Influence of Horizontal Restraints on the Behaviour of Concrete Slabs

Safwat A. H. Ibrahim

A Thesis
in
The Department
of
Civil Engineering

Presented in Partial Fulfillment of the Requirements
for the Degree of Doctor of Philosophy at
Concordia University
Montreal, Quebec, Canada

November 1994

ISBN 0-612-01274-3

Canada

ABSTRACT

Influence of Horizontal Restraints on the Behaviour of Concrete Slabs

Safwat A. H. Ibrahim

A study dealing with the influence of horizontal restraints on the behaviour of concrete slabs subjected to central concentrated loads is presented. As a part of this study, an experimental program was performed on strips of concrete slabs with horizontally restrained boundaries subjected to concentrated loads at midspans. The tested strip slabs were provided with minimum structural reinforcement to eliminate a sudden collapse at the moment of failure. Comparable tests were carried out on strip slabs that were simply supported and horizontally non-restrained with maximum reinforcement ratio.

The tests showed that the carrying capacities of the horizontally restrained strip slabs with minimum reinforcement ratio were similar to the capacities of horizontally non-restrained strip slabs with maximum reinforcement ratio. The enhanced carrying capacity of horizontally

restrained strip slabs can be explained as a result of an arch action at failure due to the horizontal restraints.

In addition, an analytical study based on the plastic theory was carried out to analyze strip slabs with full and partial horizontal restraints. As a result, a plastic analysis method was developed for these strip slabs. This method was extended to analyze horizontally restrained square slabs subjected to concentrated loads. Also, non-linear finite element analysis for the horizontally restrained square slabs and strip slabs was carried out.

By considering the influence of horizontal restraints on a wide range of applications of reinforced concrete slabs, a significant amount of reinforcement can be saved without reducing the carrying capacities of the slabs.

ACKNOWLEDGEMENTS

The author is indebted to Professor Z. A. Zielinski for his invaluable advice, guidance and constructive criticism throughout the research and preparation of this thesis.

The author thanks Dr. Jan Walczak from ADINA R&D for his help during the running of program Adina. He also thanks the Structural Laboratory Personnel especially Andrew Chociwski and Daniel Roy.

Finally, the author wishes to express his sincere gratitude to his wife Amal for her understanding and support as well as for her technical assistance during the course of this research.

To my parents and my family

CONTENTS

LIST OF FIGURES

LIST OF TABLES

LIST OF NOTATIONS

The definitions of the notations used in the text are as given below unless indicated in the text otherwise:

A Cross-section area of a structural member

a Depth of Whitney rectangular compression block (in Chapter 3, 'a' is a span length)

A_s Cross section area of steel bars

B Depth of a slab segment

b Width of cross sections of strip slabs or beams

C Compressive forces

c_d Vertical distance from the extremity of the compression fibers to the neutral axis of a cross section of a concrete member

d_1 Vertical distance between top and bottom reinforcement

E Modules of elasticity

F Force

f'_c Compression strength of concrete

f'_{cm} Compression strength of mortar

F_{ui} Axial force acting in the member number 'i' due to the application of a unit force at the joint and in the direction where the deflection needs to be calculated

f_y Tension strength of the steel reinforcement

h Depth of slabs or beams

H Height or a height of a slab segment

H_x Height at a horizontal distance 'x'

I Moment of inertia

i Number of a member in structural system

k Spring constant or the stiffness of elastic support

k_b The axial stiffness of the strip slab (or beam)

L Length of a structural member or span of a beam

M Bending moment

M_f Fixed end bending moment

P Applied concentrated load

q Compression stress acting on a tip of a slab segment

r Lever arm or the rise of structural system

R Relative strength of the strip slabs

R_h Horizontal reaction at a support

R_v Vertical reaction at a support

R_x Reaction located at a horizontal distance 'x'

s Axial deformation of member subjected to axial force

s_i Shortening of member number 'i' due to the application of the actual forces on the structural system

T Tension forces

u In-plane displacement

u_x In-plane displacements of slabs or strip slabs in x direction

w Deflection of slabs or beams

w_h Horizontal displacement or horizontal deflection

X, Y, Z General Cartesian coordinates

μ Coefficient of friction

ν Poisson's ratio

ε Strain or the axial strain of a concrete member

σ Stress or the compression stress of the concrete

β Taken as 0.85 for concrete strength f_c' up to and including 30 MPa and beyond this it is reduced continuously at a rate of 0.08 for each additional 10 MPa of strength, but with a minimum value of 0.65

ρ_{act} Actual reinforcement ratio

σ_c Compression strength of concrete $= f_c'$

ρ_{max} Maximum reinforcement ratio

ρ_{min} Minimum reinforcement ratio

ε_x Strain in x direction

Chapter 1

Introduction

1-1 General

Many publications dealt with the problem of concrete slabs subjected to concentrated loads. However, few publications took into account the effects of horizontal restraints on the behaviour of such slabs. Horizontal restraints might change the behaviour and carrying capacity of concrete slabs. If horizontal restraints have a significant influence on the behaviour of slabs, then, the effects of the horizontal restraints need to be considered in the calculations of the carrying capacities and deflections of slabs subjected to lateral loads. The present study examines some types of concrete slabs subjected to concentrated loads, taking into consideration the influence of horizontal restraints on the behaviour of these slabs.

1-2 Concrete Slabs Subjected To Concentrated Loads

Designing reinforced concrete slabs subjected to either concentrated loads or loads not distributed over the entire slab area is usually a difficult task to perform due to the complexity of the problem. The designers of such slabs usually deal with this problem either by

replacing the actual loads with equivalent loads uniformly distributed over the entire area of the slab, or by using methods that consider the concentrated loads, such as the elastic plate theory or the yield line method. Methods which consider concentrated loads are demonstrated in Chapter 2.

The solution which is based on the use of equivalent uniformly distributed loads is often recommended by codes of practice. The values of these uniformly distributed loads are sometimes specified by building codes, but more often, the values of the equivalent loads are left to the judgement of the designer. For example, the National Building Code of Canada[1] specifies 12 kN/m^2 to be used as an equivalent uniformly distributed live load for designing slabs of garages for loaded buses and trucks. To estimate the shear force under the wheel load, the same code replaces the equivalent uniformly distributed live load by a concentrated live load of 54 kN to be placed anywhere on the slab. It is doubtful that this method will produce the most economical slabs. In addition, the use of an equivalent load may be conservative for the moment at one location in a slab yet not conservative for the moment at another location. Also, according to codes[2, 3, 4] dealing with wheel load on the slabs of bridge decks, it is permissible to substitute the concentrated wheel loads by a specified uniform load. Other examples where equivalent loads are usually used are wheel loads from fork lift trucks in manufacturing

buildings or warehouses, and heavy machinery loads distributed over small areas.

Although it is obvious that moments due to concentrated loads need to be considered in the design of most floor slabs, the complexity of the necessary analysis makes the computations of such moments difficult and impractical. Therefore, in most cases, computations based on equivalent uniform loads over the entire slab are used, which may or may not yield consistent or correct results.

On the other hand, solving this problem by using methods that consider the concentrated loads, such as the elastic plate theory or the influence surface which is based on the elastic theory (demonstrated in Chapter 2) is not economical either. In addition to the complexity of these methods, laboratory investigations on models and full scale tests have shown that the slabs that are designed using such methods, especially those forming bridge decks, appear to resist loads by a mechanism different from that assumed. This leads to load capacities greater than predicted.

The accidental failure[77] of a slab is a highly visible demonstration of inadequacy in design. However, the other extreme, where the design is shown to be overly conservative, is also possible. It is the latter that has become apparent in the analysis and design of reinforced concrete slabs subjected to concentrated loads.

1-3 Influence of Horizontal Restraints

The influence of horizontally restrained boundaries on the behaviour of reinforced concrete slabs subjected to lateral loads has became an important topic of research in recent years[38,46,47]. Horizontally restrained reinforced concrete beams and slabs exhibit greater carrying capacities than that which they have been designed[46]. Yet horizontally non-restrained simply supported concrete beams and slabs exhibit in-plane (horizontal) displacements due to the applications of lateral loads[45].

The tendency of concrete slabs to exhibit in-plane displacements are restrained, to some degree, by the lateral stiffness of supporting members such as beams or walls. Adjacent slab panels also form extremely stiff diaphragms which oppose the expansions of the laterally loaded slab. Restraining the in-plane displacement results in membrane compressive forces (arch or dome action) and enhances the carrying capacity of the slabs. As a part of this study, experimental and analytical research work has been carried out to examine the behaviour of horizontally restrained concrete slabs subjected to central concentrated loads.

1-4 Applications of Horizontal Restraints

Taking advantage of the effects of the horizontal restraints on the

behaviour of horizontally restrained slabs can result in reducing the flexural reinforcing steel. Moreover, reducing the steel enhances the durability of concrete against the effect of steel corrosion. The influence of horizontal restraints on the behaviour of slabs has many engineering applications. Structural engineers can use advantageously the effects of horizontal restraints on several types of slabs. According to the present codes of practice, several types of structural slabs which are horizontally restrained are designed without taking advantage of their horizontal restraints. The main reason of that is either shortage of information on this subject (the influence of horizontal restraints on the behaviour of slabs) or that the subject is not yet widely known. To provide additional information on this subject, many experimental programs are required on horizontally restrained slabs subjected to different patterns of loading such as uniformly distributed loads and concentrated loads. Advantage of the influence of horizontal restraints can be taken for some types of slabs such as two-way floor systems, joist floor systems and some bridge slab decks. Some of these types will be demonstrated hereinafter.

1-4-1 Two-way slabs supported on beams

The degree of horizontal restraint depends on the horizontal stiffness of the member that provides the horizontal restraint. When this stiffness is very high in comparison with the vertical stiffness of the

slab, the degree of horizontal restraint is considered very high. In a hypothetical case, if the horizontal stiffness of the member that provides the horizontal restraints is infinity, the degree of the horizontal restraint is 100% or there is full horizontal restraint.

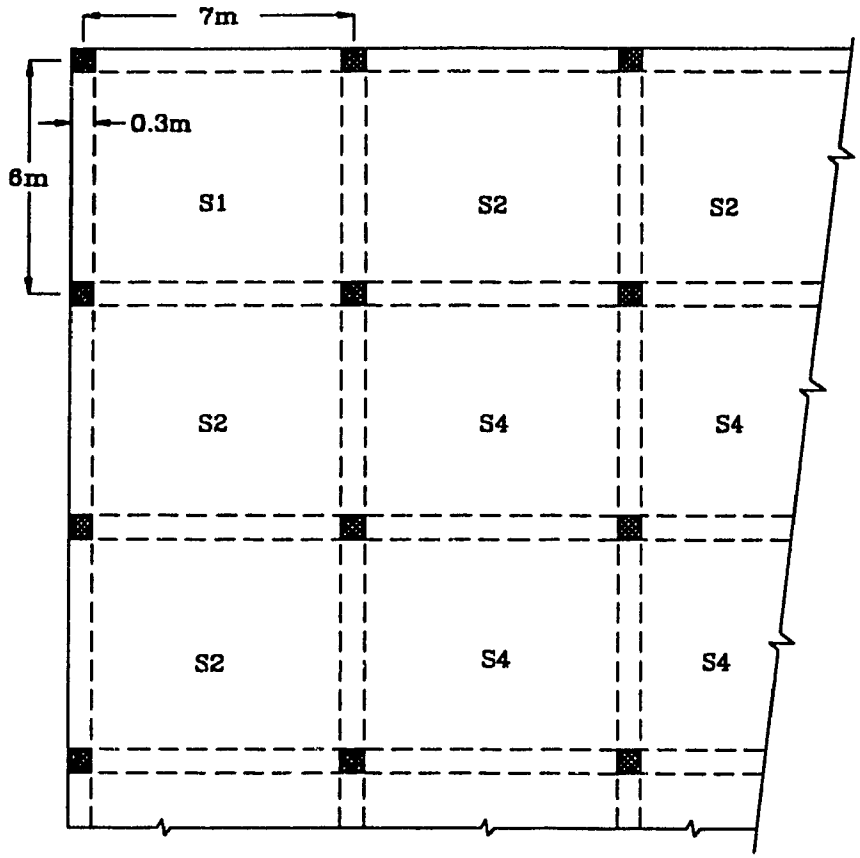

Figure 1-1 Two-way slabs supported on beams

All slab panels shown in Figure 1-1 are horizontally restrained. Slab panel 'S4' is horizontally restrained by the adjacent panels. These adjacent panels provide very stiff horizontal restraints. Therefore slab

panel 'S4' can be considered highly horizontally restrained. On the other hand, slab panel 'S1' is horizontally restrained by the supporting beams. These beams provide only partial horizontal restraint.

1-4-2 One-way joist floor systems

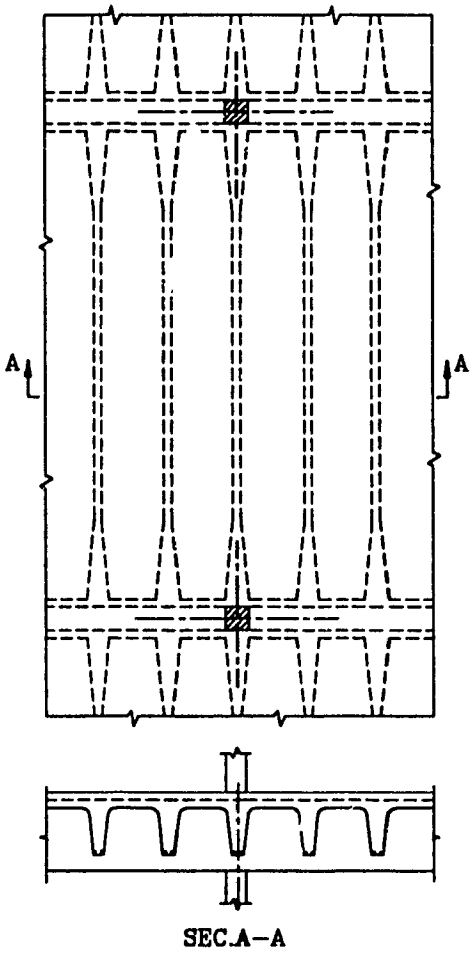

Figure 1-2 One-way joist floor system

As shown in Figure 1-2, the one-way slab panels are supported by joists. These slab panels are horizontally restrained by the adjoining

panels. The adjoining panels provide extremely stiff horizontal restraints. Therefore, advantage can be taken from these horizontal restraints by enhancing the carrying capacity of these one-way slab panels. Also, the reinforcement of the ribs can be reduced due to their horizontal restraints.

1-4-3 Two-way joist floor systems

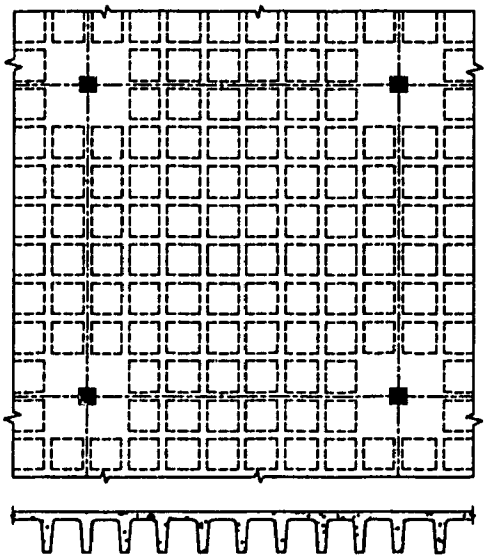

Figure 1-3 Two-way joist floor (waffle slab)

As shown in Figure 1-3, the two-way slab cells are supported by a grid of joists. These slab cells are horizontally restrained by the adjoining slab cells and the joists. The adjoining slab cells and the joists provide extremely stiff horizontal restraints. Therefore, advantage can

be taken from these horizontal restraints by reducing the flexural reinforcement of these two-way joist floor systems.

1-4-4 Concrete slab supported on box girders

As shown in Figure 1-4, the concrete slab deck is supported by box girders. These box girders provide partial horizontal restraints. Taking advantage of these horizontal restraints can result in reducing the flexural reinforcement of this deck slab.

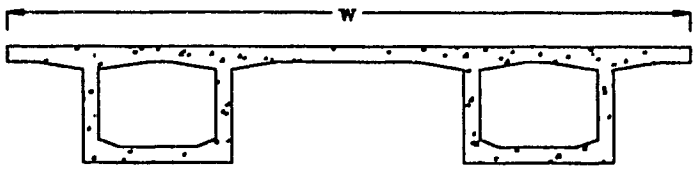

Figure 1-4 Concrete slab supported on box girders

1-4-5 Concrete slab supported on multicell box girders

The concrete slab deck that is shown in Figure 1-5 is supported by multicell box girders. The internal concrete slab panels are horizontally restrained by the adjoining slab panels and by the vertical walls of the box girders. The exterior slab panels are horizontally restrained by the vertical walls of the box girders. Taking advantage of these horizontal restraints can result in reducing the flexural reinforcement of this deck slab.

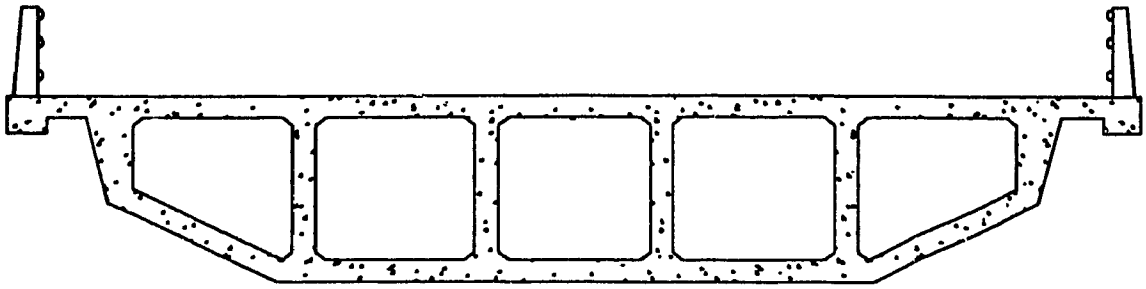

Figure 1-5 Cross section of multicell box girder bridge

1-5 Scope of the Study

The subject of this research is the influence of horizontal restraints on the behaviour and on the strength of some types of concrete slabs subjected to central concentrated loads. During the course of this research, experimental tests, analytical study and finite element analysis were performed.

An experimental program was carried out on strips of concrete slabs with horizontally restrained boundaries and subjected to central concentrated loads. Additional comparable tests were carried out on simply supported horizontally non-restrained strip slabs.

Analytical studies based on the theory of elasticity and the theory of plasticity were carried out. A plastic analysis method based on an iterative procedure for simply supported and horizontally restrained strip slabs was developed.

The research has been extended to analyze horizontally restrained square concrete slabs subjected to central concentrated loads. The internal stresses that are acting on the segments of the square slab were examined by the finite element method. The finite element program "ADINA"[5] was used to perform the analysis. An approximate solution, based on the theory of plasticity, for square slabs with horizontal restraints on the boundaries, subjected to central concentrated loads is presented.

Chapter 2

Literature Survey and Review of Methods of Analysis

2-1 Introduction

Several methods of analysis are used to predict the behaviour of reinforced concrete slabs under the action of concentrated loads. Some of these methods deal with slabs or plates in the elastic range, and others deal with slabs or plates in the ultimate state condition. Also, some of these methods solve only for moments, and some others solve for moments and shears (shear force at any location in the slab and punching shear at the vicinity of the concentrated load or column). Each one of these methods has its own assumptions. However, all of these methods disregard the in-plane displacements of the slabs.

2-2 The Elastic Theory

The most common method of analysis is the elastic plate theory. This method can be more correctly described as the theory of the bending of elastic plates with small deflections. Timoshenko and Woinowsky-

Krieger[6], in their introduction to what has become a standard reference for the subject, describe the assumptions, the method and the solutions (for some applications) given by this theory. Several numerical examples and illustrations using this theory are given by Rudolph Szilard[7], Park and Gamble[8], among others. This theory represents the behaviour of an elastic plate subjected to lateral loads in a fourth order, non-homogeneous, partial differential equation, governed by the deflection 'w' of the plate and given in the following form:

$$\frac{\partial^4 w}{\partial x^4} + 2\frac{\partial^4 w}{\partial x^2 \partial y^2} + \frac{\partial^4 w}{\partial y^4} = \frac{P_z(x,y)}{D}$$

The elastic plate theory presents solutions for plates of various loading and boundary conditions[6]. Laboratory tests have shown discrepancies between the theoretical analysis obtained by using this theory and the results that are obtained from experimental tests for some boundary conditions. The discrepancies are mainly due to ignoring the in-plane displacement.

Several techniques are used either to solve the differential equation of the elastic plate theory directly or to use the result of the elastic plate theory to produce solutions for the problem of plates subjected to concentrated loads in different forms. The differential equation may, of

course, b solved by the use of finite difference method[9, 10]. Also, the results of the elastic plate theory have been used by Pucher[11] and Woodring[12], among others, to produce an influence surface to obtain the values of the bending moments for plates subjected to concentrated loads in arbitrary positions with various boundary conditions. Hrennikoff[13] and Lightfoot[14] described the method of a grid framework analogy for laterally loaded plates. The grid framework analogy is based on replacing the plate by means of a gridwork of beams and the lateral loads to be placed on those beams. The gridwork method is also based on the elastic theory and its accuracy is similar to the accuracy of the elastic theory.

2-3 Influence Surface

An influence surface can be generated by applying a unit concentrated load to numerous points of the plate and evaluating the required effect (moment, shear, etc.), produced at an observation point (ξ, η). The results are then plotted as ordinates at the point of applications (x_i, y_i) of the unit load. Although such an approach is straightforward, its use is discouraged because of the large amount of computational work involved.

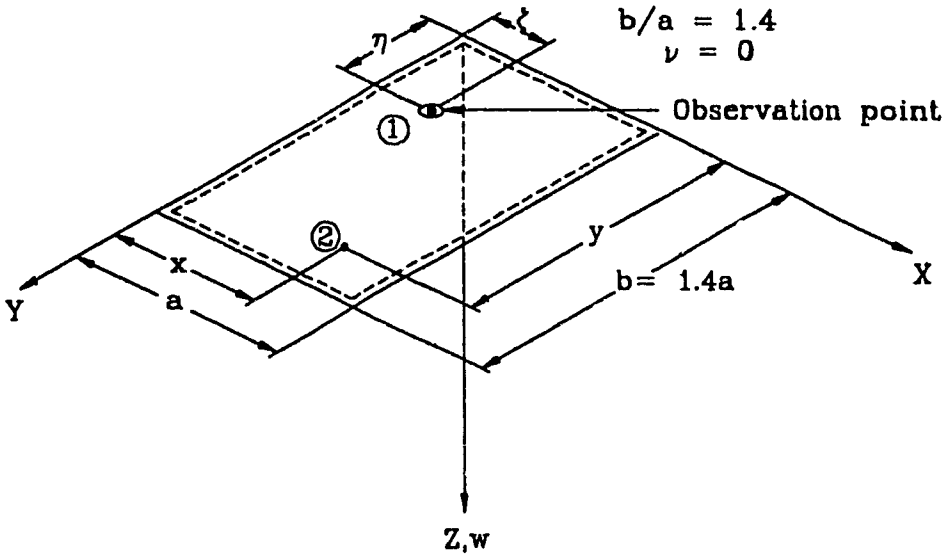

(a)

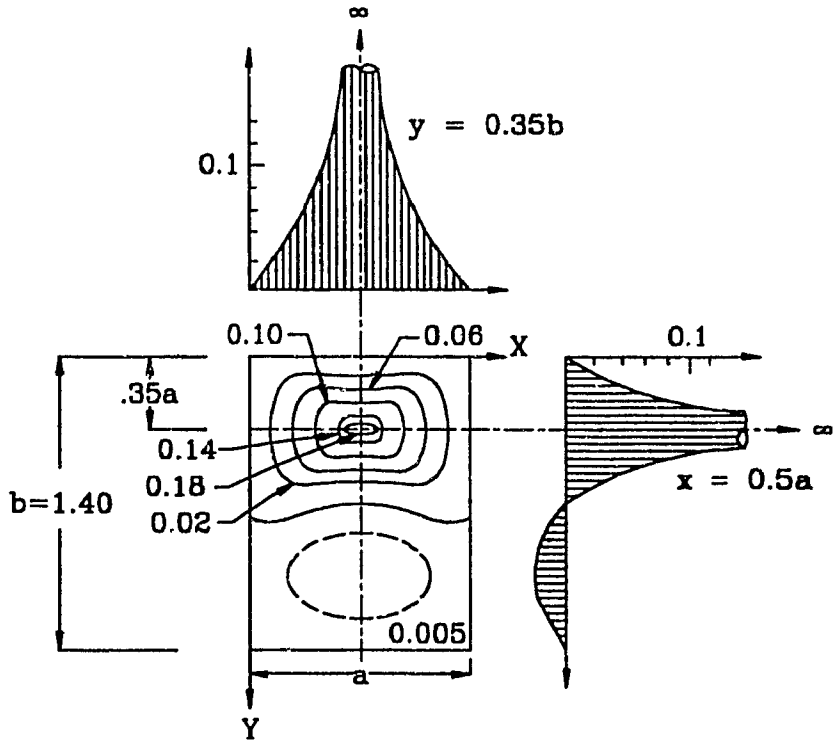

(b)

Figure 2-1 Example of influence surface for bending moment,

(a) rectangular plate, (b) ordinates of influence surface

Instead, Maxwell's theorem of reciprocal deflection[11] is applied, which states that an influence surface may be cor idered as a deflected plate surface due to an affine unit motion introduced at the observation point (see Figure 2-1). Because the influence surface solutions are based on the principles of the elastic plate theory, the accuracy of the results of the two methods are identical.

2-4 Plastic Theory

A structural analysis based on the elastic theory fails to assess the real load carrying capacity of slabs at failure. In most cases, an elastic design is excessively conservative. Consequently, information obtained on the factor of safety against collapse is not accurate. Since a knowledge of the real factor of safety is mandatory to be able to design structures within economical limits, and since plastic analysis is able to estimate the real carrying capacity of reinforced concrete slabs, the plastic theory becomes the natural replacement of the elastic theory.

The mathematical theory of plasticity of plates is often more complex than its elastic counterpart[15, 16]. The most common technique utilizing the plastic behaviour of reinforced concrete slabs is the yield line analysis.

2-5 Yield Line Analysis

After introducing the plastic analysis for beam and frame structures, which is based on the deformation pattern of a structure on the verge of collapse or what is known as the failure mechanism due to the formation of plastic hinges, Johansen[17] in 1943 extended the plastic analysis to reinforced concrete slabs by presenting the concept of yield lines, which are the two dimensional counterparts of plastic hinges for beams and frames. When a laterally loaded slab verges on collapse, yield lines are formed at the locations of the maximum positive and negative moments. These yield lines subdivide the slab into plane segments. The slab segments rotate as rigid bodies along the yield lines (see Figure 2-2). The assumptions used in yield line analysis are available in many publications dealing with this topic[18 to 28].

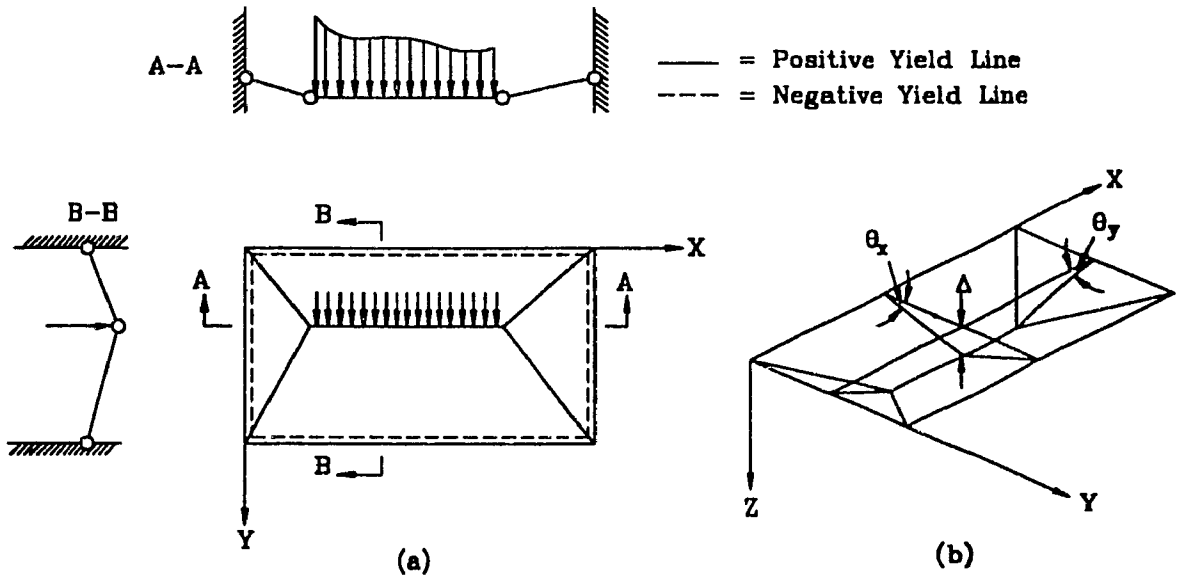

Figure 2-2 Failure mechanism of a rectangular slab

The ultimate load of a given slab, for a certain distribution of load, may be determined by using either the work method (sometimes called the energy method) which is considered an upper bound method or the equilibrium method which provides a lower bound solution[29, 30].

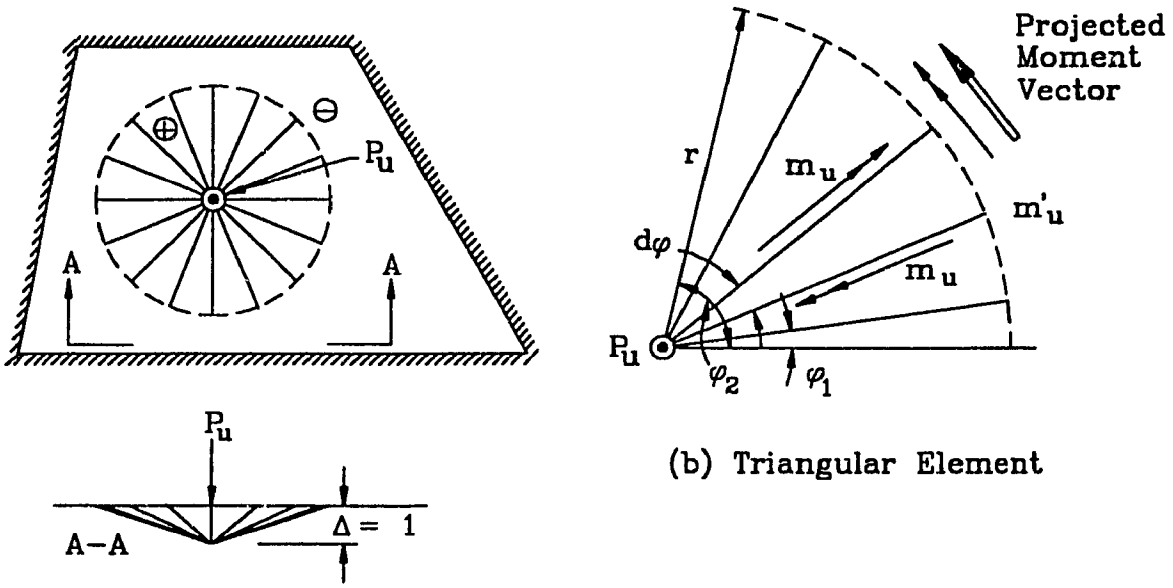

Figure 2-3 Localized failure under a concentrated load

As shown in Figure 2-3, the failure of a slab under a concentrated load is a localized slab collapse[7]. Positive yield lines radiate straight from the point of application of the concentrated load until they intersect with a curved, negative yield line, which bounds the conical failure mechanism[31]. Such a collapse mode is called a fan-type failure mechanism[32].

Although the yield line analysis has advantages over the elastic plate theory due to the utilization of the plastic range, the assumptions of the yield line theory, as with the assumptions of the elastic plate theory, do not recognize the in-plane displacements. This means that when there is restraint against the in-plane displacement on the boundaries, this restraint is not recognized by either theory, which results in disregarding the additional carrying capacity. This additional capacity has been demonstrated by laboratory tests[38,45,47]. In addition, the maximum deflections, which might control the design, cannot be estimated through the yield line analysis, moreover, theoretically, the law of superposition is not valid.

2-6 Punching Shear Analysis

Quite often the punching shear strength, rather than the moment resistance, limits the load carrying capacity for slabs subjected to point loads. The theoretical solution of the problem is quite complex. Therefore, designs for punching shear are based on empirical equations, formulated to fit the results of laboratory testing. In all the shear formulas, the shear stress is assumed to act on a critical section at some fixed distance from the perimeter of the loaded area of the slab. In most cases, the critical section is assumed to be at a distance of one half the effective depth of the slab from the loaded area[33, 34, 35]. However,

British codes[36, 37] use a distance of 1.5 times the total depth of the slab. Most codes consider the shear stress to be constant around the critical section for slabs of constant depth (assuming cases without moment transfer). Also, they consider the shear strength to be proportional to the square root of the concrete cylinder strength.

Most codes and specifications consider the shear strength due to punching shear to be largely independent of flexural conditions existing in the region of the concentrated load, and also independent of the boundary conditions of the slab. Kuang and Morley[38] and others[39, 40], through their experimental programs, proved that the value of the punching shear is affected by the boundary conditions, and the punching shear strength is enhanced if the in-plane displacement is restrained. This enhanced capacity is the result of compressive membrane action caused by providing the restraints. Present design procedures for punching failure in reinforced concrete slabs subjected to concentrated loads are based largely on experimental studies of the behaviour and strength of simply supported horizontally non-restrained slabs. Consequently, punching shear provisions incorporated in various codes of practice are a direct result of the empirical procedures, and they do not usually provide an accurate prediction of the ultimate load capacity of a restrained slab, as no direct account is taken of the considerable enhancement due to the in-plane restraint in many types of reinforced

concrete slab systems[38].

2-7 Finite Element Analysis

In the last twenty five years, the finite element method has been applied extensively to the analysis of reinforced and plain concrete structures[41, 42, 43, 44]. The earlier applications of the finite element method were only for two dimensional problems using linear analysis. Recently, the advancement of non-linear finite element analysis and better understanding of the non-linear behaviour of concrete under the triaxial state of stresses have increased the importance of analyzing concrete slabs using the finite element method. Non-linear finite element analysis can be considered a better method to predict the behaviour of concrete slabs subjected to concentrated loads.

The finite element method has several advantages over the methods that have been mentioned above. However, it also has some disadvantages. The advantages of the non-linear finite element method are:

- Generally, it can be used for several types of loading (concentrated load, uniformly distributed load, ...etc.) applied separately or simultaneously to a slab.
- It can be used for slabs having different dimensions and different boundary conditions.

- It can predict strain or displacement at a given location for a loaded slab in the plastic state.
- It can predict stresses or forces at a given location for a loaded slab in the plastic state.

The disadvantages of the finite element method are:

- The failure criteria considered in each program are different.
- It requires expensive computer facilities.
- It requires a great amount of time to learn and run one of the available programs to solve a simple problem.
- It requires an even greater amount of time to create a program to solve a simple problem.

Applications of three dimensional non-linear finite element analysis were carried out in this research using a commercial program called ADINA[5]. The results of the finite element analysis will be compared to the results obtained from the experimental work and to results obtained from the developed analytical methods.

2-8 Influence of Horizontal Restraints

Several publications[78 through 83] dealt with the problem of the horizontal restraints effect on the behaviour of concrete slabs and beams.

Hyttinen[45] in 1970 studied the influence of restrained boundaries on the behaviour of reinforced concrete square slabs subjected to central concentrated loads. In his research, slabs with different boundaries, such as simply supported and fixed boundaries, were tested. Enhanced carrying capacity was recorded due to the dome action of reinforced concrete slabs with restrained boundaries.

Vecchio and Tang[46] in 1990 discussed the influence of compressive membrane action in reinforced concrete slabs. Two reinforced strip slab specimens, each supported on two columns, were tested under concentrated midspan loads. One slab was restrained against lateral expansion at the ends, while the other was free to elongate. The laterally restrained specimen developed membrane compressive forces, which resulted in enhanced load capacity.

Kuang and Morley[38] in 1992 reported the results of punching shear tests on restrained reinforced concrete square slabs subjected to central concentrated loads. The slab panels were supported and restrained on all four sides by edge beams. The punching shear strengths observed were higher than those predicted. The enhanced punching shear capacity was a result of compressive membrane action caused by restraining the slab boundaries.

Fang et al. [47] in 1994 reported the test results of partially restrained reinforced concrete slabs with isotropic reinforcement under

central concentrated loads. The dimensions of the tested rectangular slab panels were 1000 mm by 2300 mm. The slabs were supported on two edge beams along their long sides. The tested reinforced slabs exhibited additional carrying capacities due to the compressive membrane action caused by the partially restrained boundaries.

Most of the previous research studies were performed on reinforced concrete slabs and did not provide a complete method of analysis to formulate the influence of horizontal restraints on slabs subjected to concentrated loads. Therefore, additional research work to study the influence of horizontal restraints on non-reinforced concrete slabs is required. Also, a method of analysis needs to be established.

Chapter 3

Elastic Analysis of Horizontally Restrained Slabs

3-1 The Importance of the Elastic Theory

The elastic theory is an important step toward an advanced analysis using plastic theory. The formulation of the elastic plate theory ignores the effects of horizontally restrained boundaries on the behaviour of slabs subjected to lateral loads. To examine the effects of the horizontal restraints using plastic theory, it is necessary first to examine these effects using elastic theory. In addition, their existence needs to be considered by the elastic theory, which might provide some guidance in developing the experimental program and in further developing the required plastic analysis. In this chapter, observation on the behaviour of horizontally restrained slabs will be considered and an elastic analysis will be carried out.

3-2 Behaviour of Reinforced Concrete Slab Subjected to a Point Load

Westergaard and Slater[48], who in 1921 tested a number of full scale slab panels supported on four sides and loaded to ultimate capacity, and Westergaard[47], who in 1930 studied stresses caused in bridge slabs

by wheel loads, encountered larger ultimate load capacity than was expected. At that time, a satisfactory account could not be made for the unexpectedly high strength exhibited by the slabs.

In recent publications, Hyttinen[45] and others[46, 50], were able to find out the reason for the observed additional carrying capacity of slabs restrained at the boundaries against in-plane expanding and subjected to transverse concentrated loads. This additional carrying capacity was due to a compressive arch action caused by the restraints at the boundaries.

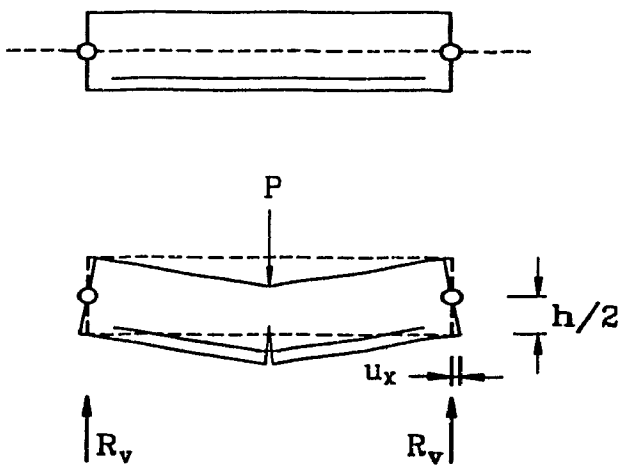

Figure 3-1 In-plane displacements 'u_x' due to the rotation of the segments of the slab

Consider the performance of a one-way simply supported reinforced concrete slab or a beam subjected to a concentrated load at midspan (as shown in Figure 3-1). Hinged supports are located at the horizontal middle surface plane of the slab. At the ultimate load, the

slab will be divided into segments. The maximum deflection will occur at midspan. This deflection is a result of the rotation of each segment at its yield line at midspan and at the hinged boundary. The presence of the in-plane displacements 'u_x' is due to the rotation of the segment, (see Figure 3-1). If these in-plane displacements are restrained, the ultimate carrying capacity of the slab would be enhanced, as will be explained below.

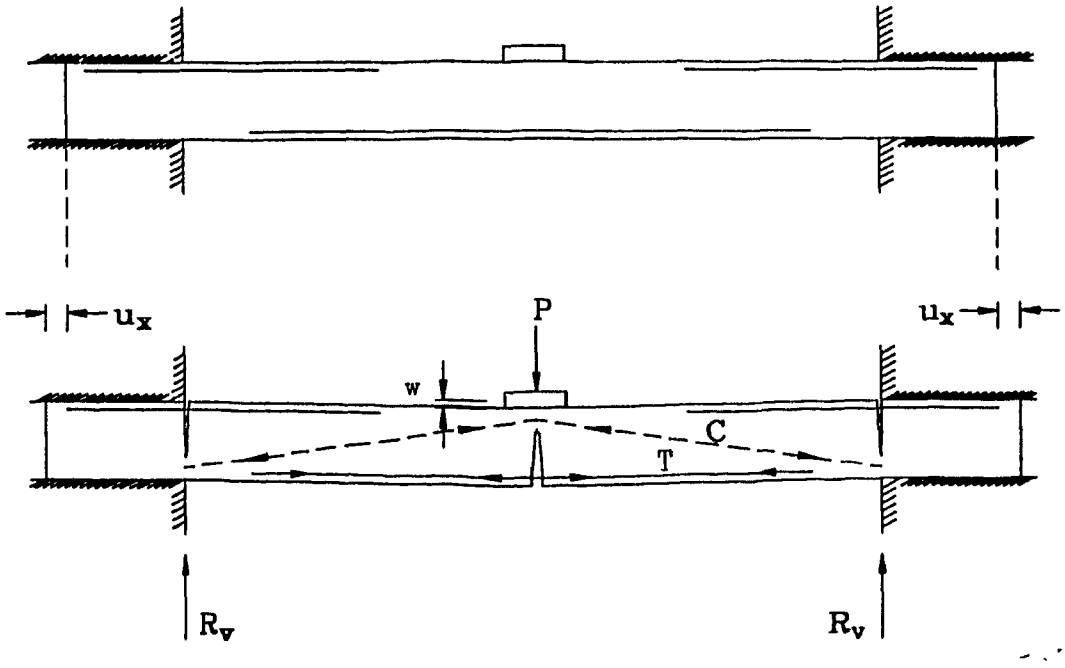

Figure 3-2 Development of the arch action

Consider the behaviour of a reinforced concrete slab subjected to a concentrated load, where the rotations at the supports are restrained and the in-plane displacements are non-restrained (as shown in Figure 3-2). Applying a small concentrated load, compressive membrane stresses will

be generated. The tension stresses will be carried totally by the concrete (for very small loads). As the load increases to reach its ultimate value, the slab deflects and the compressive membrane stresses in the concrete increase to reach its crushing value. The tension stresses will be carried totally by the reinforcement, which reaches its yielding state, with the generation of principal cracks in the tension faces of the concrete. Despite the restrained boundaries against rotations, the edges of the slab will undergo rotations, which will produce cracks in the top fibres and expansions of the bottom fibres near the supports, resulting in in-plane displacements 'u_x' (see Figure 3-2). In this case, the compressive membrane forces 'C' in the concrete are balanced by tension forces 'T' in the reinforcing steel.

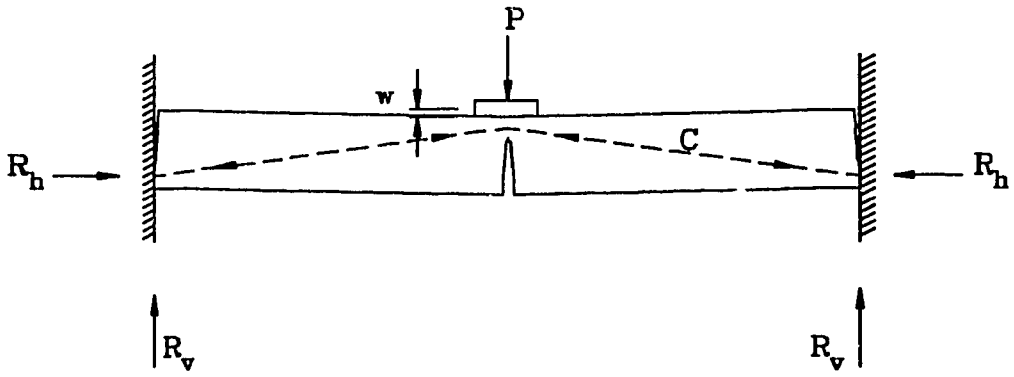

Figure 3-3 Slab with fixed boundary subjected to a concentrated load

As shown in Figure 3-3, for non-reinforced concrete slabs with boundaries restrained against in-plane displacements, the compressive membrane forces in the concrete will be balanced by horizontal reaction

forces 'R_h' at the boundaries.

In most slab structures, the tendency to expand will be prevented, to some degree, by the lateral stiffness of supporting beam or walls. Also, adjoining slab panels will form an extremely stiff diaphragm which will oppose the expansion of the loaded slab. When the in-plane displacements are restrained, the ultimate flexural capacity, the shearing capacity and the punching shear capacity will increase.

3-3 Mathematical Formulations by The Elastic Theory

Several recent publications link the observed additional carrying capacity of slabs subjected to a concentrated load to the in-plane restraints provided at the boundaries of these slabs. However, completely satisfactory mathematical explanations to describe this relation between the additional carrying capacity and the in-plane restraints are not yet perfectly established. Also, a mathematical solution to calculate the in-plane displacement is not yet entirely formulated.

As was mentioned earlier, the main reason for causing the in-plane displacement of simply supported reinforced concrete slabs subjected to concentrated loads is due to the rotation of the slab segments at the yield lines and/or at the boundaries. It is possible to calculate the in-plane displacement of such slabs as will be demonstrated in the following sections.

To determine the value of the in-plane displacement due to the rotations of the edges of a simply supported slab subjected to a concentrated load, the elastic plate theory will be used. To calculate the angles of rotation of the elastic curve at the edges of the deflected slab, the moment area method will be used.

3-4 Slopes of Elastic Surface of Plates Under Lateral Loads

The moment area method is usually used in the computation of the deflections and slopes of elastic lines for beams and frames[51, 52, 53]. In this section, the moment area method will be used to obtain the angles of rotations of plates subjected to lateral loads.

Referring to Figure 3-4, consider portion ACB of the elastic curve of a slab that was initially straight and continuous in the position A_0-B_0 in its unstressed condition. The tangents to the elastic curve at points A and B are as shown. The angle $\Delta\theta_{AB}$ is the change in the slope between the tangents at points A and B. The inclination of any tangent to the elastic curve is so small that an angle such as θ_A is approximately equal to its sine and its tangent, and its cosine is approximately equal to unity.

Consider a differential element of this curve having a horizontal projection dx, and draw the tangents to the elastic curve at each end of this element. The change in slope between these tangents is the angle $d\theta$, and its value can be obtained by considering Figure 3-5.

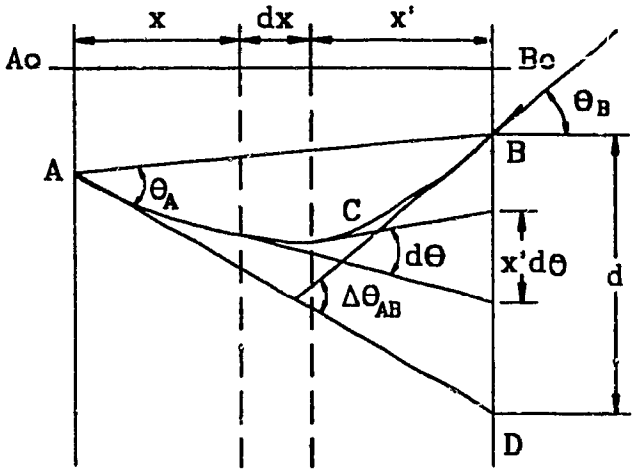

Figure 3-4 Derivation of the moment area theorems

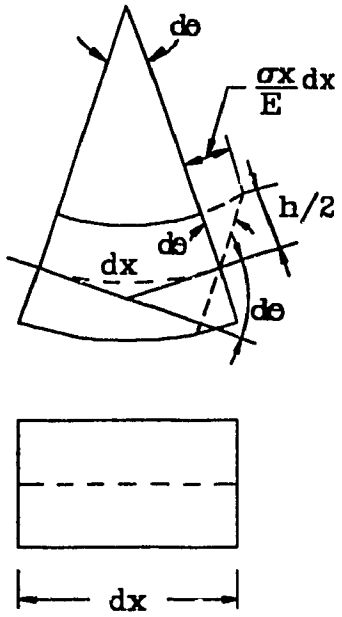

Figure 3-5 Differential change in the slope

$$d\theta = \frac{\sigma_x}{E(h/2)}\,dx \quad \ldots\ldots\ldots\ldots\ldots\ldots \quad (3\text{-}1)$$

The total change in the slope θ, between the tangents at A and B is the sum of all the angles dθ for all the elements dx along the elastic curve ACB.

$$\theta_{AB} = \int_A^B d\theta \quad \ldots\ldots\ldots\ldots\ldots\ldots \quad (3\text{-}2)$$

Using relations between stress and strain, given by the theory of elasticity, (the complete method of how they are derived is available in many publications dealing with this topic[7, 54, 56]), the following equations are obtained;

$$\sigma_x = \frac{E}{1 - \nu^2}(\varepsilon_x + \nu\,\varepsilon_y) \quad \ldots\ldots\ldots\ldots\ldots\ldots \quad (3\text{-}3)$$

$$\sigma_y = \frac{E}{1 - \nu^2}(\varepsilon_y + \nu\,\varepsilon_x) \quad \ldots\ldots\ldots\ldots\ldots\ldots \quad (3\text{-}4)$$

From the elastic theory of plates, the following equations are given by Timoshenko[6] and Szilard[7]. These equations are relations between strain and displacement and between moment and displacement.

$$\varepsilon_x = -\frac{h}{2} \times \frac{\partial^2 w}{\partial x^2} \quad \ldots\ldots\ldots\ldots\ldots\ldots \quad (3\text{-}5)$$

$$\varepsilon_y = -\frac{h}{2} \times \frac{\partial^2 w}{\partial y^2} \quad \ldots\ldots\ldots\ldots\ldots\ldots \quad (3\text{-}6)$$

Also, the bending moments M_x and M_y (for plates with constant depth having different shapes and boundary conditions) are expressed in terms of the lateral deflection 'w', as follows:

$$M_x = - \frac{E h^3}{12 (1 - \nu^2)} \left(\frac{\partial^2 w}{\partial x^2} + \nu \frac{\partial^2 w}{\partial y^2}\right) \quad \ldots\ldots\ldots \quad (3\text{-}7)$$

$$M_y = - \frac{E h^3}{12 (1 - \nu^2)} \left(\frac{\partial^2 w}{\partial y^2} + \nu \frac{\partial^2 w}{\partial x^2}\right) \quad \ldots\ldots\ldots\ldots \quad (3\text{-}8)$$

Substituting from Equations (3-5), (3-6) and (3-7) into Equation (3-3), we obtain;

$$\sigma_x = \frac{6}{h^2} M_x \quad \ldots\ldots\ldots\ldots\ldots\ldots \quad (3\text{-}9)$$

Substituting from Equation (3-9) into Equations (3-1) and (3-2), the following equation is obtained;

$$\theta_x = \frac{12}{h^3 E} \int_A^B M_x \, dx \quad \ldots\ldots\ldots\ldots\ldots \quad (3\text{-}10)$$

Following the same method, the following equation is obtained;

$$\theta_y = \frac{12}{h^3 E} \int_A^B M_y \, dy \quad \ldots\ldots\ldots\ldots\ldots \quad (3\text{-}11)$$

The above two Equations (3-10) and (3-11) represent the change in slopes between two points A and B of the elastic curve for a deflected simply supported plate, at given sections in x and y directions

respectively, for given bending moments M_x and M_y.

3-5 In-Plane Displacement of Reinforced Concrete Slabs

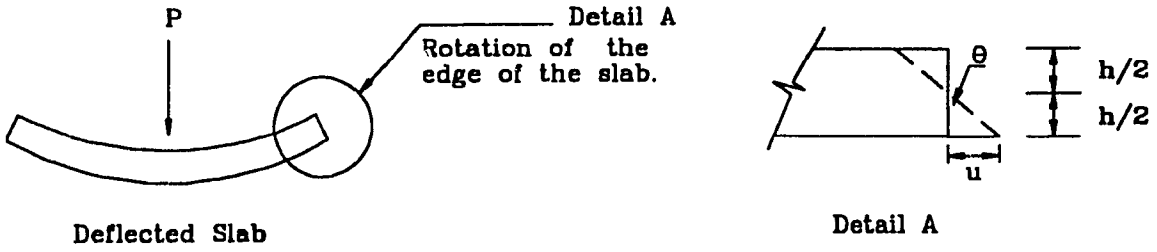

Figure 3-6 The rotation of the edge of the slab producing in-plane displacement

As shown in Figure 3-6, if the value of the angle of rotation at the boundary is known, the value of the in-plane displacement can be obtained as follows,

$$\theta \approx \tan\theta = \frac{u}{h/2}$$

$$u = \theta\,(h/2) \quad \ldots\ldots\ldots\ldots\ldots\ldots \quad (3\text{-}12)$$

Now, let us consider the case of an infinitely long simply supported plate, as shown in Figure 3-7. The expression for the bending moment M_x of this plate, for given section x, at y=0, is given in Timoshenko and Woinowsky- Krieger[6] as follows:

$$M_x = \frac{(1+\nu)P}{2\pi} \sum_{m=1}^{\infty} \frac{1}{m} \times \sin\frac{m\pi\xi}{a} \times \sin\frac{m\pi x}{a}$$

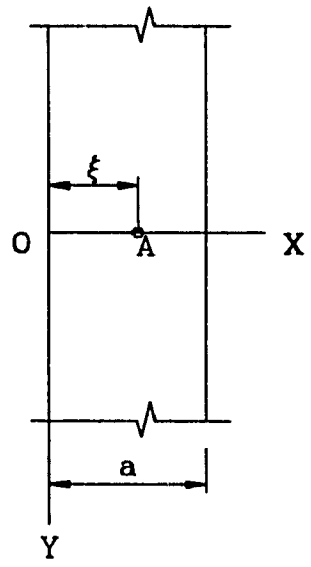

Figure 3-7 Infinitely long simply supported plate

Substituting from the above equation into Equation (3-10), the following equation will be obtained.

$$\theta_x = \frac{12(1+\nu)P}{2h^3 E\pi} \sum_{m=1}^{\infty} \frac{1}{m} \times \sin\frac{m\pi\xi}{a} \times \int \sin\frac{m\pi x}{a} dx$$

By integrating the above equation we get

$$\theta_x = - \frac{6(1+\nu)Pa}{h^3 E \pi^2} \sum_{m=1}^{\infty} \frac{1}{m^2} \times \sin\frac{m\pi\xi}{a} \times \cos\frac{m\pi x}{a} + C$$

Where C is the constant of the integration.

To find out the value of C, let us consider the following case;

$$\xi = \frac{a}{2}$$

$$x = \frac{a}{2}$$

The value of θ, in this location, must equal zero, and the summation part of the slope equation will become zero, which means;

$$\sum_{m=1}^{\infty} \frac{1}{m^2} \times \sin \frac{m\pi}{2} \times \cos \frac{m\pi}{2} = 0$$

Which leads to C = 0, and the slope of the elastic surface in x direction will become;

$$\theta_x = - \frac{6(1+\nu)Pa}{h^3 E \pi^2} \sum_{m=1}^{\infty} \frac{1}{m^2} \times \sin \frac{m\pi\xi}{a} \times \cos \frac{m\pi x}{a}$$

Substituting from the above equation into Equation (3-12), the in-plane displacement for a simply supported plate, with very long length, can be obtained as shown below;

$$u_x = - \frac{3(1+\nu)Pa}{h^2 E \pi^2} \sum_{m=1}^{\infty} \frac{1}{m^2} \times \sin \frac{m\pi\xi}{a} \times \cos \frac{m\pi x}{a} \quad \ldots\ldots \quad (3\text{-}13)$$

3-6 Illustrative Example (1)

Hyttinen[45] did some experimental work on reinforced concrete slabs subjected to centrally concentrated loads with varying dimensions and varying boundary conditions. He used, in some cases, slabs with a width of 1400 mm and depth of 60 mm which were able to support a considerably heavy concentrated load. In this example, consider a one way slab with a span of 1400 mm and depth of 60 mm, having very long length, and a concentrated load of 20 kN applied at the centre of the slab, as shown in Figure 3-8. To get the in-plane displacement, use Equation (3-13) with the following values;

$\xi = a/2$, $x = 0$,

$E = 29400$ MPa, $h = 60$ mm,

$P = 20000$ N, $a = 1400$ mm

and $\nu = 0.25$

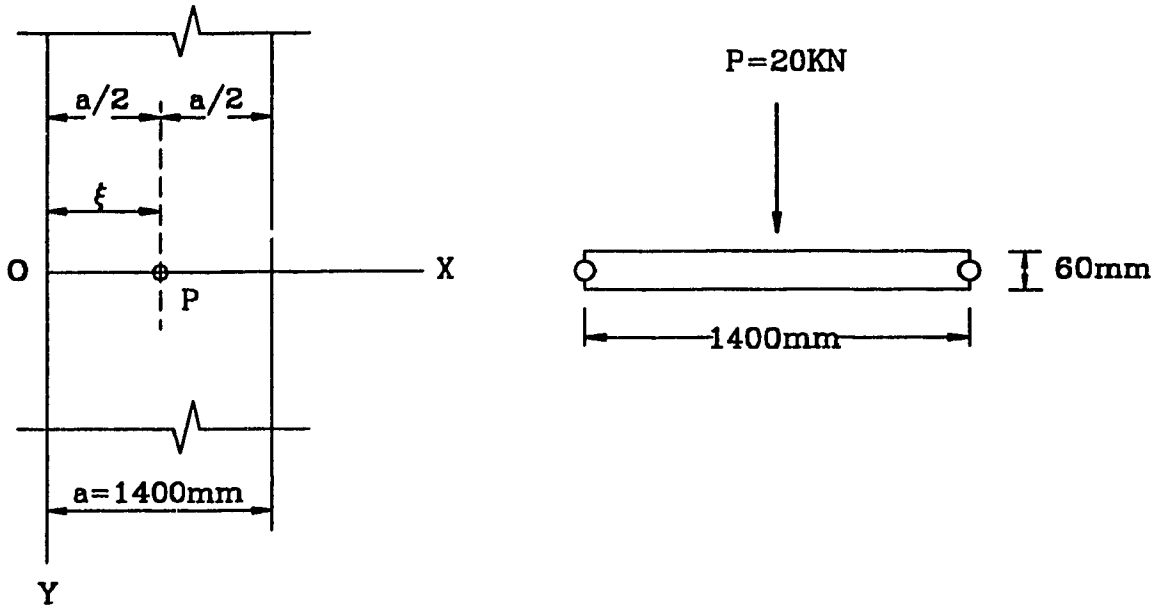

Figure 3-8 Simply supported and infinitely long slab (horizontally non-restrained) subjected to a point load

Substituting the above values into Equation (3-13), we obtain

$$u_x = 0.1\,mm$$

In the above method, the value of the in-plane displacement was obtained by using elastic theory. It may also be possible to obtain the in-plane displacement by using plastic theory as will be shown in Chapter 5.

3-7 The Effects of Restraining the In-Plane Displacement

Assuming a horizontal restraining force 'F' per linear width is applied to the bottom fibers of the slab to prevent it from expanding, the

value of this restraining force 'F' at x=0 and at x=a needs to be obtained.

Knowing the in-plane displacements that will occur on both sides of the slab, the strain ε_x can be obtained. Knowing the strain, the stress that is required to put back this strain to zero can also be obtained as shown in Figure 3-9.

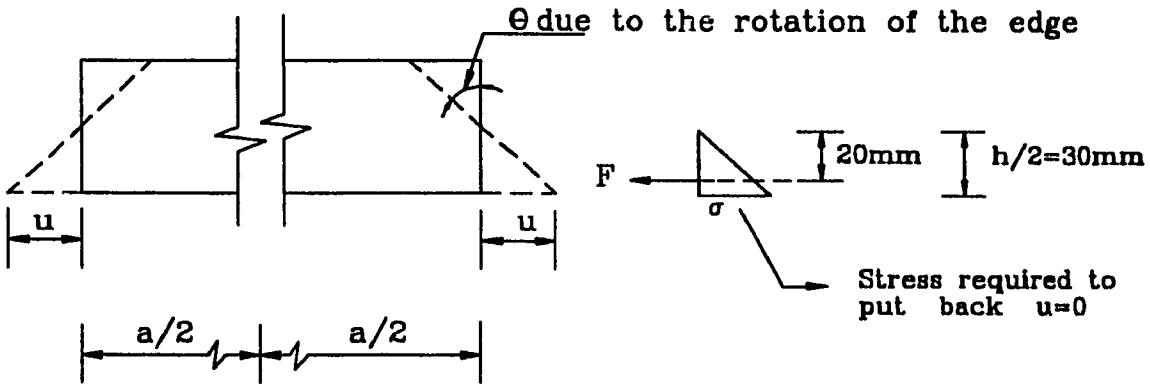

Figure 3-9 Stress required to bring back the strain to zero

$$\varepsilon_x = \frac{u}{a/2} = \frac{0.1}{1400/2} = 0.0001$$

The stress results due to this strain is calculated as follows:

$$= E \times \varepsilon_x = 29400 \times 0.0001 = 4.2 \ MPa$$

The distribution of the stress σ required to put this strain to zero is shown in Figure 3-9. The resultant force 'F' due to the stress σ is calculated as follows:

$$F = \sigma \times \frac{30\,mm}{2} = 15\,\sigma$$

The stress at the bottom fibres of the slab due to the application of the resultant force 'F' must be equal to 4.2 MPa per mm width along x axis. The value of the stress σ required to prevent the in-plane dispalcement of the slab can be calculated as follows:

$$4.2\ MPa = \frac{F}{60\times1} + \frac{F\times20}{1\times(60^2/6)} = \frac{15\,\sigma}{60\times1} + \frac{15\,\sigma\times20}{1\times(60^2/6)} = 0.75\,\sigma$$

$$\sigma = \frac{4.2}{0.75} = 5.6\ MPa$$

The value of the resultant force 'F' (or the restraining force) due to the σ stress is calculated as follows:

$$F = 5.6\,MPa \times \frac{30\,mm}{2} = 84\,N\ per\ mm\ of\ width$$

The force F is located at a distance of $\frac{2}{3}\times\frac{h}{2}$ (20 mm) from the neutral axis of the slab (see Figure 3-9). Thus, a negative bending moment equal to the product of this force times the 20 mm will be obtained and this moment will oppose the positive bending moment

produced by the concentrated load. In other words, by restraining the in-plane displacement of slabs, an effect similar to prestressing is generated. This effect is activated due to the application of the concentrated load and is caused by restraining the in-plane displacement of the slab.

3-8 Illustrative Example (2)

Consider a case of a simply supported and infinitely long reinforced slab subjected to a linear load of 78 N/mm applied at midspan as shown in Figure 3-10. The span and the depth of this slab are 2400 mm and 100 mm respectively. To calculate the in-plane displacement due to the applied load, a strip of this slab will be considered. Assume the width of this strip is 200 mm. By considering a strip taken from this slab, this problem, actually, will be reduced to the case of a simply supported beam having cross section dimensions of width and depth equal to 200 mm and 100 mm respectively.

Solution

It is known that the value of the maximum bending moment at midspan of this beam is equal to $\frac{P \times a}{4}$ and the value of the slope of the angle θ at the supports is equal to $\frac{P \times a^2}{16 \times EI}$. Referring to Figure 3-6 and

Figure 3-9, and considering the slope of the angle θ is so small that it is approximately equal to its tangent, then the value of the in-plane displacement 'u' that is given by Eq. (3-12) can be obtained as follows:

$$u = \frac{h}{2} \times \frac{P \times a^2}{16 \times EI}$$

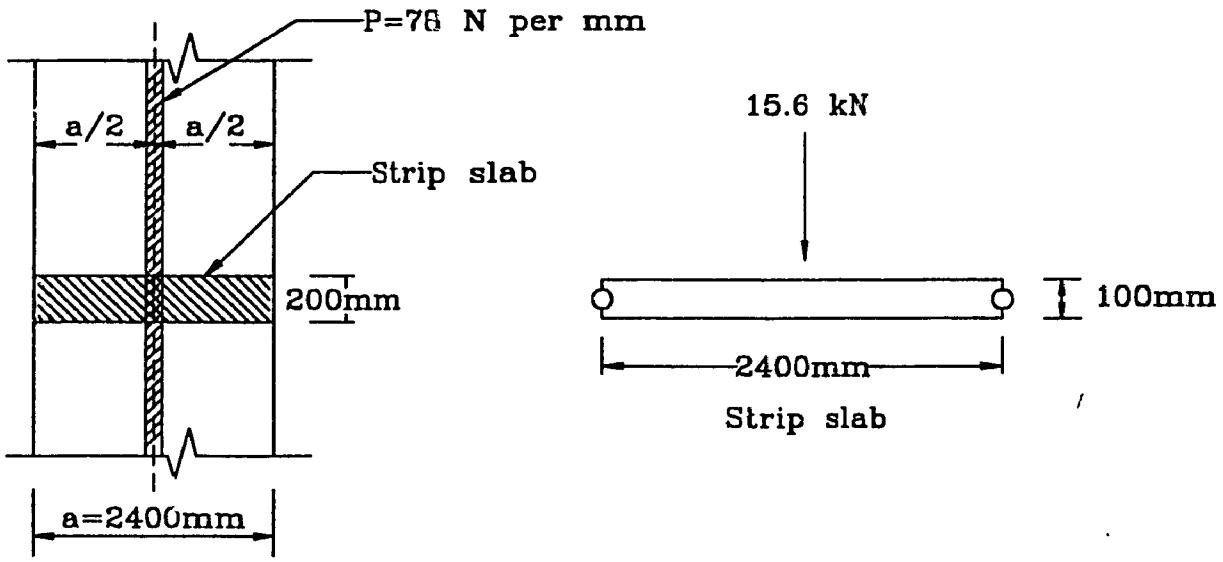

Figure 3-10 Infinitely long slab subjected to linear load at midspan

As has been mentioned earlier, the restraining force 'F' that needs to put back the value of the in-plane displacement to zero can be obtained through the following steps.

The value of the strain ε_x due the in-plane displacement is

$$\varepsilon_x = \frac{u}{a/2} = \frac{h}{2} \times \frac{P \times a^2}{16 \times EI} \times \frac{2}{a} = \frac{P \times a \times h}{16 \times EI}$$

The value of the stresses due to this strain is calculated as follows:

$$= E \times \varepsilon_x = E \times \frac{P \times a \times h}{16 \times EI} = \frac{P \times a \times h}{16 \times I}$$

where $I = \frac{h^3 \times b}{12}$

$$\text{i.e. } E \times \varepsilon_x = \frac{3 \times P \times a}{4 \times h^2 \times b} = \frac{3 \times 15.6 \times 10^3 \times 2400}{4 \times 100^2 \times 200} = 14.04 \ MPa$$

The distribution of the stress σ required to put this strain to zero is shown in Figure 3-9. The resultant force 'F' due to the stress σ is calculated as follows:

$$F = \sigma \times \frac{30\,mm}{2} \times 200 = 3000\,\sigma$$

The stress results at the bottom fibres of the slab due to the application of the resultant force 'F' must be equal to 14.04 MPa. The value of the stress σ required to prevent the in-plane dispalcement of the strip slab can be calculated as follows:

$$4.04\ MPa = \frac{F}{b \times h} \times \frac{F \times 20}{b \times (h^2/6)} = \frac{3000\sigma}{200 \times 100} \times \frac{3000\sigma \times 20}{200 \times (100^2/6)} = 0.33\,\sigma$$

$$\text{i.e } \sigma = 42.55 \ MPa$$

As shown in Figure 3-9, the value of the restraining force 'F' can be obtained as follows:

$$\text{i.e. } F = 3000\,\sigma = 127.64 \times 10^3\ N = 127.64\ kN$$

The above expression presents the value of the horizontal reaction 'F' that is required to prevent the horizontal displacement of the strip slab. The above restraining force 'F' is calculated using elastic theory with the angle of the slope of the elastic curve at the support. As will be shown in Chapter 5, the failure load of this strip slab, calculated by plastic analysis, is actually 15.6 kN as given in this example. Also, the value of the restraining force 'F' that will be obtained using plastic analysis is much greater than the above obtained value.

Chapter 4

Experimental Program

4-1 Objectives of the Research

The purpose of this research is to achieve the following objectives:

1- To better understand the behaviour of concrete slabs subjected to concentrated loads, taking into account the effects of horizontally restrained boundaries.

2- To develop a method of analysis, based on the theory of plasticity, which takes into account the effects of the in-plane restraints on the behaviour of strip slabs and square slabs subjected to central concentrated loads.

4-2 The Experimental Program

The experimental program was designed to test simply supported strips of concrete slabs with and without horizontally restrained boundaries. The tested slabs were subjected to central concentrated loads.

The choice of strip slabs for testing was based on the fact that they

simulate, to some degree, one way slabs and shallow beams. Also, they may provide guidance in understanding the behaviour of two way slabs restrained against in-plane displacements and in preparing for future tests for two way slabs.

The experimental tests were carried out on two similar series of slabs. The results of the first series were examined and evaluated, and, accordingly, some modifications were introduced to the tests of the second series.

4-3 Description of the Slabs and Boundary Conditions

The test program included twelve concrete slabs divided into two series, each series consisting of six slabs. All twelve slabs had the nominal cross section dimensions of 100 mm depth by 200 mm width. The spans of the slabs of the first series were equal to 2400 mm. Due to modifications implanted on the set-up for the tests of the second series, spans of 2421 mm were used for the horizontally restrained slabs and spans of 2400 mm for the horizontally non-restrained slabs. Each series consisted of the following type of slabs:

1- Two reinforced concrete slabs were tested as simply supported horizontally non-restrained as well as having heavy reinforcement reaching the balanced condition (maximum reinforcement ratio). Rollers were placed at supports. The purpose of testing these strip slabs was to compare their carrying capacity to the carrying capacity of the horizontally restrained strip slabs with minimum reinforcement

ratio.

2- Four concrete strip slabs were tested with their boundaries restrained against horizontal displacement and with minimum reinforcement ratio (approximately 0.3%) as required by the Canadian code[57]. The purpose of this reinforcement was to prevent the sudden collapse of slabs at failure stage.

The details of the tested slabs are shown in Figure 4-1 and Figure 4-2. Additional reinforcements were provided to the extremities of the slabs to prevent them from early collapse during the tests. The details of the reinforcement at the extremities are shown in Figure 4-1 and Figure 4-4. In Figure 4-2, the steel hangers used to carry the slab during transportation are shown in the details of the cross-sections d-d and e-e. The details of the wood forms are shown in Figure 4-3.

4-4 Testing Set-up

The general arrangement for the tests is shown in Figure 4-5 and Figure 4-10. Figure 4-6 and Figure 4-10 show how the central concentrated load is applied. The details of the support for strip slabs with restrained in-plane displacements, for the first series of tests, are shown in Figure 4-7 and Figure 4-11. The details at the support for the second series of tests are shown in Figure 4-8 and Figure 4-12. As can be seen in Figure 4-8 and Figure 4-12, a rectangular steel bar was placed

under the extremity of the strip slabs to reduce the support area. A special mortar[58], which has early high compression strength, was used to create the horizontal restraint as shown in Figure 4-11 and Figure 4-12. The details of the end conditions for simply supported horizontally non-restrained slabs are shown in Figure 4-9 and Figure 4-13. All the tested strip slabs are shown in Figure 4-14.

4-5 Material Testing

The strength of the concrete, steel bars and mortar was tested, during this experimental program, as follows:

1- Specimens of concrete cylinders having a diameter of 76.2 mm (3 inches) and a height of 152.4 mm (6 inches) were taken during the casting of the concrete slabs (cylinders available in the structural laboratory). The total number of the tested cylinders was 36, with 18 cylinders tested for each series. The compression strength of three cylinders was tested simultaneously with each slab test to measure the average compression strength of the concrete of the slab. Concrete samples are shown in Figure 4-15.

2- The tension strength of the steel bars was tested and the load-deformation curve for every test was plotted. A total of 18 tests were carried out on the steel bars, 9 tests for the steel batch of each

series. Three specimens were tested for each bar diameter. The bar diameters are 6 mm, 11 mm and 16 mm, corresponding to bar numbers 6M, 10M and 15M.

3- Three mortar cylinders were tested simultaneously with each test of a horizontally restrained slab to measure the average compression strength of the mortar. The mortar tests were carried out during the two series of tests. Error occurred during testing the mortar cylinders for slab number S10. Therefore, the mortar strength for S10 was eliminated. Mortar samples are shown in Figure 4-15.

The results of the average compression strength of the concrete cylinders are presented in Table 4-1 The results of all compression tests (three tests for each slab) are presented in Appendix A (Section A-2).

The results of the tests for the average tension strength 'f_y' of the steel are presented in Table 4-2. The graphs of the load-deformation curves that were obtained from the steel tests are given in Appendix A (Section A-4).

The results of the mortar compression strength tests are presented in Table 4-3. The results of all the mortar compression tests (three tests for each slab) are presented in Appendix A (Section A-2).

Table 4-1 The compression strength of the concrete

Test No.	Concrete strength f'_c MPa
S1	28.55
S2	31.88
S3	32.32
S4	33.23
S5	34.14
S6	32.58
S7	45.65
S8	37.55
S9	32.69
S10	37.65
S11	37.07
S12	38.60

Table 4-2 The results of the tension strength of the steel bars

	'f_y' for bars having diameter of 6 mm (MPa)	'f_y' for bars having diameter of 10 mm (MPa)	'f_y' for bars having diameter of 16 mm (MPa)
First series	504.40	535.16	441.12
Second series	456.24	536.33	370.50

Table 4-3 The compression strength of the mortar

Test No.	Mortar strength f'_{cm} MPa
S1	24.65
S2	31.60
S3	35.44
S4	31.86
S9	33.12
S10	-
S11	25.10
S12	32.99

4-6 The Test Results

The central concentrated load was applied in incremental sequences to each strip slab test. At each incremental load the value of the deflection at the center of the strip slab was recorded. A curve representing the applied load versus the deflection was plotted for each slab test. The values of the applied loads versus the deflections for all the tests are presented in Appendix A (Section A-3).

For the first test 'S1', after reaching the failure load, the slab was reloaded and subjected to another cycle of loading. However, the strip slab did not have sufficient stiffness to support additional load. For 'S1', the first cycle of loading was recorded and the second cycle has

been eliminated.

The load-deflection curves for tests 'S1' through 'S4' are shown in Figure 4-16 (horizontally restrained slabs of the first series). Figure 4-17 shows the load-deflection curves for the two simply supported horizontally non-restrained slabs of the first series. Figure 4-18 shows all the curves of the slabs of the first series. The results of the simply supported horizontally non-restrained slabs for the second series are presented in Figure 4-19. The results of the horizontally restrained slabs are presented in Figure 4-20. The results of all the tests of the second series are presented in Figure 4-21. The results of all the tests for strip slabs having horizontally restrained boundaries are presented in Figure 4-22. The results of all the tests for horizontally non-restrained strip slabs are shown in Figure 4-23. A summary of the results of the experimental program is presented in Table 4-4 and Table 4-5. The load-deflection curve for each slab test is presented in Appendix A (Section A-3, Figure A-1 through Figure A-12).

4-7 Behavioral Observations and the Sequence of Cracking

In general, the behavior of the horizontally restrained and horizontally non-restrained strip slabs differed at different load levels. The crack patterns and the sequences of cracking were different.

For horizontally non-restrained strip slabs, the crack patterns and sequence of cracking at failure load are shown in Figure 4-24. For these strip slabs, increasing the load resulted in one or two thin cracks on the bottom fibers at mid-span. Increasing the load further, the number of cracks progressed from the centers of the strip slabs toward the supports. As well, the width of the previously created cracks increased. Also, the directions of the cracks from the very bottom fibers to the tension reinforcement were vertical. The tips of the cracks changed direction at the level of the tension reinforcement and penetrated toward the point of application of the concentrated load.

For horizontally restrained strip slabs, the crack patterns and sequence of cracking at different levels of loads are shown in Figure 4-25. For these strip slabs, at very low levels of loading, one or two cracks were initiated at the bottom fibers at mid-span. Increasing the load, the width of these cracks increased and they penetrated vertically toward the point of application of the concentrated loads up to the failure of the strip slabs. These cracks divided each horizontally restrained strip slab into two segments. Each strip slab behaved as if it was composed of two members separated by the cracks at mid-span on the bottom fibers. These two members were connected at mid-span on the top fibers through the compression zone.

4-8 Discussion of the Load-Deflection Curves

The load-deflection curves represent the deflection behavior of the tested strip slabs at different levels of loading. As shown in these curves, the deflections of the horizontally restrained strip slabs before and after the failure loads differ from the deflections of the horizontally non-restrained strip slabs. Also, the failure loads of the horizontally restrained strip slabs of the first series were, in general, higher than the failure loads of the horizontally restrained strip slabs of the second series.

A comparison of load-deflection curves of the first series for horizontally and non-horizontally restrained strip slabs indicates that before reaching the failure loads horizontally restrained strip slabs had less deflection than horizontally non-restrained strip slabs. For example, a comparison of the load deflection curves of Figure 4-16 and 4-17 indicates that at a load of 15 kN the horizontally restrained strip slabs had, on average, a deflection of about 8 mm and the horizontally non-restrained strip slabs had, on average, a deflection of about 12 mm. Also, a comparison of the deflections of the strip slabs of the second series indicates similar results. For example, a comparison of the load deflection curves of Figure 4-19 and 4-20 indicates that at a load of 12.5 kN the horizontally restrained strip slabs had, on average, a deflection of

about 8 mm and the horizontally non-restrained strip slabs had, on average, a deflection of about 11 mm.

After reaching the failure loads, the horizontally restrained strip slabs had a very rapid decrease in their carrying capacities. However, the horizontally non-restrained strip slabs had a slow decrease in their carrying capacities. In the horizontally restrained strip slabs, the amount of reinforcement was minimum. Therefore, they did not have enough stiffness after reaching the failure conditions to sustain further load. In the horizontally non-restrained strip slabs, the amount of reinforcement was maximum. Therefore, they were able to sustain further loads after reaching the failure conditions.

At more advanced levels of deflections, the concrete was completely crushed, leaving only the reinforcement to act as a tensile net. For all the strip slabs, this stage is indicated by the horizontal plateau of the load-deflection curves, as shown in Figure 4-18 and Figure 4-21. The horizontal plateaus of the horizontally non-restrained strip slabs had higher values due to the very high amount of reinforcement in these strips. Due to the presence of a very little amount of reinforcement in the horizontally restrained strips, the horizontal plateaus of their load-deflection curves had low values.

Table 4-4 Experimental results for horizontally restrained strip slabs

Test No	Span mm	Dimensions of cross section mm x mm	Age of concrete Days	Concrete strength f_c' MPa	Failure load kN	Deflection at failure mm	Age of mortar Days	Mortar strength MPa
S1	2400	104 x 203	29	28.55	21.97	23.36	1	24.65
S2	2400	107 x 203	39	31.88	28.15	30.89	4	31.60
S3	2400	112 x 203	46	32.32	23.31	29.05	3	35.44
S4	2400	117 x 203	61	33.23	35.59	29.62	7	31.86
S9	2421	116 x 203	50	32.69	25.73	29.27	7	33.12
S10	2421	114 x 203	63	37.65	22.91	28.87	-	-
S11	2421	111 x 203	72	37.07	23.13	27.83	7	25.10
S12	2421	106 x 203	105	38.60	21.91	29.04	7	32.99

Table 4-5 Experimental results for simply supported horizontally non-restrained strip slabs

Test No	Span mm	Dimensions of cross section mm x mm	Age of concrete Days	Concrete strength f_c' MPa	Failure load kN	Deflection at failure mm
S5	2400	117 x 203	81	34.14	36.92	34.69
S6	2400	113 x 203	82	32.58	35.32	41.05
S7	2400	113 x 203	30	45.65	25.31	32.81
S8	2400	117 x 203	35	37.55	28.39	32.75

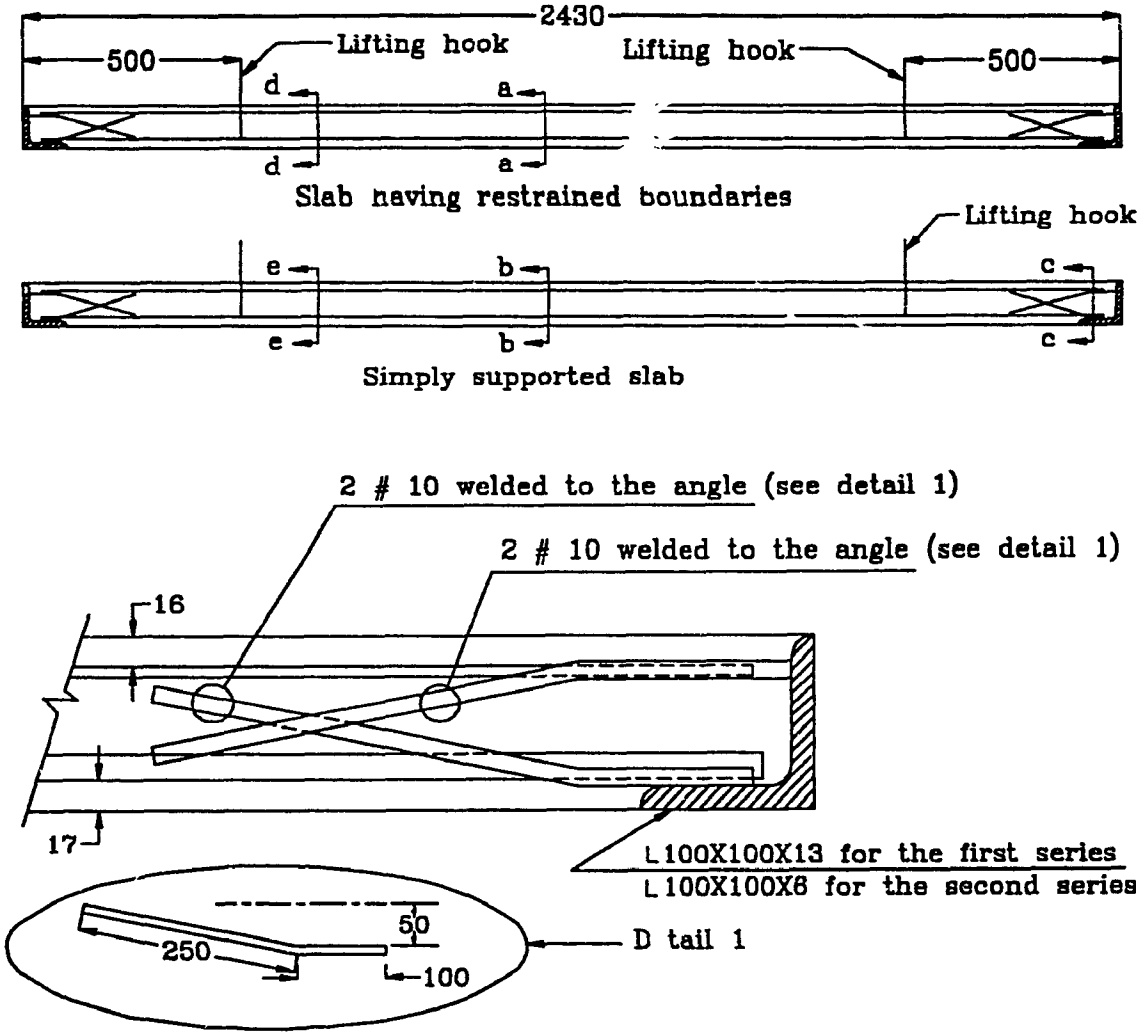

Figure 4-1 Details of the tested strip slabs (cross sections are shown in Figure 4-2)

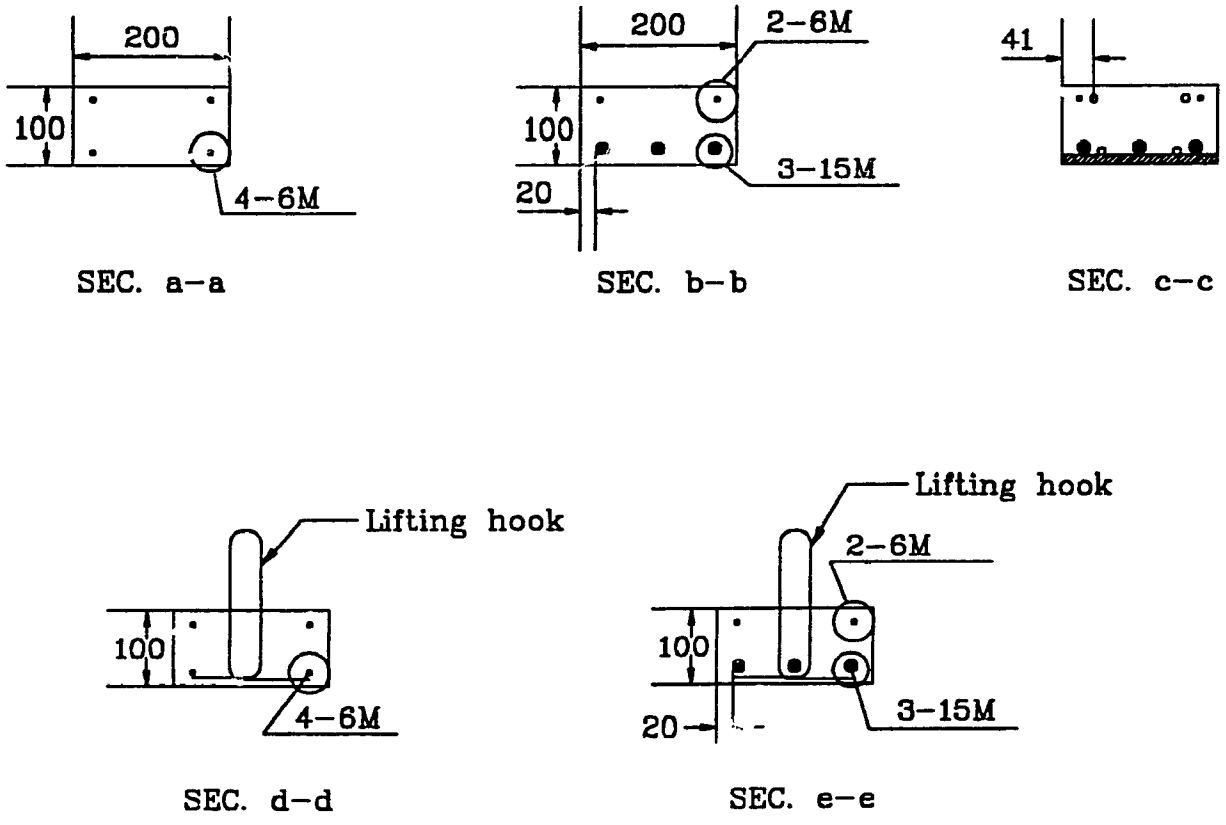

Figure 4-2 Cross-sections for the strip slabs

Figure 4-3 View of the wood form

Figure 4-4 Reinforcement used at the extremities of the strip slabs

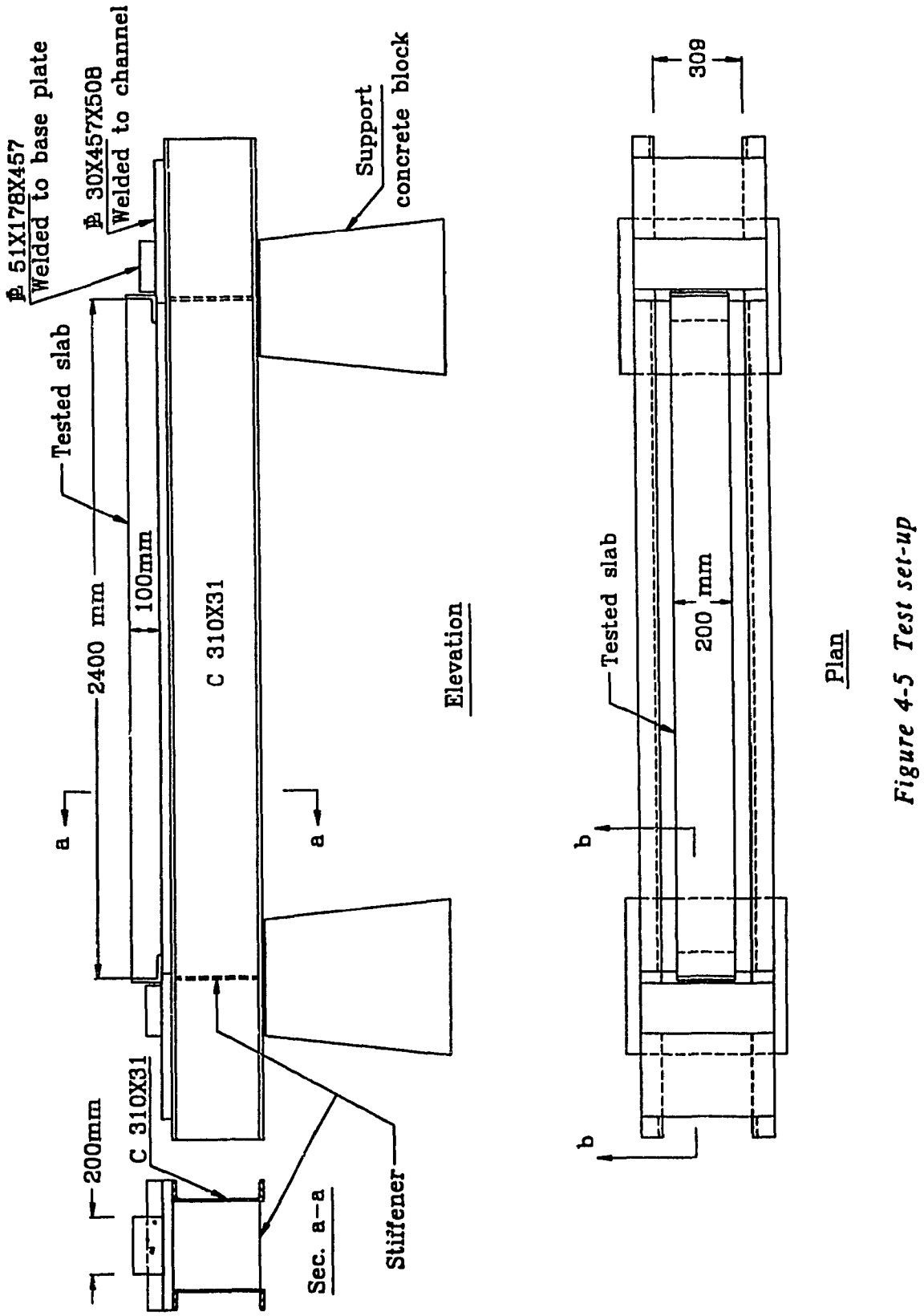

Figure 4-5 Test set-up

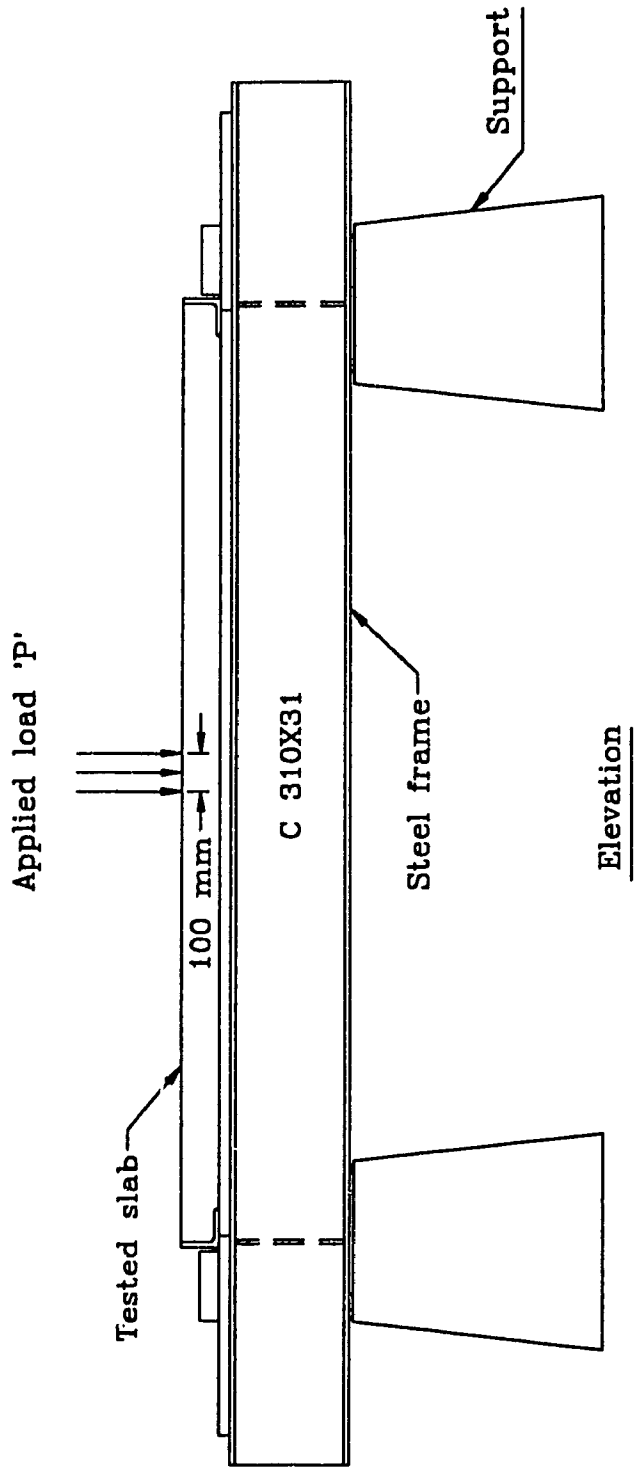

Figure 4-6 The location and the distribution of the applied load 'P'

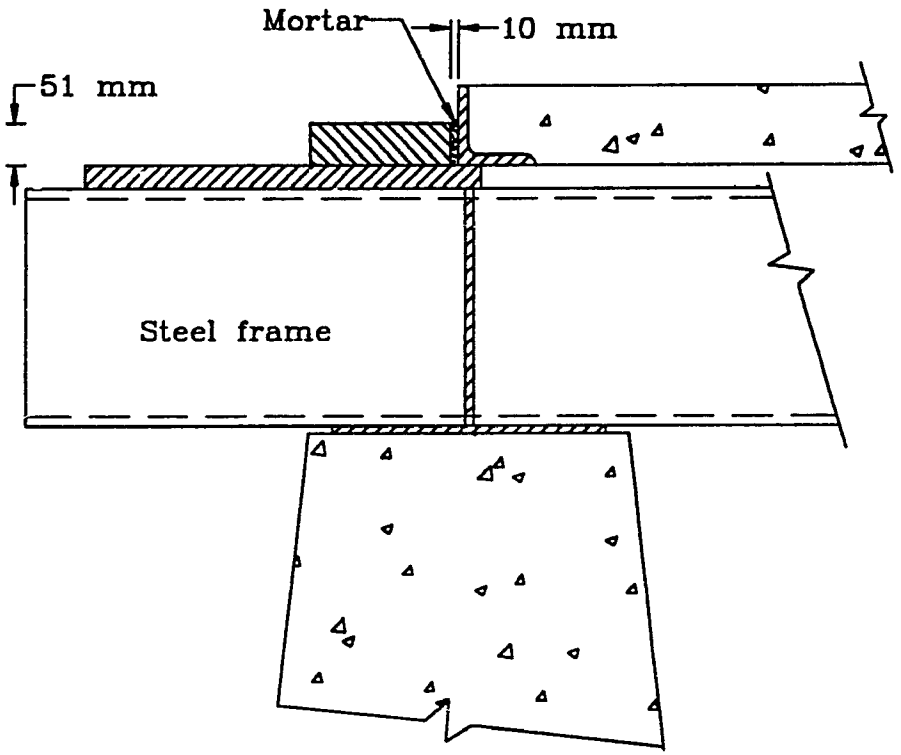

Sec. b–b (Fig. 4–5) restrained boundary for first series of tests

Figure 4-7 Details of the restrained boundary used in the first series of tests

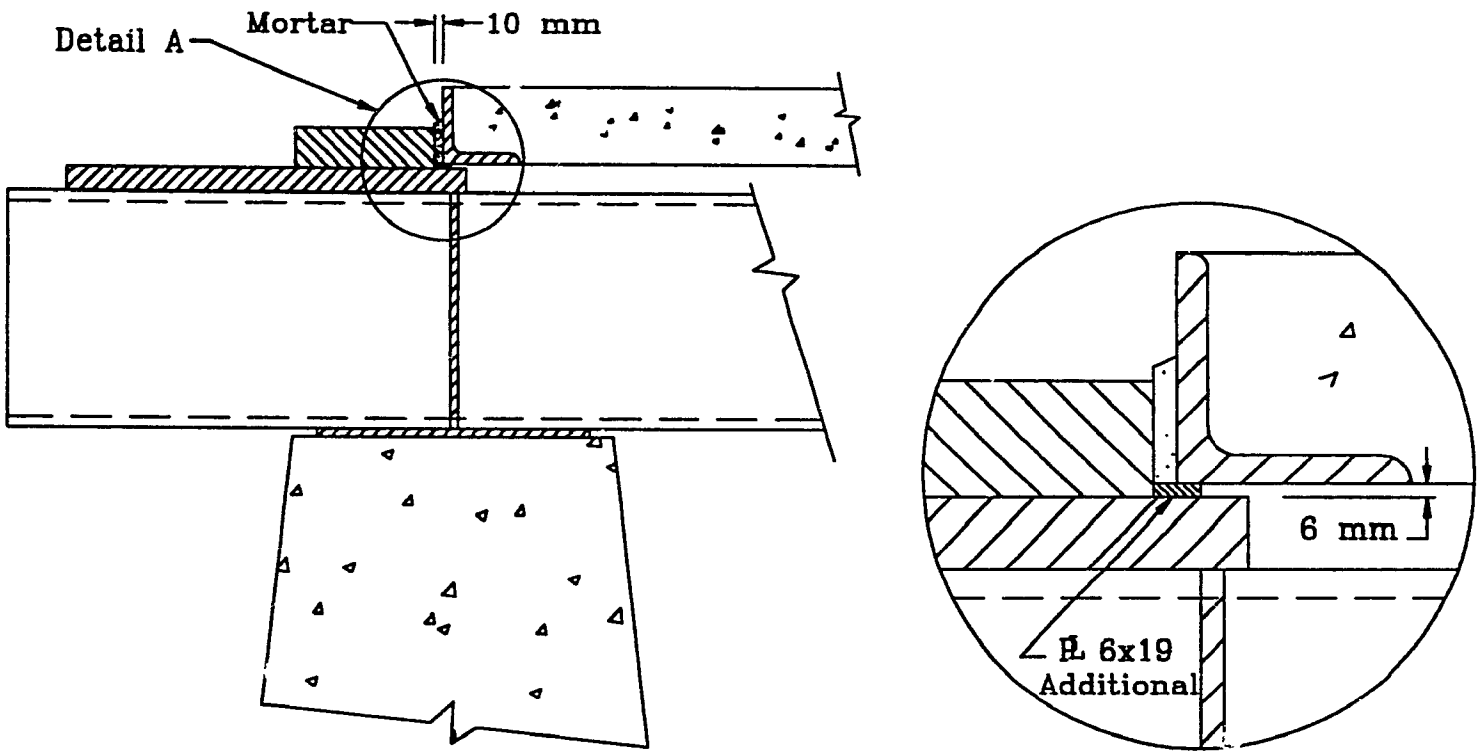

Sec. b–b (Fig. 4–5) restrained boundary for second series of tests

Detail A

Figure 4-8 Details of the restrained boundary used in the second series of tests

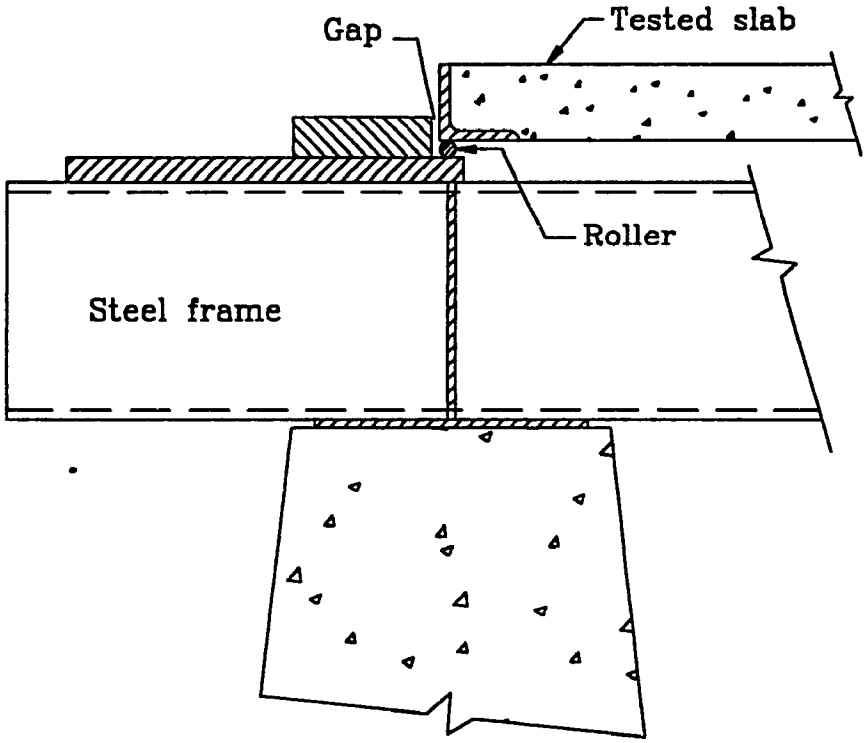

Sec. b–b (Fig. 4–5) simply supported boundary

Figure 4-9 Details of the simply supported boundary used in the tests

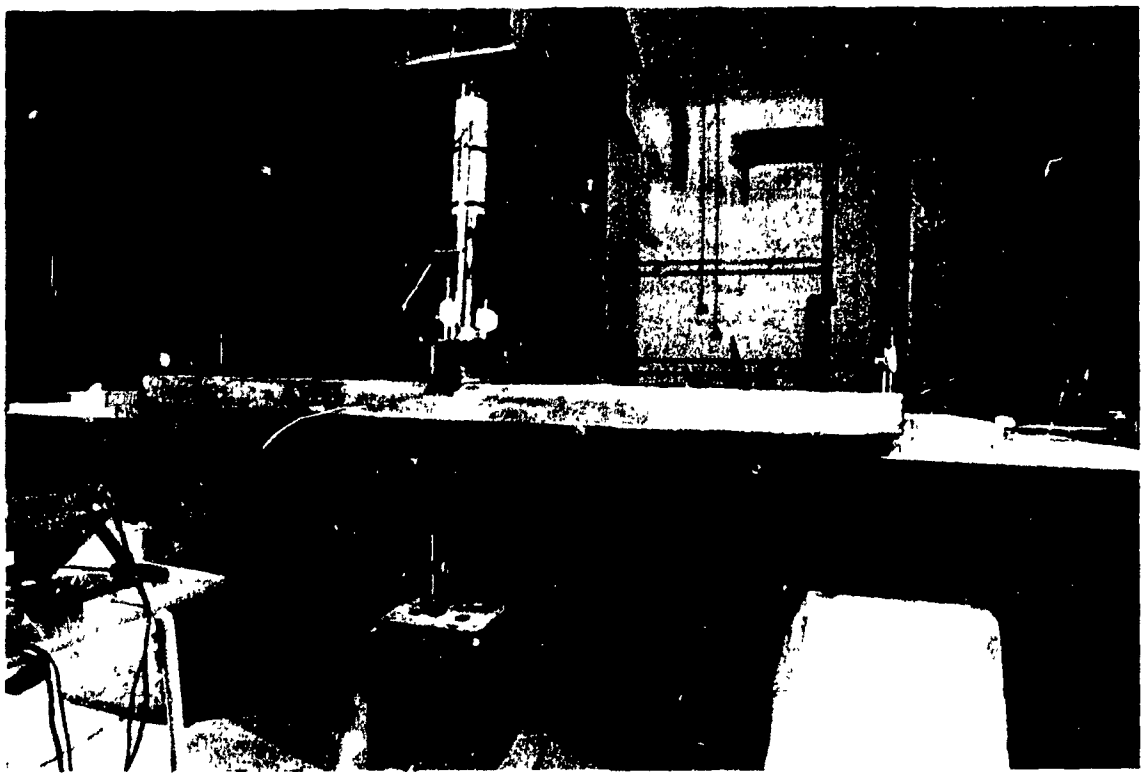

Figure 4-10 View of the test set-up

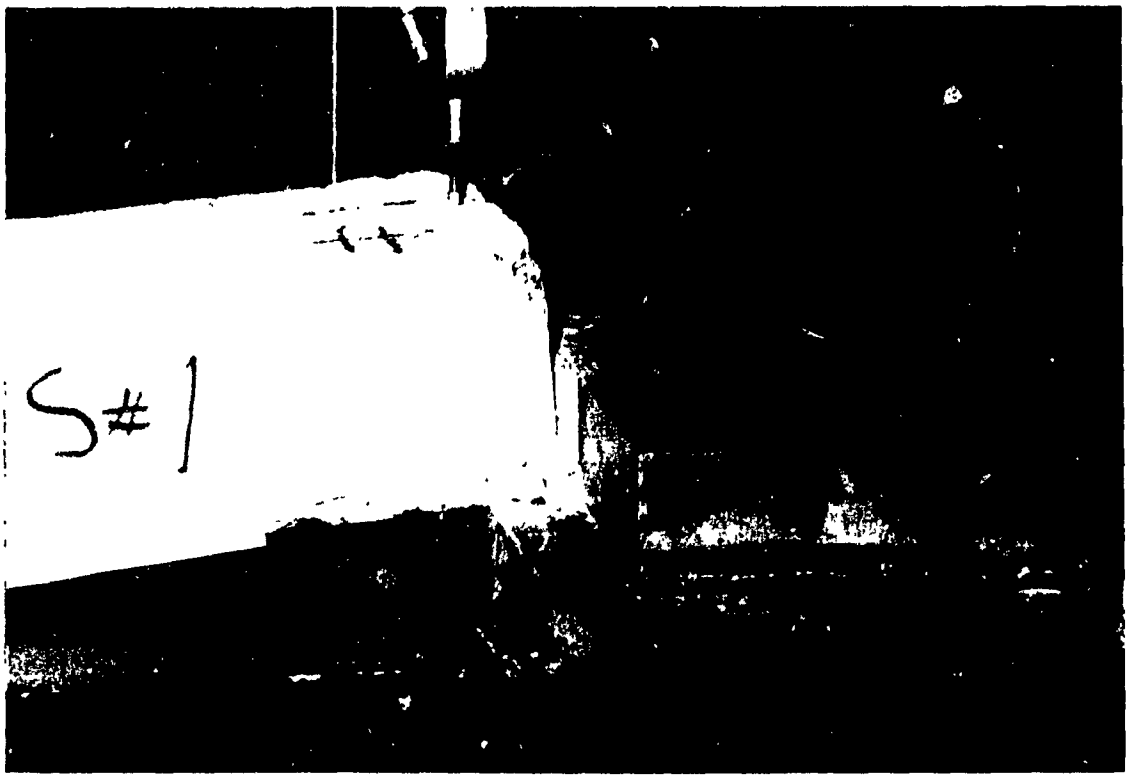

Figure 4-11 Horizontally restrained support for the first series

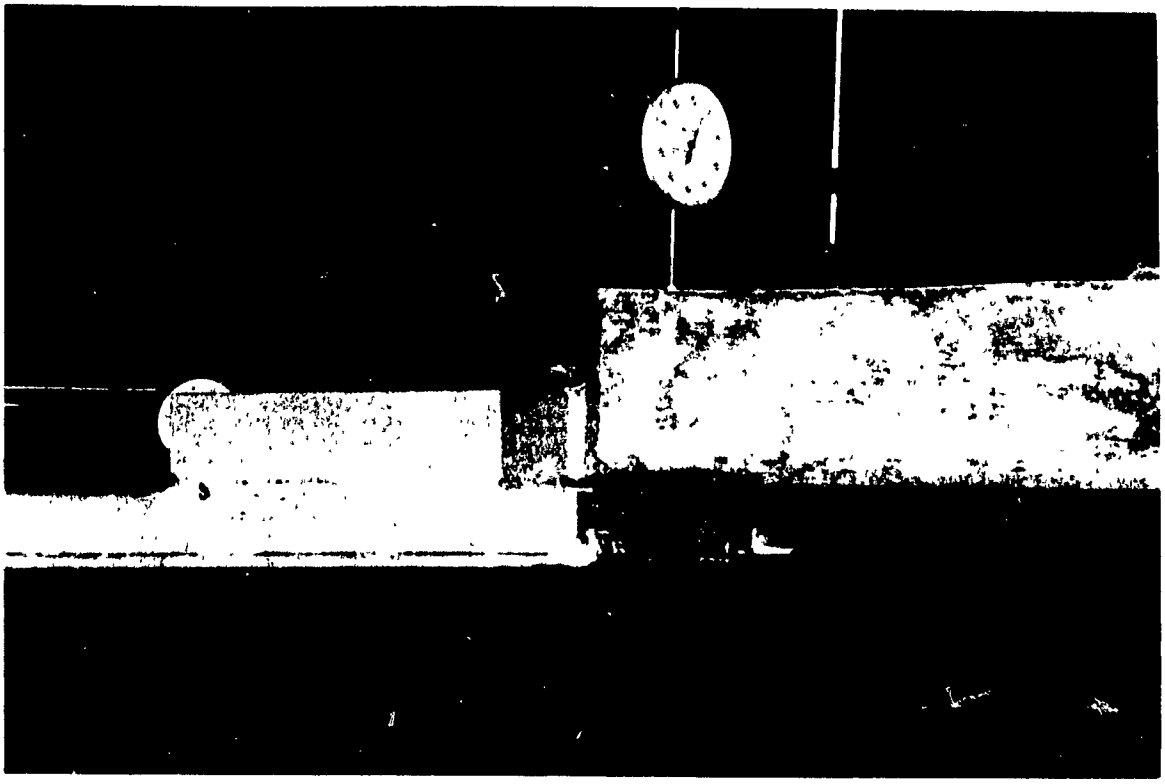

Figure 4-12 Horizontally restrained support for the second series

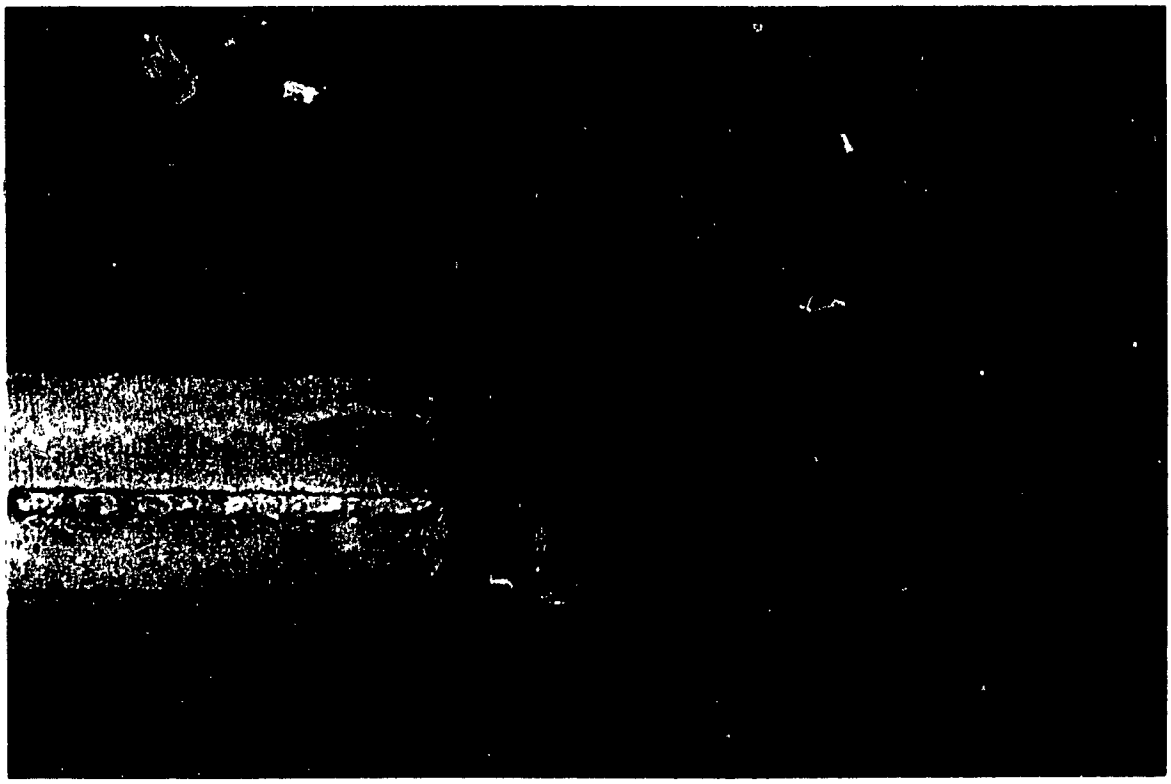

Figure 4-13 The simply supported end conditions

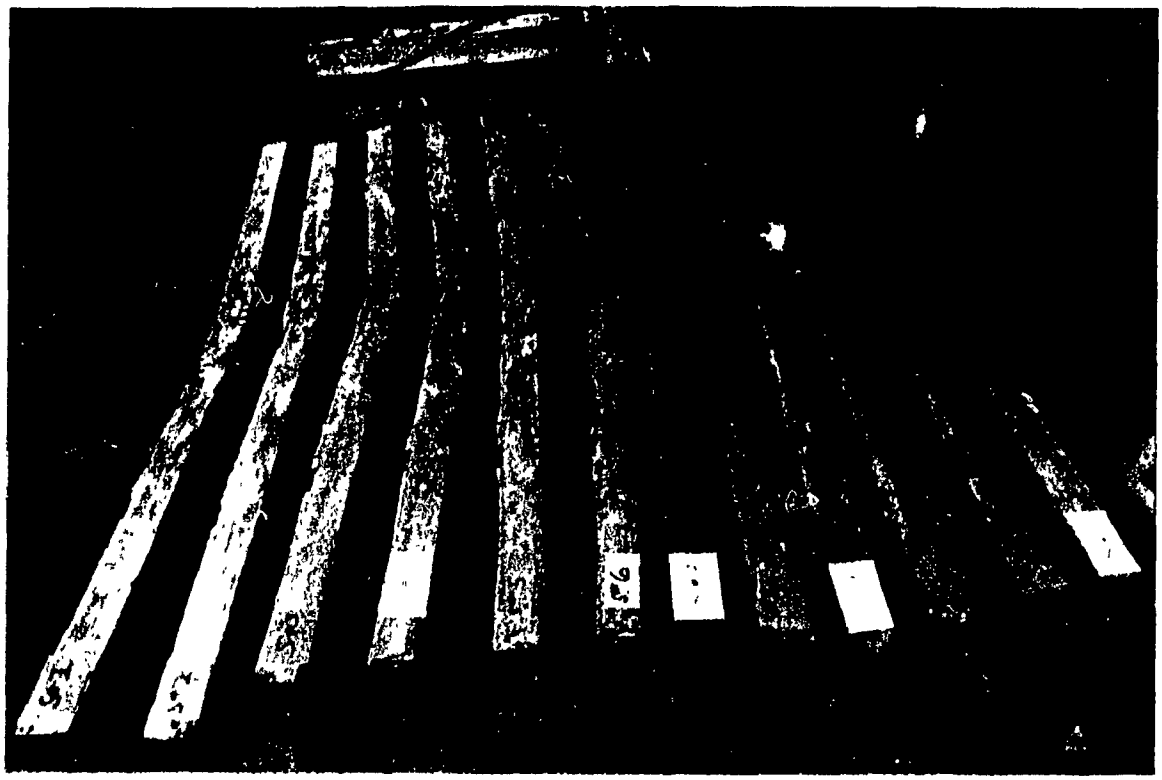

Figure 4-14 All the strip slabs after testing

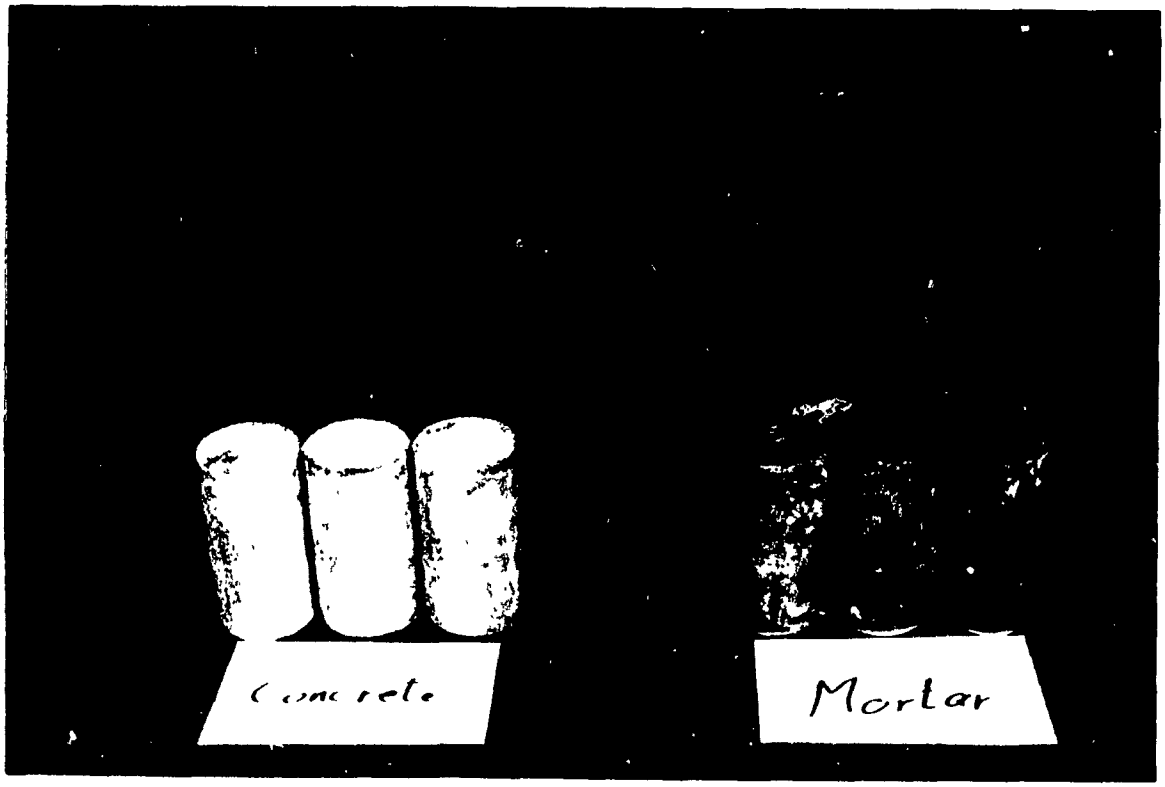

Figure 4-15 Concrete and mortar cylinders before the strength tests

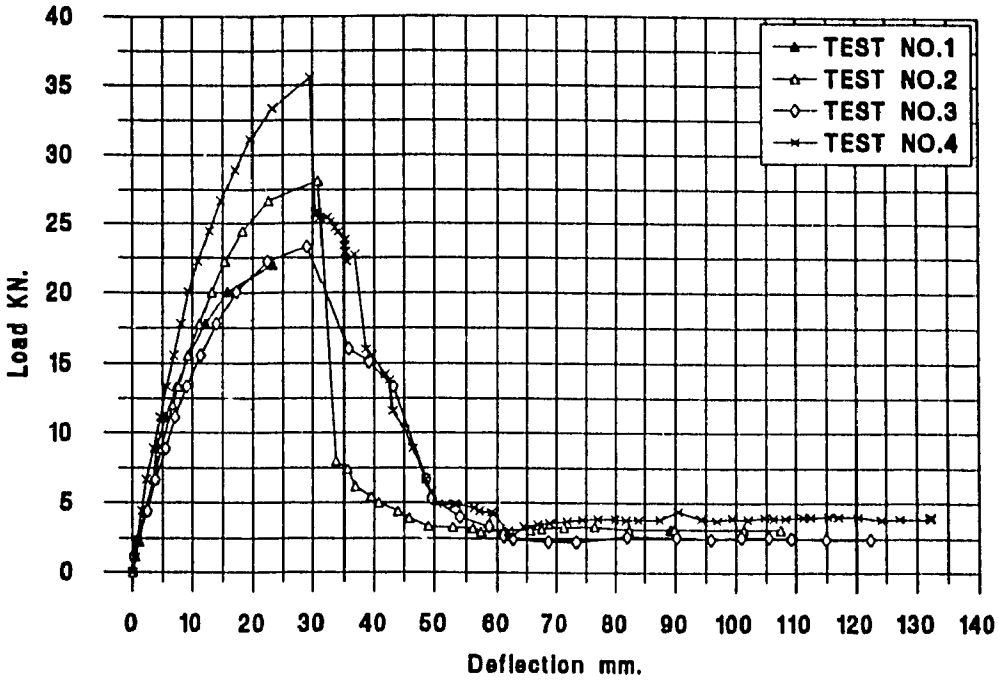

Figure 4-16 Load-deflection curves for tests of the first series (restrained boundaries)

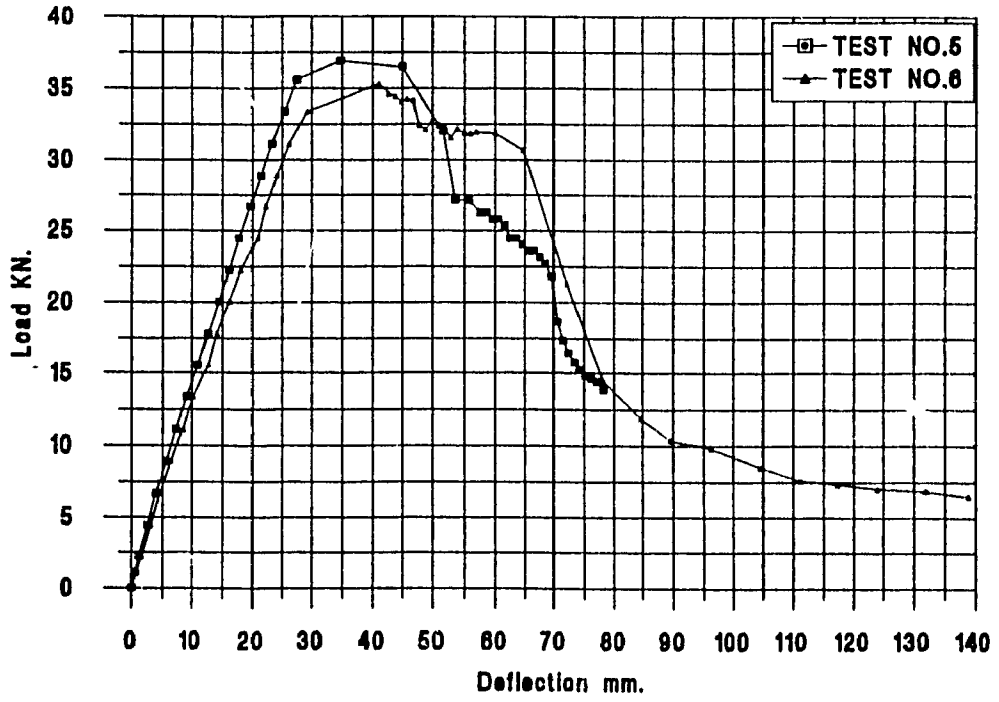

Figure 4-17 Load-deflection curves for tests of the first series (simply supported boundaries)

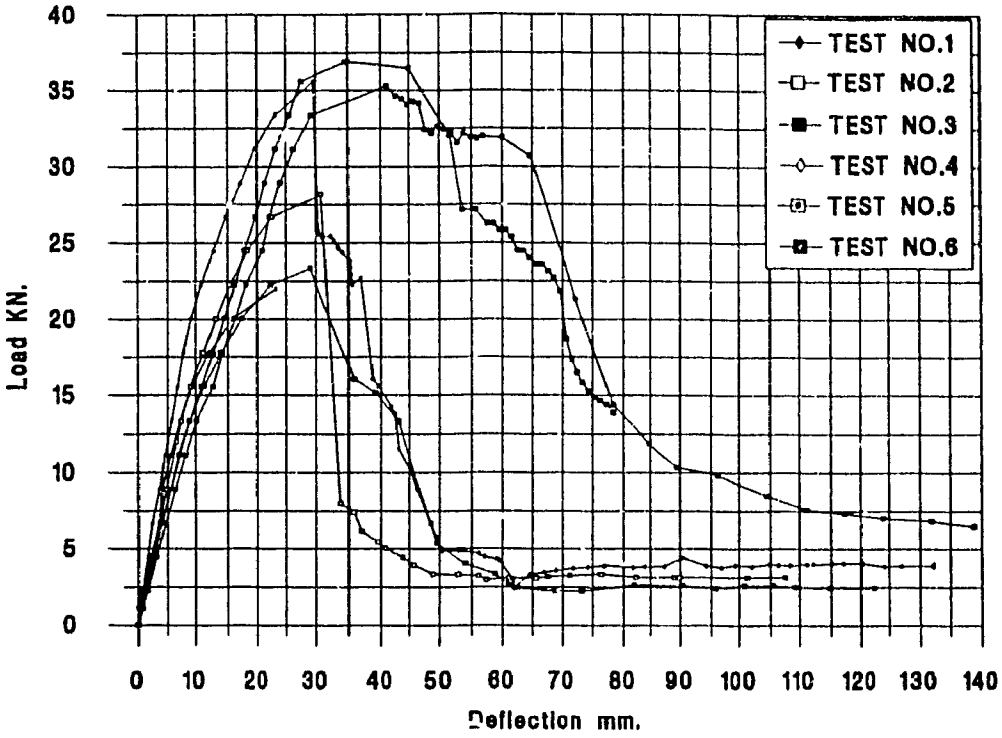

Figure 4-18 Load-deflection curves for all the tests of the first series

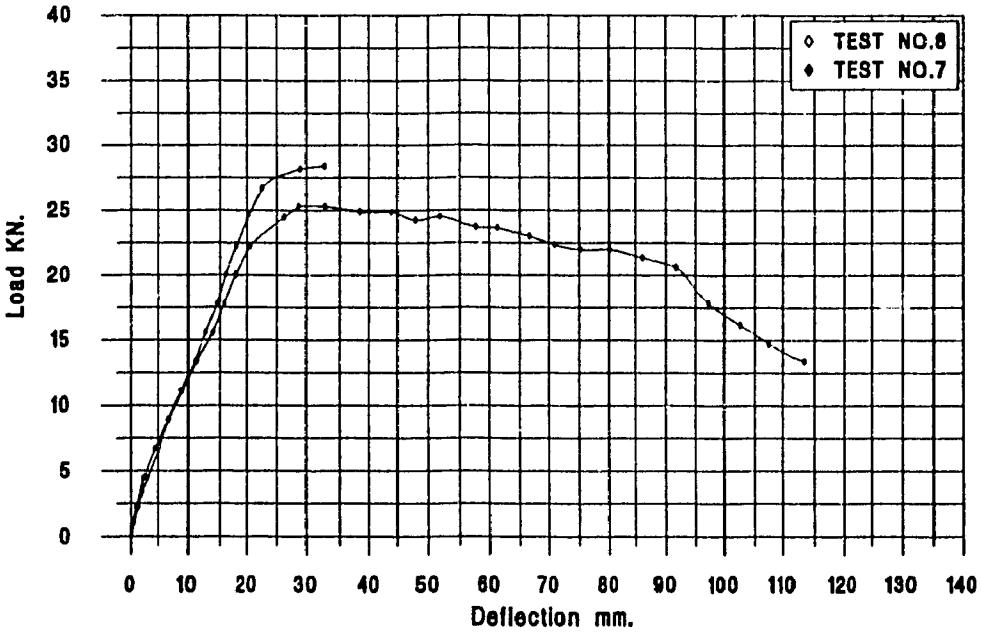

Figure 4-19 Load-deflection curves for tests of the second series (simply supported Horizontally non-restrained)

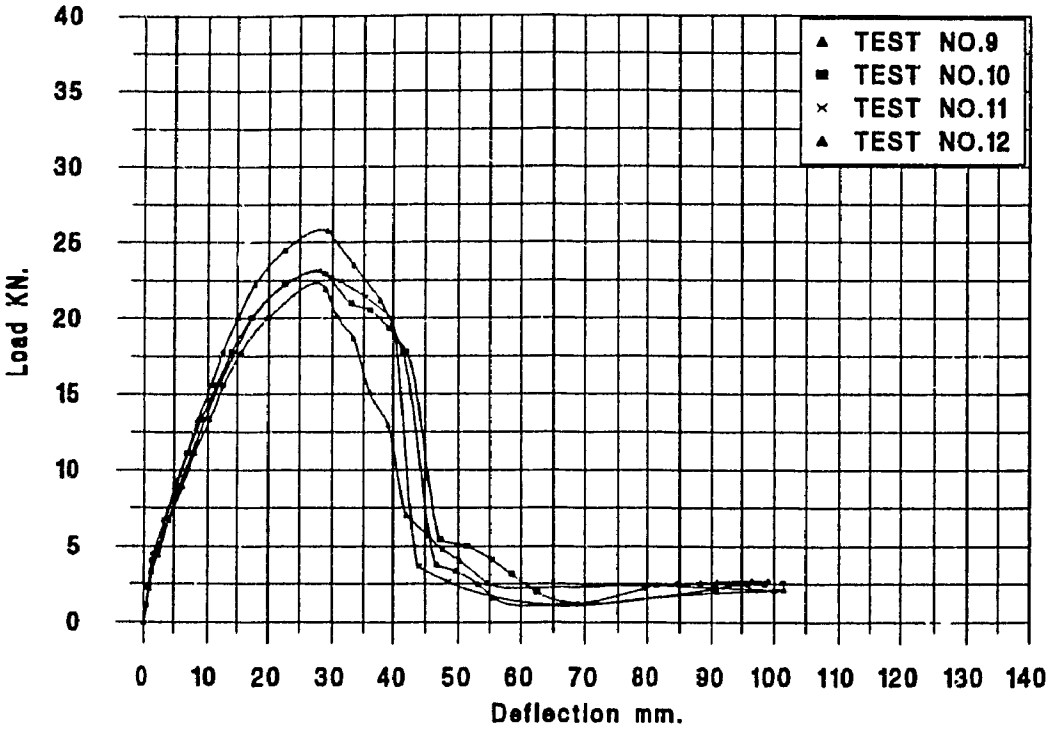

Figure 4-20 Load-deflection curves for tests of the second series (restrained boundaries)

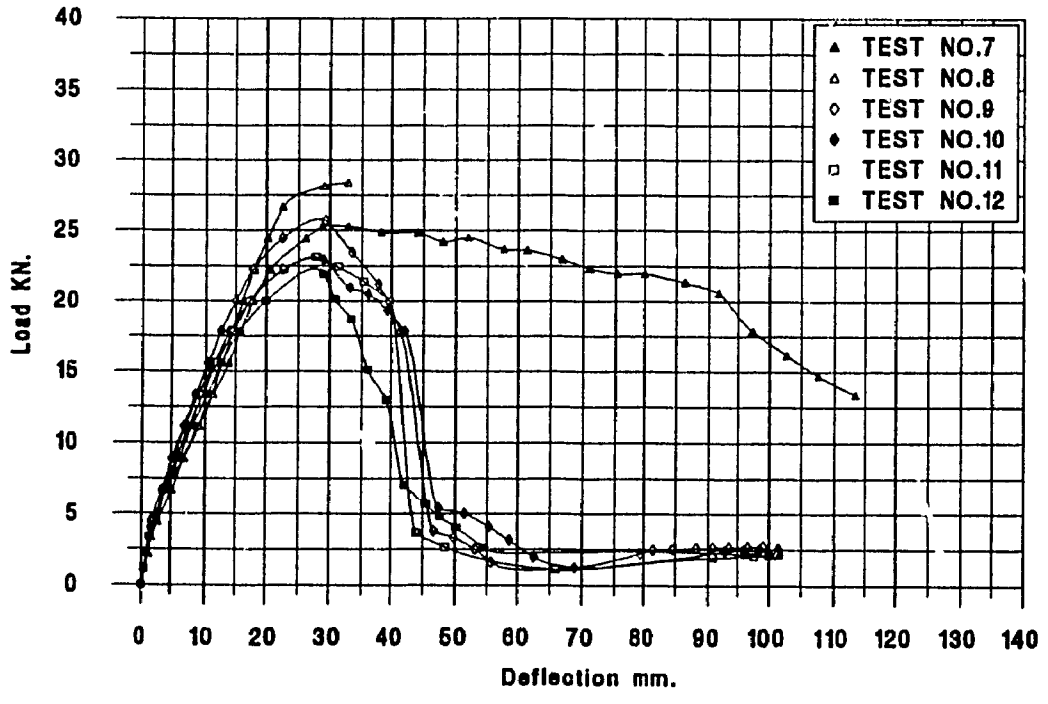

Figure 4-21 Load-deflection curves for all the tests of the second series

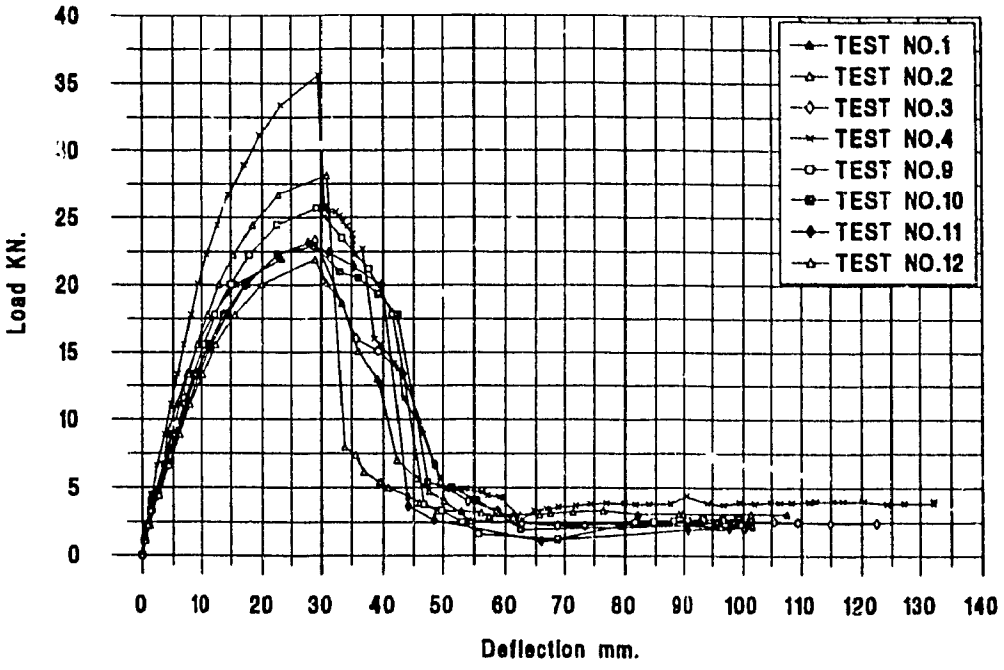

Figure 4-22 Load-deflection curves for all the tests of the strip slabs having restrained boundaries

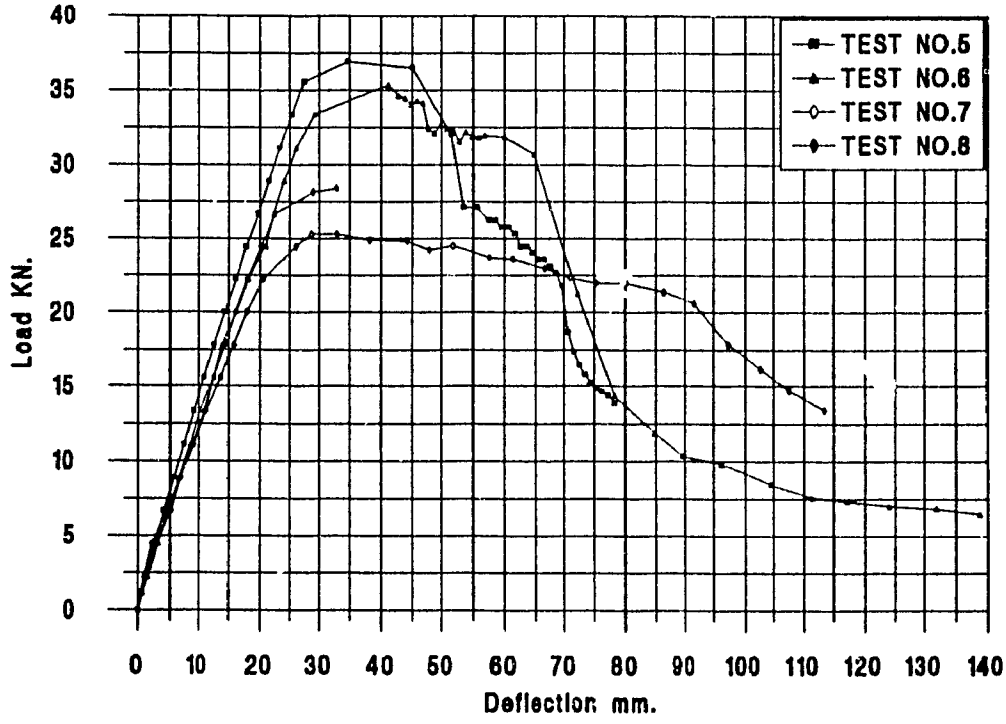

Figure 4-23 Load-deflection curves for all the tests of the simply supported strip slabs

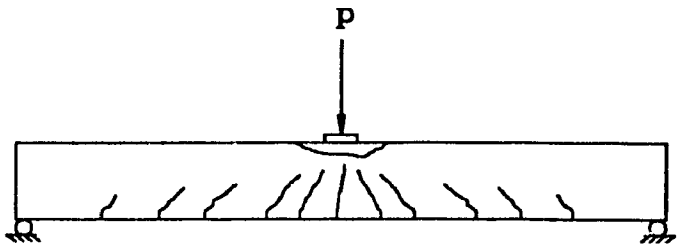

Figure 4-24 Patterns of cracks in a horizontally non-retrained strip slab (the strip was horizontally restrained at the point of application of the concentrated load)

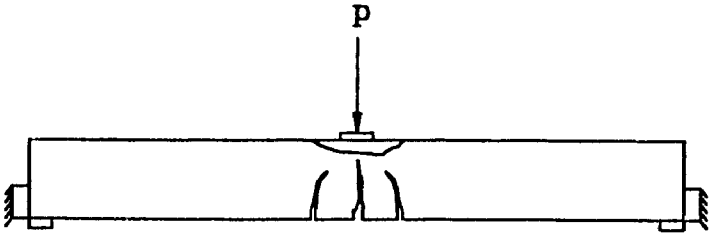

Figure 4-25 Patterns of cracks in a horizontally retrained strip slab

Chapter 5

Plastic Analysis of One Way Strip Slabs Horizontally Restrained Subjected to Central Concentrated Loads

5-1 Simply Supported Horizontally Restrained Strip Slabs

The problem of one way strip slabs subjected to a concentrated load, such the ones used in our experimental program, is similar to the problem of simply supported beams with or without horizontal restraints. In the many publications[59] dealing with this problem, the values of the reactions are given as shown in Figure 5-1.

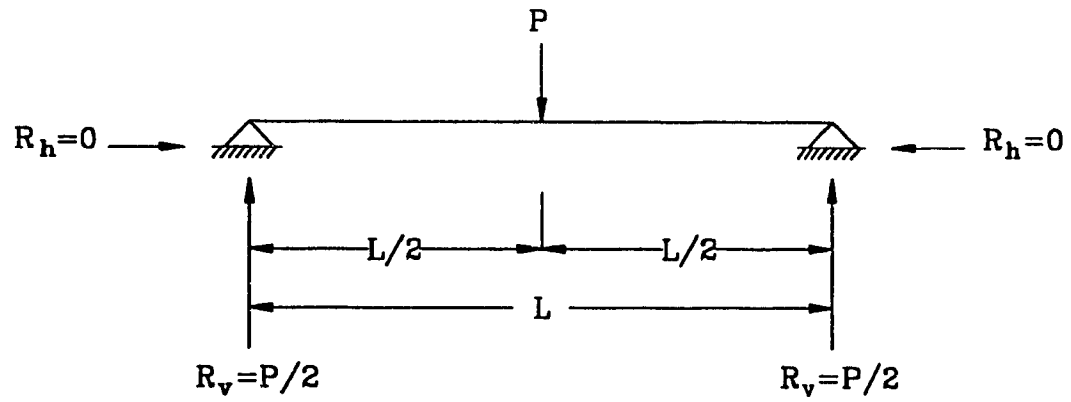

Figure 5-1 Simply supported beam with horizontally restrained boundary

The method[59] that is used to obtain the reactions shown in the above figure is one of the fundamental basics of mechanics of materials and has been widely used for reinforced concrete structures.

The accuracy of the obtained horizontal reactions has been altered after examining the results of our experimental program. The above solution ignores the horizontal reactions that act on the horizontally restrained concrete beam, which is opposite to the results of our laboratory tests that show the horizontal reactions have high values and great effects on the behavior of the concrete beams. Therefore, this problem should be looked at in a different way.

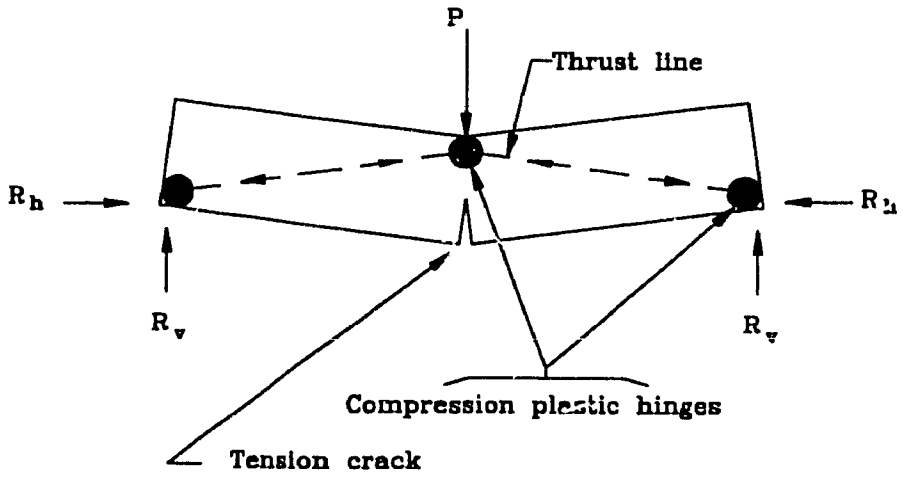

Figure 5-2 The formation of compression plastic hinges

Figure 5-2 shows a non-reinforced concrete strip slab or beam at the point of impending collapse under the application of a concentrated load at midspan. It also shows the tension crack and the plastic hinges. The plastic hinges are formed by the concrete which is on the verge of crushing. The beam is divided into two segments which are working as compression members. The compression forces are acting along the thrust lines, as shown in Figure 5-2 and Figure 5-3. The segments become members of a mechanism system, as shown in Figure 5-3.

To analyze the problem shown in Figure 5-3, the compression zones at some cross section need to be considered as shown in Figure 5-4.

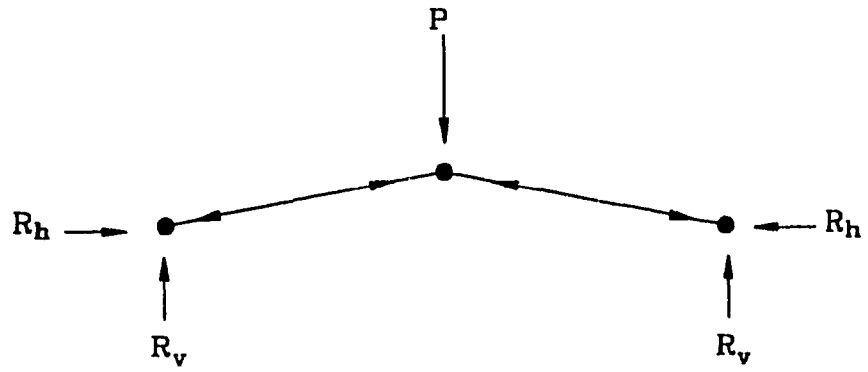

Figure 5-3 The mechanism of the strip slab at impending collapse

In Figure 5-4, the value of 'a' represents the depth of the compression zone and the value of 'w' represents the deflection at the center of the beam. The compression zone at the center of the span is located at the top fibers of the strip slab. At the extreme ends of the

span, the compression zone is located at the bottom fibers. The compression forces at section B-B must equal the compression forces at section C-C.

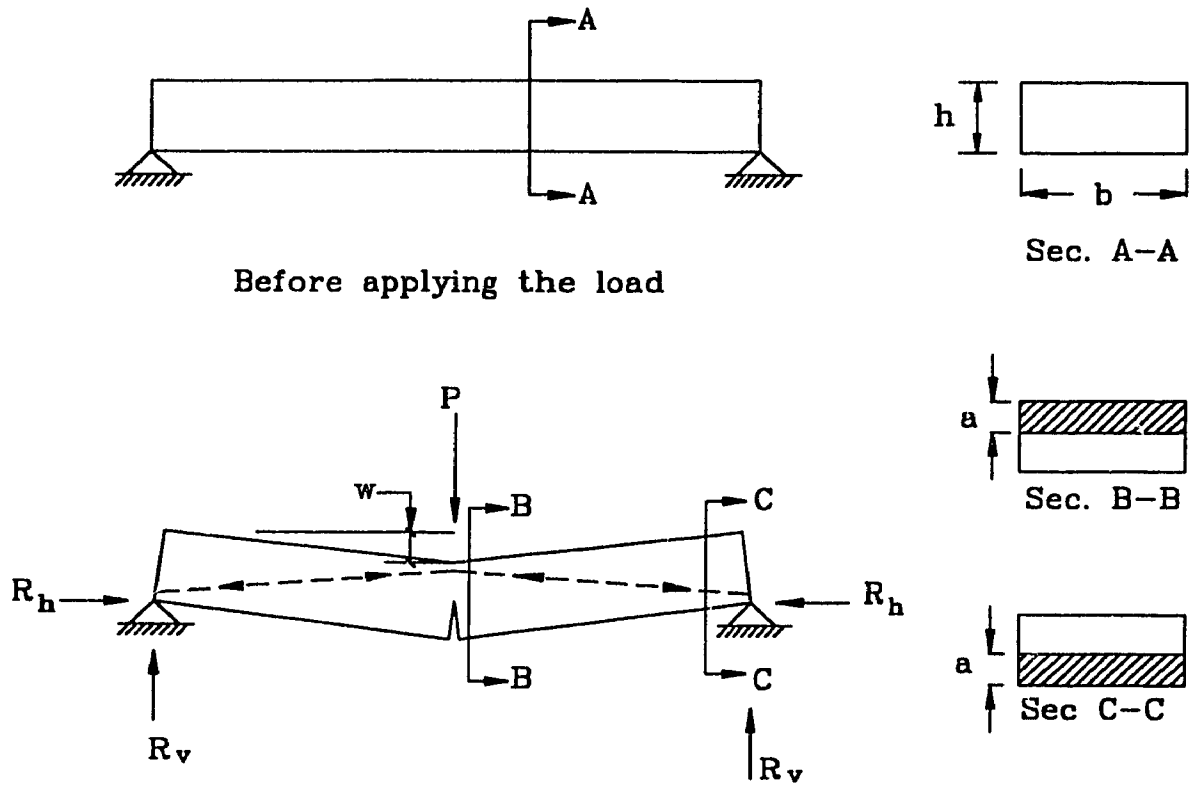

Figure 5-4 The locations of the compression zones

The internal and external horizontal forces, acting on a half beam segment of this system, are forming the resisting couple of the beam as shown in Figure 5-5. The maximum bending moment that can be carried by this beam is equal to the multiplication of these horizontal compression forces 'F_c' by the lever arm 'r' which is equal to 'h-w-a'.

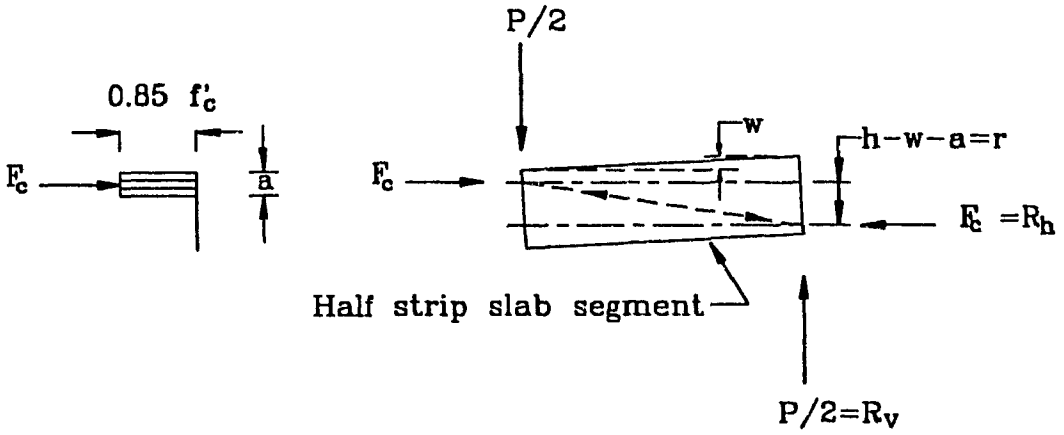

Figure 5-5 The forces that are acting on one segment of the slab

The resisting bending moment can be calculated as follows:

$$M = F_c \times r \qquad \ldots\ldots\ldots\ldots\ldots \quad (5\text{-}1)$$

$$M = F_c(h-w-a) \qquad \ldots\ldots\ldots\ldots\ldots \quad (5\text{-}2)$$

$$M = 0.85 f_c^{'} b a (h-w-a)$$

Taking, $C = Constant = 0.85 f_c^{'} b$

$$\text{i.e. } M = Cha - Cwa - Ca^2 \qquad \ldots\ldots\ldots \quad (5\text{-}3)$$

In Equation (5-1), the value of the moment 'M' is a function of the values of 'r' and 'F_c'. Different values of 'r' are shown in Figure 5-6. As shown in Figure 5-6-a, before applying the concentrated load and ignoring the own weight of the beam, the value of 'r' is given as follows:

$$r = h-w-a = h \ ,$$

Where $a = 0$ and $w = 0$

Consequently, $F_c = 0.85 f_c' b a = 0$

Substituting into Equation (5-1)

$$M = F_c \times h = 0$$

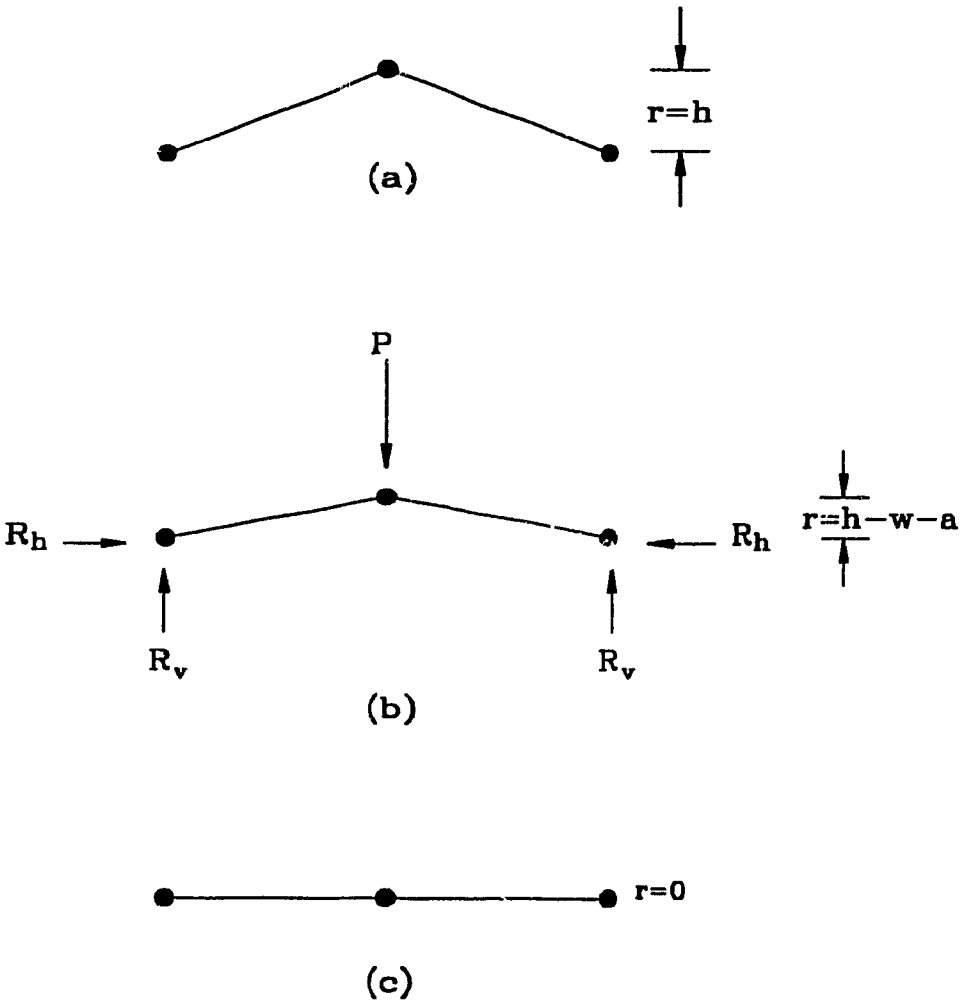

Figure 5-6 Different values of the rise 'r'

After applying the load, the values of 'r' and 'M' are given by Equation (5-2) and the value of 'r' is shown in Figure 5-6-b.

In Figure 5-6-c, the value of 'r' is given as follows:

$$r = 0$$

Where $w = h - a$

In Equation (5-3) the values of the variables 'a' and 'w' are unknown and they need to be determined. To determine the value of 'a', an assumed reasonable value can be assigned to 'w' and a curve between 'M' and 'a' for different given values of 'a' can be plotted. Curves are plotted as shown in Figure 5-7 for 'M' versus 'a' for different values of 'w'.

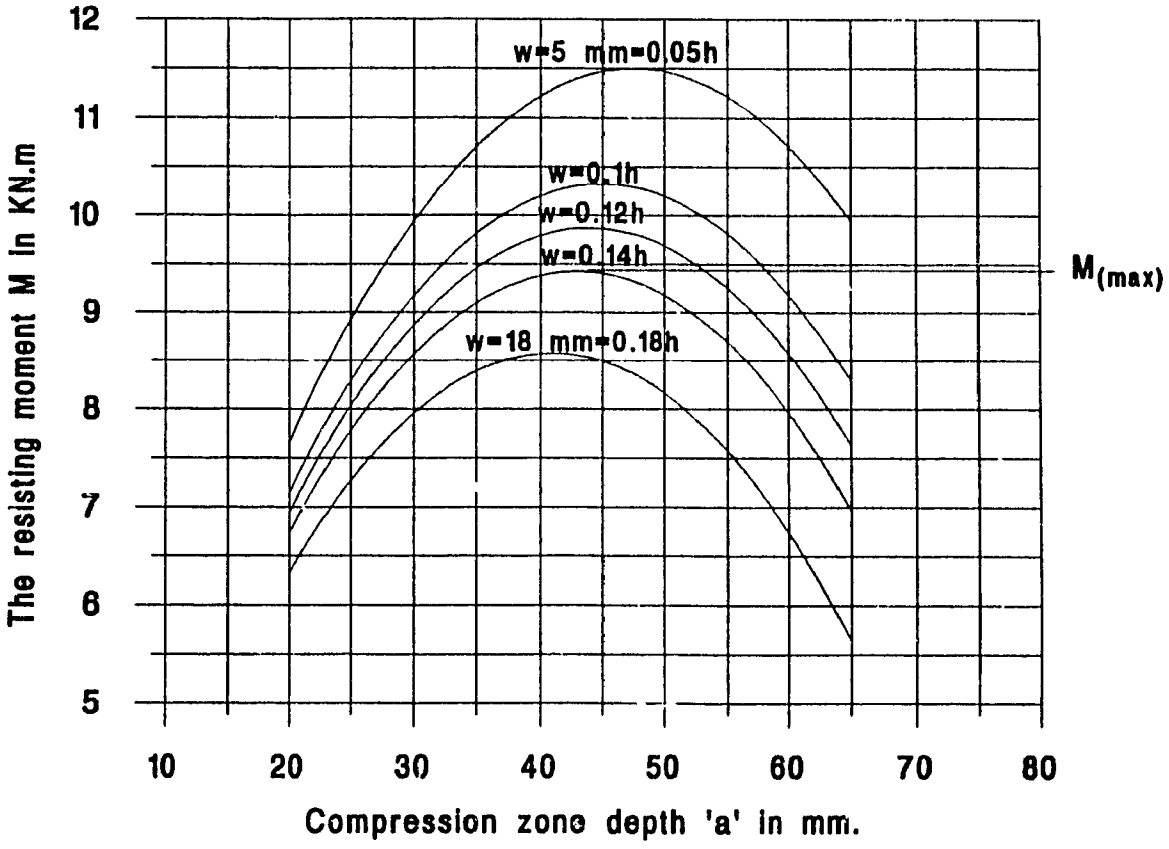

Figure 5-7 Relation between the resisting moment 'M' and the compression zone depth 'a' for different values of 'w'

The curves shown in Figure 5-7 are obtained by using values for the beam depth 'h' and the beam width 'b' equal to 100 mm and 200 mm respectively. The values of the deflection 'w' that are used to obtain these curves are shown in the figure.

From the above curves, it is obvious that the maximum moment is obtained when the slope of the tangent to a curve is zero, which means, the maximum moment 'M' can be obtained when,

$$\frac{dM}{da} = 0$$

As an example, the maximum bending moment 'M_{max}' for the curve which has a deflection value equal to 0.14h = 14 mm is shown in Figure 5-7.

Substituting from the above equation into Equation (5-3)

$$\frac{dM}{da} = Ch - Cw - 2Ca = 0$$

$$i.e.\quad h - w - 2a = 0$$

which means

$$a = \frac{1}{2}h - \frac{1}{2}w \qquad \text{.....} \qquad (5\text{-}4)$$

The above Equation (5-4) presents the depth of the compression zone 'a' as a function of the deflection 'w'. The value of 'a' in this equation corresponds to the maximum resisting moment. The maximum resisting moment results from the maximum concentrated load 'P' that can be carried by the beam. Also, Equation (5-4) indicates that the value of the depth of the compression zone 'a' at the maximum load 'P' will be, always, less than 0.5h (less than half the total depth of the beam).

The deflection 'w' in Equation (5-4) is unknown and it needs to be determined. To calculate the deflection 'w' for the structure shown in Figure 5-3 the method of virtual work[51, 52, 53] will be used. The deflection should be calculated using a plastic analysis. This means the constitutive stress-strain relations need to be considered.

5-2 Stress-Strain Relations

Bathe[60] et al., used stress-strain curves, which had been introduced by Kupfer[61, 62] et al. and Saenz[63]. The plastic stress-strain relations introduced by Kupfer in 1969, were examined by Chen[15] in 1982. The stress-strain curve of Kupfer et al. will be adopted in this study. The compression part of this curve is shown in Figure 5-8.

By performing a regression analysis[9] on the coordinates of the curve shown in Figure 5-8, a polynomial equation presenting this curve can be obtained as follows:

$$y = \sigma/\sigma_c = -0.003 + 1054.36\varepsilon - 324118.98\varepsilon^2 + 2316471.79\varepsilon^3 \quad \ldots\ldots \quad (5\text{-}5)$$

Equation (5-5) is valid from $\varepsilon = 0$ to $\varepsilon = 0.00315$

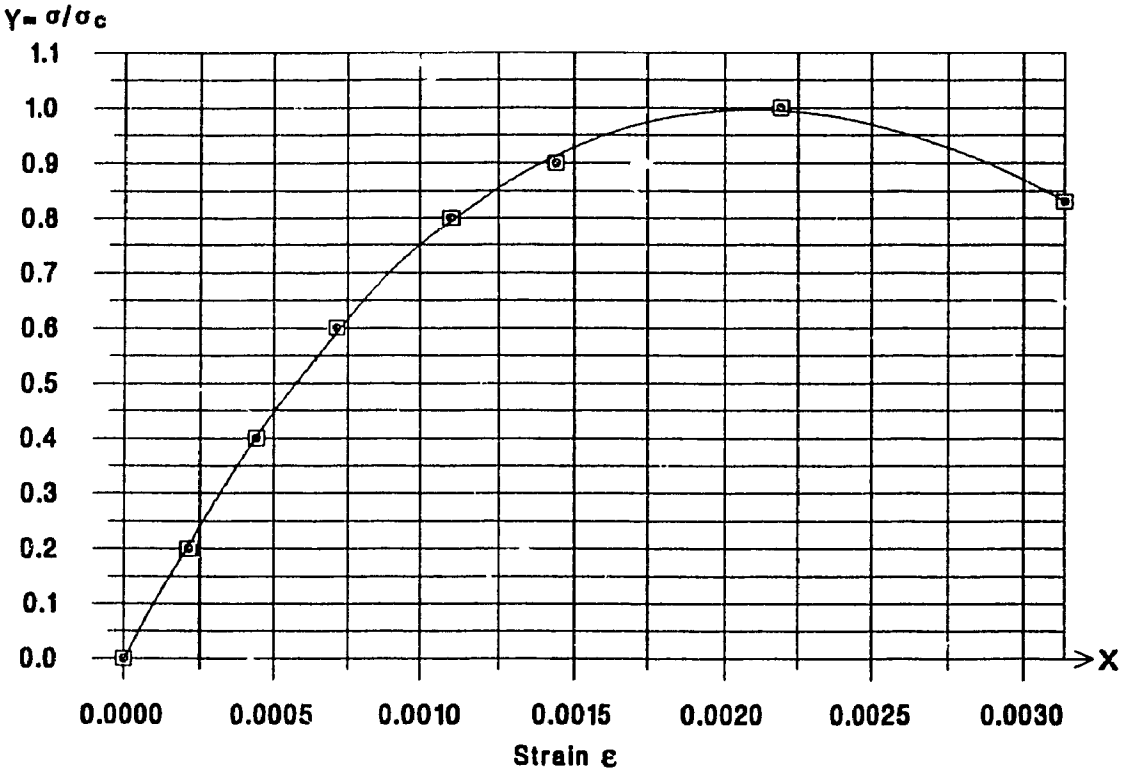

Figure 5-8 Stress-strain curve

Equation (5-5) presents the stresses as a function of the strain, which means for a given value of a strain the equivalent stress can be calculated. However, in some cases, the stress is known and the strain needs to be obtained. Therefore, by reversing the coordinates of the curve shown in Figure 5-8, a new curve can be obtained which is shown

in Figure 5-9.

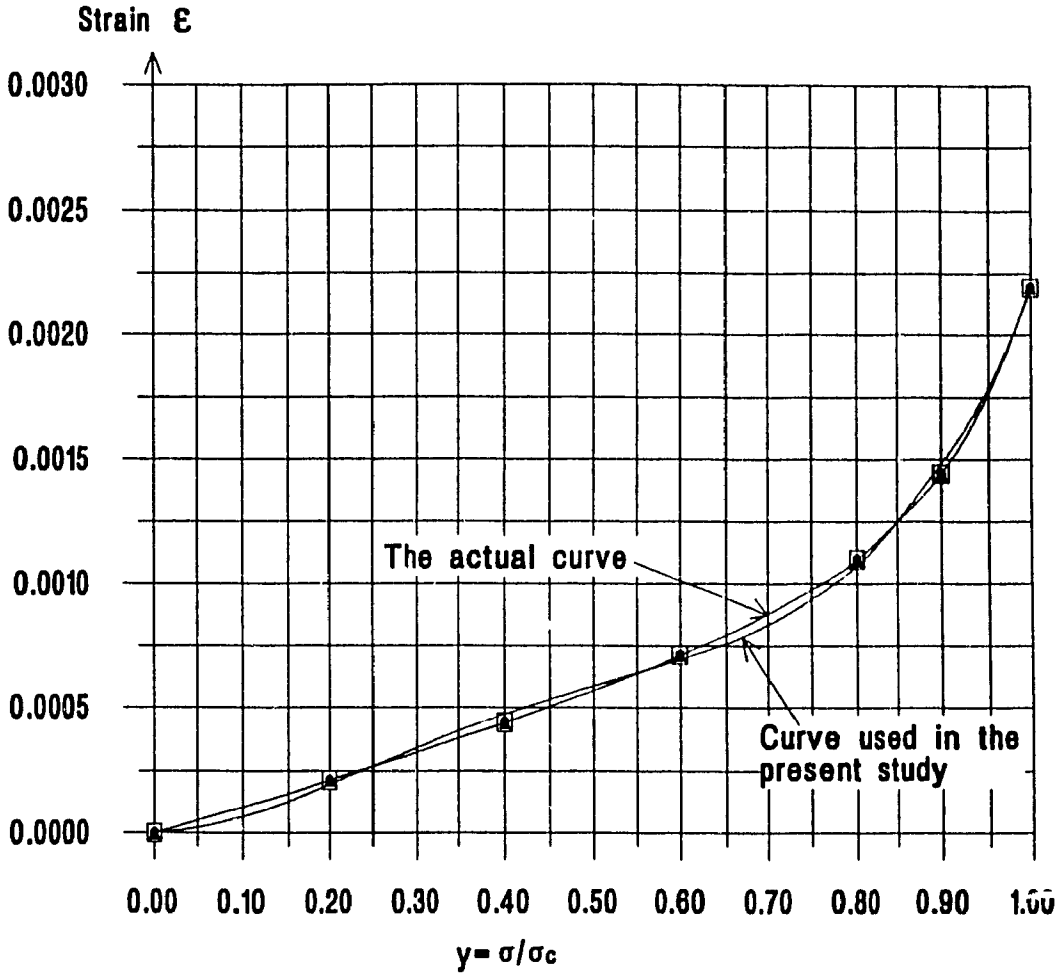

Figure 5-9 Strain-stress curve

Using regression analysis, the polynomial equation of the curve that is shown in Figure 5-9, where the strain is presented as a function of the stress, is given as follows:

$$\varepsilon = 0.00003y + 0.0071y^2 - 0.01434y^3 + 0.00939y^4 \quad \ldots\ldots \quad (5\text{-}6)$$

Where y is equal to σ/σ_c

It can be seen in Figure 5-9 that the deviation between the actual curve and the curve represented by Equation (5-6) is negligible. The value of the coefficient of multiple determination[9] for the curve represented by Equation (5-6) is 0.999. This coefficient measures the accuracy of the coordinates of the points of the curve represented by Equation (5-6) in compression with the coordinates of the points represented by the actual curve. Equation (5-6) presents the value of the strain for a given value of stresses and is valid from $y=0$ to $y=1$. The values of y and ε for the curves of Figures 5-8 and 5-9 are tabulated as shown in Table 5-1.

Table 5-1 Stress-strain values

$y = \sigma/\sigma_c$	ε
0	0
0.2	0.000212
0.4	0.000442
0.6	0.000712
0.8	0.001096
0.9	0.001442
1.0	0.002192
0.83	0.003153

5-3 Plastic deformation by the virtual work method

The virtual work method[51, 52, 53] is used widely in calculating the deflections (or deformations) of structures using elastic analysis. To calculate deflections using the virtual work method, for a structure composed of several members, the deformations of the individual members need to be calculated. In the elastic analysis, the deformations are calculated using modulus of elasticity 'E'. In this study a plastic analysis will be considered. Thus, equation (5-6) will be used to calculate the deformation 's' of a member subjected to axial force 'F' as shown in Figure 5-10.

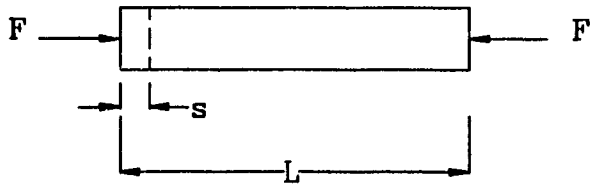

Figure 5-10 Shortening of a member due to axial compression loads

The value of '$y=\sigma/\sigma_c$' that is shown in Figures 5-8 and 5-9 is calculated as follows:

$$y = \sigma/\sigma_c = \frac{F}{A\ f_c'} \qquad \text{..... (5-7)}$$

Where:

A = the cross-section area of the member

f_c' = σ_c = the compression strength of the concrete

σ = the compression stress in the concrete

Equation 5-7 is valid for members subjected to axial compression force 'F' as shown in Figure 5-10. Substituting the value of 'y' in Equation (5-6) or in Table 5-1, the value of the strain 'ε' can be obtained. Knowing the value of the strain 'ε', the axial deformation 's' can be calculated as follows:

$$s = \varepsilon L \quad \ldots\ldots\ldots\ldots\ldots\ldots \quad (5\text{-}8)$$

where L= The length of the member

The deflection 'w' of a structure that consists of members which are subjected to axial forces only, using the virtual work method, is given as follows:

$$w = \sum F_{ui} \times s_i \quad \ldots\ldots\ldots\ldots\ldots\ldots \quad (5\text{-}9)$$

Where 'F_{ui}' is the value of the axial force acting in the member number 'i' of the structure. The value of 'F_{ui}' is due to the application of a unit force at the joint and in the direction where the deflection needs to be calculated. And 's_i' is the shortening of the member number 'i'

due to the application of the actual forces.

5-4 Partial Horizontal Restraint

The degree of rigidity of the horizontal restraint may vary depending on the horizontal stiffness of the members that are providing these restraints. For an interior slab panel of a floor system, the surrounding slabs provide almost full horizontal restraints for this interior slab. This full restraint is due to the great rigidity of the surrounding slabs in the horizontal directions. On the other hand, for a single slab supported by four beams (depending on the rigidity of the beams in the horizontal directions), the horizontal restraints of the slab can be considered partial horizontal restraints.

The problem of partial horizontal restraint of a strip slab can be treated similarly to what has been mentioned above for a strip slab with full horizontal restraint. To treat this problem, the rigid horizontal supports shown in Figure 5-3 will be replaced by horizontal elastic supports as shown in Figure 5-11. The value of the spring constant 'k' for the elastic horizontal support is defined as the value of the reaction 'R_h' required to produce a unit horizontal deflection for the spring. The inverse of 'k', which is '1/k', is defined as the horizontal deflection of the spring due to a value of 'R_h' equal to a unit force.

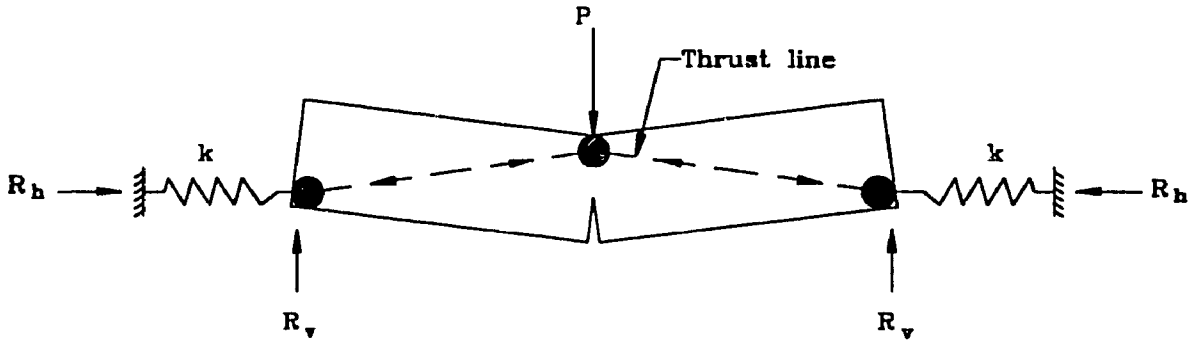

Figure 5-11 Elastic horizontal supports

5-5 Illustrative Example

The dimension of the strip slabs that have been used in our experimental program will be used in this numerical example. As shown in Figure 5-12, the span of the non-reinforced concrete beam is 2400 mm, the depth and the width of the cross section are 100 mm and 200 mm respectively. The compression strength of the concrete is 30 MPa. The maximum value of the concentrated applied load 'P' is required. Solve this problem, first assuming the supports provide full horizontal restraints, and compare the obtained maximum load by the maximum load that can be carried by this strip beam if it is simply supported without horizontal restraints having maximum reinforcement ratio (assuming 'fy' is equal to 400 MPa). Second, solve the problem considering elastic horizontal supports having spring constant 'k' equal to 625 kN per mm (the value of 'k' was calculated for the structural scheme of the test set-up as given in Appendix C Section C-1).

Solution

For this problem, the maximum compression depth 'a' should be smaller than 0.5h, as has been discussed earlier concerning Equation (5-4). The value of 'a' will be assumed equal to 0.5h = 50 mm. Also, the value of the deflection 'w' is unknown. Therefore, it will be assumed equal to an unity (1 mm).

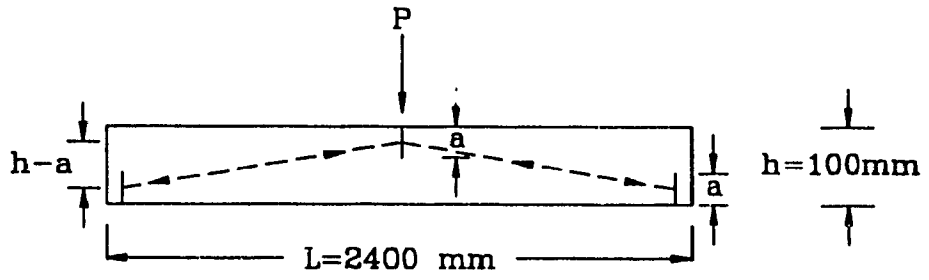

Before deflection

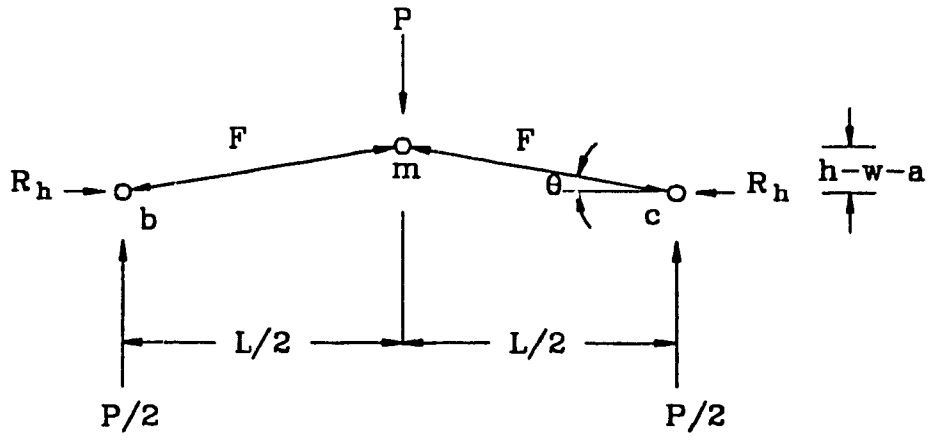

After deflection

Figure 5-12 Dimensions and forces for the illustrative example

Because the convergence of the solution of this problem will require more than one trial, the assumed values of 'a' and 'w' will be modified during the solution until their exact values are reached. In the first trial, the assumed compression depth 'a' is 50 mm and the assumed deflection is 1 mm. Therefore, the vertical distance 'r' between joint 'm' and joints 'b' or 'c' is equal to the depth of the beam 'h' minus the compression depth 'a' and minus the deflection 'w', as shown in Figure 5-12, which is equal to 49 mm.

$$r = h - a - w = 100 - 50 - 1 = 49 \ mm$$

The value of cos θ (see Figure 5-12) can be calculated as follows:

$$\tan\theta = \frac{r}{0.5L} = \frac{49}{1200} = 0.04083$$

$$i.e \quad \theta = 2.338^{\circ}$$

$$\cos\theta = 0.999$$

The ultimate compression forces 'F' in the members of the beam are calculated as follows:

$$F = F_c \times \frac{1}{\cos\theta} = 0.85 f_c' a b \left(\frac{1}{\cos\theta}\right) = 0.85 \times 30 \times 50 \times 200 \times \frac{1}{0.999} \times 10^{-3} = 255.26 \ KN$$

Now, the value of the horizontal reaction 'R_h' can be obtained as follows:

$$R_h = F \cos\theta = 255.26 \times 0.999 = 255 \ KN$$

By taking the moment at joint 'm', the maximum value of the load 'P' can be calculated and modified in the following trials until its exact value is obtained.

$$R_h \times 49 = \frac{P}{2} \times 1200$$

$$P = R_h \times 49 \times \frac{2}{1200}$$

$$P = 255 \times 49 \times \frac{2}{1200} = 20.8\ KN$$

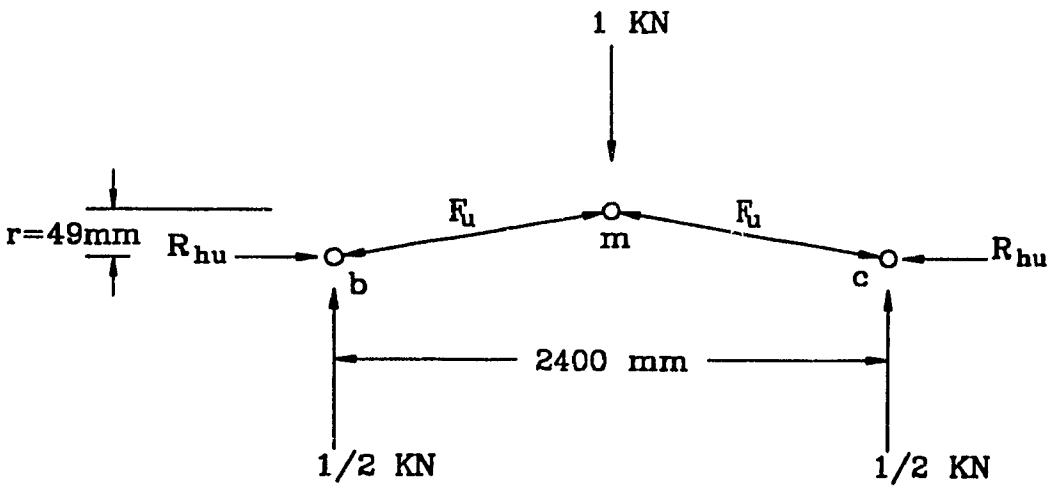

Figure 5-13 Forces used in the virtual work method

As shown in Figure 5-13, the method of virtual work is used. Taking the moment at joint 'm', the values of the horizontal reaction 'R_{hu}' and the compression force 'F_u' that acts in the members due to the

application of a unit load at joint 'm' can be obtained as follows:

$$R_{hu} = \frac{1}{2} \times \frac{1200}{49} = 12.25\ KN$$

$$F_u = \frac{R_{hu}}{\cos\theta} = \frac{12.25}{0.999} = 12.26\ KN$$

Using Equation (5-7), the value of $y = \sigma/\sigma_c$ can be calculated due to the application of the load 'P' at joint 'm' as shown in Figure 5-12,

$$y = \sigma/\sigma_c = \frac{F}{A\ f_c'} = \frac{255.26 \times 10^3}{100 \times 200} \times \frac{1}{30} = 0.425$$

Substituting in Equation (5-6),

$$\varepsilon = 0.000501$$

or by interpolation in Table 5-1,

$$\varepsilon = 0.000508$$

Using the value obtained from Equation (5-6), the value of the axial shortening 's' of a member in this structure, due to the application of the load 'P' at joint 'm', can be calculated by Equation (5-8) as follows:

$$s = \varepsilon \frac{L}{2 \times \cos\theta} = 0.000501 \times \frac{1200}{0.999} = 0.6015\ mm$$

The deflection 'w' is calculated by Equation (5-9) as follows:

$$w = \sum F_u \times s = 2 \times F_u \times s$$

$$w = 2 \times 12.26 \times 0.6015 = 14.75 \ mm$$

Using Equation (5-4), the assumed value of the depth of the compression zone 'a' can be checked whether it is due to the required maximum load 'P'. This value has been assumed earlier as 50 mm,

$$a = \frac{1}{2}h - \frac{1}{2}w = 50 - \frac{14.75}{2} = 42.63 \ mm$$

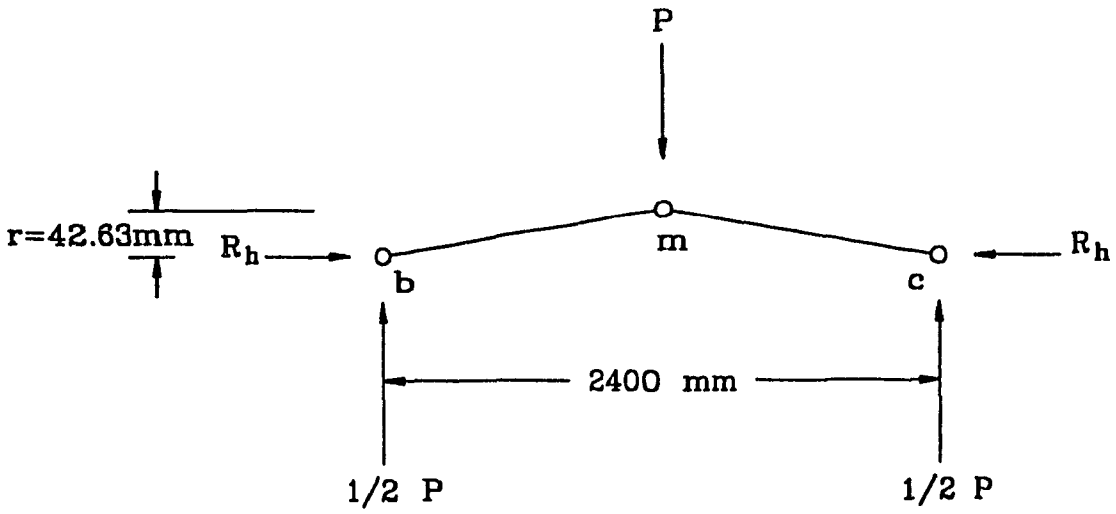

Figure 5-14 The configuration that is considered in the second trial

The obtained values of 'a' and 'w' do not match the assumed values. Therefore, a second trial should be performed using values of 'a' and 'w' that have been obtained from the first trial equal to 42.63 mm and 14.75 mm respectively. The new values of 'a' and 'w' lead to a structure having a vertical distance 'r' between joint 'm' and joints 'c' or 'b' equal to 42.63 mm as shown in Figure 5-14.

$$r = h - a - w = 100 - 42.63 - 14.75 = 42.63 \ mm$$

Table 5-2 The results of the first part of the illustrative example

Trial No.	Assumed Compres. Depth 'a' mm	Obtained Compres. Depth 'a' mm	Applied Load 'P' kN	Assumed Deflect. 'w' mm	Obtained Deflect. 'w' mm	Horizontal Reaction 'R_h' kN
1	50	42.63	20.80	1	14.75	255.00
2	42.63	42.85	15.43	14.75	14.31	217.36
3	42.85	42.84	15.59	14.31	14.32	218.48
4	42.84	42.84	15.59	14.32	14.32	218.45
5	42.84	42.84	15.59	14.32	14.32	218.45

The convergence is reached very rapidly, and for practical engineering purposes, the second or third trial will give satisfactory

results. The results of the additional trials are presented in Table 5-2. As can be seen in Table 5-2, the variation of the value of the applied load 'P' from trial number 2 and the value obtained from the last trial is about one percent.

According to the Canadian Code, a maximum load of 18.17 kN can be carried by this strip slab if it is horizontally unrestrained and if it has maximum reinforcement ratio of $\rho_{max} = 0.032513$ corresponding to the balanced conditions. From the above results, the maximum load that can be carried by the horizontally restrained non-reinforced strip slab is equal to 86% of the load that can be carried by this strip slab if it is simply supported without horizontal restraints and with maximum reinforcement ratio.

To solve the second part of the problem, where horizontal elastic supports are assumed to be resisting the horizontal reactions as shown in Figure 5-11, the elastic supports will be replaced by horizontal members as shown in Figure 5-15.

The shortening of these horizontal members will be calculated as follows:

$$s_1 = \frac{1}{k} \times F_1 = \frac{1}{k} \times R_h \qquad \text{..... (5-10)}$$

Where 's_1' is the shortening of an elastic support or the shortening of a horizontal member as shown in Figure 5-15. This horizontal

shortening is due to the horizontal reaction 'R_h' that is equal to the force 'F_1'. The value of the spring constant 'k' for the elastic supports used in this problem is the actual value for the spring constant of the test set-up used in our experimental program.

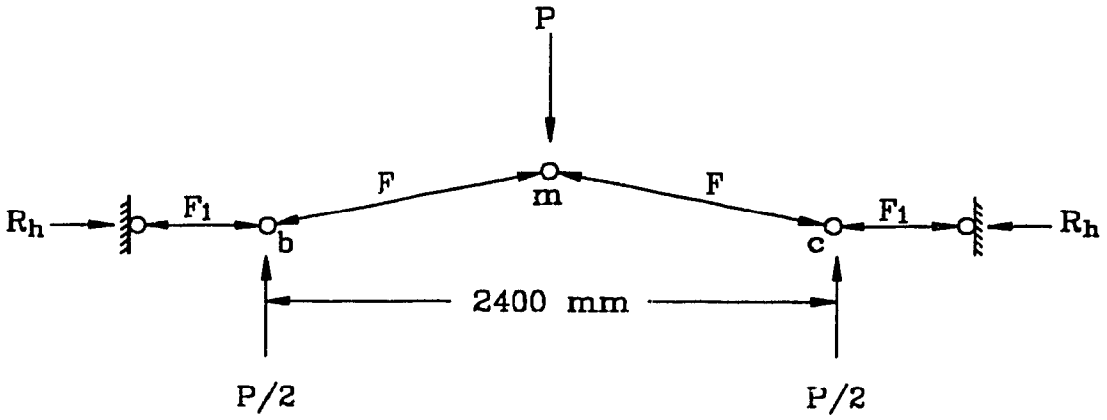

Figure 5-15 Horizontal members replacing the elastic supports

The solution of the second part of this problem is similar to the first part except for taking into consideration the effects of these additional horizontal members. The first trial will be represented hereinafter as has been done in the first part. The depth of the compression zone 'a' and the deflection 'w' will be assumed equal to 50 mm and 1 mm respectively.

$$\cos\theta = 0.999 \qquad \text{(See the first part)}$$

$$F = 0.85 f_c' a b \left(\frac{1}{\cos\theta}\right) = 0.85 \times 30 \times 50 \times 200 \times \frac{1}{0.999} \times 10^{-3} = 255.26 \ KN$$

$$R_h = F_1 = F \cos\theta = 255.26 \times 0.999 = 255 \ KN$$

By using Equation (5-10)

$$s_1 = 0.0016 \times 255 = 0.408 \ mm$$

Taking the moment at joint 'm' and calculating P (see the first part),

$$P = 255 \times 49 \times \frac{2}{1200} = 20.8 \ KN$$

Using the virtual work method as shown in Figure 5-16,

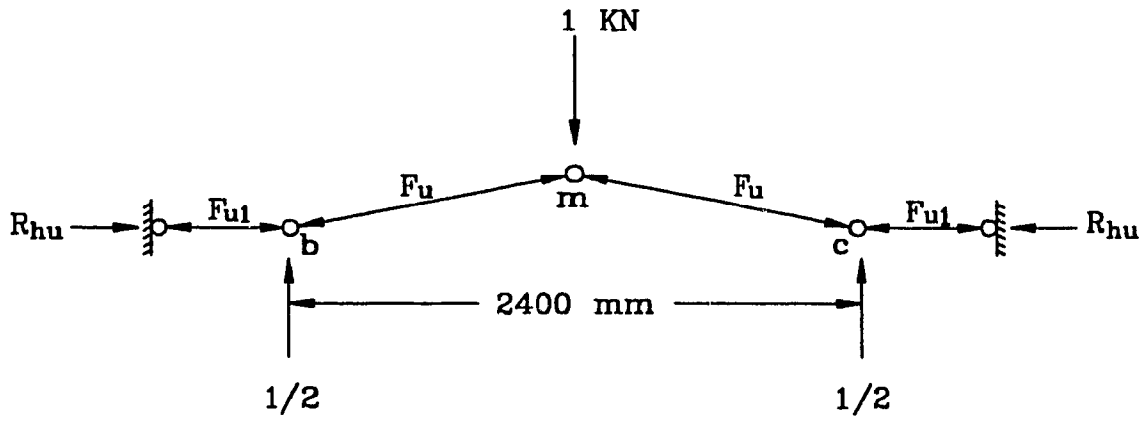

Figure 5-16 The forces produced by a unit load

Taking the moment at joint 'm' and calculating 'F_u',

$$R_{hu} = F_{u1} = \frac{1}{2} \times \frac{1200}{49} = 12.25 \ KN$$

$$F_u = \frac{F_{u1}}{\cos\theta} = \frac{12.25}{0.999} = 12.26\ KN$$

Using Equation (5-7),

$$y = \sigma/\sigma_c = \frac{F}{A\ f_c'} = \frac{255.26 \times 10^3}{100 \times 200} \times \frac{1}{30} = 0.425$$

Substituting in Equation (5-6),

$$\varepsilon = 0.000501$$

The value of the axial shortening 's' of a diagonal member in this structure is given in as follows:

$$s = \varepsilon \times \frac{L}{2 \times \cos\theta} = 0.000501 \times \frac{1200}{0.999} = 0.6015\ mm$$

The deflection 'w' is given in Equation (5-9) as follows:

$$w = \sum F_{ui} \times s_i = (2 \times F_u \times s) + (2 \times F_{u1} \times s_1)$$

$$w = (2 \times 12.26 \times 0.6015) + (2 \times 12.25 \times 0.408) = 24.74\ mm$$

Check whether the depth of the compression zone 'a' is due to the required maximum load 'P',

$$a = \frac{1}{2}h - \frac{1}{2}w = 50 - \frac{24.74}{2} = 37.63\ mm$$

The obtained values of 'a' and 'w' do not match the assumed values. In the second trial, the assumed values of the compression depth 'a' and the deflection 'w' that will be used are 37.63 mm and 24.74 mm respectively. The trials are to be continued until convergence is reached. Convergence is considered to be reached when the assumed values of 'a' and 'w' at the beginning of one trial are equal to the obtained values at the end of the trial. The results of the following trials are represented in Table 5-3.

As can be seen in Table 5-3, the convergence of the solution is reached very rapidly, and acceptable results can be obtained from trial number 2 or 3 or a higher order. This rapid convergence is due to the rate of the value of 'k' that is used in this problem. The speed of convergence is a function of the value of 'k'. For a very high value of 'k', the convergence will be rapid and for a very low value of 'k' the convergence will be slow.

Because of the presence of horizontal displacements 'w_h' as shown in Table 5-3 (the horizontal displacements that are shown in the table are the total horizontal displacements due to the deformation of the two elastic horizontal supports), there is a variation between the maximum load 'P' that is obtained from the first part of the problem (where rigid supports are used) and the maximum load 'P' that is obtained from the

second part of the problem (where elastic supports are used).

Table 5-3 The results of the second part of the illustrative example

Trial No.	Assumed Compres. Depth 'a' mm	Obtained Compres. Depth 'a' mm	Applied Load 'P' kN	Assumed Deflect. 'w' mm	Obtained Deflect. 'w' mm	Horizo. React. 'R_h' kN	Total 'w_h'* mm
1	50	37.63	20.80	1	24.74	255.00	0.82
2	37.63	38.11	12.03	24.74	23.78	191.76	0.61
3	38.11	38.09	12 33	23.78	23.82	194.17	0.62
4	38.09	38.09	12.32	23.82	23.82	194.07	0.62
5	38.09	38.09	12.32	23.82	23.82	194.08	0.62
6	38.09	38.09	12.32	23.82	23.82	194.08	0.62

*w_h = Horizontal displacement due to the deformations of both supports.

5-6 Horizontally Restrained Reinforced Concrete Strip Slab

It is important to examine the case of horizontally restrained reinforced concrete beam or strip slab. Most of concrete beams or slabs are reinforced. This case is demonstrated through an illustrative example.

5-6-1 Illustrative Example II

A strip slab similar to the one used in the illustrative example of the preceding section is used in this section. The dimensions of the cross section and the span of the strip slab are shown in Figure 5-17. This strip slab is reinforced with two bars having area steel equal to 28.27 mm^2 each (the diameter of each bar is 6 mm). The stiffness of the horizontal elastic support is 625 kN per millimeter of horizontal displacement (this is the actual value of the experimental set-up). Determine the maximum value of the concentrated load 'P' that can be carried by the strip slab.

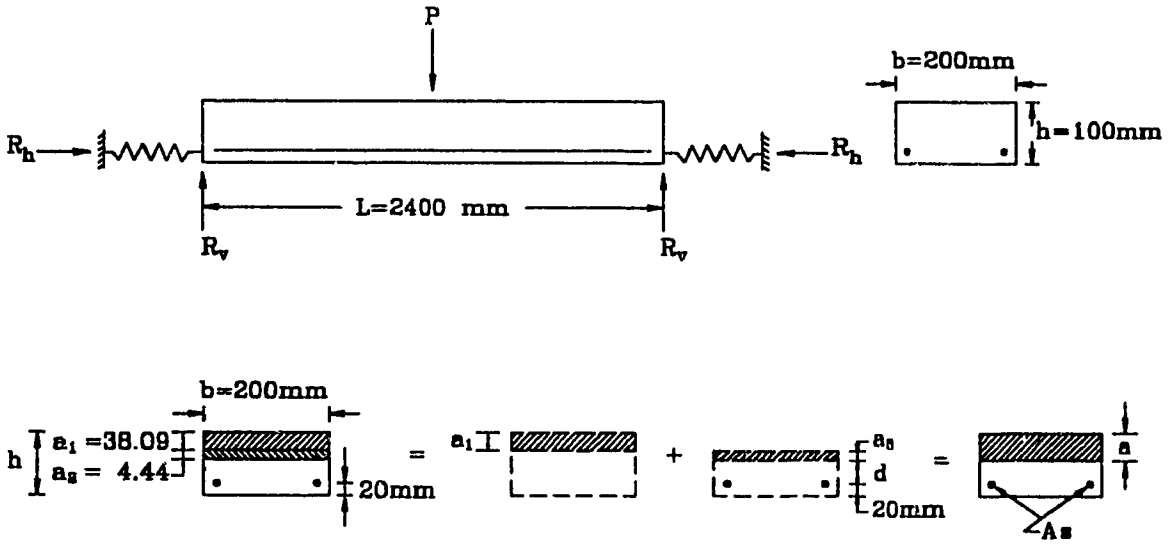

Figure 5-17 Horizontally restrained reinforced strip slab

The tension force in the reinforcement is calculated as follows:

$$A_s \times F_y = 2 \times 28.27 \times 400 = 22616 \ N$$

The depth 'a' of the compression zone is given as follows:

$$a_2 = \frac{A_s \times F_y}{0.85 \times f_c' \times b} = \frac{22616}{0.85 \times 30 \times 200} = 4.44 \ mm$$

Where 'a_2' is the depth of the compression zone due to the presence of the reinforcement and 'a_1' is the depth of the compression zone due to the horizontal restraint and is obtained from Table 5-3 (trial No. 6).

The moment resistance 'M' due to the reinforcement is equal to

$$M = A_s \times F_y (d - \frac{a_2}{2}) = 22616(41.91 - \frac{4.44}{2})10^{-6} = 0.9 \ kN.m$$

Where 'd' is equal to =h-cover-a_1=100-20-38.09=41.91 mm

The additional load 'P_2' that can be carried by the strip slab due to the presence of the reinforcement can be calculated as follows:

$$P_2 = \frac{M \times 4}{L} = \frac{0.9 \times 4}{2.4} = 1.5 \ kN$$

Assuming the deflection is linearly proportional to the applied concentrated load, the deflection 'Δ' due to unit load can be calculated as follows (the values of the deflection and the load are obtained from the illustrative example in the preceding section):

$$\Delta = (23.82 \text{ mm})/(12.32 \text{ kN}) = 1.93344 \text{ mm}$$

The additional deflection 'w_2' due to load P_2 is calculated as follows:

$$w_2 = \Delta \times P_2 = 1.933442 \times 1.5 = 2.9 \ mm$$

To maintain the compatibility, this additional deflection must be added to equation (5-4) as an imposed deflection, which results in a decrease in the value of the depth of the compression zone 'a'.

$$\text{Modified } a = \frac{h}{2} - \frac{(w_1 + w_2)}{2} = \frac{100}{2} - \frac{23.82 + 2.9}{2} = 36.64 \ mm$$

where w1 is the vertical deflection due to the horizontal restraint

From Figure 5-12, the compression force 'F', the horizontal reaction 'R_h' and the rise of the strip slab are calculated as follows:

$$F = 0.85 \times f_c' \times a \times b \times \frac{1}{\cos\theta} = 0.85 \times 30 \times 36.64 \times 200 \times \frac{1}{0.999} \times 10^{-3} = 187.05 \ kN$$

$$R_h = F \times \cos\theta = 187.05 \times 0.999 = 186.86 \ kN$$

$$r = h - w - a = 100 - 26.72 - 36.64 = 36.64 \ mm$$

From Figure 5-12, the value of 'P_1' due to the horizontal restraint can be calculated by taking the moment at joint 'm'.

$$P_1 = \frac{R_h \times r \times 4}{L} = \frac{186.86 \times 36.64 \times 4}{2400} = 11.41 \ kN$$

$$P = P_1 + P_2 = 11.41 + 1.5 = 12.91 \ kN$$

$$\text{Total } a = 36.64 + 4.44 = 41.08 \ mm$$

$$\text{Total deflection } w = 23.82 + 2.9 = 26.72 \ mm$$

In the above iteration a new value for the depth of the compression zone 'a_1' was obtained which results in new value for 'd'. Therefore, additional iterations are required until convergence is reached. The subsequent iterations are given in Table 5-4.

Table 5-4 Results of the horizontally restrained reinforced strip slab

Trial NO	a_1 mm	a_2 mm	a_{total} mm	P_1 kN	P_2 kN	P_{total} kN	w_1 mm	w_2 mm	w_{total} mm
1	36.64	4.44	41.08	11.41	1.50	12.91	23.82	2.90	26.72
2	37.47	4.44	41.91	11.93	1.55	13.93	22.06	3.00	25.06
3	37.00	4.44	41.44	11.63	1.52	13.15	23.07	2.94	26.01
4	37.27	4.44	41.71	11.81	1.54	13.35	22.49	2.97	25.46
5	37.11	4.44	41.55	11.71	1.53	13.24	22.83	2.95	25.78
6	37.2	4.44	41.64	11.76	1.53	13.29	22.64	2.96	25.6
7	37.15	4.44	41.59	11.73	1.53	13.26	22.74	2.96	25.70
8	37.18	4.44	41.62	11.75	1.53	13.28	22.68	2.96	25.64
9	37.16	4.44	41.60	11.74	1.53	13.27	22.72	2.96	25.68

To insure that the stress in the reinforcing steel is equal to its yielding stress, the maximum depth of the compression zone 'a_{max}' needs to be greater or equal to the total depth 'a_{total}'. The maximum depth of the compression zone 'a_{max}' is calculated as follows:

$$a_{max} = \beta \times c_d = 0.85 \frac{600}{600 + f_y} d = 0.85 \frac{600}{600 + 400} 80 = 40.8\,mm \approx 41.6\,mm$$

5-7 Summary

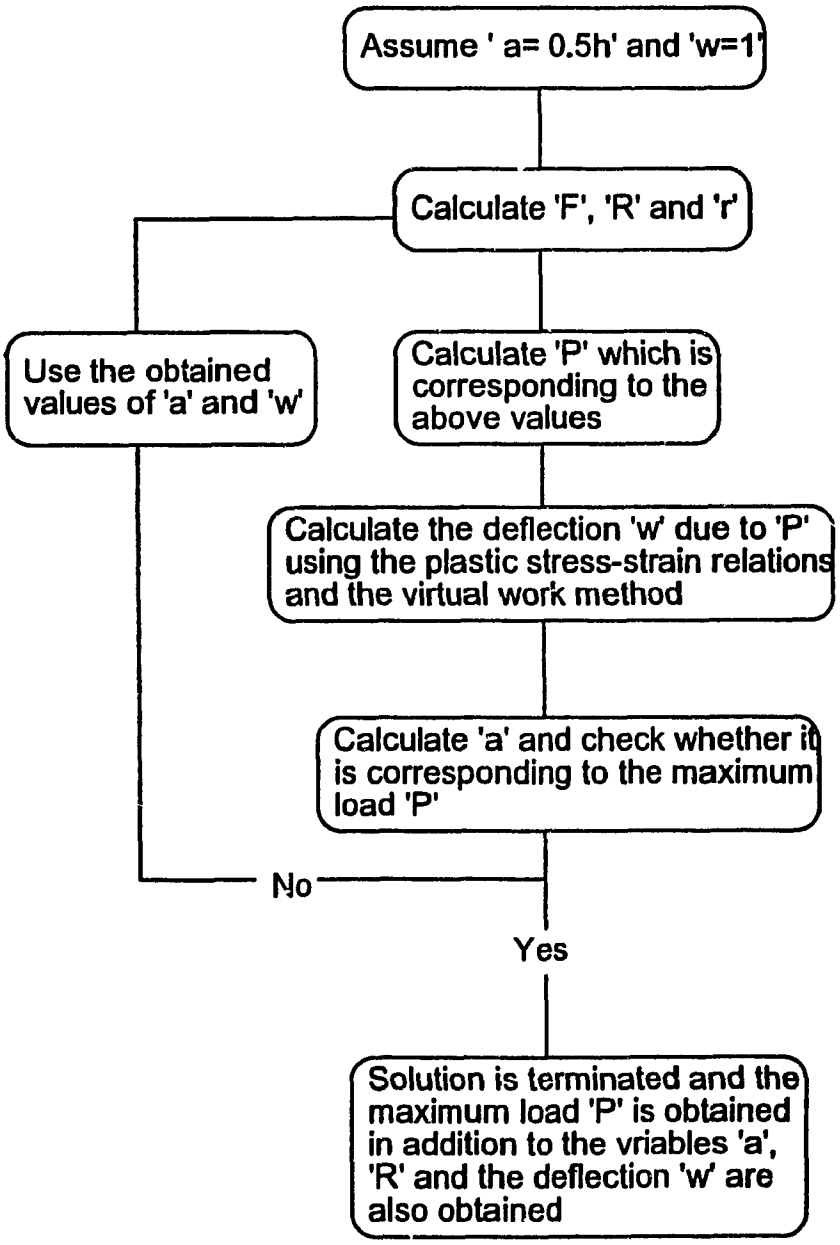

Figure 5-18 The flow chart of the plastic analytical method

Plastic analysis method for non reinforced concrete strip slabs or beams horizontally restrained subjected to concentrated loads at mid-spans was presented. Through this analysis, we were able to establish the values of the maximum load that can be carried by the strip slabs, the maximum deflection and the value of the horizontal reaction. This method can be used for strip slabs (or beams) fully or partially horizontally restrained. The flow chart of the plastic analytical method is shown in Figure 5-18.

Chapter 6

Finite Element Analysis and Parametric Study

6-1 Introduction

A review of reported applications of the finite element method to the analysis of concrete slabs shows that over the last 20 years many comprehensive and sophisticated techniques have been developed. These are apparently capable of modeling many of the aspects of concrete and reinforced concrete slab behavior that commonly used methods of analysis ignore.

During the period of the 60s to early 70s many papers were published dealing with the linear finite element method[64, 65, 66], mainly to model beams and walls, also to model elastic slabs[67], mostly using three-node triangular elements.

In the period of the late 70s, the non-linear finite element method dominated the publications dealing with concrete slabs. Ghoneim[68] in 1978 and Jackson[69] in 1979 among others worked with layered non-linear finite element models for concrete slabs which are considered to be

'first generation' models. They used quadrilateral plate bending elements to model the slabs.

During the 80s and up to the present time, most of the non-linear finite element publications[70, 71, 72] that deal with three-dimensional models of concrete slabs use or refer to brick elements of 8 and 20 nodes. In these models the non linearities of reinforced and non reinforced concrete slabs are simulated to a high degree of accuracy.

In this study, the commercial program ADINA[5] was used to analyze the model of the experimental specimen. This program is capable of performing three dimensional non-linear analysis using triaxial stress envelopes for compression and tension stresses, to simulate the multiaxial stress conditions that occur within a prism of concrete subjected to external loads. Also, it is capable of taking into account the increase of the values of the strength parameters, namely the stress-strain parameters, for models under multiaxial stress conditions.

Bathe[60] et al. in 1989 presented a paper that includes the assumptions of this program. The failure criteria were not mentioned in the published paper or in the manual of the program. However, through communications with the designer of program ADINA, he indicated that the failure criterion is reached when the maximum strain is reached.

For non-reinforced concrete, the program has great difficulties performing convergence for the constitutive relation of the stress-strain

curve. The incremental load method[73] is used in the analysis performed by the program. For some load increments (near the maximum load), the user needs to modify the value of the load increment by trial and error to choose the proper value that will allow the program to perform a successful convergence. In some cases, the program has to be run many times to test each modified load increment to be able to get the proper value that will result in successful convergence. In some other cases, even after running the program several times, the proper load increment can not be obtained, and the analysis stops. The value of the concentrated load that is obtained from such unsuccessful running is less than the maximum load that can be carried by the beam, and the deviation between the obtained value and the maximum value is unknown.

In the analysis of the strip slab, we encountered such unsuccessful running of the program. The designer of the program admitted the difficulties of convergence for non-reinforced concrete beams and directed us to use some technique to overcome this problem. However, this technique was also based on trial and error and requires running the program several times.

Despite the difficulties that have been encountered using program ADINA, the program uses very advanced techniques to model the three dimensional aspects of non-linearity of concrete and reinforced concrete

structures which most other programs ignore. Also, the program has a plotting software package which is capable of drafting many applications.

The cross sectional dimensions of the non-linear finite element model are 100 mm in depth and 200 mm in width. A view of the model and the boundary conditions is shown in Figure 6-1.

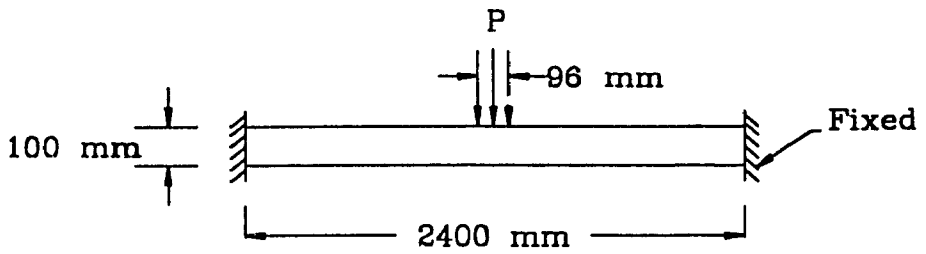

Figure 6-1 The model analyzed by ADINA

In the 3-D model, eight-node brick elements were used in the finite element mesh that represent the strip slab. The value of the maximum load obtained was higher than expected. Also, the value of the deflection was smaller than expected. The designer of program ADINA recommended the use of twenty-node brick elements (it better simulates non-reinforced concrete) to model the strip slab. The command program using eight-node brick elements is presented in Appendix B (Sections B-1) as program SS2.

Twenty-node brick elements and non-reinforced concrete with a

compressive strength of 30 MPa are used to simulate the strip slab. The concentrated load P was uniformly distributed over 96 mm at midspan and on the top fibers.

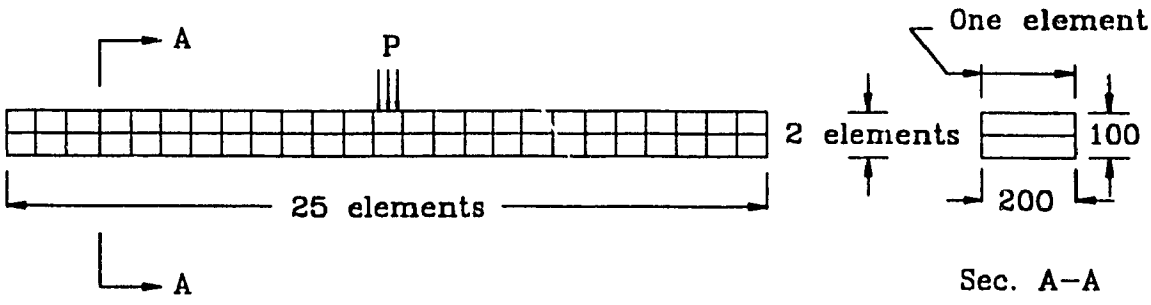

Figure 6-2 The 3-D element mesh used to analyze the model

The span length of the model was divided to accommodate 25 elements. The width of 200 mm was divided to accommodate one element and the depth of 100 mm was divided to accommodate 2 elements, which means the model was divided into 50 elements as shown in Figure 6-2. The command programs that were used to run program Adina, for the model is given in Appendix B (Sections B-2) as program SS4. A command program recommended by the designer of Adina to help reduce the difficulty of convergence is also included in Appendix B (Section B-3).

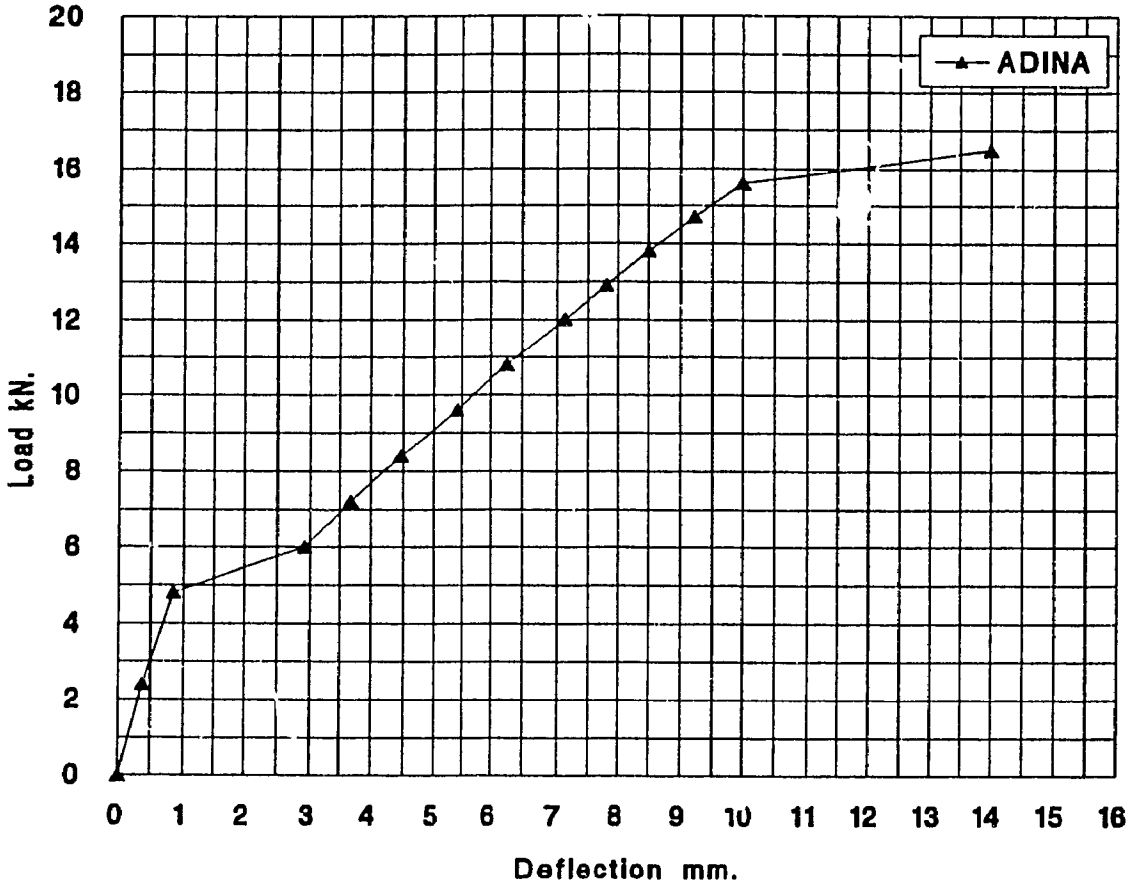

Figure 6-3 Load-deflection curve from the finite element analysis for the strip slab of the 2400 mm span

The maximum load and deflection for the model of the twenty-node brick elements were 16.50 kN and 14.0 mm respectively without any difficulties reaching convergence. The load-deflection curve for the model is shown in Figure 6-3.

Comparison between the results that are obtained form the finite element method and the analytical method that was presented earlier in Chapter 5 is presented in Table 6-1. The results of the analytical

analysis are shown in Table 5-2.

Table 6-1 Comparison between results obtained from the finite element method and the analytical method

	Finite element method (A)	Analytical method (B)	Ratio of (A)/(B)
Failure load 'P' kN	16.50	15.59	1.058
Deflection 'w' mm	14.00	14.32	0.978

6-2 Parametric Study

It is important to examine the effects of some of the parameters that influence the carrying capacity of the considered strip slab. Examining the influence of these parameters can be useful in establishing a design procedure for horizontally restrained strip slabs or beams. The influences of three parameters were examined. These parameters are: the variation of the reinforcement ratio in the horizontally restrained strip slab, the degree of the horizontal restraints (the variation of the stiffness of the horizontal elastic support) and the span to depth ratio. Program ADINA was used to perform this parametric study. To optimize the use of the computer facilities, two dimensional models were used in the analysis. Taking advantage of the symmetry of the strip slab(or beam),

one half was simulated in the analysis.

6-2-1 Influence of the Reinforcement Ratio

The model used to examine the influence of the reinforcement ratio on the behavior of horizontally restrained strip slabs or beams is shown in Figure 6-4. As shown, the span of one half of the beam was divided into 6 elements and the depth was divided into three elements. At the center line of the span, horizontal restraints were provided and vertical displacement was not restrained. At the support, the elements located at the bottom fibers were horizontally restrained. Also, a vertical restraint was provided.

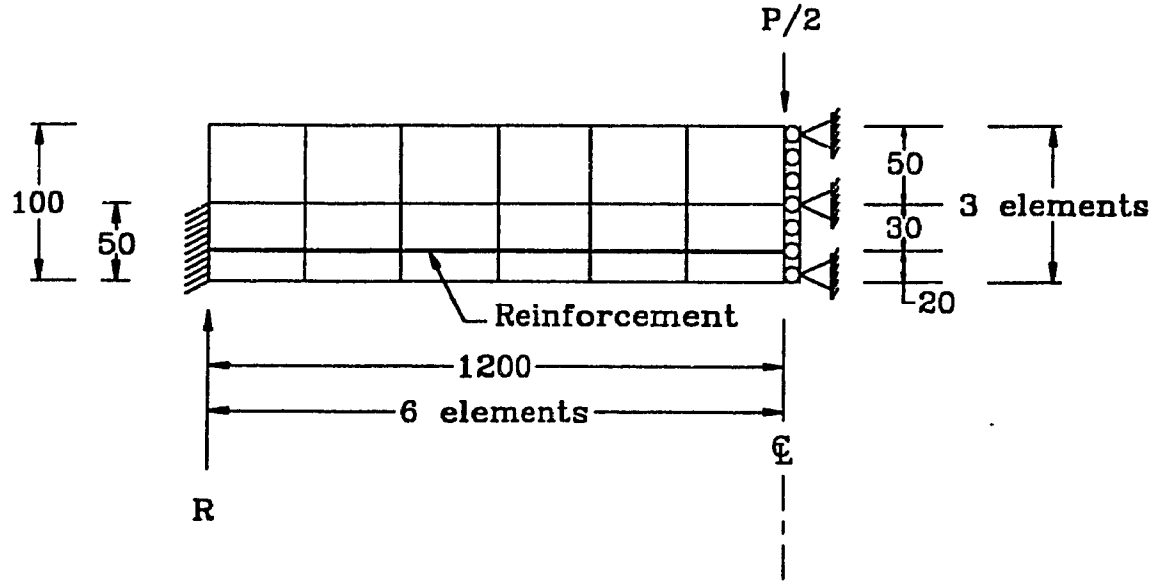

Figure 6-4 Model used to examine the influence of the reinforcement ratio

In the analysis that was presented in the preceding chapter, the reinforcement ratio was considered to be null. In this section, different reinforcement ratios were used and the maximum concentrated load that can be carried by the beam was obtained for every case. Several analyses were carried out. In the first analysis the reinforcement ratio was considered to be zero and in the subsequent analyses this ratio was increased to become maximum at the last analysis.

Figure 6-5 shows the value of the maximum load versus the ratio of the reinforcement. While running that analysis, the finite element program had difficulties performing convergence. Therefore, the path of the curve connects the ordinates that have upper concentrated load values.

The results obtained from the curve indicate that at zero reinforcement ratio the maximum concentrated load was 16.02 kN, which confirms the results that were obtained from the 3 dimensional analysis in the preceding section. In every subsequent analysis, the area of the steel was increased 50 mm^2 until it became 550 mm^2, which is slightly higher than maximum area steel (maximum area steel is 520.2 mm^2) required by the Canadian Code. The maximum area steel corresponds to a reinforcement ratio equal to 0.032513. At maximum reinforcement ratio, the maximum value of the concentrated load was 21.2 kN.

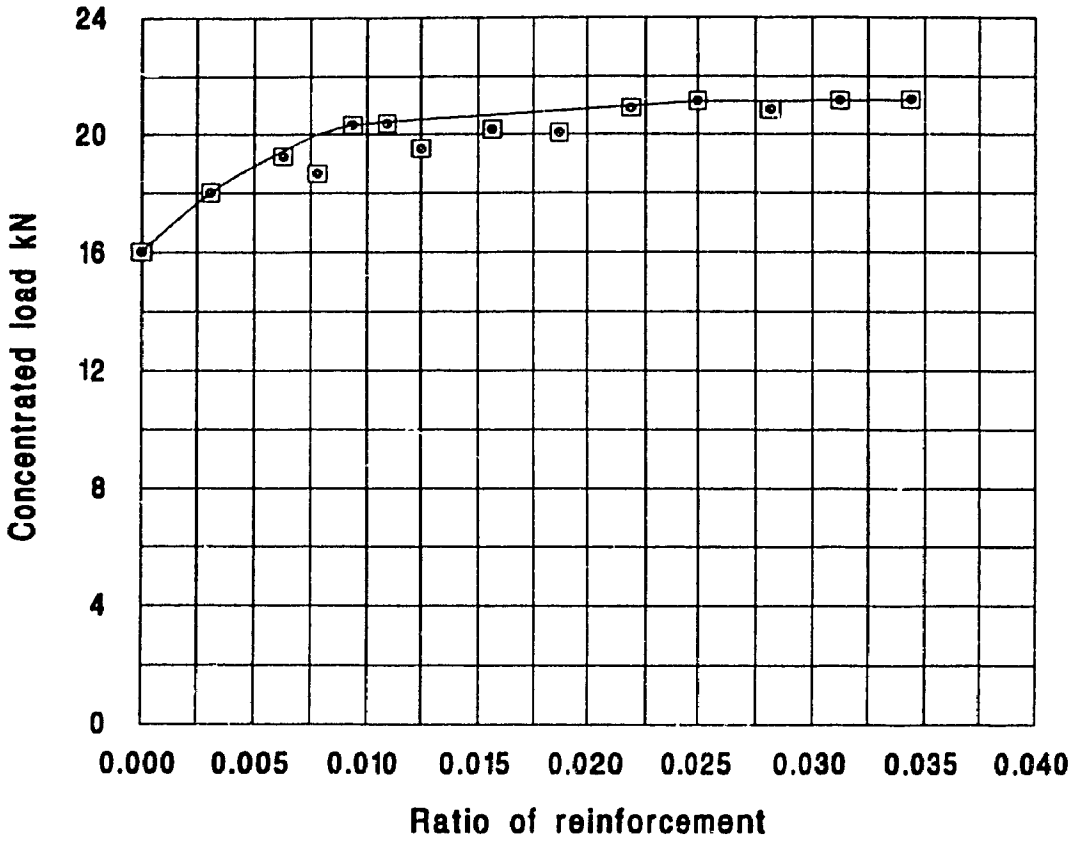

Figure 6-5 The reinforcement ratio versus the maximum load

As shown in the graph, there is an increase in the carrying capacity of the beam due to the presence of the reinforcement. Up to a reinforcement ratio equal to 0.01, which corresponds to area steel approximately equal to 150 mm^2, the maximum load was 20.32 kN which represents approximately a 20 percent addition in the carrying capacity. Increasing the area steel from 150 mm^2 to 550 mm^2 results in increase of the load from 20.32 kN to 21.20 kN which represents less than a 5 percent increase in the carrying capacity. From these results it can be

concluded that using more than 0.01 reinforcement ratio for the horizontally restrained strip slab (or beam) will result in a negligible increase in the carrying capacity and will also result in using additional steel that is not required. A sample of the programs that are used to perform the analysis presented in this section is given in Appendix B (Section B-4). This sample is for the case of area steel equal to 150 mm^2.

6-2-2 Influence of the Span to Depth Ratio

Finite element analyses were carried out to examine the influence of the span to depth ratio on the behavior of horizontally restrained strip slabs. During the analyses, different strip slabs were examined with shear span to depth ratio 'S/h', varying from zero to 20. The boundary conditions that were used in the analysis are shown in Figure 6-6.

A curve representing the shear span to depth ratio versus the concentrated load is presented in Figure 6-7. As can be seen from the presented curve, at a shear span to depth ratio equal to 20, the load that can be carried by the strip slab is 5.64 kN. This shear span 'S' is 2.0 meters with a depth of 0.1 meter. For the horizontally restrained non-reinforced strip slab, this load of 5.64 kN is approximately 5.6 times greater than its carrying capacity if it is horizontally non-restrained (assuming 30 MPa and 3 MPa as compression and tensile concrete strengths respectively and a cross section width equal to 200 mm).

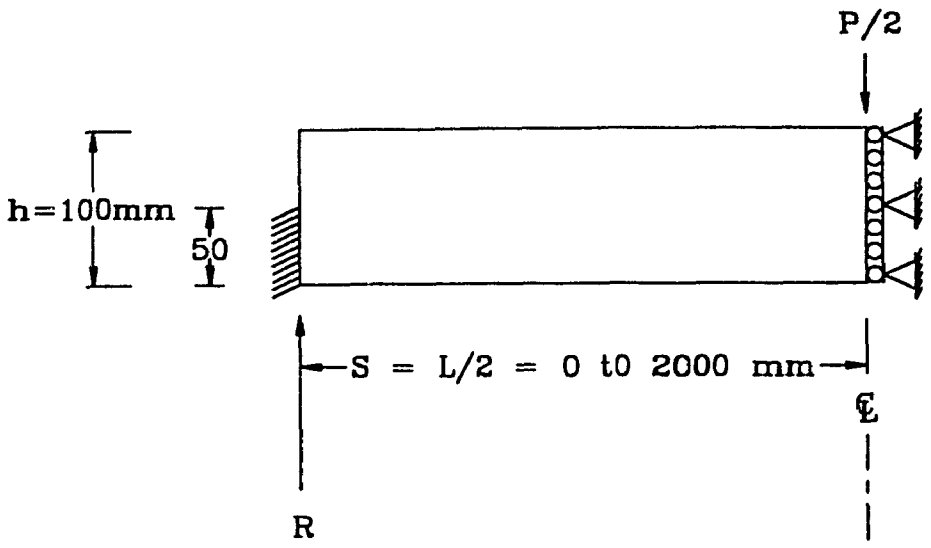

Figure 6-6 The boundaries used to examine the influence of the shear span to depth ratio

Decreasing the span of the strip slab (which decreases the shear span to depth ratio), the corresponding carrying capacity increases. When the shear span to depth ratio is approximately 6, the carrying capacity of the strip slab is controlled by its shearing strength. When this ratio is less than 6, the carrying capacity of the strip slab increases very rapidly. When the ratio is less than 1, the strip slab start to behave as a column. When the span of the strip slab is reduced to zero, that means, the span of the element which transfers the load to the support becomes null, that results in zero carrying capacity. A sample of the programs that are used to perform the analysis presented in this section is given in Appendix B (Section B-5). This sample is for the case of a shear span to depth ratio equal to 8 which corresponds to a span equal to 1.6 meter.

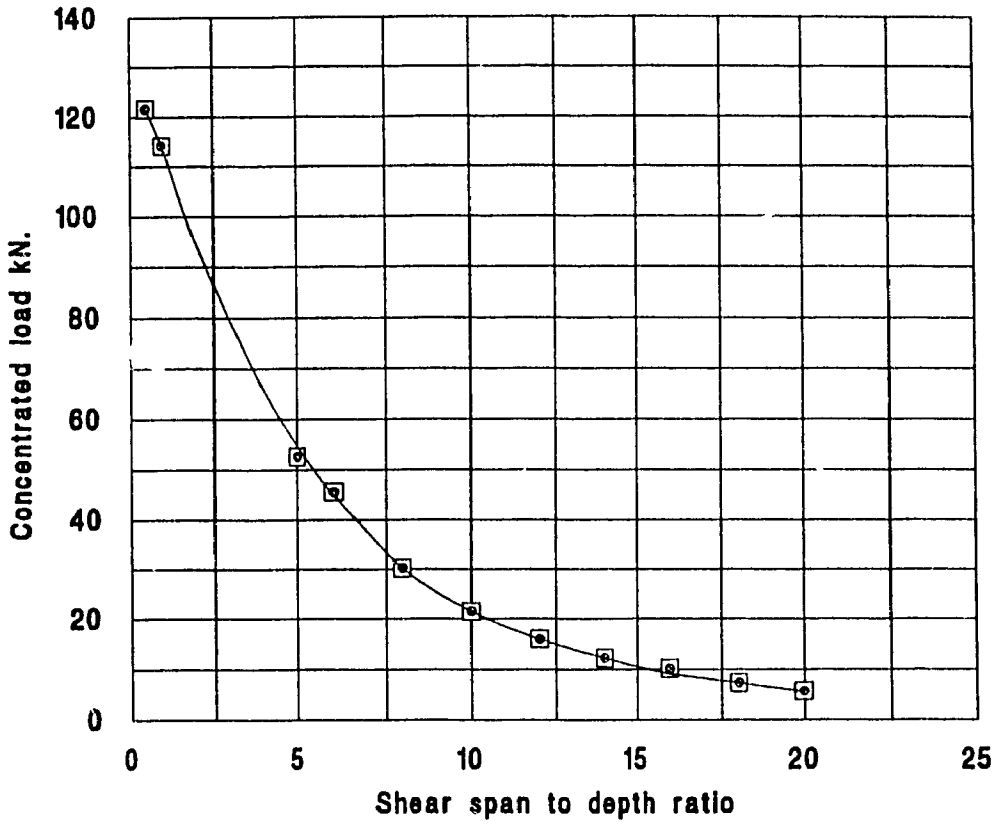

Figure 6-7 The shear span to depth ratio 'S/h' versus the concentrated load

6-2-3 Influence of the Stiffness of the Horizontal Elastic Support

The value of the stiffness of the horizontal elastic support has great influence on the value of the concentrated load that can be carried by the strip slab. For non-reinforced horizontally restrained strip slabs, when the value of the stiffness of the horizontal supports approaches infinity, the concentrated load can reach its maximum value. When this stiffness value is zero (a horizontally non-restrained strip slab), the carrying capacity will be controlled by the moment resistance of the

cross section of the strip slab at midspan.

The model shown in Figure 6-8 is used to examine the influence of the stiffness of the horizontal elastic support on the behavior of the strip slab. Spring elements were placed at bottom fibers of the strip slab at the location of the support to provide the horizontal restraints. Several analyses were carried out, each with a different stiffness value for the spring support.

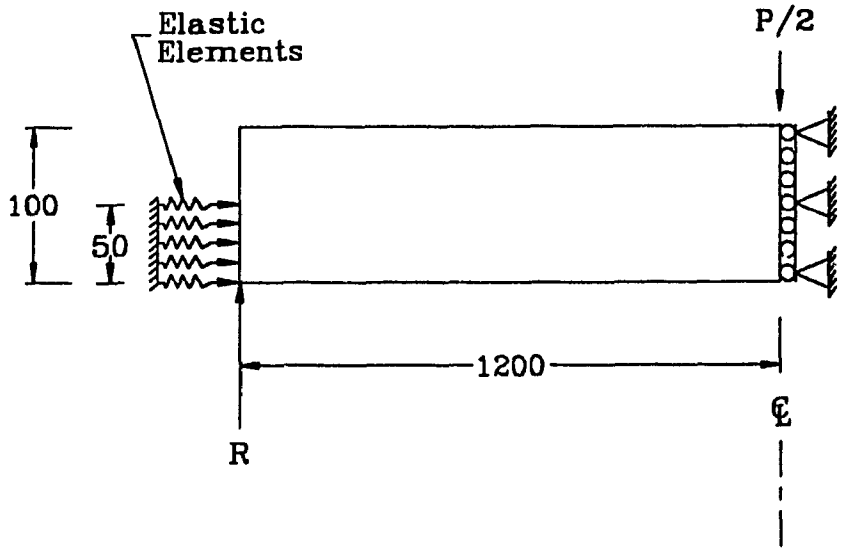

Figure 6-8 Model used to examine the influence of the stiffness of the elastic support

In the analysis, the values of the stiffness of the elastic supports were varied from zero (a strip slab horizontally non-restrained) to 625 kN per mm. To present the results, a ratio of the stiffness of the elastic support to the axial stiffness of the strip slab was used. The axial

stiffness of the strip slab (or beam) 'k_b' is defined as the axial force that can produce a unit axial deformation of the strip slab and is given as follows:

$$k_b = \frac{A \times E}{L}$$

where:

A is the cross section area $= 200 \times 100 = 20000\ mm^2$

E is the modulus of elasticity of the concrete $= 27368\ MPa$

L is the span of the strip slab $= 2400\ mm$

$$k_b = \frac{20000 \times 27368}{2400} \times 10^{-3} = 228.22\ kN\ per\ mm$$

The ratio of the stiffness of the elastic support '**k**' to the axial stiffness of the strip slab 'k_b' is equal to $\frac{k}{k_b}$. A curve representing the ratio of the elastic support stiffness to the strip slab axial stiffness versus the maximum load is presented in Figure 6-9. When the elastic support stiffness is zero, the carrying capacity of the strip slab is due to its flexural resistance at midspan and the load that can be carried by this strip slab is 2.7 kN.

Increasing the value of the elastic support stiffness from zero results in a rapid increase in the carrying capacity of the strip slab up to

a ratio (the ratio of the elastic support stiffness to the longitudinal strip slab axial stiffness) approximately equal to 0.75, which corresponds to a support stiffness equal to 180 kN. The load that can be carried by a strip slab at this ratio is approximately equal to 12.2 kN. After this ratio, increasing the stiffness of the support results in a slow increase in the carrying capacity of the strip slab. For example, when the stiffness of the support is increased to 625 kN (this value representing the experimental program value) which corresponds to a ratio approximately equal to 2.75, the concentrated load is increased to 13.36 kN (similar to the value obtained from the analytical analysis presented in Section 5-5).

When the support stiffness approaches infinity, the value of the concentrated load is increased to 16.02 kN as has been mentioned in the preceding section. It can be concluded that a horizontal elastic support having stiffness equal to or greater than 0.75 of the axial stiffness of the strip slab will result in a major increase in the carrying capacity of the strip slab. A sample of the programs that are used to perform the analysis that is presented in this section is given in Appendix B (Section B-6). This sample is for the case of an elastic support stiffness of approximately 180 kN per mm, which is equivalent to a ratio of approximately 0.75.

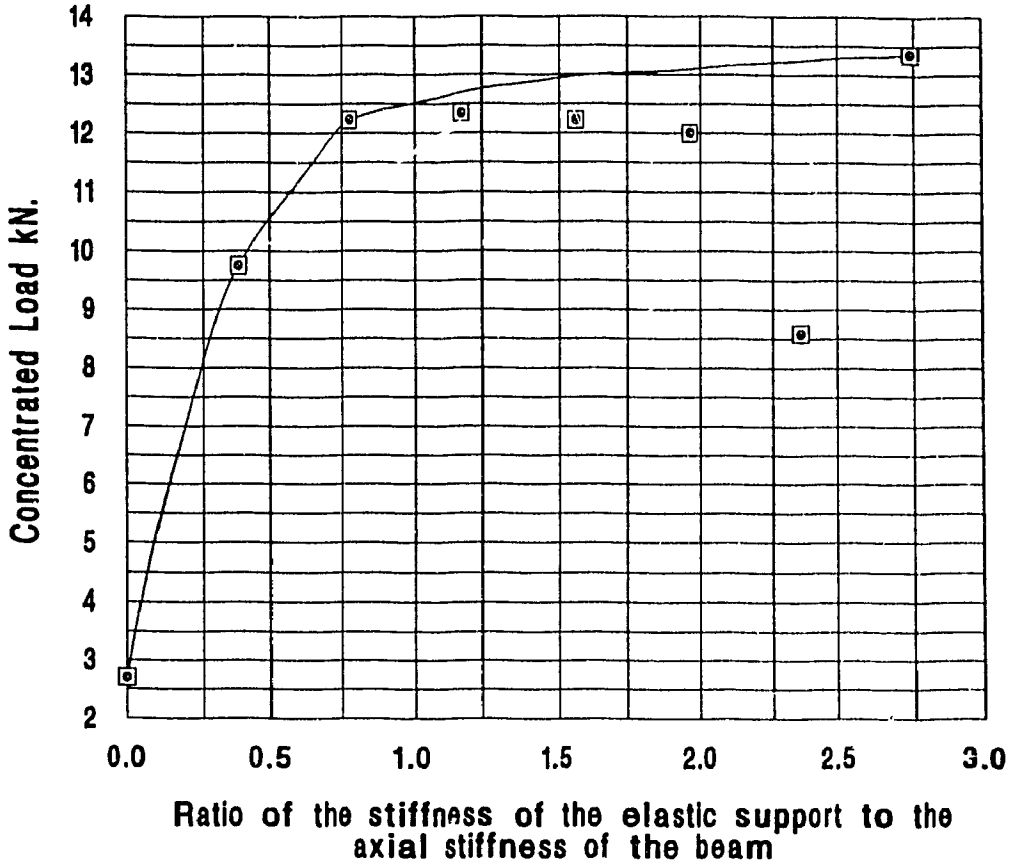

Figure 6-9 Influence of the ratio of the elastic support stiffness to the strip slab axial stiffness on the maximum load

6-3 Membrane Action (Arch Action) Versus Bending Effects

Several publications dealt with membrane action in slabs[84,85,86,87]. Membrane action has long been noted in both full-scale slabs and laboratory tests[46]. The earliest observations were made by Westergaard and Slater[48] in testing a number of full-scale slab panels. The tests indicated that the ultimate load attained was larger than expected. This

unexpected strength was due to membrane action.

Consider the behavior of a reinforced concrete slab under a transverse load at mid-span. As the slab deflects under the load, the concrete on the tension face cracks and the reinforcement is stretched. The strains on the tension face will be greater in magnitude than those on the compression face. The net tensile strain resulting at the slab mid-span causes the slab to expand, producing outward horizontal displacements at the slab ends. Restraining the horizontal displacements will induce compressive membrane forces in the slab. This compressive membrane action is called arch action.

The carrying capacities of horizontally restrained slabs (slabs working by arch action) are affected by the magnitude of the vertical deflections. Large vertical deflections negate the beneficial influences of arch action. On the other hand, the flexural resistance of horizontally non-restrained reinforced concrete slabs is independent of vertical deflection.

In horizontally non-restrained reinforced concrete slabs, the moment resistance of the slabs is due to a couple of compression force in the concrete and tension force in the reinforcements. In reinforced concrete beams or slabs, if the reinforcement is behaving as a tie, compressive membrane forces will be developed in the concrete, which will result in arch action. Usually, the reinforcement does not behave as

a tie, in all cases. Therefore, the carrying capacities of these beams and strip slabs are due to their bending moment resistance at mid-span. However, if these beams and strip slabs are horizontally restrained, their carrying capacity would be due to the arch action.

6-4 Influence of the Mortar as an Element in the Mesh

As shown in Figure 4-12 and 4-13 in Chapter 4, the tested strip slabs were horizontally restrained by a 50 mm thick steel plate. A 10 mm vertical layer of mortar was placed between the ends of the strip slabs and the steel plate. In the analysis that was presented in Chapter 5 and in the comparison between the experimental and theoretical results that will be presented in the next chapter, the layer of mortar is assumed to have negligible effects on the obtained results. Since the layer of mortar was subjected to compression stresses, this layer would deform. The deformation of the mortar would result in a horizontal displacement. The carrying capacity of the strip slabs would be reduced if this horizontal displacement had any significant value. Since the compression strength of the mortar is similar to or slightly less than the compression strength of the concrete (according to experimental results), the deformation of a layer of mortar that has 10 mm of thickness under compression stress is negligible.

A finite element analysis was carried out to examine the effect of

this layer of mortar. The model used in the analysis is shown in Figure 6-10. A mortar layer was placed at the bottom fibers at the end of the strip slab. Also, a horizontal elastic support was placed at the other end of the mortar layer. The stiffness of the elastic support was 625 kN per mm, which is the value of the experimental set-up.

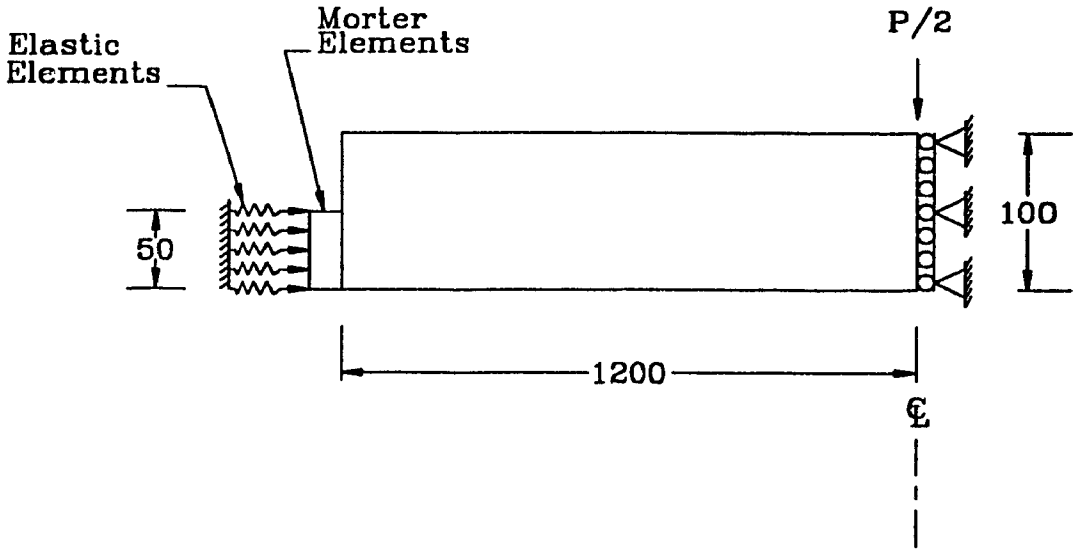

Figure 6-10 The model used to simulate the effect of the mortar

As was mentioned earlier, a very thin layer of mortar has no effect on the carrying capacity of the strip slab. Greatly increasing the thickness of the layer of the mortar will slightly affect the carrying capacity of the strip slab. For example, increasing the thickness of the mortar layer to 200 mm will result in a carrying capacity of 11.52 kN. This means that increasing the thickness of the layer of the mortar 20 times results in decreasing the concentrated load by less than 14 percent

(the concentrated load that was obtained for a similar case in the preceding section was 13.36 kN). It can be concluded that the presence of a layer of mortar having a thickness of 10 mm will result in negligible effect on the carrying capacity of the strip slabs. The program that was used to perform the analysis for the case of a layer of mortar having a thickness of 200 mm is given in Appendix B (Section B-7).

Chapter 7

Comparison of Theoretical Analysis Results and Experimental Results

A comparison between the theoretical analysis results and the experimental results will be carried out, as will be shown below, for the two series of tests. Before comparing between the results of the theoretical analysis presented in Chapter 5 and the experimental results presented in Chapter 4, some factors which enhance the carrying capacity of the tested horizontally restrained strip slabs will be analyzed. These factors are the presence of reinforcement in each strip slab and the existence of partial restraints against rotations at the extremities of each strip slab.

7-1 Factors Affecting the Carrying Capacities of the Tested Slabs

One of the factors that affect the value of the maximum concentrated loads that were carried by the tested horizontally restrained strip slabs was their light amount of tension and compression reinforcement. This reinforcement enhances the carrying capacity of the strip slabs.

For the strip slabs with horizontal restraints, 4 reinforcement bars with a diameter of 6 mm were used. Two bars were placed at the top fibers and two bars at the bottom fibers. The vertical distance between the top and bottom bars was 61 mm, measured from the center of the bars. The cross sections of these slabs are shown in Figure 7-1.

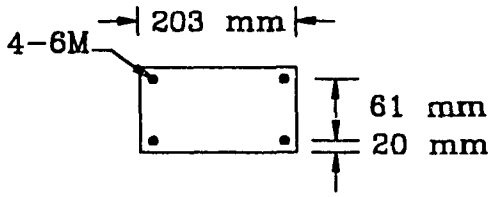

Figure 7-1 Cross section for slabs with horizontal restraints

Tension tests on the 6 mm diameter steel bars indicate that their yield strength 'f_y' is 504.4 MPa and 456.24 MPa for the bars of the first series and the second series respectively (see Chapter 4).

When a non-reinforced horizontally restrained strip slab is on verge of collapse, it has at midspan a significant depth 'a' of the compression zone. The resisting bending moment of this strip slab is controlled by the depth 'a' of the compression zone and the compression strength of the concrete. For a horizontally restrained strip slab that has compression and tension reinforcement where the amount of the compression reinforcement is equal to the amount of the tension reinforcement, there is an additional bending moment due to this

reinforcement. Assuming the tension force that is acting in the tension reinforcement is equal to the compression force that is acting in the compression reinforcement and that both forces are corresponding to the maximum force that can be carried by the reinforcement at its yielding conditions, this additional bending moment, for the first series, is calculated as follows:

$$M_1 = f_y \times A_s \times d_1$$

$$M_1 = 504.4 \times 56.55 \times 61 \times 10^{-6} = 1.74 \ KN.m \quad \ldots\ldots\ldots \quad (7\text{-}1)$$

And for the second series,

$$M_2 = f_y \times A_s \times d_1$$

$$M_2 = 456.24 \times 56.55 \times 61 \times 10^{-6} = 1.574 \ KN.m \quad \ldots\ldots\ldots \quad (7\text{-}2)$$

Where 'A_s' is the area steel of two bars of 6 mm in diameter and is equal to 56.55 mm^2, 'd_1' is the distance between the top and bottom bars and is equal to 61 mm and 'f_y' is the yield strength of the steel and equal to 504.4 MPa and 456.24 MPa for the steel of the first and the second series respectively.

For simply supported beams subjected to concentrated loads at midspan, the bending moment 'M' at midspan is given as:

$$M = \frac{P \times L}{4}$$

Where L is the span of the beam.

If the bending moment 'M' is given, the concentrated load 'P' can be obtained as follows:

$$P = \frac{4 \times M}{L}$$

Using the above equation for the simply supported strip slabs of the first series with spans of 2.4 meters each, the above bending moments 'M_1', given by Equation (7-1), can be produced by a concentrated load 'P_1' equals to 2.90 kN placed at the center of the strip slabs. Similarly, for the simply supported strip slabs of the second series with spans of 2.421 meters each, the above bending moments 'M_2', given by Equation (7-2), can be produced by a concentrated load 'P_1' equal to 2.60 kN placed at the center of the strip slabs. This amount of additional load 'P_1' (due to the presence of tension and compression reinforcement) and its effects must be added to the load that is calculated from the analysis presented in Chapter 5.

As has been mentioned in Chapter 4, each series consisted of 6 strip slabs. In the second series of tests, some modifications were introduced to the supports. For the first series, the strip slabs with horizontal restraints were supported as shown in Figure 7-2.

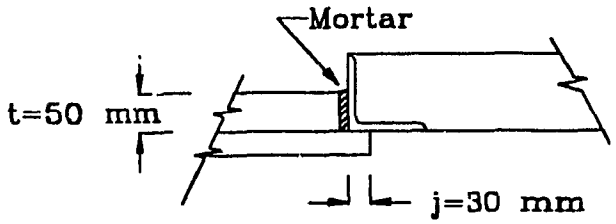

Figure 7-2 End conditions for slabs with horizontal restraint (first series)

As shown in Figure 7-2, an end of the horizontally restrained strip slab, in the first series, is resting on a support 30 mm in width and is restrained horizontally by a vertical support 50 mm in depth. Normally, rotations of the end edges over the supports are to be expected due to the application of the concentrated load at the center of the slab. However, this arrangement (shown in Figure 7-2) is partially restraining the rotations of the ends of the strip slabs over the support and is introducing fixed end bending moment 'M_f'.

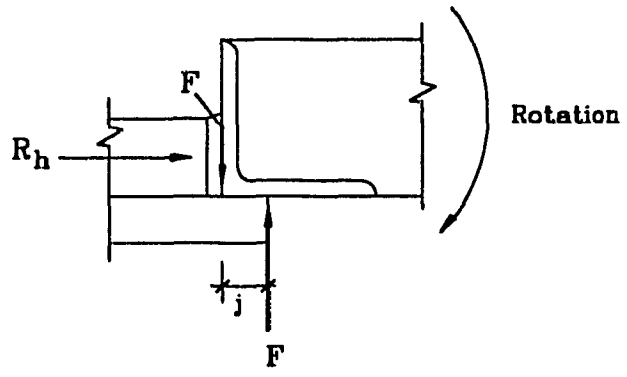

Figure 7-3 Forces restraining rotation at the support

As shown in Figure 7-3, due to the presence of the horizontal reaction 'R_h' a vertical friction force 'F' was introduced between the vertical end surface of the slab and the mortar. The end rotation was partially restrained by a couple of forces 'F': the vertical friction force at the extreme end of the strip slab and an equivalent force at the edge of the support. The value of the friction force 'F' due to the presence of the horizontal reaction 'R_h' is as follows:

$$F \leq \mu \times R_h \qquad \text{..... (7-3)}$$

Where μ is the friction coefficient.

The value of bending moment 'M_f' due to the presence of this couple is calculated as follows:

$$M_f = F \times j = \mu \times R_h \times j$$

Where j is shown in Figure 7-3.

The value of the moment 'M_f' given by the above equation is a function of the value of the friction force 'F' and, in turn, the value of the friction force is a function of the horizontal reaction 'R_h' and the coefficient of friction 'μ'. The value of the friction coefficient 'μ' is a

function of the smoothness of the texture and the strength of the mortar.

It can be concluded from the above discussion that in the first series of tests, fixed end bending moments were produced at the extremities of the strip slabs due to the partial restraints against rotation.

The value of the coefficient of friction 'μ' between the mortar and the steel is unknown. According to Murashev[74] et al. this coefficient varies within wide limits.

According to the Canadian Code CSA[57], the coefficient of friction 'μ' for concrete placed against as-rolled structural steel is 0.6. The coefficient of friction 'μ' for mortar placed against steel should be less than the friction coefficient of the concrete because the components of the mixture of the mortar do not have coarse aggregates. Therefore, the texture of the mortar has a lesser degree of roughness than the concrete.

In spite of the above discussion, an assumed maximum value of 0.6 for the coefficient of friction 'μ' between the mortar and the steel was used to establish an upper limit to the friction force 'F' as given by Equation (7-3). Assuming an average horizontal reaction 'R_h' equal to 270 kN, the maximum friction force 'F_{max}' at the ends of the strip slabs can be calculated as follows:

$$F \leq 270 \times 0.6 = 162 \; kN$$

$$F_{max} = 270 \times 0.6 = 162 \; kN$$

The actual value of 'F' can be equal to or less than 162 kN. Since its upper limit is equal to 162 kN, then a lower limit value needs to be established. The average value between the upper and the lower limits will be used in calculating the fixed end moment 'M_f'.

Since the surface of the mortar must have a certain degree of roughness and since the mortar is cementitious mortar which has a certain adhesion between its surface and the steel, the minimum friction coefficient cannot be zero. According to Murashev[74] et al., the adhesion between an ordinary concrete and steel surface varies from 2.5 to 3.9 N/mm^2. Since the minimum value of the coefficient of friction between the mortar and the steel cannot be determined, an average value of 3.2 N/mm^2 for the adhesion based on the values given by Murashev was used.

Although the adhesion value given by Murashev[74] et al. is for ordinary concrete, this value was used for the mortar because the adhesion of the concrete as well as the adhesion of the cementitious mortar is due to the cement content and the water ratio in the mixture. The lower limit of the value of 'F', which is 'F_{min}' can be calculated as follows:

$$F_{min} = t \times b \times the\ adhesion$$

$$F_{min} = 50 \times 203 \times 3.2 \times 10^{-3} = 32.5 \ kN$$

Where 't' and 'b' are the depth and the width of the support which is providing horizontal restraint and are 50 mm and 203 mm respectively ('t' is shown in Figure 7-2). The value of the adhesion is 3.2 N/mm^2.

The average value of 'F' can be calculated as follows:

$$F = \frac{F_{max.} + F_{min}}{2} = \frac{162 + 32.5}{2} = 97.2 \ kN$$

The fixed end bending moment 'M_f' at the extremities of the horizontally restrained strip slabs of the first series can be calculated as follows:

$$M_f = F \times j$$

$$M_f = 97.2 \times 0.03 = 2.9 \ KN.m$$

Where the value of 'j' is shown in Figure 7-3.

The presence of the fixed end bending moment 'M_f' will increase the carrying capacity of the simply supported horizontally restrained strip slabs. This additional carrying capacity must be taken into account during the comparison between the theoretical analysis and the results

obtained from the experimental tests.

As shown in Figure 7-4, the load 'P_2' that can produce a fixed end bending moment equal to 2.9 kN.m can be obtained assuming partial restraints against rotation at joints 'b' and 'c'. Also, by performing the analysis that is presented in Chapter 5 on the strip slabs with horizontal restraints, the exact depth 'r' of the structure (or the rise of the structure) can be calculated.

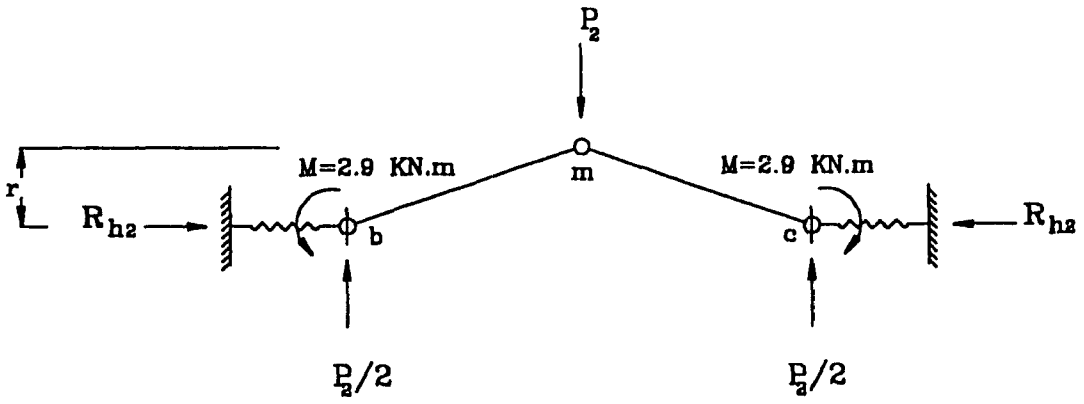

Figure 7-4 Effects of partial restraints against rotations

This load 'P_2' and its effects will be added to the maximum analytical load 'P_c' which is calculated from the analysis of Chapter 5 and to the load 'P_1' which is obtained due to the presence of the tension and compression reinforcement.

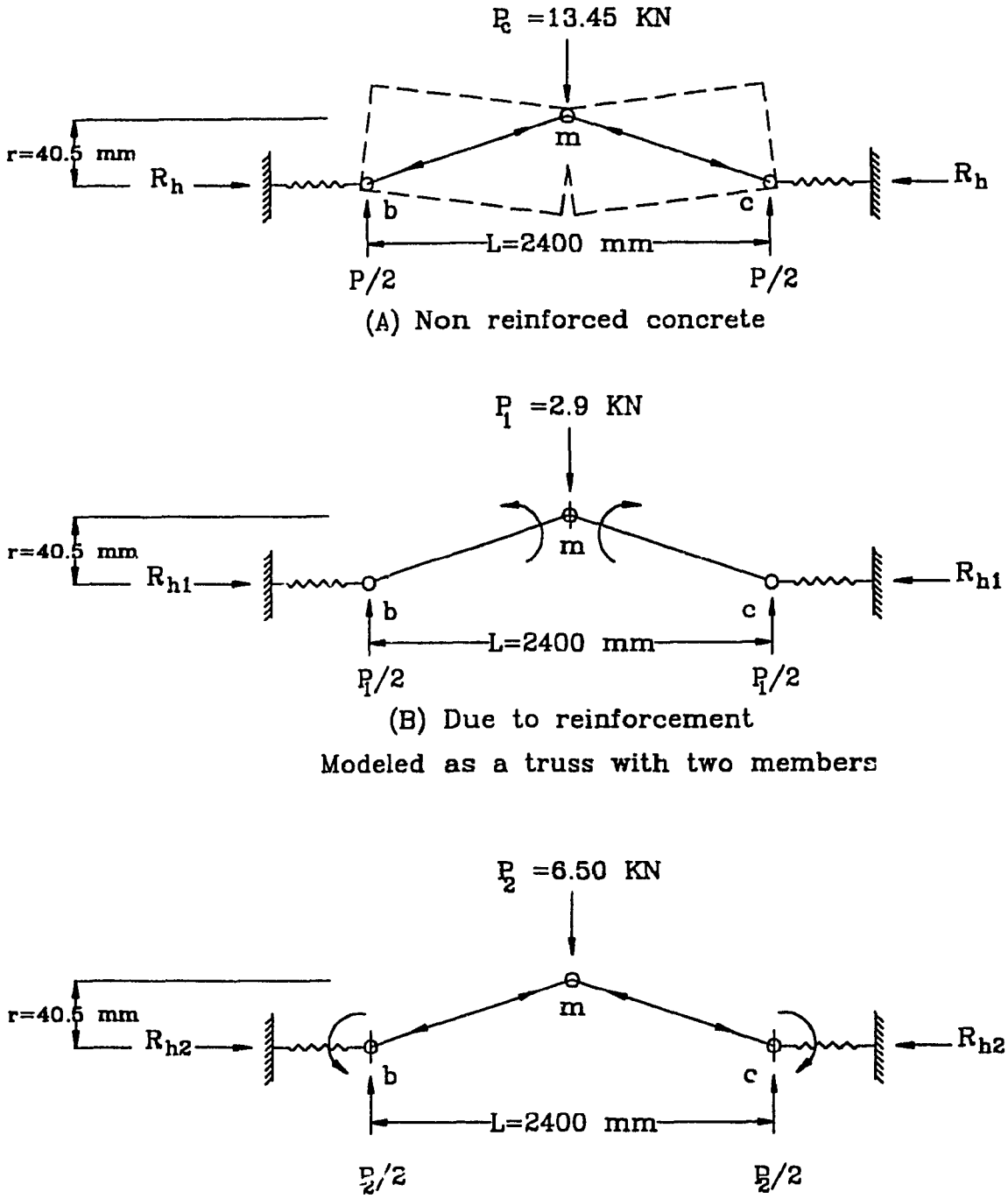

Figure 7-5 Loads acting on the horizontally restrained strip slabs

7-2 First Series of Tests

The dimensions and properties of the concrete of each strip slab are presented in Chapter 4. For the strip slab of test S1, the load and deflection calculated by the analysis of Chapter 5 are shown in Figure 7-5-A and presented in Table 7-1. The additional load 'P_1' due to the presence of the tension and the compression reinforcement is shown in Figure 7-5-B. Also, a restraint is provided at joint 'm' in Figure 7-5-B to indicate that there is a bending moment due to the presence of the reinforcement at midspan.

The additional load 'P_2' due to the fixed end bending moment at the extremities of strip slab S1 is shown in Figure 7-5-C. Also, partial restraints are provided at joints 'b' and 'c'.

A value of a spring constant 'k' equal to 625 kN/mm was used in the calculation presented in Table 7-1. This value is the actual spring constant of the set-up used in the experimental program. The structural scheme of the set-up is presented in Appendix 'C' (Section C-1). The value of the spring constant 'k' is obtained by applying horizontal loads (which are actually the horizontal reactions 'R_h') as shown in Appendix 'C' (Section C-1) and calculating the corresponding horizontal deflections 'w_h'. Then, knowing these values, a value for the load that can produce a unit deflection was calculated as follows:

$$k = \frac{R_h}{w_h}$$

Where the value of this load is the required spring constant 'k' (or the spring stiffness) and is defined as the value of the load that can deflect the spring support one unit.

The value of the load 'Pc', that is shown in Figure 7-5, was obtained assuming this load is acting alone on the strip slab (the corresponding value of the horizontal reaction was 199.3 kN). To maintain compatibility (to take into account the effect of the other loads 'P1' and 'P2' considering that they act on the strip slab simultaneously with 'Pc'), the vertical deflections due to loads 'P1' and 'P2' were used as an imposed deflection to modify the value of the depth of the compression zone 'a' obtained from Equation (5-4).

$$a = \frac{h}{2} - \frac{w_1 + w_2}{2} = \frac{104}{2} - \frac{23.01 + 3.96}{2} = 38.52\ mm$$

Where 'w_1' is the deflection due to the load 'Pc'

'w_2' is the deflection due to the loads 'P1' and 'P2' =1.22+2.74

The value of the force 'F' (as shown in Figure 5-12) can be calculated as follows:

$$F = 0.85 \times f_c' \times a \times b \times \frac{1}{\cos\theta} = 0.85 \times 28.55 \times 38.52 \times 203 \times \frac{1}{0.999} \times 10^{-3} = 189.93\ kN$$

The value of the horizontal reaction 'R_h' is

$$R_h = F \times \cos\theta = 189.93 \times 0.999 = 189.74 \ kN$$

The modified rise of the structure 'r' is

$$r = h - (w_1 + w_2) - a = 104 - (23.01 + 3.96) - 38.52 = 38.52 \ mm$$

The modified value of the load 'Pc' due to the additional deflection obtained from loads 'P1' and 'P2' is

$$Pc = \frac{R_h \times r \times 4}{L} = \frac{189.74 \times 38.52 \times 4}{2400} = 12.18 \ kN$$

Table 7-1 Calculated loads, deflections and reactions acting on slab S1 at failure

Type of Load	Load kN	Deflection mm	Horizontal Reaction kN	Vertical Reaction kN
Pc	12.18	23.01	189.74	6.09
P1	2.90	1.22	11.03	1.45
P2	6.50	2.74	24.73	3.25
Total	21.58	26.97	225.5	10.79

Table 7-2 Calculated loads, deflections and reactions acting on slab S2 at failure

Type of Load	Load kN	Deflection mm	Horizontal Reaction kN	Vertical Reaction kN
Pc	14.60	23.73	219.54	7.30
P1	2.90	1.07	10.43	1.45
P2	6.44	2.38	23.18	3.22
Total	23.94	27.18	253.15	11.97

Table 7-3 Calculated loads, deflections and reactions acting on slab S3 at failure

Type of Load	Load KN	Deflection mm	Horizontal Reaction KN	Vertical Reaction kN
Pc	17.06	23.33	238.91	8.53
P1	2.90	0.93	9.87	1.45
P2	6.45	2.06	21.96	3.22
Total	26.41	26.32	270.74	13.20

Table 7-4 Calculated loads, deflections and reactions acting on slab S4 at failure

Type of Load	Load kN	Deflection mm	Horizontal Reaction kN	Vertical Reaction kN
Pc	19.89	23.16	261.61	9.95
P1	2.90	0.80	9.32	1.45
P2	6.46	1.79	20.76	3.23
Total	29.25	25.75	291.69	14.63

A similar analysis for the tested strip slabs S2, S3 and S4 was performed and the results are presented in Tables 7-2, 7-3 and 7-4 respectively. All results were calculated considering the actual compression strength of the concrete and the exact dimensions of the cross section of each specimen.

The value of the maximum loads 'P' obtained from the theoretical analysis and the experimental tests for strip slabs horizontally restrained differ very much from the maximum concentrated load 'P' that can be calculated according to present codes of practice. The cause of this discrepancy is due to ignoring the effects of the horizontal restraints on the behavior of the slabs in the codes of practice. According to present

codes of practice, horizontally restrained flexural members would be treated as if they were simply supported without horizontal restraints.

A comparison of the theoretical and the experimental results is presented in Table 7-5. The rises 'r' (shown in Figure 7-5) are calculated according to the analysis presented in Chapter 5 (assuming the load 'Pc' is acting alone on the strip slab). The ratios of the theoretical failure loads 'P_{theo}' to experimental failure loads 'P_{exp}' are also presented. The maximum variation between theoretical and experimental loads is about 18%.

Table 7-5 Comparison of theoretical and experimental results for slabs S1, S2, S3 and S4 (slabs with horizontal restraints)

Test No.	Dimension of Cross Sections h * b mm*mm	Concrete Strength f'_c MPa	Experimental Failure Load 'P_{exp}' kN	Theoretical Failure Load 'P_{theo}' kN	Ratio Of 'P_{theo}' Over 'P_{exp}'	Experimental Deflection 'w_{exp}' mm	Theoretical Deflection 'w_{theo}' mm	Rise 'r' mm
S1	104x203	28.55	21.97	21.58	0.982	23.36	26.97	40.50
S2	107x203	31.88	28.15	23.94	0.850	30.89	27.18	41.64
S3	112x203	32.32	23.31	26.41	1.133	29.05	26.32	44.34
S4	117x203	33.23	35.59	29.25	0.822	29.62	25.75	46.94

A comparison of the theoretical load 'P_c', that can be carried by the horizontally restrained strip slabs calculated according to the analysis of Chapter 5, and the maximum load 'P_{cod}' calculated according to the present codes of practice is presented in Table 7-6. The loads 'P_{cod}' and their corresponding deflections were calculated assuming simply supported horizontally non-restrained non-reinforced strip slabs. The loads 'P_c' and their corresponding deflections were calculated based on the structural scheme shown in Figure 7-6 and assuming non-reinforced concrete strip slabs.

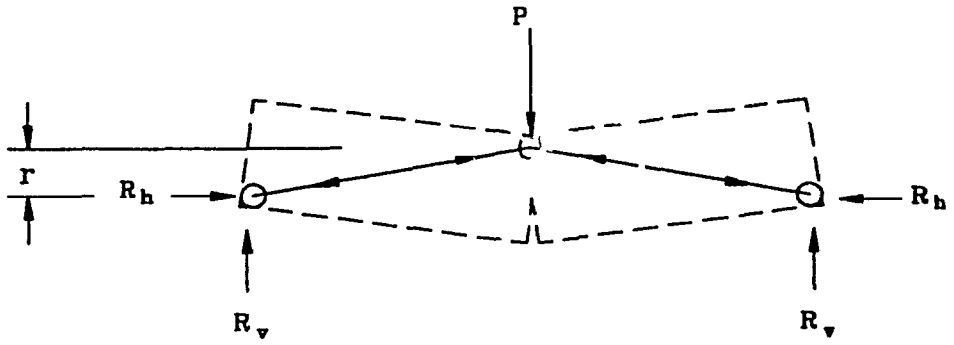

Figure 7-6 Structural scheme to calculate theoretical loads and deflections (assuming infinitely rigid horizontal supports)

In Figure 7-6, the loads 'P_{cod}' were calculated according to the present codes of practice assuming non-reinforced strip slabs. The deflections corresponding to the loads 'P_{cod}' were calculated using the beam theory. A sample of the calculation of 'P_{cod}' and its corresponding

deflection is presented in Appendix 'C' (Section C-2) for strip slab S1.

A comparison of the experimental results and the results obtained from an analysis according to present codes of practice for the fully reinforced simply supported horizontally non-restrained strip slabs of the first series is presented in Table 7-7. The tension reinforcement of these slabs is 3-15M (3 bars with diameter of 16 mm each) and the compression reinforcement is 2 bars of 6 mm diameter each.

Table 7-6 Comparison of results obtained according to the analysis presented in Chapter 5 and results obtained according to present codes of practice for strip slabs S1, S2, S3 and S4

Test No	Theoretical Failure Load 'P_c' kN	Load Due to Codes 'P_{cod}' kN	Ratio Of 'P_{cod}'/'P_c'	Deflection Due to Load 'P_c' mm	Deflection Due to Load 'P_{cod}' mm
S1	16.69	1.96	0.117	13.79	1.11
S2	20.06	2.19	0.109	13.41	1.07
S3	22.83	2.41	0.106	12.83	1.03
S4	26.17	2.69	0.103	12.29	0.99

The theoretical failure loads 'P_{theo}' presented in Table 7-7 are

calculated according to the Canadian Code CSA. These capacities were predicted ignoring horizontal restraint effects. The reduction factors presented in this code are ignored. A sample of these calculations is presented in Appendix 'C' in Section C-3 (calculations for theoretical failure load for slab S5).

For the first series of tests, the yield strength 'f_y' for bars of 16 mm in diameter and 6 mm in diameter was 441.12 MPa and 504.4 MPa respectively. These values were obtained from experimental tension tests that were carried out on the steel bars (the results of these tests are presented in Chapter 4). The cross sections of the fully reinforced simply supported horizontally non-restrained strip slabs of the first series are as shown in Figure 7-7. The above mentioned values of the yield strength 'f_y' and the cross section dimensions shown in Figure 7-7 were used in calculating the failure loads 'P_{theo}' presented in Table 7-7

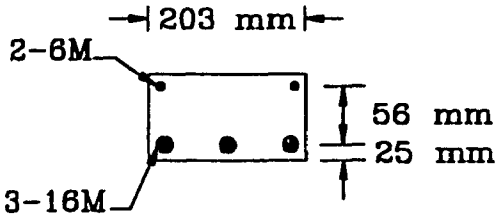

Figure 7-7 Cross section for simply supported strip slabs

Load deflection curves presented in Chapter 4 show the experimental results of strip slabs with and without horizontal restraints.

To compare the experimental results of these two types of slabs accurately, several variables should be considered such as the concrete strength f'_c and the cross-sectional dimensions.

Table 7-7 Comparison of theoretical and experimental results for slabs S5 and S6 (simply supported, without horizontal restraints)

Test No	Dimension of Cross Sections h * b mm*mm	Concrete Strength f'_c MPa	Experimental Failure Load 'P_{exp}' kN	Theoretical Failure Load 'P_{theo}' kN	Ratio Of 'P_{theo}' Over 'P_{exp}'
S5	117x203	34.14	36.92	30.34	0.822
S6	113x203	32.58	35.32	28.17	0.798

Table 7-8 shows a comparison of the experimental failure loads of slab S4 which was horizontally restrained and slab S5 which was fully reinforced horizontally non-restrained. Both slabs have similar cross sectional dimensions and concrete strength. A similar comparison of slabs S3 and S6 is presented. In Table 7-8, the 'P_{exp1}' and 'P_{exp2}' are the experimental failure loads for slabs with horizontal restraints and slabs without horizontal restraints respectively. The ratio of experimental failure loads 'P_{exp1}' to 'P_{exp2}' is also presented.

Table 7-8 A comparison of the experimental failure loads for strip slabs with and without horizontal restraints

Support Conditions	With Horizontal Restraints	Without Horizontal Restraints	With Horizontal Restraints	Without Horizontal Restraints
Test No	S4	S5	S3	S6
Dimensions	117x203	117x203	112x203	113x203
f_c' MPa	33.23	34.14	32.32	32.58
P_{exp1} kN	35.59	-	23.31	-
P_{exp2} kN	-	36.92	-	35.32
Ratio P_{exp1}/P_{exp2}	0.964		0.660	

The concrete strength and the cross sectional dimensions vary for each slab test. To eliminate the effect of these variables on the comparison of the failure loads for all the strip slabs of the first series, the relative strength 'R' was considered. This relative strength 'R' can be defined as the maximum relative concentrated load (dimensionless) that can be carried by a strip slab having cross section area equal to a unity as well as having a concrete with compression strength equal to a unity. The relative strength 'R' is calculated as follows:

$$R = \frac{P_{exp}}{(h \times b \times f_c')}$$

where:

'P_{exp}' is the experimental failure load

'h' and 'b' are the depth and width of the cross section

A comparison of the relative strength 'R' for all the slab tests of the first series is presented in Table 7-9.

Table 7-9 Relative strength of all the strip slabs of the first series

Test No	Experimental Failure Load 'P_{exp}' kN	Relative Strength R 10^{-3}	Horizontal Restraints
S1	21.97	36.45	Restrained
S2	28.15	40.65	Restrained
S3	23.31	31.72	Restrained
S4	35.59	45.09	Restrained
S5	36.92	45.53	Non
S6	35.32	47.26	Non

7-3 Second Series of Tests

In the second series of tests, the two fully reinforced horizontally non-restrained strip slabs 'S7' and 'S8' were tested first. A comparison

between the theoretical failure load 'P_{theo}' according to present codes of practice and the experimental failure load 'P_{exp}' is presented in Table 7-10. The cross sections and the reinforcement of these slabs are shown in Figure 7-7. The steel yield strength 'f_y' for bars of 6 mm and 16 mm in diameter is equal to 456.24 MPa and 370.5 MPa respectively (obtained from experimental tension tests on the steel bars of the second series).

Table 7-10 Comparison of theoretical and experimental results for slabs S7 and S8 (simply supported, without horizontal restraints)

Test No	Dimension of Cross Sections h * b mm*mm	Concrete Strength f_c' MPa	Experimental Failure Load 'P_{exp}' kN	Theoretical Failure Load 'P_{theo}' kN	Ratio Of 'P_{theo}' Over 'P_{exp}'
S7	113x203	45.65	25.31	27.00	1.067
S8	117x203	37.55	28.39	27.40	0.965

The cross sections for the strip slabs with horizontal restraints in the second series of tests are shown in Figure 7-1. The bending moment that can be carried by the provided tension and compression reinforcement is given by Equation (7-2) and equals 1.574 kN.m. The load 'P_1' which can produce the above bending moment for a simply

supported beam with a span of 2.421 meters is 2.60 kN. Similarly to the analysis presented for the first series, this load and its effects should be added to the load 'P_c' calculated according to the analysis presented in Chapter 5.

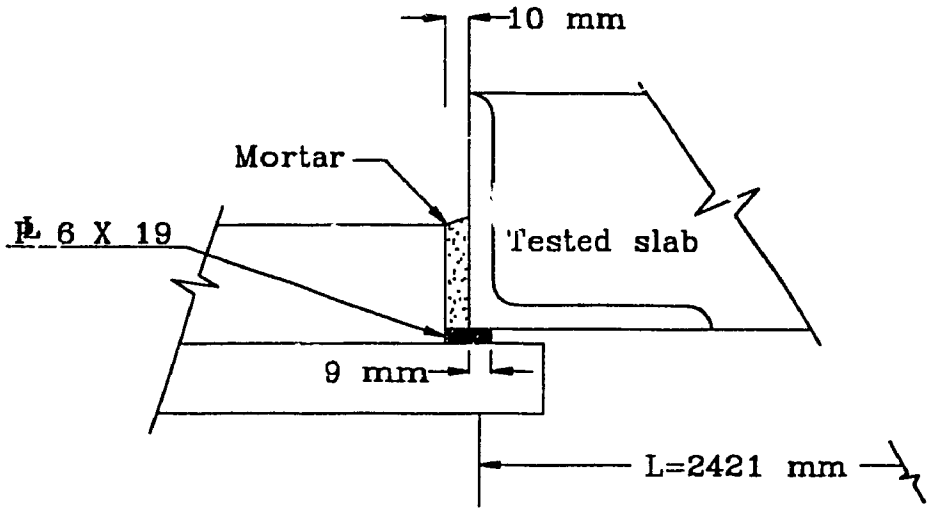

Figure 7-8 Details of the modified end conditions for second series

Modifications to the supports of the test set-up to minimize the partial restraint against rotations are shown in Figure 7-8. These modifications reduced the fixed end bending moment at the extremities of the horizontally restrained strip slabs in the second series to become 33% of the value of the first series. Therefore, the value of the fixed end bending moment due to the partial restraint against rotations used in the second series is 0.97 kN.m. Due to these modifications, the span of the strip slabs changed to become 2421 mm (as shown in Figure 7-8). The calculated loads and deflections for the tested strip slabs of the second

series, numbers S9, S10, S11 and S12, are presented in Tables 7-11, 7-12, 7-13 and 7-14.

Table 7-11 Calculated loads, deflections and reactions acting on slab S9

Type of Load	Load kN	Deflection mm	Horizontal Reaction kN	Vertical Reaction kN
Pc	19.41	23.34	257.41	9.70
P1	2.60	0.76	8.56	1.30
P2	2.15	0.63	7.08	1.07
Total	24.16	24.73	273.05	12.07

Table 7-12 Calculated loads, deflections and reactions acting on slab S10

Type of Load	Load kN	Deflection mm	Horizontal Reaction kN	Vertical Reaction kN
Pc	20.53	25.15	284.13	10.27
P1	2.60	0.76	8.43	1.30
P2	2.11	0.62	6.84	1.05
Total	25.24	26.48	299.40	12.62

Table 7-13 Calculated loads, deflections and reactions acting on slab S11

Type of Load	Load kN	Deflection mm	Horizontal Reaction kN	Vertical Reaction kN
Pc	18.74	25.28	269.32	9.37
P1	2.60	0.83	8.73	1.3
P2	2.11	0.68	7.09	1.05
Total	23.45	26.79	285.14	11.72

Table 7-14 Calculated loads, deflections and reactions acting on slab S12

Type of Load	Load kN	Deflection mm	Horizontal Reaction kN	Vertical Reaction kN
Pc	16.73	26.32	259.69	8.37
P1	2.60	0.94	9.10	1.30
P2	2.09	0.76	7.31	1.04
Total	21.42	28.02	276.10	10.71

A comparison of the results obtained from the theoretical analysis and the experimental tests of the second series is presented in Table 7-15. Also, the rise 'r' for each strip slab is presented. The maximum variation between the theoretical and experimental failure loads is about 10%.

Table 7-15 Comparison of theoretical and experimental results for slabs S9, S10, S11 and S12 (slabs with horizontal restraints)

Test No.	Dimension of Cross Sections h * b mm*mm	Concrete Strength f'_c MPa	Experimental Failure Load 'P_{exp}' kN	Theoretical Failure Load 'P_{theo}' kN	Ratio Of 'P_{theo}' Over 'P_{exp}'	Experimental Deflection 'w_{exp}' mm	Theoretical Deflection 'w_{theo}' mm	Rise 'r' mm
S9	116x203	32.69	25.73	24.16	0.939	29.27	24.73	46.33
S10	114x203	37.65	22.91	25.24	1.102	28.87	26.53	44.42
S11	111x203	37.07	23.13	23.45	1.014	27.83	26.79	42.86
S12	106x203	38.60	21.91	21.42	0.978	29.04	28.02	39.84

A comparison of the maximum load 'P_c' that can be carried by the strip slabs of the second series and the maximum load calculated according to the present codes of practice is presented in Table 7-16.

The capacities according to the present codes of practice were predicted ignoring horizontal restraint effects. The structural scheme of the calculated theoretical failure load 'P_c' is shown in Figure 7-6.

Table 7-16 Comparison of results obtained according to the analysis presented in Chapter 5 and results obtained according to present codes of practice for strip slabs number S9, S10, S11 and S12

Test No	Theoretical Failure Load 'P_c' kN	Load Due to Codes 'P_{cod}' kN	Ratio Of 'P_{cod}'/'P_c'	Deflection Due to Load 'P_c' mm	Deflection Due to Load 'P_{cod}' mm
S9	24.88	2.58	0.104	12.61	1.01
S10	27.44	2.68	0.098	12.83	1.03
S11	25.26	2.52	0.100	13.17	1.06
S12	23.38	2.34	0.100	13.77	1.10

A comparison of the experimental results obtained for strip slabs with horizontal restraints(S10 and S9) and strip slabs fully reinforced without horizontal restraints (S7 and S8) is presented in Table 7-17. Strip slabs S7 and S10 have similar concrete strength and cross sectional

dimensions. Strip slabs S8 and S9 have the same similarities as S7 and S10. The comparison presented in Table 7-17 indicates the effects of the horizontal restraints on the carrying capacity of the strip slabs.

Table 7-17 Comparison of experimental results for strip slabs with and without horizontal restraints

Support Conditions	With Horizontal Restraints	Without Horizontal Restraints	With Horizontal Restraints	Without Horizontal Restraints
Test No	S10	S7	S9	S8
dimensions	114x203	114x203	116x203	117x203
f_c' MPa	37.65	45.65	32.69	37.55
P_{exp1} kN	23.13	-	25.73	-
P_{exp2} kN	-	25.31	-	28.39
Ratio P_{exp1}/P_{exp2}	0.914		0.906	

A comparison of the relative strength 'R' for all the slab tests of the second series is presented in Table 7-18.

Table 7-18 Relative strength of all the strip slabs of the second series

Test No	Experimental Failure Load 'P_{exp}' kN	Relative Strength R 10^{-3}	Horizontal Restraint
S7	25.31	24.17	Non
S8	28.39	31.83	Non
S9	25.73	33.43	Restrained
S10	22.91	26.29	Restrained
S11	23.13	27.69	Restrained
S12	21.91	26.38	Restrained

7-4 Summary

Generally, the theoretical results in comparison with the results of the experimental tests for the strip slabs with horizontal restraints are within acceptable limits. Because of the modifications that were introduced to the supports of the set-up of the second series of tests, the theoretical results are closer to the experimental results in the second series than in the first series. The difference between theoretical results and results obtained from experimental tests varies from -18% to +13%. As shown in Table 7-19, the average variation between the calculated

theoretical failure loads 'P_{theo}' and the obtained experimental failure loads 'P_{exp}' is -2.2%. The average variation between the calculated theoretical deflections 'w_{theo}' and the obtained experimental deflections 'w_{exp}' is -6.2%.

A summary of results of all strip slabs with horizontal restraints is presented in Table 7-19. A summary of the results of all simply supported fully reinforced horizontally non-restrained strip slabs is presented in Table 7-20. A sample of the calculations of the actual reinforcement ratio 'ρ_{act}', the maximum reinforcement ratio 'ρ_{max}' and the minimum reinforcement ratio 'ρ_{min}' in Table 7-20 is presented in Appendix 'C' in Section C-4 (calculations for the reinforcement ratios for slab S5).

Load deflection curves presenting a comparison of the experimental results of the fully reinforced horizontally non-restrained strip slabs and the experimental results of horizontally restrained strip slabs are shown in Chapter 4.

Table 7-21 shows the relative strength 'R' of all the strip slabs, as well as, the maximum, minimum and actual reinforcement ratios for each strip slab, calculated according to the Canadian Code CSA. Despite the great difference in the reinforcement ratios of horizontally restrained slabs (minimum ratio) and horizontally non-restrained slabs (maximum ratio), the values of relative strength shown in Table 7-21 do not, on

average, vary too much for both cases. The average relative strength values are similar for the slabs of the first group (S1 through S4) and for the slabs of the second group (S5 through S8), where the slabs of the first group are horizontally restrained and the slabs of the second group are horizontally non-restrained. For the horizontally restrained slabs of the third group (S9 through S12) the average relative strength value is smaller, because the fixed end moment was minimized due to the modifications introduced to the supports.

Table 7-22 shows a comparison of the maximum load that can be carried by each strip slab (calculated according to the present code of practice, assuming all the strip slabs are simply supported horizontally non-restrained) and the experimental failure load. The amount of reinforcement in the tested strip slabs were considered in calculating the maximum loads according to the present code of practice.

Table 7-19 Comparison of theoretical and experimental results for strip slabs with horizontal restraints

Test No.	Dimension of Cross Sections h * b mm*mm	Span 'L' mm	'f_y' for Bars with Diameter 6 mm MPa	Concrete Strength f_c' MPa	Experimental Failure Load 'P_{exp}' kN	Theoretical Failure Load 'P_{theo}' kN	Ratio Of 'P_{theo}' Over 'P_{exp}'	Experimental Deflection 'w_{exp}' mm	Theoretical Deflection 'w_{theo}' mm	Ratio Of 'w_{theo}' Over 'w_{exp}'	Rise 'r' mm
S1	104x203	2400	504.40	28.55	21.97	21.58	0.982	23.36	26.97	1.155	40.50
S2	107x203	2400	504.40	31.88	28.15	23.94	0.850	30.89	27.18	0.884	41.64
S3	112x203	2400	504.40	32.32	23.31	26.41	1.133	29.05	26.32	0.906	44.34
S4	117x203	2400	504.40	33.23	35.59	29.25	0.822	29.62	25.75	0.869	46.94
S9	116x203	2421	456.24	32.69	25.73	24.16	0.939	29.27	24.73	0.845	46.33
S10	114x203	2421	456.24	37.65	22.91	25.24	1.102	28.87	26.53	0.919	44.42
S11	111x203	2421	456.24	37.07	23.13	23.45	1.014	27.83	26.79	0.963	42.86
S12	106x203	2421	456.24	38.60	21.91	21.42	0.978	29.04	28.02	0.965	39.84
Average	-	-	-	-	-	-	0.978	-	-	0.938	-

Table 7-20 Comparison of theoretical and experimental results for strip slabs without horizontal restraints

Test No	Dimension of Cross Sections h * b mm*mm	Span 'L' mm	'f_y' for Bars with Diameter 6 mm MPa	'f_y' for Bars with Diameter 16 mm MPa	Concrete Strength f'_c MPa	Experimental Failure Load 'P_{exp}' kN	Theoretical Failure Load 'P_{theo}' kN	Ratio Of 'P_{theo}' Over 'P_{exp}'
S5	117x203	2400	504.40	441.12	34.14	36.92	30.34	0.822
S6	113x203	2400	504.40	441.12	32.58	35.32	28.17	0.798
S7	113x203	2400	456.24	370.50	45.65	25.31	27.00	1.067
S8	117x203	2400	456.24	370.50	37.55	28.39	27.40	0.965
av.	-	-	-	-	-	-	-	0.913

Table 7-21 Relative strength of the strip slabs

Test No	Failure Load 'P_{exp}' kN	Relative Strength R 10^{-3}	Average Relative Strength R 10^{-3}	Minimum Reinforcement Ratio ρ_{min}	Actual Reinforcement Ratio ρ_{act}	Maximum Reinforcement Ratio ρ_{max}	Ratio Of ρ_{act} Over ρ_{max}	Horizontal Restraint
S1	21.97	36.45		0.00278	0.0033	0.0240	0.138	Restrained
S2	28.15	40.65		0.00278	0.0032	0.0259	0.124	Restrained
S3	23.31	31.72	38.48	0.00278	0.0030	0.0258	0.117	Restrained
S4	35.59	45.09		0.00278	0.0029	0.0260	0.111	Restrained
S5	36.92	45.53		0.00317	0.0321	0.0321	1.000	Non
S6	35.32	47.26		0.00317	0.0336	0.0316	1.064	Non
S7	25.31	24.17	37.20	0.00378	0.0336	0.0482	0.697	Non
S8	28.39	31.83		0.00378	0.0321	0.0432	0.743	Non
S9	25.73	33.43		0.00307	0.0029	0.0299	0.0972	Restrained
S10	22.91	26.29		0.00307	0.00296	0.0327	0.0906	Restrained
S11	23.13	27.69	28.45	0.00307	0.00306	0.0326	0.0939	Restrained
S12	21.91	26.38		0.00307	0.00324	0.0338	0.0960	Restrained

Table 7-22 Comparison of results obtained according to present codes of practice and experimental results for all the strip slabs

Test No	Experimental Failure Load 'P_{exp}' kN	Calculated* Failure Load 'P_{cod}' kN	Ratio of P_{theo} / P_{exp}	Horizontal Restraint
S1	21.97	2.41	0.110	Restrained
S2	28.15	2.56	0.091	Restrained
S3	23.31	2.80	0.120	Restrained
S4	35.59	3.04	0.085	Restrained
S5	36.92	30.34	0.821	Non
S6	35.32	28.17	0.798	Non
S7	25.31	27.00	1.067	Non
S8	28.39	27.40	0.965	Non
S9	25.73	2.70	0.105	Restrained
S10	22.91	2.62	0.114	Restrained
S11	23.13	2.49	0.108	Restrained
S12	21.91	2.28	0.104	Restrained

*P_{cod} was calculated as for simply supported horizontally non-restrained beam (these capacities were predicted ignoring horizontal restraint effects).

Chapter 8

Analysis of Square Slabs Subjected to Central Concentrated Loads

8-1 Introduction

In Chapter 5, a plastic analysis method for horizontally restrained concrete strip slabs was developed. Strip slabs simulate beams and one way slabs. In this chapter, the developed plastic analysis method will be extended to analyze two way horizontally restrained concrete slabs subjected to concentrated loads. The simplest form of two way slabs subjected to concentrated loads is a square slab subjected to a central concentrated load.

In this chapter, for horizontally restrained square slab with given dimensions and given concrete strength, the value of the maximum central concentrated load 'P' that can be carried by the slab, the maximum deflection 'w' at the center of the slab and the value of the horizontal reactions at the boundaries will be established using the developed plastic method.

When applying a central concentrated load to a horizontally

restrained square slab, the slab cracks. When the collapse of the slab is impending, the cracks divide the slab into segments. The segments of the cracked slab share in carrying the central concentrated load. To extend the developed plastic method presented in Chapter 5 to analyze square slabs, the pattern of cracks due to central concentrated loads needs to be examined.

8-2 Pattern of Cracks

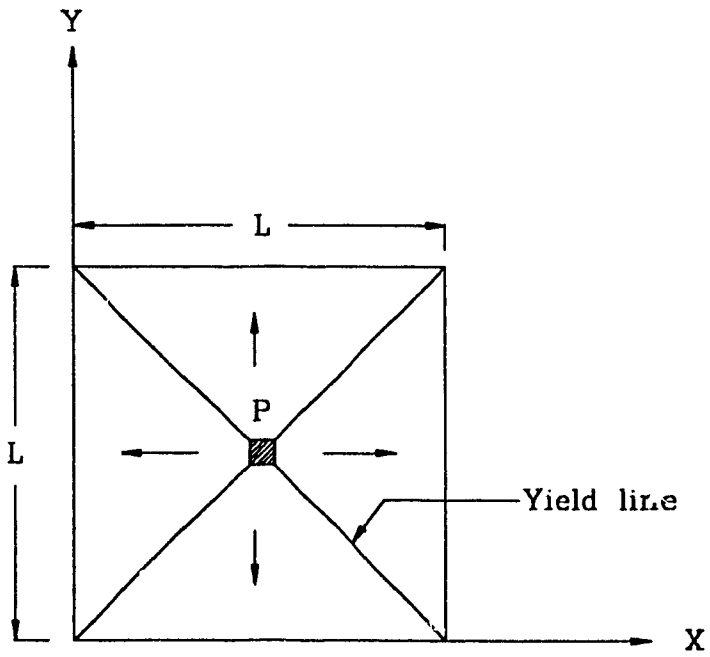

Figure 8-1 The pattern of cracks for a slab on the verge of collapse due to a central concentrated load 'P'

According to the yield line theory, the pattern of the cracks of a simply supported square slab on the verge of collapse due to a central

concentrated load 'P' is as shown in Figure 8-1. The slab cracks diagonally due to the failure load 'P'. The diagonal cracks are along the diagonal yield lines and they divide the slab into four segments.

Since the yield line theory ignores the effect of horizontal restraints, the cracks that are shown in Figure 8-1 occur to simply supported horizontally non-restrained square slabs. However, Kwang and Morley[38], also, Taylor and Hayes[79] tested horizontally restrained reinforced concrete square slabs subjected to central concentrated loads and the pattern of cracks of the tested slabs was identical to the pattern shown in Figure 8-1.

8-3 Assumed Horizontal Reaction Acting on a Segment of a Square Slab

As shown in Figure 8-1, the load 'P' is distributed in two perpendicular directions 'X' and 'Y'. Half the load 'P' is carried by the two segments in 'Y' direction and the other half carried by the two segments in 'X' direction. When the slab is on the verge of collapse, the segments of the cracked slab form a mechanism system. In this mechanism system, the forces that are acting on each segment need to be determined to be able to establish the values of the maximum load 'P', the maximum deflection 'w' and the horizontal reactions 'R_h'.

To determine the forces that are acting on each segment, the

problem shown in Figure 8-1 can be simplified by assuming that each two segments of the cracked slab facing each other are carrying half the load 'P' as shown in Figure 8-2. Also, assume the stresses that are acting on the diagonal yield lines in comparison with the stress that acting on the tip of the segment are negligible. The validity of these assumptions will be evaluated.

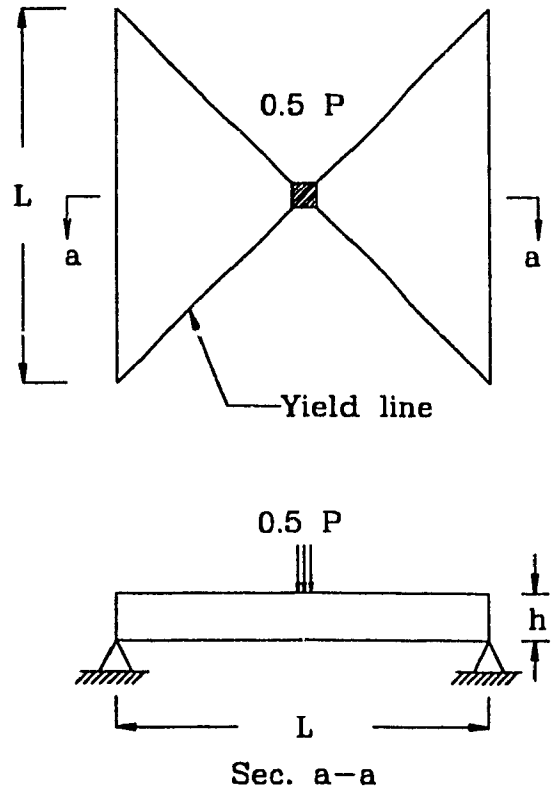

Figure 8-2 The two segments of a square slab carrying half the applied central concentrated load

The problem shown in Figure 8-2 reduces the original three

dimensional problem to a two dimensional problem. This problem is similar to problems that are dealt with in Chapter 5. The difference between this problem and the problems of Chapter 5 is that the segments of this problem have variable cross-sections.

When the slab is on the verge of collapse, the system shown in Figure 8-2 will be divided into two segments. The stresses and the reactions that are acting on one segment will be examined. One segment will be isolated to examine the distribution of the horizontal reaction that is acting on it as it is shown in Figure 8-3.

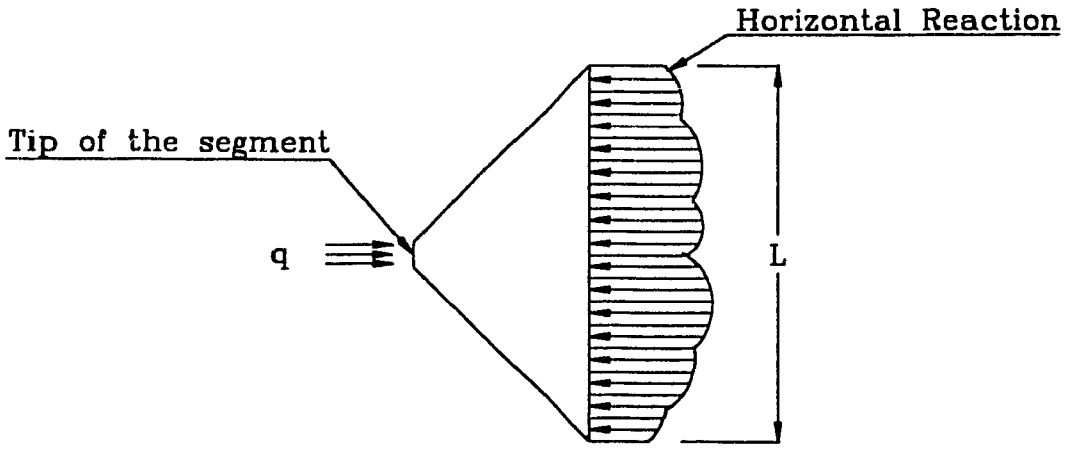

Figure 8-3 The assumed stress and reaction acting on a segment of a square slab

The horizontal stresses that are acting on the tip of one segment are due to the formation of a compression zone at the cross section of the

tip. The horizontal stresses of the compression zone are assumed to be uniformly distributed (according to the beam theory). The distribution of the horizontal reaction that is acting on the boundary of the segment as shown in Figure 8-3 is unknown.

To obtain the distribution of the horizontal reaction due to the horizontal restraint, a finite element analysis using program Adina is carried out on the segment shown in Figure 8-3. The command program to perform this analysis is presented in Appendix D Section D-1. The dimensions and the finite element mesh of this segment are shown in Figure 8-4. The dimensions of the cross section of the tip of this segment are 160 mm in width and 100 mm in depth.

Since the shape of the distribution of the reaction forces on the boundary of the segment needs to be obtained and since the value of the compression stress 'q' that is acting on the tip of the segment is unknown, therefore, an assumed maximum value for the compression stress 'q' will be used.

The maximum value for the compression stress 'q' will be used because the horizontal reaction that will be obtained from the analysis of the segment shown in Figure 8-3 will be compared to the horizontal reaction that will be obtained from analyzing a complete square slab subjected to a central concentrated load. If the value of the horizontal reaction that will be obtained from analyzing the segment shown in

Figure 8-4 is less than that of the horizontal reaction that will be obtained from analyzing a complete square slab, then, the importance of the stresses that are acting on the diagonal yield lines will be concluded.

Assuming that the depth of the compression zone 'a' at the tip of the segment shown in Figure 8-3 is half the thickness of the slab 'h' (assuming a=0.5h) where 'h' is 100 mm. The value of the stress that is acting on this compression zone is equal to $0.85f_c'$. Taking f_c' equal to 30 MPa, then, the stress of the compression zone is equal to 25.5 MPa.

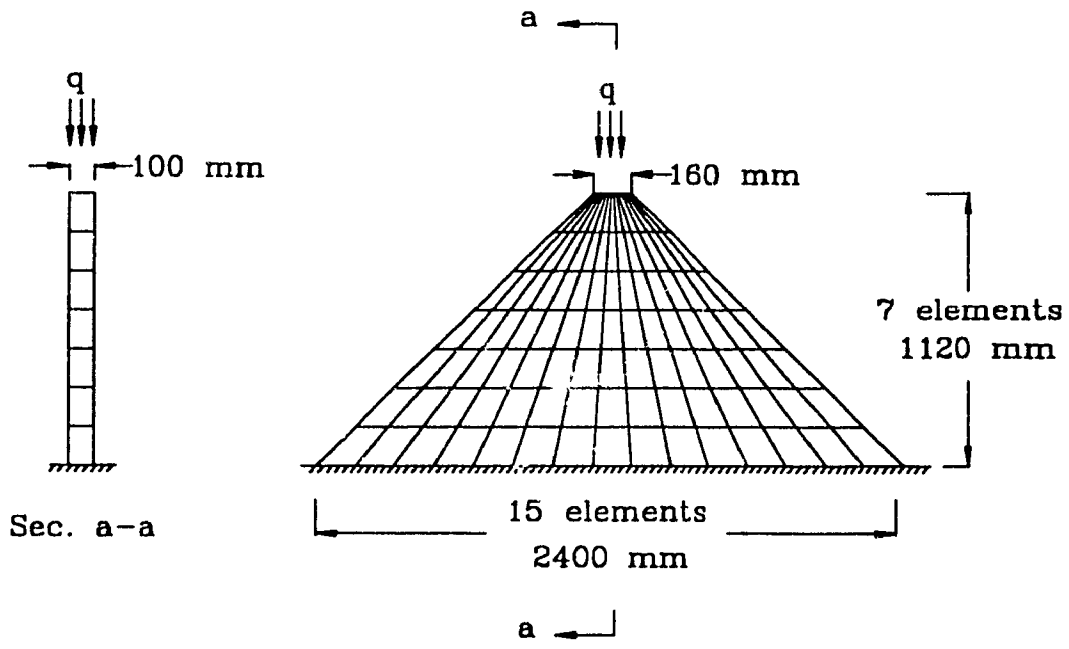

Figure 8-4 The mesh of a segment of a slab analyzed by the finite element method

Since only the distribution of the reaction at the base of the segment is needed, then, for the finite element analysis, the stress that is

acting on the compression zone will be redistributed over the entire area of the tip. Since the area of the assumed compression zone is half the area of the tip, then, the value of the compression stress 'q' that was used in the analysis is equal to 12.75 MPa. The compression force 'F' that is acting on the tip of the segment is calculated as follows:

$$F = q \times a \times width\ of\ the\ tip$$

$$F = 0.85 \times f_c' \times 0.5 \times 100 \times 160 = 204 \times 10^3\ N = 204\ kN \quad \ldots\ldots \quad (8\text{-}1)$$

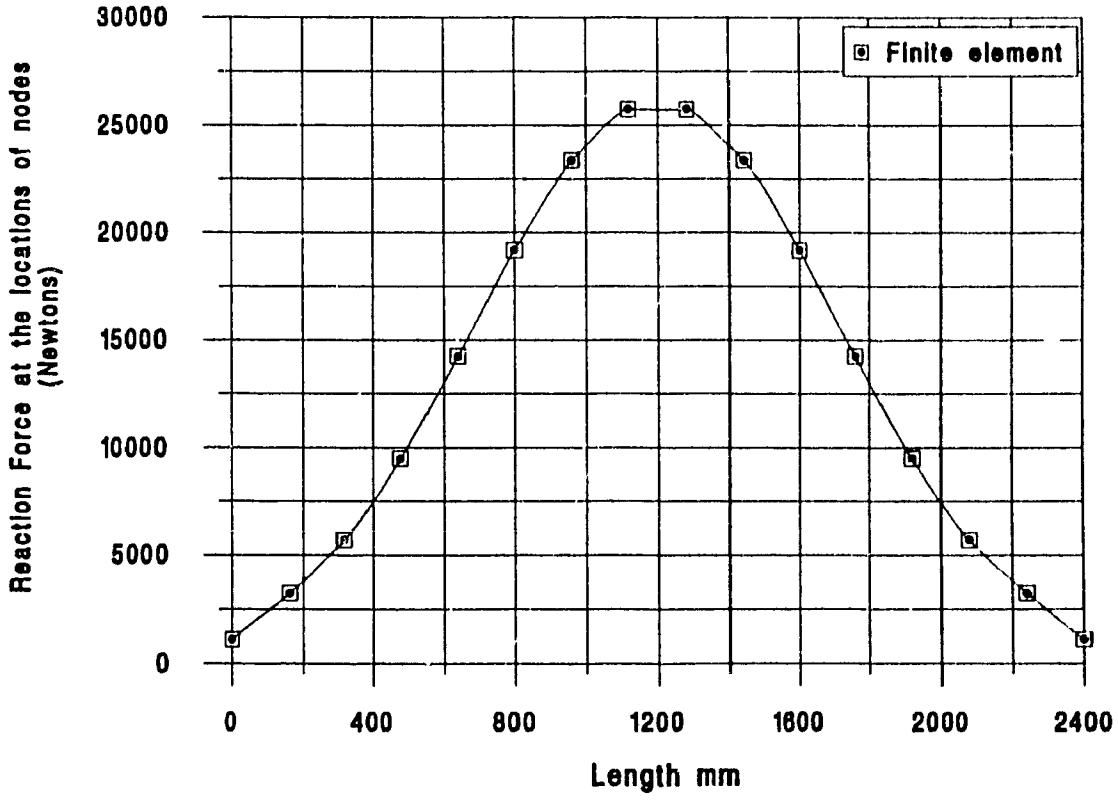

Figure 8-5 The distribution of the horizontal reaction obtained from

The results of the finite element analysis for the segment shown in Figure 8-4 are obtained. The distribution of the horizontal reaction forces at the locations of the nodes is plotted against the width of the base of the segment and is presented in Figure 8-5.

8-4 Mathematical Formulation for the Reaction Acting on the Segment

To mathematically formulate the shape of the distribution of the reaction that is presented in Figure 8-5, considering the segment shown in Figure 8-6, and assume that the support of this segment can take only reaction perpendicular to the plane defined by the line o-n.

A strip taken from the segment shown in Figure 8-6 will be isolated to analyze the in plane stresses acting on it. Since we are interested in evaluating the reaction 'R_x', then only the stresses acting in the direction of the reaction 'R_x' will be considered. Summing the stresses acting in the direction of the reaction 'R_x' can lead to the following equation:

$$(q+\frac{\partial q}{\partial x}dx)\times B\times H_x - q\times B\times H_x = R_x\times dx\times B$$

Eliminating the depth of the segment 'B' and the shear stress 'q'

from both sides of the above equation will lead to Equation (8-2), which defines the value of reaction stress 'R_x' at a given horizontal distance 'x', as shown below.

$$\frac{\partial q}{\partial x} H_x = R_x \quad \ldots\ldots\ldots\ldots\ldots\ldots \quad (8\text{-}2)$$

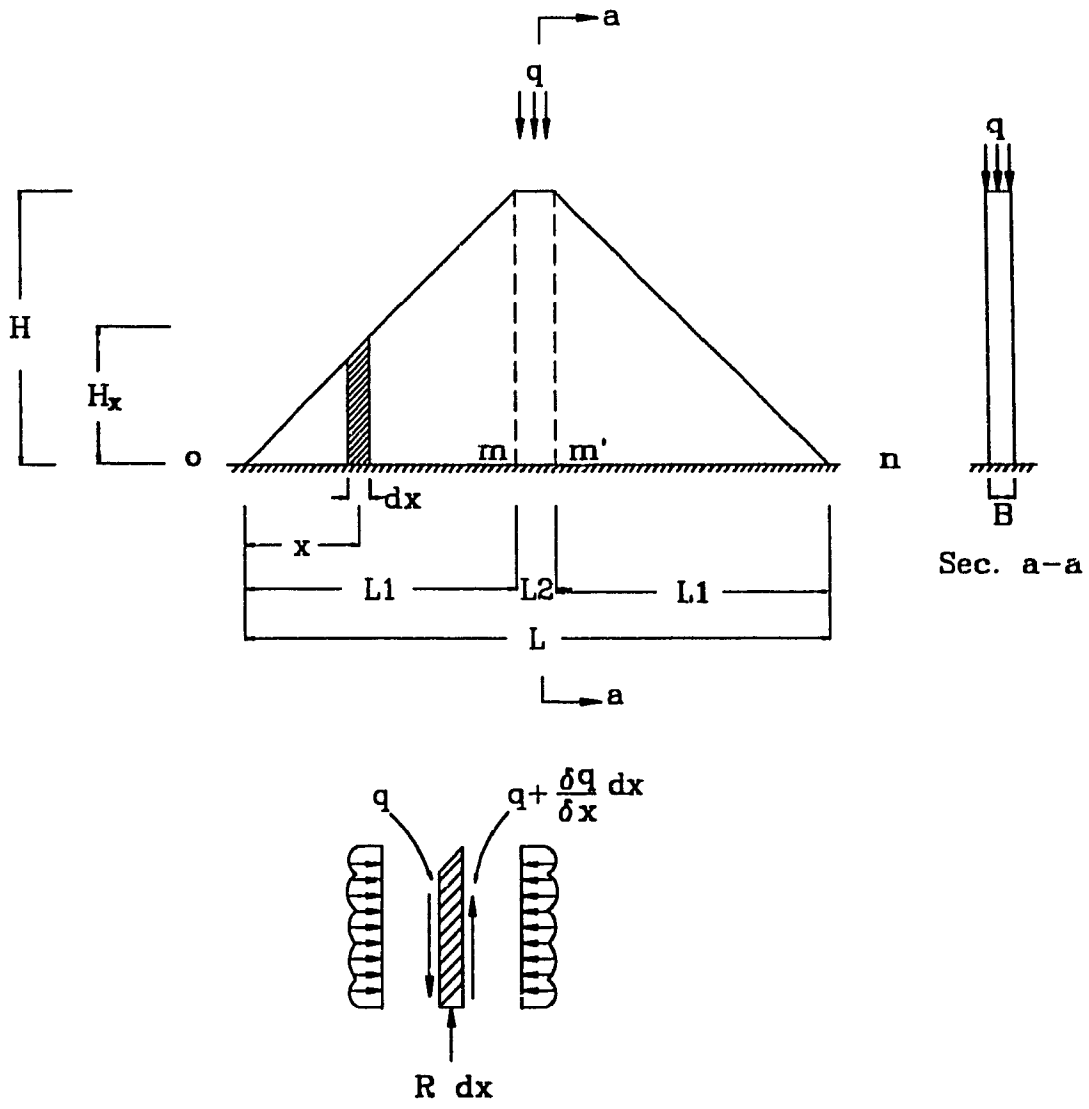

Figure 8-6 Mathematical formulation for the stresses acting on a strip taken from a segment of a slab

In the above equation, the reaction 'R_x' is a function of 'H_x' and '$\partial q/\partial x$'. The value of 'H_x' changes linearly from zero at point 'o' to maximum at point 'm'. Also, the value '$\partial q/\partial x$' changes linearly from point 'o' to point 'm' (because there is not any external load applied within this interval). Since the value of 'H_x' is zero at point 'o', the value of 'R' is also zero at point 'o'. In addition, since the values of 'H_x' and '$\partial q/\partial x$' change linearly from point 'o' to point 'm', then, the value of 'R_x' will be maximum at point 'm' which leads to a distribution shape of the reaction as shown in Figure 8-7.

Since the volume of the segment shown in Figure 8-6 will be needed, this volume can be calculated as follows:

$$V = 2 \times \frac{L1 \times H}{2} \times B \; + \; L2 \times H \times B$$

$$V = H \times B \; (L1 + L2)$$

As shown in Figure 8-7, the value of the reaction stress 'R_x' at any horizontal distance 'x' is proportional to 'H_x' (see Figure 8-6). Also as shown in the same figure, the shape of the distribution of the reaction is a mirror image of the physical shape of the segment. Consequently, the value of 'R_x' at any distance 'x' can be calculated as follows (the value

of 'F' is given in Equation 8-1):

$$R_x = \frac{F}{V} H_x$$

$$R_x = \frac{F}{H \times B(L1+L2)} H_x$$

Multiplying the left side of the above equation by L/L:

$$R_x = \frac{F}{H \times B(L1+L2)} H_x \times \frac{L}{L}$$

Rearranging the above equation,

$$R_x = \frac{F}{B \times L} \left(\frac{H_x}{H} \times \frac{L}{L1+L2}\right) \quad \ldots\ldots\ldots\ldots\ldots \quad (8\text{-}3)$$

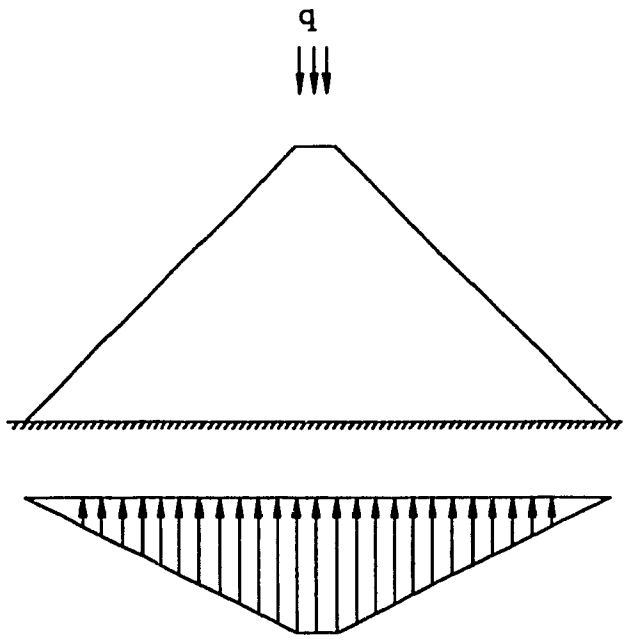

Figure 8-7 Reaction distribution on one segment due to the stress 'q'

Equation (8-3) represents the value of the reaction distribution 'R_x' (at any distance 'x') as a function of 'H_x'. A comparison between the results obtained from finite element analysis (see Figure 8-5) and the results obtained from Equation (8-3) are presented in Figure 8-8. The results that are obtained from the finite element analysis are reaction forces at the locations of the nodes. To compare between the results obtained from finite element analysis and those obtained from an analysis based on Equation (8-3), the reaction forces at the locations of the nodes are calculated based on the results that are obtained from Equation (8-3) and are presented by the curve called 'Present study' in Figure 8-8.

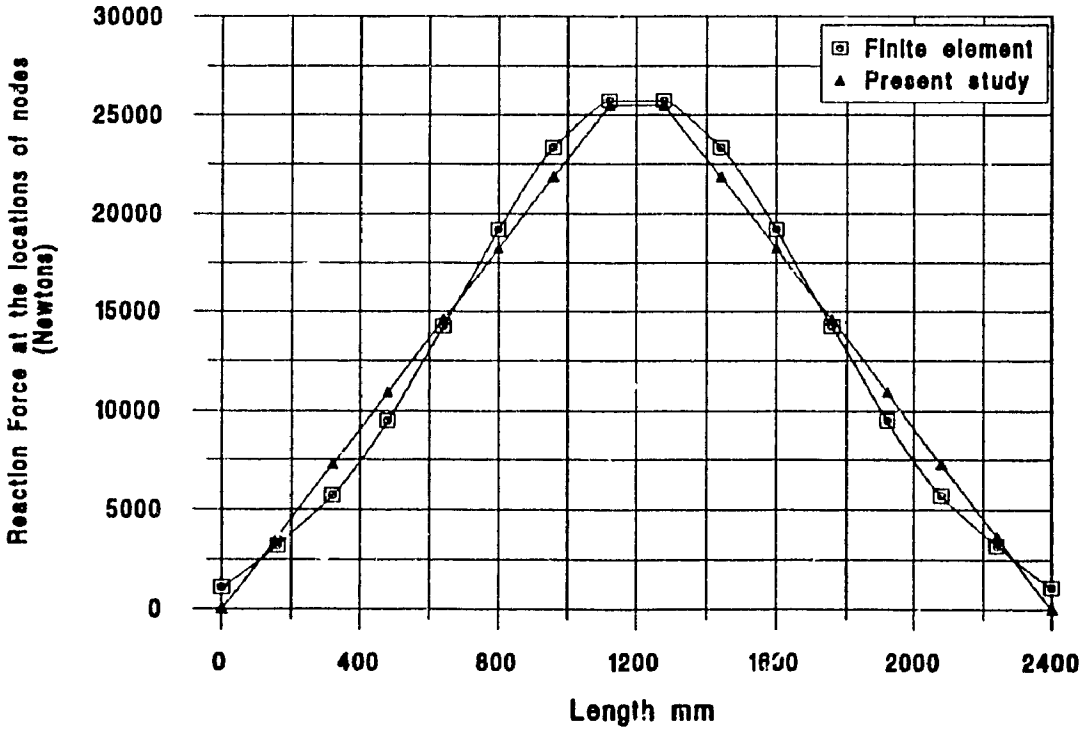

Figure 8-8 A comparison between horizontal reactions obtained by using finite element analysis and by an analysis based on Equation (8-3)

In Figure 8-8, the ordinates of the curve obtained from Equation (8-3) are calculated by multiplying the values of 'R_x' by the depth of the segment 'B' which is equal to 100 mm and by the width of the element which is 160 mm. The ordinates of this curve (curve shown as 'Present study') are the reaction forces at the location of the nodes. Taking that into account, the width of the elements at line o-n is 160 mm (see Figures 8-4 and 8-6).

From mechanics of materials, the equation that presents the stress 'σ' due to the application of the force 'F' on a given cross section area 'A' is defined as follows:

$$\sigma = \frac{F}{A} = \frac{F}{B \times L}$$

Equation (8-3) is found to be similar to the above equation with the exception of the additional term $(\frac{H_x}{H} \times \frac{L}{L1+L2})$. This term modifies the value of the stress that is acting on the base of the segment to take into account the shape of the segment.

8-5 Finite Element Analysis of a Horizontally Restrained Square Slab

In the preceding section, the shape of the distribution of the horizontal reaction was presented for the case where two segments facing

each other (see Figure 8-2) are assumed to carry half the central concentrated load that is applied on the square slab. The other half is carried in the perpendicular direction. For the case studied in the preceding section, the stresses that are acting on the diagonal yield lines are assumed to be negligible in comparison with the stress acting on the tip of the segment. To examine the validity of these assumptions, a complete square slab was analyzed and the shape of the horizontal reaction distribution was obtained and will be compared to the reaction shown in Figure 8-5.

A finite element analysis, using program Adina, was performed on a square slab subjected to a central concentrated load to record the stresses and the reactions that are acting on the segments of the slab and also to record the maximum central concentrated load that can be carried by this slab and the maximum deflection.

The dimensions of the analyzed slab are 2400 mm in length, 2400 mm in width and 100 mm in depth. The length and the width were each divided into 15 elements, each element having a length and width of 160 mm and 160 mm respectively. The depth of the slab was divided to accommodate 3 layers of elements, each layer having a depth of 33.33 mm. Figure 8-9 shows the mesh of the slab. The command program to perform the analysis of this slab is presented in Appendix D Section D-2.

The boundary conditions for the square slab is shown in Figure

8-9. The perimetric surface of the bottom layer of elements was considered to be restrained against displacements in the horizontal and vertical directions. When the boundaries are restrained at the perimetric surface of the bottom layer of elements, partial rotations are permitted at the edges of the slab which present a better modeling for a slab with horizontally restrained boundaries.

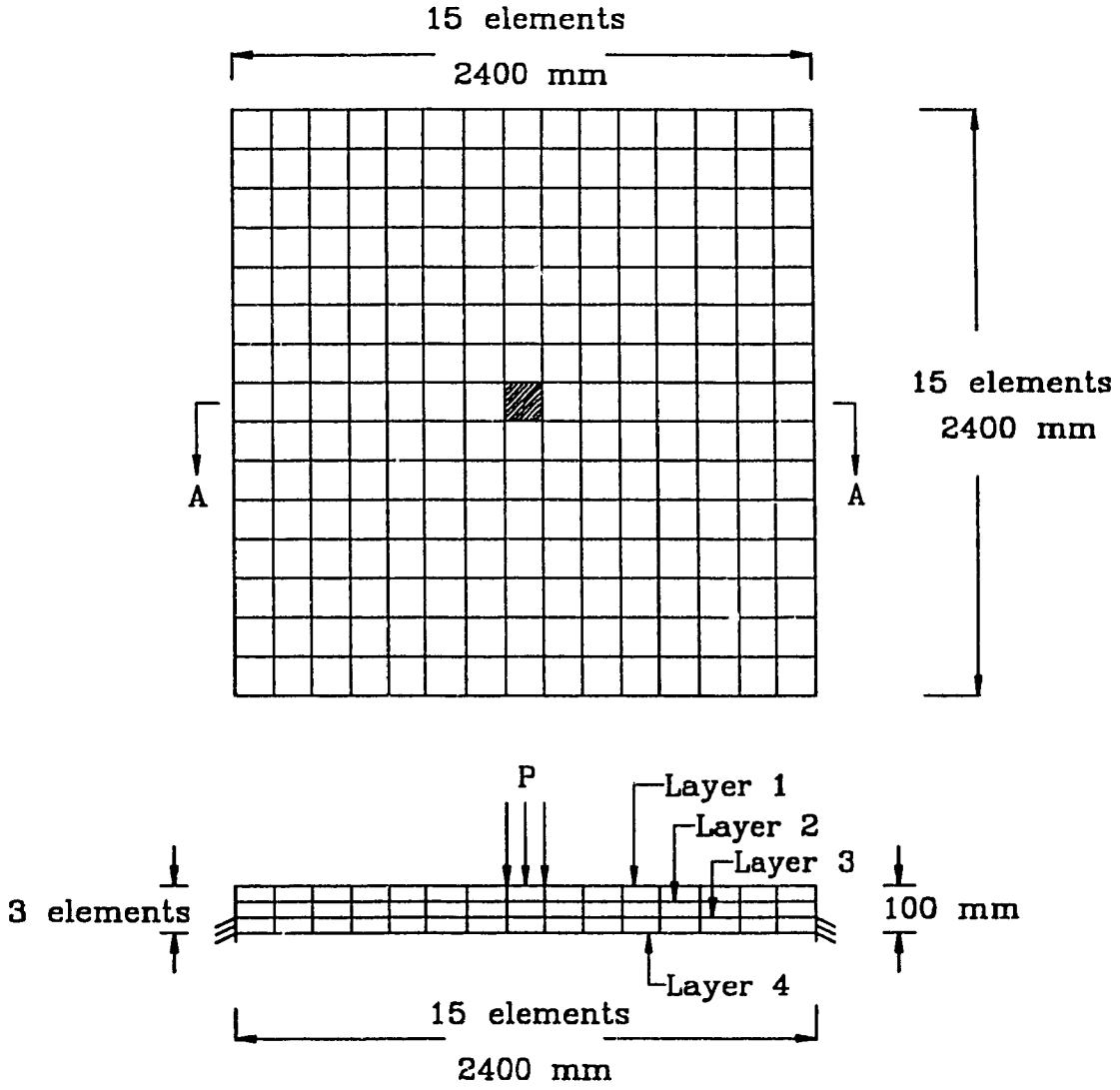

Figure 8-9 A square slab analyzed by the finite element method

As can be seen in Figure 8-9, the depth of the slab is accommodating three layers of elements and four layers of nodes. The layers of nodes are numbered in ascending order. The top layer of nodes (where the load is applied) is called layer 1 and the bottom layer of nodes is called layer 4.

The summation of the vertical reaction forces at the locations of the nodes at the boundary of one side of the slab is presented as shown in Figure 8-10. The value of the vertical coordinate that are shown in Figure 8-10 represent the downward reaction with negative numbers and the upward reaction is presented with positive numbers.

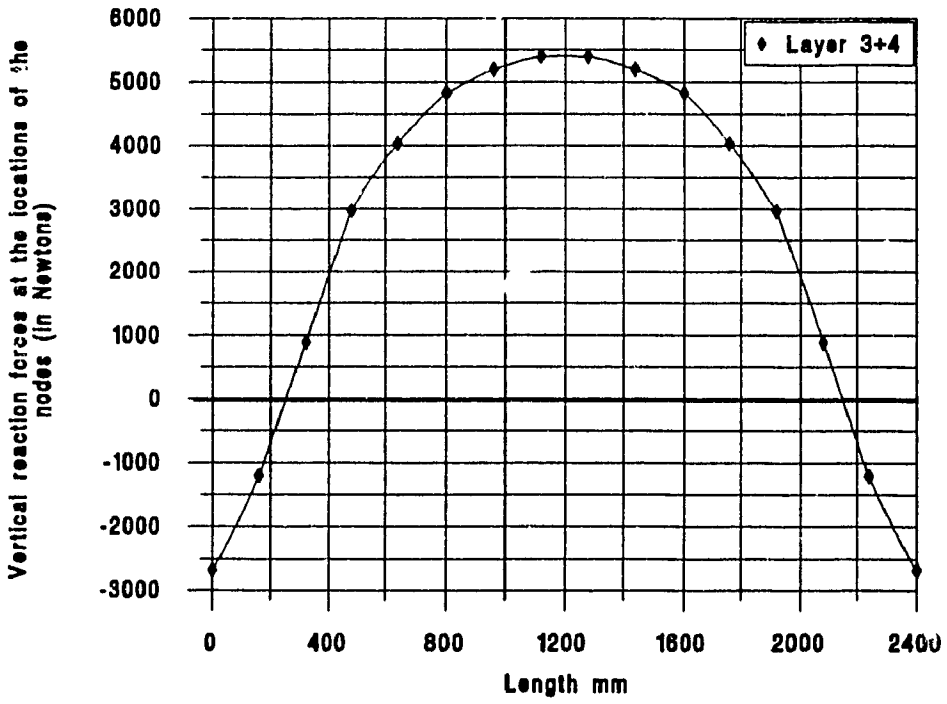

Figure 8-10 The vertical reactions at one side of the square slab

In Figure 8-11, the compression horizontal reaction forces at the bottom fibers of the slab at its boundaries are presented. This horizontal reaction is acting at the bottom layer of nodes.

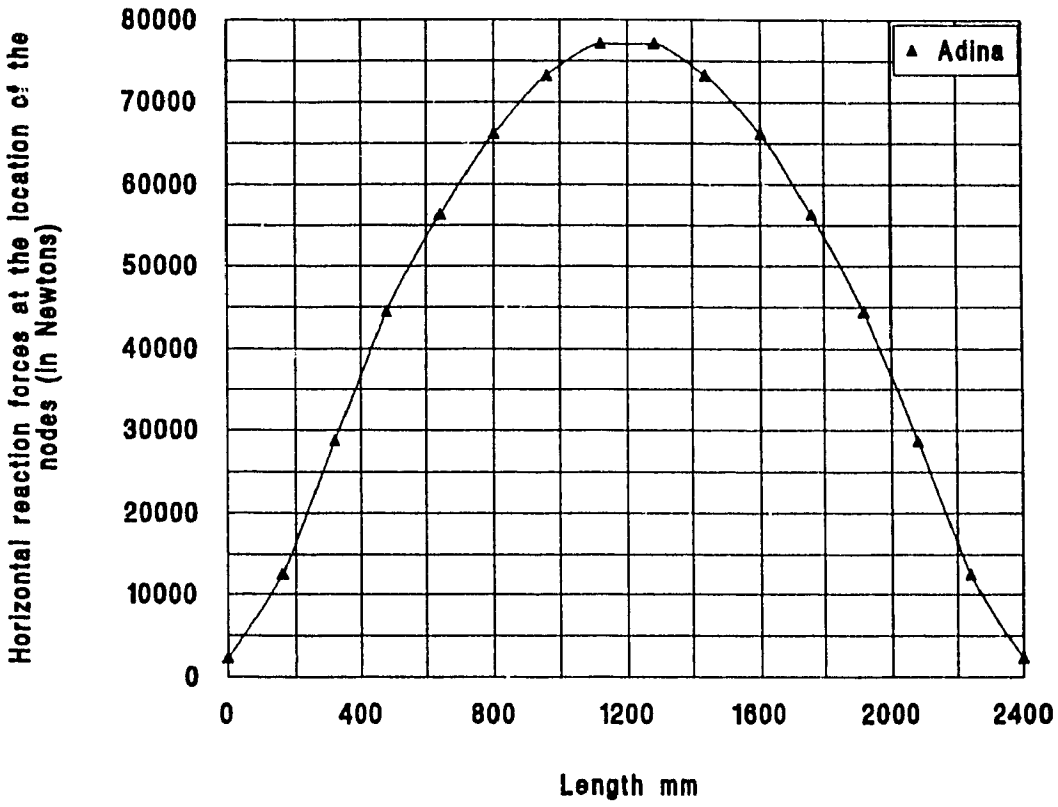

Figure 8-11 The shape of the horizontal reaction distribution at the boundaries of the slab

A comparison between the values of the horizontal reaction distribution presented in Figure 8-5 and the values of the horizontal reaction distribution presented in Figure 8-11 shows that the values of

the two curves are different. The curve shown in Figure 8-11 has higher reaction values than the curve presented in Figure 8-5. The curve presented in Figure 8-5 was due to the force acting on the tip of the segment only, ignoring the forces acting on the diagonal lines. From this comparison, it may be concluded that the forces that are acting on the diagonal yield lines for slabs with horizontally restrained boundaries are important.

The comparison between the two curves proves that the assumptions presented earlier are not valid for square slabs with horizontally restrained boundaries. These assumptions are that the horizontal reaction is equal to the in-plane force that acts on the tip of the segment and that the forces that act on the diagonal lines of the segment are negligible.

It may be conclude from the above comparison that the four segments of the cracked square slab are dependent on each other in carrying the applied central concentrated load. In addition, the forces that act on the diagonal yield lines are of great importance and can not be ignored.

The forces that are acting on the diagonal yield lines are obtained from the finite element analysis performed on the square slab that is shown in Figure 8-9. Before presenting the values of these forces, their directions need to be demonstrated. The directions of the forces that are

acting on the diagonal yield lines are presented in Figure 8-12.

The values of the forces that are acting on the diagonal lines at the locations of the nodes in a direction perpendicular to the base of the segment (corresponding to Figure 8-12-A) are presented in Figure 8-13. The values of the forces presented in Figure 8-13 are obtained from the finite element analysis at each layer of nodes as explained earlier. The length of the diagonal line is presented by the horizontal coordinate. In the following graphs and for the vertical coordinates, the negative sign represents a tension force and the numbers having positive values represent compression forces.

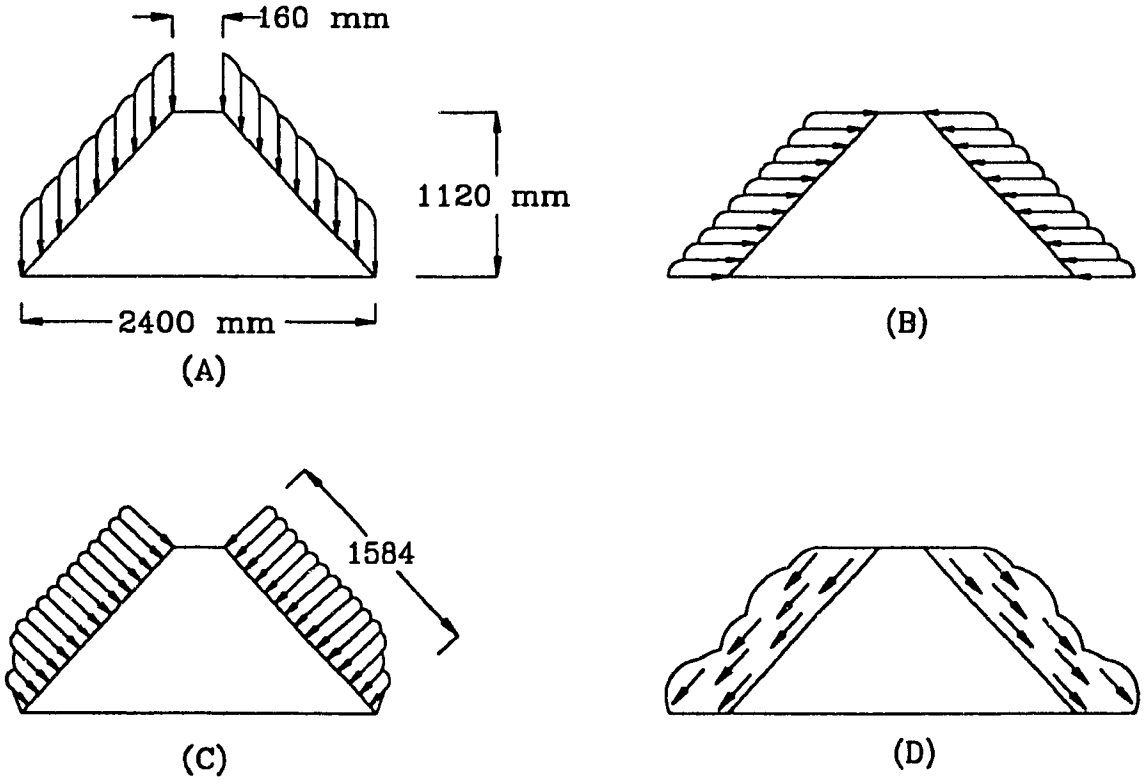

Figure 8-12 Directions of forces that are acting on the diagonal lines

As can be seen in Figure 8-13, the curve called 'Layer 1+2' represents the compression forces that are acting at the top surface of the slab and it shows higher compression forces in the vicinity of the concentrated load. The curve called 'Layer 3+4' represents the tension forces that are acting at the bottom surface of the slab and it shows higher values in the vicinity of the load.

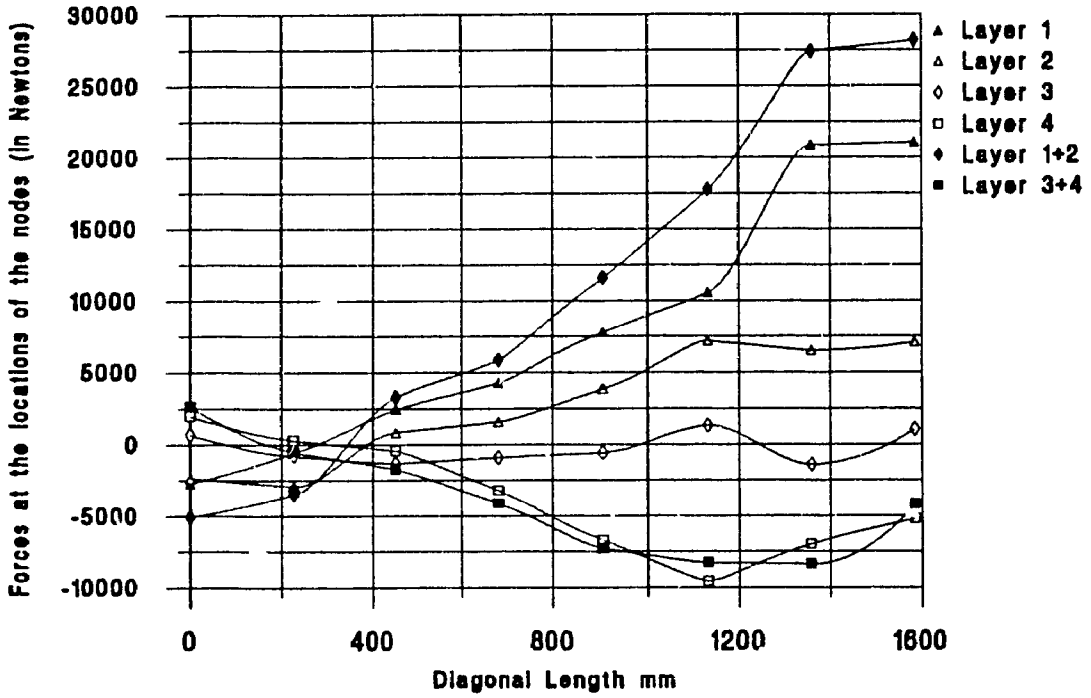

Figure 8-13 Forces acting on the diagonal lines in a direction perpendicular to the base of the segment

Similar values for the forces that are acting on the diagonal lines and acting in a direction parallel to the base of the segment are presented

in Figure 8-14. The direction of these forces corresponds to the direction that is shown in Figure 8-12-B.

The values of the forces presented in Figure 8-14 are used in combination with the values presented in Figure 8-13 to obtain the values of the forces presented in Figure 8-15 and Figure 8-16.

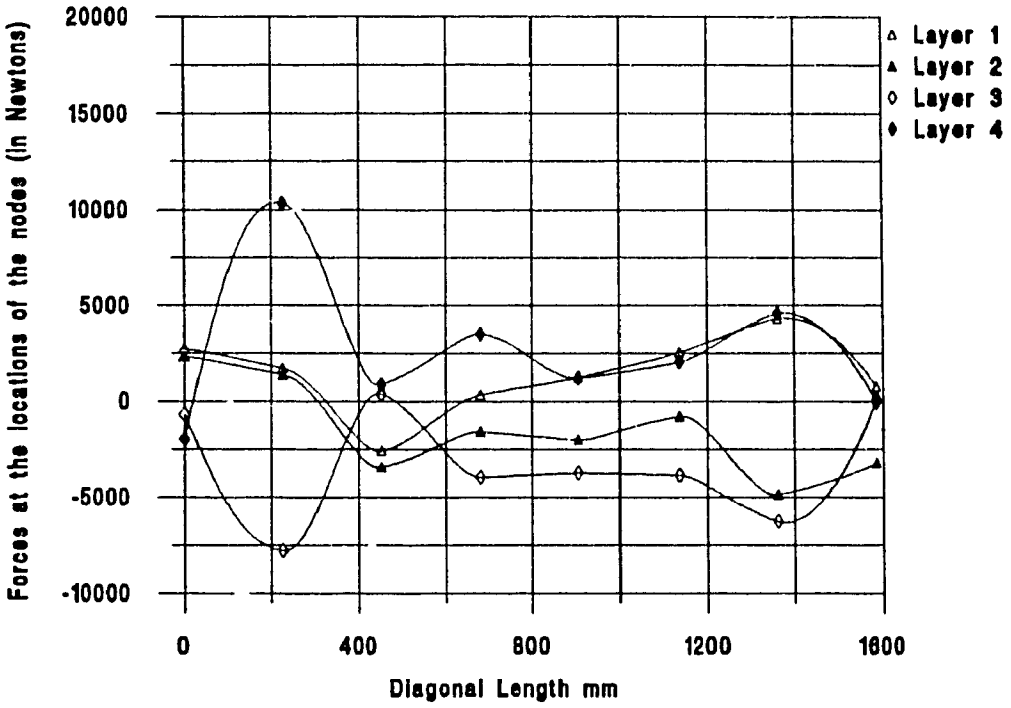

Figure 8-14 Forces acting on the diagonal lines in a direction parallel to the base of the segment

The forces that are acting in a directions perpendicular and parallel to the diagonal lines (corresponding to Figure 8-12-C and Figure 8-12-D respectively) are calculated from the results that are presented in Figure 8-13 and Figure 8-14. The forces perpendicular and parallel to the

diagonal lines are presented in Figure 8-15 and Figure 8-16 respectively. Since the results that are shown in Figure 8-13 and Figure 8-14 are the forces in directions 'X' and 'Y' acting on the nodes, their components at 45° (in directions perpendicular and parallel to the diagonal lines of the segment) can be calculated.

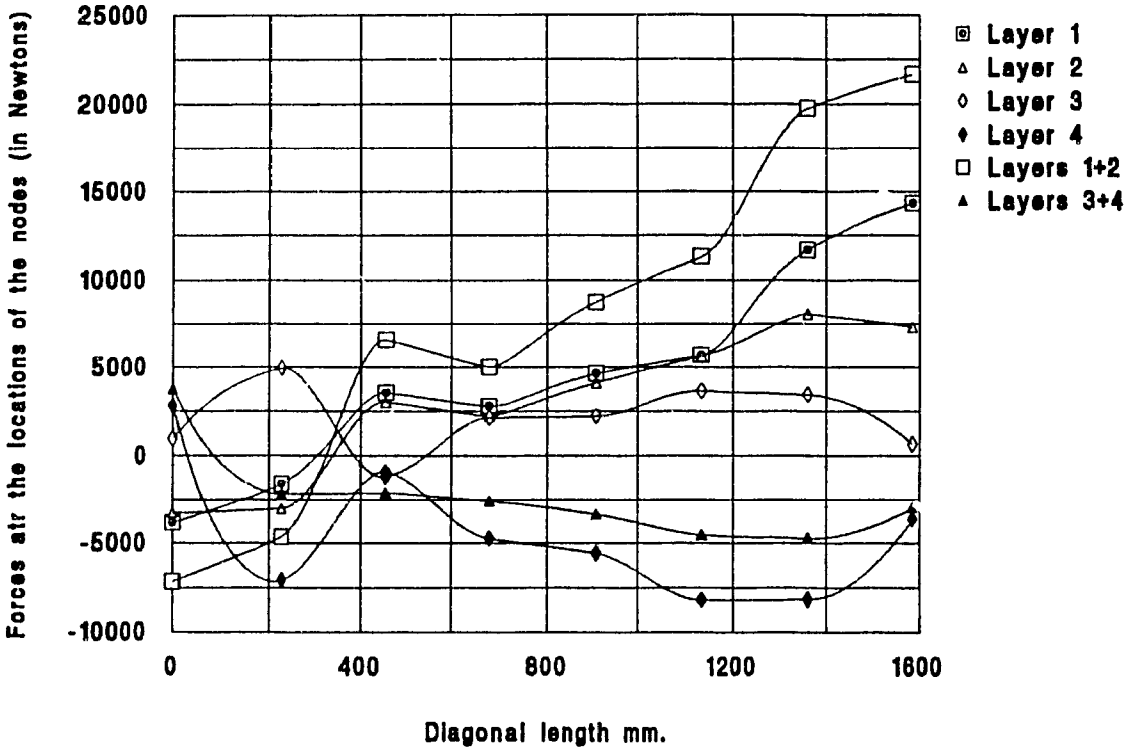

Figure 8-15 Forces perpendicular to the diagonal lines

As shown in Figure 8-15, the summation of the forces acting on layer 1 and layer 2 is represented by the curve called 'Layer 1+2'. Also, the summation of the forces acting on layer 3 and layer 4 is represented by the curve called 'Layer 3+4'. The forces perpendicular

to the diagonal yield lines at the top fibers of the slab and represented by the curve called 'Layer 1+2' are mainly compression forces. The forces that are acting at the bottom fibers of the slab and represented by the curve called 'Layer 3+4' are mainly tension forces.

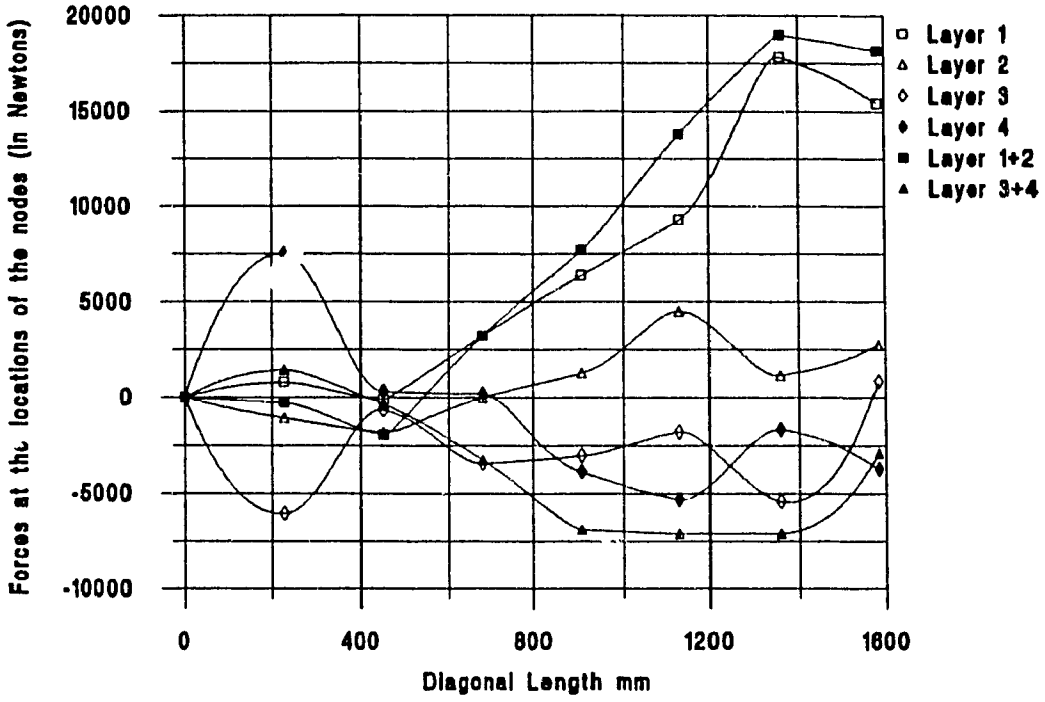

Figure 8-16 Forces parallel to the diagonal lines

As shown in Figure 8-16, the summation of the forces acting on layer 1 and layer 2 is represented by the curve called 'Layer 1+2'. Aiso, the summation of the forces acting on layer 3 and layer 4 is represented by the curve called 'Layer 3+4'. The curve called 'Layer 1+2' has higher values in the vicinity of the concentrated load.

The forces that are represented by the curves called 'Layer 1+2' in

Figure 8-15 and Figure 8-16 are drawn to scale and presented in Figure 8-17 and Figure 8-18 respectively.

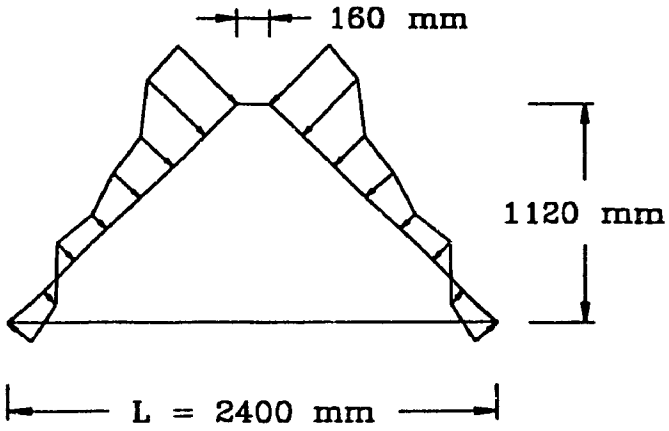

Figure 8-17 Forces perpendicular to the diagonal lines

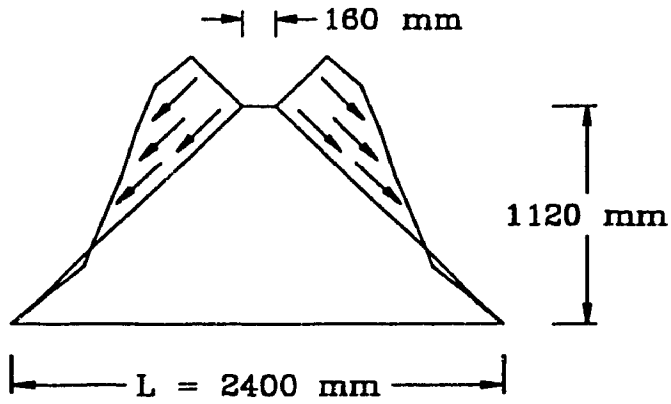

Figure 8-18 Forces parallel to the diagonal lines

As can be seen in Figure 8-17 and 7-18, the diagonal lines of a segment of a square slab are subjected to biaxial forces. In other words,

these diagonal lines are subjected to biaxial stresses. The failure stress envelope for biaxial stress of concrete is given by Pillai and Kirk[75] based on studies by Kupfer et al.[66] and Tasuji et al.[76] and indicates the biaxial compression strength of concrete is $1.25 f_c'$. Since the segments (of square slabs subjected to central concentrated loads) are subjected to biaxial stresses, the value of $1.25 f_c'$ will be used in the analysis that will be presented in the following sections instead of the value of the uniaxial compression strength of the concrete f_c'.

8-6 Finite Elements Analysis of a Square Slab with Fixed Boundaries

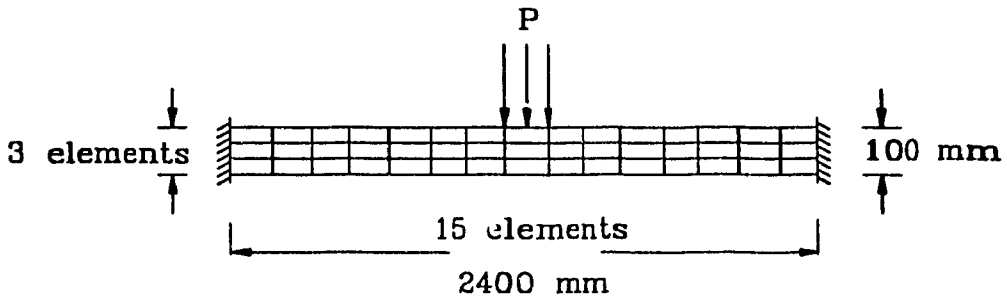

Figure 8-19 A slab with fixed boundaries

A square slab with fixed boundaries subjected to a central concentrated load was also analyzed by program Adina. The boundaries of the slab are shown in Figure 8-19. The mesh of the slab is identical to the mesh of the slab shown in Figure 8-9. The command program to run program Adina for this slab is presented in Appendix D Section D-3.

The purpose of analyzing such a slab is to know whether horizontally restrained square slabs behave similarly to square slabs with fixed boundaries. The forces acting on the diagonal lines on a segment of this slab were obtained from the finite element output and are presented in Appendix D Section D-3. The curves of the forces acting on the diagonal lines of a segment of the slab that are shown in Appendix D are similar to the curves of the square slab horizontally restrained which are presented in Figure 8-13 through Figure 8-16. In addition, both slabs have similar carrying capacity and maximum deflection. These results indicate that horizontally restrained square slabs and square slabs with fixed boundaries have similar behavior.

When a square slab with fixed boundaries subjected to a concentrated load is on the verge of collapse, a perimetric crack penetrates at the top surface of the slab in the vicinity of the boundary and transfers the boundaries shown in Figure 8-19 to boundaries similar to the case shown in Figure 8-9. The output of the finite element analysis indicates the existence of such a perimetric crack.

8-7 Tentative Solution for Horizontally Restrained Square Slabs Subjected to Central Concentrated Loads

As can be seen from the results of the finite element analysis, the problem of a square slab subjected to a central concentrated load is

complex. However, considering a tentative solution that deals with the slab as a structural system composed of four members (or segments) seems possible and may provide acceptable results for such a complicated problem.

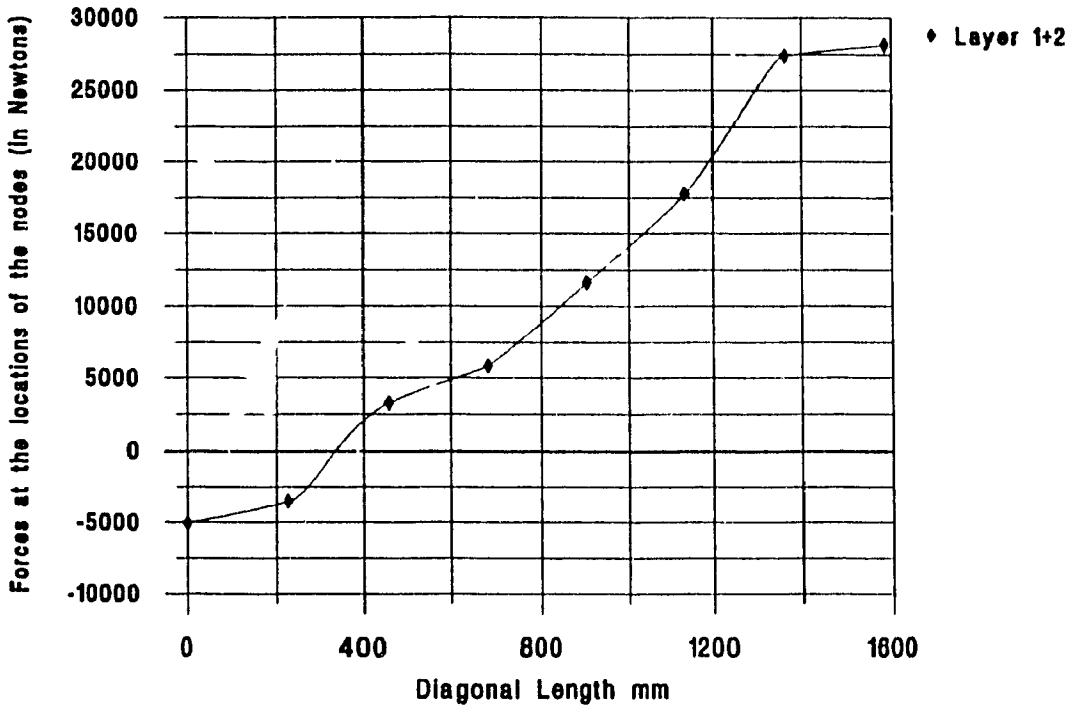

Figure 8-21 The forces that are acting on the diagonal lines of the square slab obtained from summing the forces of layer 1 and 2

For a horizontally restrained square slab, the horizontal reaction (the in-plane reaction) on one side of the boundary of the slab (or on a segment of the slab) is due to the in-plane forces that act on the tip and

on the diagonal lines of the segment in a direction opposite to the direction of the horizontal reaction (see Figure 8-12-A). The curve called 'Layer 1+2' in Figure 8-13 is isolated and is presented as shown in Figure 8-21. This curve represents the forces that are acting on the diagonal lines of a segment of the slab in a direction perpendicular to the base of the segment. The curve presented in Figure 8-21 is drawn to scale and is presented as shown in Figure 8-22.

Now, assume the forces that are acting on the diagonal lines of a segment as shown in Figure 8-22 can be replaced by uniformly distributed forces having the same value as the forces shown in Figure 8-22. These uniformly distributed forces are assumed to be acting on the tip of the segment as shown in Figure 8-23.

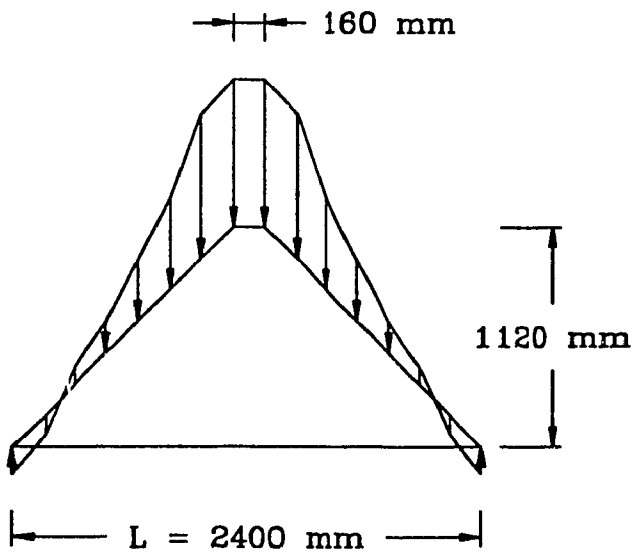

Figure 8-22 Forces acting on the diagonal lines of the square slab

In other words, the actual forces that are acting on the diagonal lines of the square slab as shown in Figure 8-22 are replaced by uniformly distributed stress acting on the tip of the segment as shown in Figure 8-23.

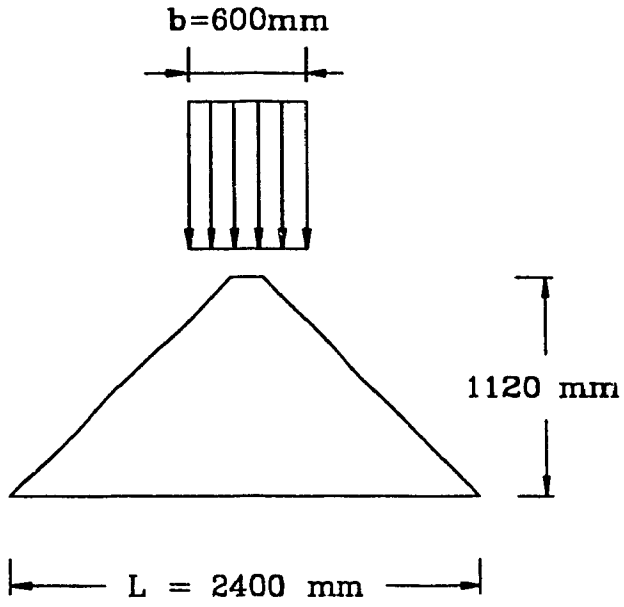

Figure 8-23 Uniformly distributed forces acting on the tip of the segment

To be able to use the analysis presented in Chapter 5, an average width 'b_1' for each segment will be considered. As shown in Figure 8-24, the average width 'b_1' will be taken at line 'o-p' and will be equal to 'L/2'. In other words, the segment shown in Figure 8-24 will be replaced by the segment shown in Figure 8-25. Also, the uniformly distributed stress that acts on the tip of the original segment as shown in Figure 8-23 is considered to be acting on the new segment as shown in Figure 8-25.

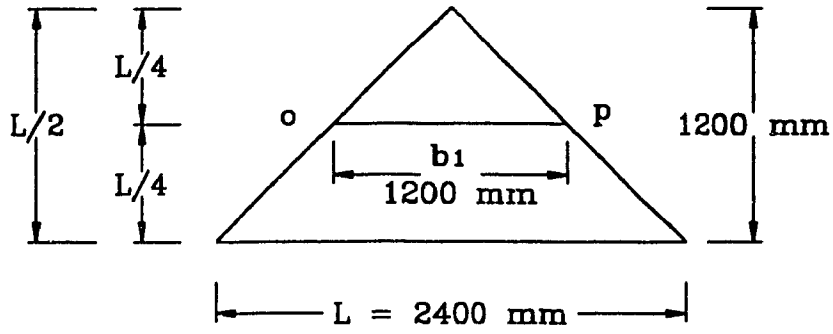

Figure 8-24 The average width 'b1' of the segment

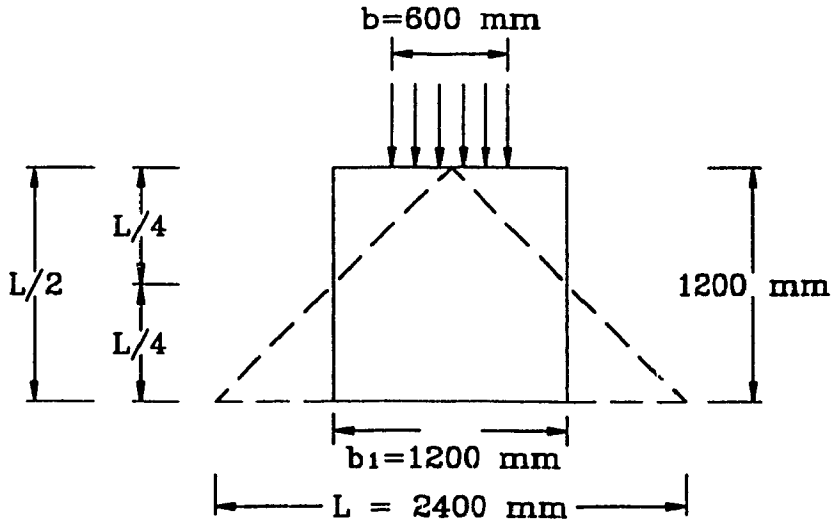

Figure 8-25 Simulation of the original segment of the slab by a segment to be used in the analysis

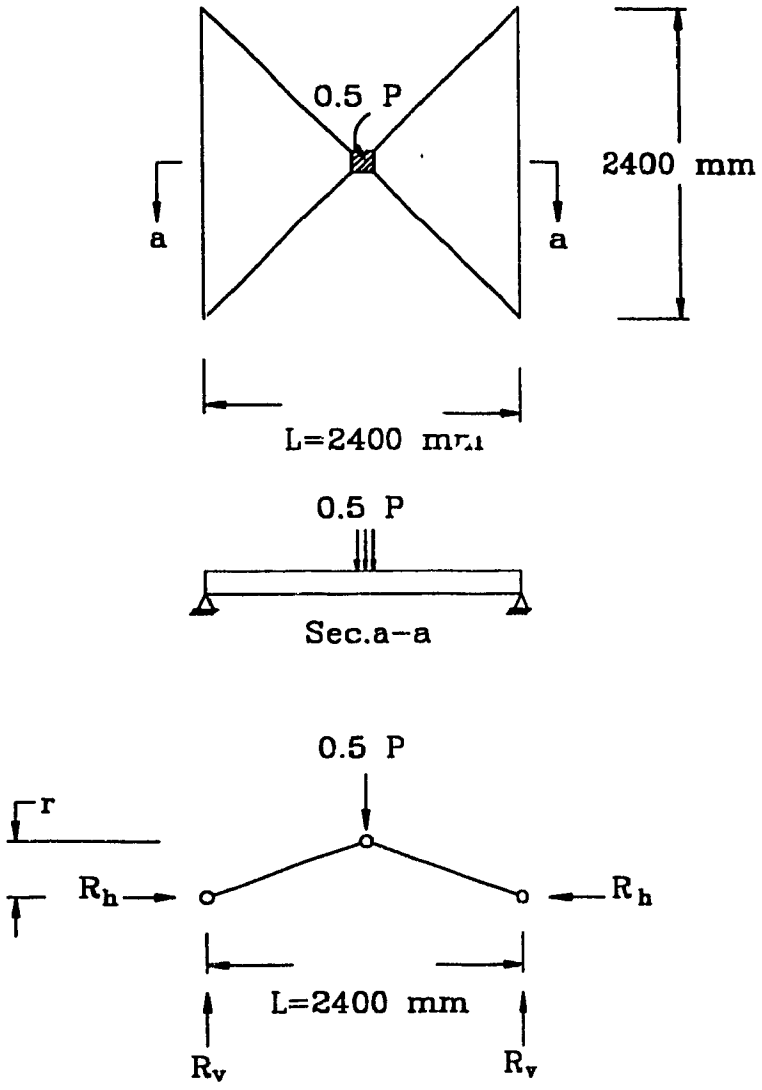

Figure 8-26 The system used in the analysis

To calculate the load that can be carried by the system shown in Figure 8-26, the analysis presented in Chapter 5 will be used. The maximum load that can be carried by this system is half the maximum load that can be carried by the square slab. A summary of the steps of the analysis presented in Chapter 5 is given below.

$$F = 0.85 \times 1.25 \times f_c' \times a \times b \times \frac{1}{\cos\theta}$$

Where 'b' is as shown in Figure 8-23 and Figure 8-25 and the compression depth 'a' is assumed to be equal to half the thickness of the slab 'h' for the first trial. For concrete subjected to biaxial stress, the compression strength is taken as $1.25\, f_c'$.

$$R_h = F \cos\theta$$

$$r = h - a - w$$

The deflection 'w' is assumed to be equal to 1 mm for the first trial.

$$0.5P = R_h \times r \times \frac{4}{L}$$

Where 'L' is 2400 mm and is shown in Figure 8-26. The deflection 'w' can be calculated by using the virtual work method.

$$R_{hu} = 0.5 \times \frac{L}{2r}$$

$$F_u = \frac{R_{hu}}{\cos\theta}$$

$$y = \frac{\sigma}{\sigma_c} = \frac{F}{h \times b_1}$$

Where 'b_1' is as shown in Figure 8-24 and Figure 8-25.

$$\varepsilon = 0.00003y + 0.0071y^2 - 0.01434y^3 + 0.00939y^4$$

$$s = \varepsilon \times \frac{L}{2\cos\theta}$$

$$w = 2 \times F_u \times s$$

Using the following equation to check whether the value of 'a' is corresponding to the maximum load.

$$a = \frac{h}{2} - \frac{w}{2}$$

The above steps need to be repeated until convergence is reached. The results obtained using the above procedure are presented in Table 8-1. In Table 8-1, the deflection that is presented is the maximum deflection at the center of the slab. The load '0.5P' is half the load that can be carried by the square slab. The total maximum load 'P' that can be carried by the square slab is 141.17 kN.

Table 8-1 Results of the solution presented by the present study

Trial No.	Assumed Compression Depth 'a' mm	Obtained Compression Depth 'a' mm	Applied Load '0.5P' kN	Assumed Deflection 'w' mm	Obtained Deflection 'w' mm	Horizontal Reaction 'R_h' kN
1	50	46.93	78.09	1.00	6.14	956.25
2	46.93	47.09	70.13	6.14	5.83	896.63
3	47.09	47.08	70.60	5.83	5.84	899.63
4	47.08	47.08	70.59	5.84	5.84	899.54
5	47.08	47.08	70.59	5.84	5.84	899.54

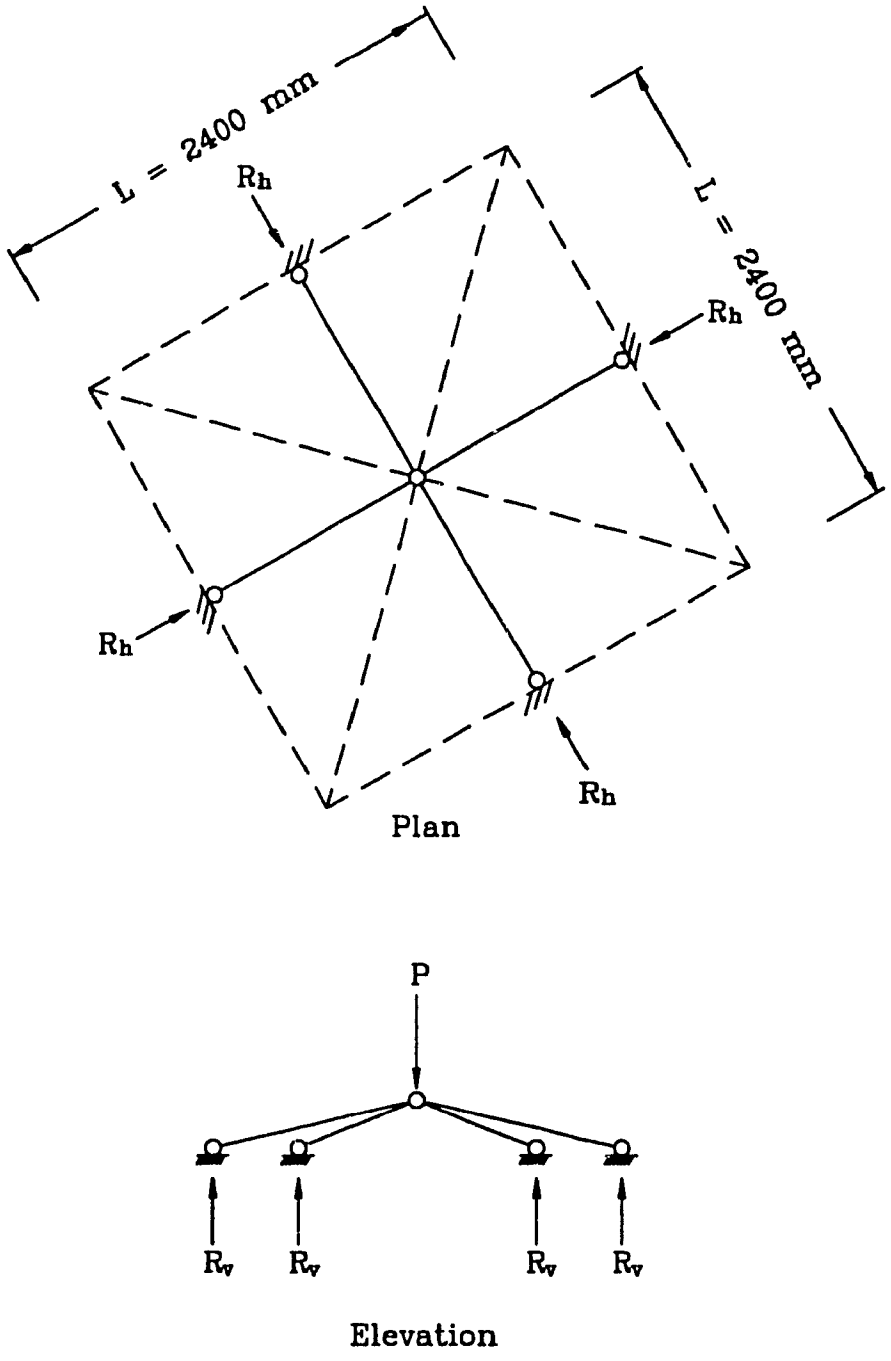

Figure 8-27 The segments of the slab carrying the concentrated load

According to the above analysis, the maximum load 'P' that can be carried by the square slab is actually carried by four segments as shown in Figure 8-27. These segments are replacing the original slab. The average width 'b_1' of each segment is 'L/2' as shown in Figure 8-24 and Figure 8-25. The load that act on the tip of each segment is acting on a width 'b' equal to 'L/4' as shown in Figure 8-25.

To validate the accuracy of the above tentative solution, the results of this solution need to be tested against future experimental results. Therefore, a future experimental program to test horizontally restrained non-reinforced concrete square slabs subjected to central concentrated loads is highly recommended.

8-8 Comparison Between Results Obtained From Finite Element Analysis and Results Obtained From Present Study

As was mentioned in Chapter 5, running program Adina for models having eight node brick elements results in higher carrying capacity and smaller deflection. Therefore, the slab shown in Figure 8-9 was reanalyzed by program Adina using 20 node brick elements. Using 20 node brick elements in the analysis usually consumes great time and storage capacity of the computer. Therefore, taking advantage of the symmetry of the slab, only, a quarter of the slab was analyzed as shown in Figure 8-28.

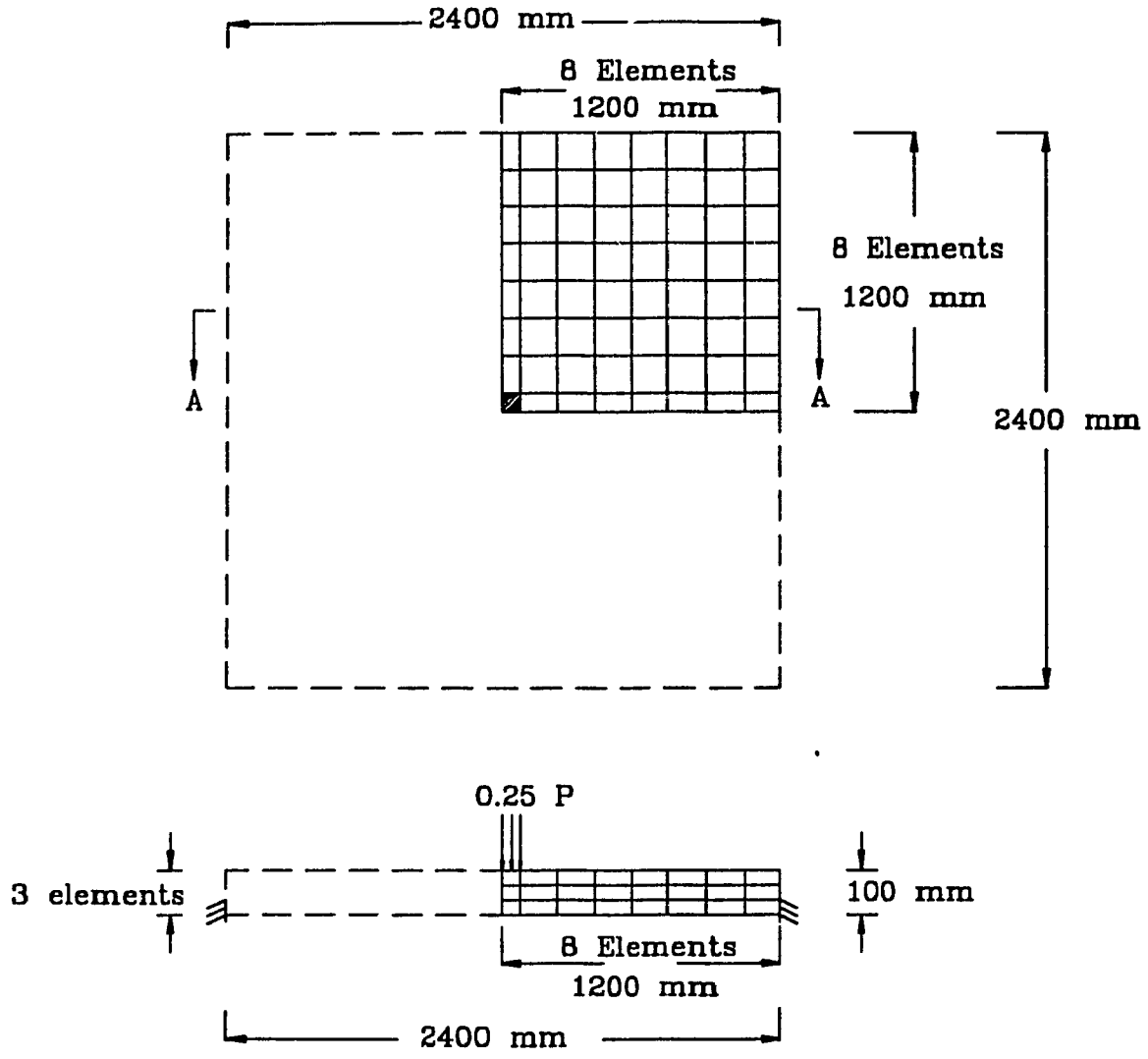

Figure 8-28 Mesh of the slab analyzed using 20 node brick elements

For the analyzed quarter slab, on the axes of symmetry there are six degrees of freedom for each node, three degrees of freedom representing displacements in 'X', 'Y' and 'Z' directions and three

degrees of freedom representing rotations also in 'X', 'Y' and 'Z' directions. For each node along the axes of symmetry two degrees of freedom representing displacements are assumed to be non-restrained, the displacements in a direction perpendicular to the plane of the slab and in a direction parallel to each axis of symmetry. The command program to run program ADINA for this slab is presented in Appendix D Section D-4.

The results of the finite element analysis are compared to the results of the tentative solution presented in the preceding section. The comparison is shown in Table 8-2.

Table 8-2 Comparison of results obtained from finite element analysis and results obtained from present study (tentative solution)

	Finite element analysis (A)	Analysis from the present study (B)	Ratio of (B)/(A)
Load 'P' kN	140.00	141.17	1.008
Deflection 'w' mm	5.79	5.84	1.009
Horizontal reaction 'R_h' kN	879.01	899.54	1.023

Chapter 9

Summary, Conclusions and Recommendations

9-1 Summary

A study dealing with the influence of the horizontal restraints on the behaviour of concrete slabs subjected to central concentrated loads is presented. As a part of this study, an experimental laboratory program was carried out to examine the behaviour of horizontally restrained strip slabs subjected to central concentrated loads. The reinforcement ratio of these strip slabs was similar to the minimum reinforcement ratio required by the Canadian code. The purpose of this reinforcement is to prevent a sudden collapse at the moment of failure of the strip slabs.

Additional comparable tests were carried out on strip slabs that were simply supported and horizontally non-restrained with maximum reinforcement ratio corresponding to the reinforcement ratio at the balanced condition[33]. The purpose of testing these simply supported slabs is to compare their carrying capacities with the carrying capacities of the horizontally restrained strip slabs. The results of the experimental program are presented in Chapter 4.

In addition, an analytical study based on the plastic theory was

carried out to analyze the horizontally restrained strip slabs having full and partial horizontal restraints. As a result, a plastic analysis method was developed for these strip slabs. Also, non-linear finite element analysis for the horizontally restrained strip slabs was carried out. The finite element program ADINA[5] was used to perform the required analysis. The analytical study, its results and the results of the finite element analysis are presented in Chapter 5.

A comparison of the results obtained from the experimental tests and those obtained from the analytical study is presented in Chapter 6. A comparison of the results of the experimental tests for the horizontally restrained strip slabs and the experimental results of the simply supported strip slabs without horizontal restraints is also included in Chapter 6.

An analytical study and finite element analysis were carried out on horizontally restrained square slabs subjected to central concentrated loads. These are presented in Chapter 7. A comparison between the results obtained from the finite element analysis and those obtained from the analytical study are also included in Chapter 7.

9-2 Conclusions

As a result of the experimental program, analytical study and finite element analysis, the following conclusions can be made:

a) The horizontal reactions of horizontally restrained slabs can be obtained by using the elastic theory.

b) Experimental tests prove that the horizontal restraints increase significantly the flexural carrying capacities of the tested strip slabs (or beams).

c) The carrying capacities of horizontally restrained strip slabs with reinforcement ratio similar to the minimum ratio required by the Canadian code are almost equivalent to the carrying capacities of simply supported strip slabs without horizontal restraints having maximum reinforcement ratio (which indicates that the enhanced carrying capacity due to the horizontal restraint can be replaced with equivalent amount by using additional flexural reinforcement).

d) In some cases for horizontally restrained slabs, the flexural reinforcement might not be required. Experimental tests prove that horizontal restraints can reduce or eliminate the flexural reinforcement.

e) At failure load, the segments of the strip slabs or beams are working as members in a mechanism system forming an arch action. These members are connected to each other and to the boundaries by plastic hinges.

f) The proposed method of plastic analysis proves to be accurate and efficient in predicting the maximum concentrated load that can be carried by strip slabs or beams, also in predicting the value of the maximum deflection associated with this load.

g) The proposed method can take into account the effects of full and partial horizontal restraints on the carrying capacities of the strip slabs or beams.

h) The segments of a cracked horizontally restrained square slab subjected to a central concentrated load are dependent on each other in carrying the applied concentrated load.

i) The proposed plastic analysis method can be extended to analyze horizontally restrained square slabs subjected to central concentrated loads.

j) Using the proposed plastic analysis method instead of the finite element analysis can save time and does not need sophisticated computer facilities.

k) The influence of horizontal restraints can be advantageously used in many structural applications. Most of the concrete slabs are, to some degree, horizontally restrained either by beams or adjacent slabs.

l) By considering the influence of horizontal restraints on a wide range of applications of reinforced concrete slabs, a significant

amount of reinforcement can be saved without reducing the carrying capacities of the slabs.

m) This reduced amount of steel has the additional benefit of enhancing the durability of concrete structures against the effect of steel corrosion.

9-3 Recommendations For Further Research

Some types of horizontally restrained slabs are designed without taking advantage of their horizontal restraints. The shortage of information on the subject of the influence of horizontal restraints on the behavior of slabs or the fact that the subject is not yet widely known are reasons for ignoring the effects of horizontal restraints. To provide adequate information on this subject, further research studies and experimental programs are recommended. Some of the recommended research programs are as follows:

a) To validate the accuracy of the proposed plastic method for horizontally restrained non-reinforced square slabs subjected to central concentrated loads, the results of this method need to be tested against results to be obtained from future experimental programs.

b) For horizontally restrained slabs, the problem of shear needs to

be addressed both analytically and experimentally.

c) Additional research investigations are required to examine horizontally restrained two-way slabs with different length to width ratios.

d) Experimental and analytical research are required to examine horizontally restrained slabs subjected to different patterns of loading such as uniformly distributed loads.

REFERENCES

REFERENCES

1- Associate Committee on the National Building Code, National Research Council of Canada " National Building Code of Canada " Ottawa, 1990.

2- Canadian Standards Association "Design of Highway Bridges", CAN3-S6-M78, 1978.

3- Ministry of Transport and Communications, "Ontario Highway Bridge Design Code", Ontario, Canada, 1983.

4- American Association of State Highway Officials, "Standard Specification for Highway Bridges", 11th ed., 1973.

5- Program Adina version 6.1, produced by Adina R & D, Inc. 71 Eiton Avenue, Watertown, MA 02172, USA.

6- Timoshenko and Woinowsky-Krieger "Theory Of Plates And Shells", McGraw-Hill Book Company, New York, 1959.

7- Rrudolph szilard "Theory And Analysis Of Plates, Classical and Numerical Methods", Prentice-Hall, New Jersey, 1974.

8- Park, R. and Gamble, W. L. "Reinforced Concrete Slabs", Wiley, 1980.

9- Al-Khafaji, A. W. and Tooley J. R. "Numerical Methods In Engineering Practice", Holt, Rinehart and Winston, New York, 1986.

10- Lapidus, L and George, F. P. "Numerical Solution of Partial Differential Equation In Science and Engineering", John Wiley and Sons, New York, 1982.

11- Pucher, A. "Einflussfelder Elastischer Platten" Springer-Verlag, Vienna, 1951 and 1964.

12- Woodring, R. E. and Siess, C. P. "An Analytical Study of the Moments in Continuous Two-Way Slabs Produced by Concentrated Loads", Civil Engineering Studies, Structural Research Series No. 264, University of Illinois, Ph.D. Thesis, 1963.

13- Hrennikoff, A. "Solution of the problem of elasticity by framework method", Journal of applied mechanics. Transaction of ASME, A-169 A-175, Dec. 1941.

14- Lightfoot, E. "A grid framework analogy for laterally loaded plates", International Journal of Mechanical Sciences, Great Britain, June 1964.

15- Chen, W.F. "Plasticity in reinforced concrete" McGraw Hill Book company, New York, 1982.

16- Westergaard, H.M. "Theory of elasticity and plasticity", Dover publications, New York, 1952 and 1964.

17- Johansen, K. W. "Brudlinieteorier",J. Gjelerup. Copenhagen 1943.

18- Johansen, K. W. "Yield Line Theory", Cement and Concrete Association, London, 1962.

19- Dutch Committee for Concrete Research (C.U.R.) "Examples of Slab Design By The Yield-Line Theory" C & CA Library, Translation number 121, A translation of report 26c, published originally by the Betonvereniging, The Hague, Translation made by C.V. Amerongen, Cement and Concrete Association, London, 1962.

20- Johansen, K. W. "Yield Line Formulae for Slabs", Translated from the third (1968) edition of the Danish book *Pladeformler*, Cement and Concrete Association, London, 1972.

21- Hognestad, E. "Yield Line Theory for the Ultimate Flexural Strength of Reinforced Concrete Slabs", ACI Journal, Proceedings, 49, pp. 637-656, March 1953.

22- Wood, R. H. "Plastic Design of Slabs Using Equilibrium Methods", Flexural Mechanics of Reinforced Concrete. Proceeding of the International Symposium, Miami, pp. 319-336, 1964.

23- Wang, C. K. and Salmon, C. G. "Reinforced Concrete Design", Harper & Row, Publishers, New York, 4th ed., 1985.

24- Cope, R. J. and Clark, L. A. "Concrete Slabs, Analysis and Design" Elsevier applied science publishers Ltd., London, England, 1984.

25- Magazine of Concrete Research "Recent Developments in Yield-Line Theory" MCR Special Publication, Magazine of Concrete Research, Cement and Concrete Association, London, 1965.

26- Simmonds, S. H. and Ghali, A. "Yield Line Design of Slabs", Journal of the Structural Division, ASCE, Vol. 102(STI), pp. 109-123, Jan. 1976.

27- Fintel, M. "Handbcok of Concrete Engineering", Van Nostrand Reinhold Company Inc., New York, 1985.

28- Gesund, H. and Kaushik, Y. P. "Yield Line Analysis of Punching Failures in Slabs", Publ. IABSE 30-I, pp. 41-60, 1970.

29- Hopkins, H. G. and Prayer, W. "The Load Carrying Capacities of Circular plates" J. Mech. Phys. Solids, 2, pp 1-13, 1953.

30- Schumann, W. "On Limit Analysis of Plate", Quart. Appl. Math., 16, pp. 61-71, 1958

31- Rzhanitsyn, A. R. "The Shape at Collapse of Elastic-Plastic Plates Simply Supported Along the Edges", office of Naval Res., Technical Report No. 19, Division of Applied Mathematics, Brown University, Providence, R. I., Jan. 1957.

32- Jones, L. L., and Wood, R. H. "Yield Line Analysis of Slabs.", American Elsevier Publishing Company, New York, 1967.

33- Canadian Standards Association, "Design of Concrete Structures for Buildings with Explanatory Notes", CSA Standard CAN3-A23.3-M84, Ottawa, 1984.

34- American Concrete Institute-Committee 433, "Analysis and Design of Reinforced Concrete Bridges Structures", American Concrete Institute, 1977.

35- American Concrete Institute Committee 318 "Building Code Requirements For Reinforced Concrete", ACI Standard 318-89. American Concrete Institute, 1989.

36- British Standards Institution, "Code of Practice for Design of Concrete Bridges", BS 5400: Part 4, 1984.

37- British Standards Institution, "Code of Practice for the Structure Use of Concrete", CP 110, 1972.

38- Kuang, J. S. and Morley, C. T. "Punching Shear Behaviour of Restrained Reinforced Concrete Slabs" ACI Structural Journal, Vol. 89 No. 1, pp 13-14, Jan.-Feb., 1992.

39- Batchelor, B. deV. and Tong, P. Y. "An Investigation of the Ultimate Shear Strength of Two-Way Continuous Bridge Slabs Subjected to Concentrated Loads" Ontario Joint Highway Research Program, Sept., 1970.

40- Csagoly, P and Holowka, M. and Dorton, R. - Ontario Ministry of Transportation and Communications "The True Behaviour of Thin Concrete Bridge Slabs". Transportation Research Record N664 pp 171-179, 1979.

41- Hudton, R.L. and Passerello, C.E. "Finite element methods, an introduction", Marcel Dekker Inc. New York, 1984.

42- Stasa, L.F. "Applied finite element analysis for engineers", Holt, Rinehart and Winston, New York, 1985.

43- Bathe, K.J., Oden, J.T., and Wunderlich "Formulations and computational algorithms in finite element analysis", Massachusetts Institute of Technology, 1977.

44- Bathe, K.J. "Nonlinear finite element analysis and Adina", Proceedings of the 8th Adina conference, Massachusetts Institute of Technology, Pergamon Press, New York, 1991.

45- Hyttinen, E. "Dome Action of Reinforced Concrete Slabs" Nordisk Betong, In Sweden, Vol. 15 No. 2, pp. 111-128, 1971.

46- Vecchio, F. J. and Tang, k. "Membrane Action in Reinforced Concrete Slabs", Canadian Journal of Civil Engineering, Vol. 17 No. 5, pp. 686-697, Oct., 1990.

47- Fang, I-k., Lee, J.-H. and Chen C.-R. "Behavior of Partially Restrained Slabs under Concentrated Load" ACI Structural Journal, Vol. 91 No. 2, pp 133-139, March-April, 1994.

48- Westergaard, H. M., and Slater, W. A. "Moment and Stresses in Slabs", Journal of the American Concrete Institute, 17, pp 415-538, 1921.

49- Westergaard, H. M. "Computation of stresses in bridge slabs due to wheel loads", Public Roads, 11, No.1, pp 1-23, March 1930.

50- Dickson, A. R. and Buckle, I. G. and Fenwick, R. C. "The Response of Reinforced Concrete Slabs To Concentrated Loading", Ph.D. thesis, University of Auckland, Department of Civil Eng. Report No. 408, Feb., 1986.

51- Norris, C. H. and Wilbur, J. B. and Utku, S. "Elementary Structural Analysis" McGraw-Hill Book Company, 1976.

52- Au, Tung and Christiano, P. "Structural analysis", Prentice-Hall Inc., New Jersey, 1987.

53- Willems, N. and Lucas, W.M. jr. "Structural analysis for engineers", McGraw-Hill Book Company, New York, 1978.

54- Timoshenko and Goodier "Theory of Elasticity", McGraw-Hill Book Company, 1970.

55- Sabotka, Zdenek "Theory of Plasticity and Limit Design of Plates", Elsevier Science Publishing Company Inc., Printed in Czechoslovakia, 1989.

56- Heins, C. P. "Applied Plate Theory For The Engineer", Lexington Books, 1976.

57- CSA Standard CAN3-A23.3-M84, *Design of Concrete Structures for Buildings* with Explanatory Notes, Canadian Standard Association, Toronto, 1984.

58- Mortar type "M-Bed Standard, non-chloride premixed cementitious grout", produced by Sternson construction products, 403 Boul. Lebeau, St-Laurent, H4N-1S2, Quebec.

59- Beer, F.P. and Johnston, E.R. jr. "Mechanics of materials" McGraw-Hill Inc., New York, 1981.

60- Bathe, K.J., Walczak, J., Welch, A. and Mistry, N. "Nonlinear analysis of concrete structures" Computers and structures, Vol. 32, no. 3/4, pp. 563-590, Great Britain, 1989.

61- Kupfer, H., Hilsdorf, H.K. and Rusch, H. "Behavior of concrete under biaxial stresses" J. Am. Concrete Inst., vol. 66, no. 8, pp. 656-666, August 1969.

62- Kupfer, H. and Gerstle K. N. "Behavior of concrete under biaxial stresses" J. Eng. Mech. Div. ASCE, vol. 99, no. EM4, pp. 852-866, August 1973.

63- Saenz, L.P. "Discussion of the equation for the stress-strain curve of concrete by Desayi and Krishnan" Proc. Am. Con. Inst. vol. 61, no. 9, pp. 1229-1235, September 1964.

64- Ngo, D. and Scordelis, A.C. "Finite Element Analysis of reinforced concrete beams" ACI Journal, vol. 64, no. 3, pp. 152-163, March 1967.

65- Zienkiewicz, O. C. and Holister, G. S. "Stress Analysis" John Wiley & Sons Ltd, pp. 85-119 and pp. 385-424, New York, 1965.

66- Zienkiewicz, O. C. and Cheung, Y. K. "The Finite Element Method in Structural and Continuum Mechanics" McGraw-Hill Publishing Company Limited, New York, 1968.

67- Zienkiewicz, O. C. and Cheung, Y. K. "The finite element method for analysis of elastic isotropic and orthotropic slabs" Proceedings of the Institution for Civil Engineers, vol. 28, pp. 471-488, 1964.

68- Ghoneim, G.A.M. "Nonlinear finite element analysis of concrete structures" Ph.D. thesis, University of Calgary, Canada, August 1978.

69- Jackson, A.T. "Finite element analysis of compressive membrane action in slabs" University of Auckland, New Zealand, Department of Civil Engineering, Report no. 207, June 1979.

70- Hinton, E. and Owen, D.R.J. "Computational modeling of reinforced concrete structures" Pinridge Press, 1986.

71- Task committee on finite element analysis of reinforced concrete structures of the Structural Division, Committee on Concrete and Masonry Structures "Finite element analysis of reinforced concrete" American Society of Civil Engineers, New York, 1982.

72- Meyer, C., Okamura, H., Shinkokai, N.G. "Finite element analysis of reinforced concrete structures" Proceedings of seminar sponsored by the Japan Society for the Promotion of the Science and the US National Science Foundation, Tokyo, Japan, May 1985, American Society of Civil Engineers, New York, 1986.

73- Bathe, Klaus-Jürgen "Finite element procedures in engineering analysis" Prentice-Hall Inc., New Jersey, 1982.

74- Murashev, V., Sigalov, E. and Baikov, V. "Design of reinforced concrete structures", Mir Publishers, Moscow, 1976.

75- Pillai, S.U. and Kirk, D.W. "Reinforced concrete design" McGraw-Hill Ryerson Limited, Toronto, Canada, 1988.

76- Tasuji, M.E., Slate, F.O. and Nilson, A.H. "Stress-Strain Response and Fracture of Concrete in Biaxial Loading" ACI Structural Journal, Vol.75, pp 306-312, Jul. 1978.

77- Vecchio, F.J. and Collins, M.P. "Investigating The Collapse Of A Warehouse" Concrete international, Vol. 12, No. 3, pp.72-78, 1990.

78- Christiansen, K.P. "The Effect Of Membrane Stresses On The Ultimate Strength Of The Interior Panel In A Reinforced Concrete Slab" The structural engineer journal, Vol. 41, No. 1, Jan. 1963, London.

79- Taylor, R. and Hayes, B. "Some Tests On The Effect Of Edge Restraint On Punching Shear In Reinforced Concrete Slabs" Cement and Concrete Association, Magazine of concrete research, Vol. 17, No. 50 March 1965, London.

80- Park, R. "The Lateral Stiffness And Strength Required To Ensure Membrane Action At The Ultimate Load Of A Reinforced Concrete

Slab-And-Beam floor" Cement and Concrete Association, Magazine of concrete research, Vol. 17, No. 50 March 1965, London.

81- Park, R. "Ultimate Strength Of Rectangular Concrete Slabs Under Short-Term Uniform Loading With Edges Restrained Against Lateral Movement" The institution of civil engineers, Proceedings Vol. 28, session 1963-64, May 1964, London.

82- Guice, L.K. and Rhomberg, E.J. "Membrane Action In Partially Restrained Slabs" American Concrete Institute, Structural journal, Vol. 85, No. 4, pp. 365-373, 1988.

83- Hewitt, B.E. and Batchelor, B.V. " Punching Shear Strength of Restrained Slabs" Journal of the Structural Division, proceeding of the American society of civil engineers, Vol. 101, No. ST9, Sept. 1975.

84- Mufti, A.A., Jaeger, L.G., Bakht, B., Wegner, L.D. "Experimental investigation of fibre-reinforced concrete deck slabs without internal steel reinforcement" Canadian Journal of Civil Engineering, Vol. 20, No. 3, pp. 398-406, June 1993.

85- Brotchie, J.F. and Holley, M.J. "Membrane Action in Slabs" International symposium on the Cracking, Deflection, and Ultimate Load of Concrete Slab Systems, American Concrete Institution, pp. 345-377, March 1971.

86- Hopkins, D.C. and Park, R. "Test on a reinforced concrete slab and beam floor designed with allowance for membrane action" International symposium on the Cracking, Deflection, and Ultimate Load of Concrete Slab Systems, American Concrete Institution, pp. 223-250, March 1971.

87- Kirkpatrick, J., Rankin, G.I.B. and Long, A.E. " The influence of compressive membrane action on the serviceability of beam and slab bridge decks" The structural Engineer, Journal of the Institution of Structural Engineers, Vol. 64B, No. 1, pp. 6-12, March 1986.

APPENDIXES

Appendix A

A-1 The values of the applied loads versus the deflections, for each slab test, are presented as follow:

Test No. S1

Load kN.	Deflection mm.
0.000000	0.000
1.143193	0.405
2.237456	1.120
4.448222	2.110
6.672333	3.585
9.007650	4.065
11.120555	5.580
13.344666	7.340
15.568777	9.435
17.792888	12.095
20.016999	15.745
21.974217	23.360

Test No. S2

Load kN	Deflection mm.
0.000000000	0.0000
1.112055500	0.4600
2.224111000	0.9000
4.448222000	2.1250
8.896444000	4.7500
12.010199400	6.7350
13.344666000	7.6600
15.568777000	9.2000
17.792888000	11.1500
20.016999000	13.1250
22.241110000	15.3250
24.465221000	18.3350
26.689332000	22.7450
28.148348816	30.8917
8.006799600	33.7580
7.428530740	35.6688
6.183028580	36.9427
5.426830840	39.4904
5.026490860	40.7643
4.421532668	43.9490
3.914435360	45.8599
3.336166500	49.0446
3.291684280	52.8662
3.202719840	56.0510
2.935826520	57.3248
3.069273180	61.1465
3.069273180	65.6051
3.158237620	67.5159
3.247202060	71.3376
3.336166500	76.4331
3.113755400	82.1656
3.113755400	89.8089
3.113755400	89.1720
3.113755400	101.2739
3.113755400	107.6433

Test No. S3

Load kN	Deflection mm.
0.0000	0.0000
1.1121	0.2500
2.2241	0.6000
4.4482	2.4719
6.6723	3.7640
8.8964	5.5618
11.1206	7.1348
13.3447	9.0449
15.5688	11.2921
17.7929	13.8764
20.0170	17.2472
22.2411	22.4719
23.3075	29.0500
16.0136	35.7865
15.1240	39.2135
13.3447	43.1461
6.6723	48.6517
5.3379	49.5506
4.0034	53.9888
3.3362	58.6517
2.6689	61.1236
2.4465	62.5281
2.2241	68.7640
2.2241	73.3708
2.6245	81.8539
2.5800	90.2247
2.4020	95.8427
2.5800	100.8989
2.5800	105.5056
2.4910	109.3258
2.4465	114.8876
2.4465	122.3596

Test No. S4

Load kN	Deflection mm.
0.000	0.000
1.112	0.385
2.224	0.705
4.448	1.538
6.672	2.308
8.896	3.590
11.121	4.615
13.345	5.705
15.569	6.859
17.793	8.077
20.017	9.359
22.241	10.897
24.465	12.756
26.689	14.615
28.913	17.051
31.138	19.615
33.362	23.269
35.586	29.615
25.800	30.449
25.577	30.577
25.355	31.090
25.444	32.372
25.132	32.949
24.688	33.526
24.376	34.167
23.798	35.128
23.353	35.192
22.908	35.256
22.241	35.513
22.686	36.795
16.014	38.718
15.569	39.615
14.234	41.859
13.789	42.500
11.565	43.141
10.231	45.128
8.896	46.474
6.672	48.526

(cont'd)

Load kN	Deflection mm.
5.783	49.423
4.893	50.449
4.893	52.949
4.893	53.462
4.671	56.154
4.448	57.051
4.315	58.974
4.226	59.423
3.003	61.795
2.420	61.859
3.336	64.551
3.470	66.859
3.559	68.910
3.710	71.859
3.794	74.359
3.866	76.923
3.848	79.872
3.768	81.667
3.817	83.910
3.830	87.564
4.408	90.449
3.870	94.103
3.750	96.795
3.923	99.359
3.839	101.987
3.977	104.872
3.914	106.410
3.914	108.397
3.981	111.282
4.003	112.308
4.030	115.256
4.035	116.923
4.048	120.192
3.825	124.167
3.888	127.179
3.879	132.179
4.030	132.179

Test No. S5

Load kN	Deflection mm.
0.000	0.000
1.112	0.556
2.224	1.173
4.448	2.593
6.672	4.012
8.896	5.679
11.121	7.407
13.345	9.074
15.569	10.988
17.793	12.654
20.017	14.506
22.241	16.173
24.465	17.778
26.689	19.753
28.913	21.420
31.138	23.333
33.362	25.494
35.586	27.593
36.920	34.691
36.475	45.000
32.027	51.605
27.134	53.580
27.134	55.617
26.245	57.531
26.245	58.519
25.800	59.506
25.800	60.494
25.355	61.543
24.465	62.531
24.465	63.580
24.020	64.568
23.576	65.556
23.576	66.605
23.131	67.593

(cont'd)

Load kN	Deflection mm.
22.686	68.580
21.796	69.630
18.683	70.617
17.348	71.605
16.458	72.531
15.791	73.457
15.257	74.383
14.857	75.247
14.679	76.235
14.412	77.222
13.878	78.272

Test No. S6

Load kN	Deflection mm.
0.0000	0.000
1.1100	0.679
2.2200	1.605
4.4500	3.086
6.6700	4.691
8.9000	6.481
11.1200	8.457
13.3400	10.185
15.5700	12.654
17.7900	14.136
20.0200	16.173
22.2400	18.025
24.4700	20.926
26.6900	22.284
28.9100	24.136
31.1400	26.
33.3600	29.259
35.3200	41.049
34.6200	42.716
34.4500	43.765
34.0600	44.753
34.2600	45.741
34.1600	46.790
32.4200	47.716
32.1500	48.765
32.6200	49.815
32.4100	50.802
32.2700	51.852
31.5600	52.840
32.1800	53.827
31.8800	54.877
31.8400	55.864
31.9500	56.852
31.8700	60.000
30.6900	64.691

(cont'd)

Load kN	Deflection mm.
21.2800	72.222
14.3900	78.272
11.8500	84.753
10.3500	89.630
9.8200	96.235
8.4800	104.506
7.5800	111.296
7.3400	117.160
7.0100	124.012
6.8500	131.914
6.4900	138.827

Test No. S7

Load kN	Deflection mm.
0.0000	0.000
1.1120	0.375
2.2240	0.937
4.4480	2.250
6.6720	4.375
8.8960	6.812
11.1210	9.063
13.3450	11.250
15.5690	13.812
17.7930	15.812
20.0170	17.875
22.2410	20.563
24.4650	26.188
25.2880	28.770
25.3150	32.812
24.9010	38.250
24.8660	44.125
24.2290	47.937
24.5190	51.875
23.6960	57.625
23.6250	61.313
22.9840	66.688
22.3480	71.000
21.9830	75.313
21.9790	80.063
21.3600	86.250
20.6180	91.688
17.8460	97.313
16.1470	102.688
14.7190	107.563
13.3980	113.375

Test No. S8

Load kN	Deflection mm.
0.0000	0.0000
1.1121	0.5625
2.2241	1.3125
3.3362	1.8750
4.4482	2.9375
6.6723	5.1563
8.8964	6.7500
11.1206	8.8125
13.3447	11.0000
15.5688	12.6875
17.7929	14.5625
20.0170	16.1250
22.2411	18.0000
24.4652	20.1875
26.6893	22.5000
28.1483	29.0000
28.3886	32.7500

Test No. S9

Load kN	Deflection mm.
0.00000000	0.000
1.11205550	0.485
2.22411100	0.970
3.33616650	1.455
4.44822200	2.545
6.67233300	3.818
8.89644400	5.152
11.12055500	6.848
13.34466600	8.485
15.56877700	10.485
17.79288800	12.424
20.01699900	14.970
22.24111000	17.879
24.46522100	22.485
25.73296427	29.273
23.48661216	33.394
21.20467427	37.818
17.79288800	41.515
3.78098870	46.667
3.34506294	49.697
2.50434899	53.091
1.61915281	55.576
1.24550216	68.848
2.22411100	79.455
2.46431499	81.636
2.52214187	84.606
2.61110631	88.121
2.65558853	90.788
2.70451898	93.515
2.70451898	96.667
2.72231186	99.091

Test No. S10

Load kN	Deflection mm.
0.000000000	0.000000
1.112055500	0.440252
2.224111000	0.817610
4.003399800	1.572327
4.448222000	1.761006
6.672333000	3.584906
8.896444000	5.283019
11.120555000	6.981132
13.344666000	8.930818
15.568777000	11.383648
17.792888000	13.899371
20.016999000	17.421384
22.241110000	22.515723
22.908343300	28.867925
20.973366730	33.018868
20.532992752	36.100629
19.327524590	39.308176
17.792888000	42.201258
5.435727284	47.358491
5.008697972	51.383648
4.092364240	55.283019
3.140444732	58.616352
1.975010568	62.452830
2.246352110	90.566038
2.424280990	92.830189
2.482107876	95.974843
2.513245430	98.616352
2.562175872	101.383648

Test No. S11

Load kN	Deflection mm.
0.000000000	0.0000
1.112055500	0.5660
2.224111000	1.0063
3.336166500	1.5094
4.448222000	2.2013
6.672333000	4.2138
8.896444000	5.7862
11.120555000	7.5472
13.344666000	9.5597
15.568777000	11.7296
17.792888000	14.5283
20.016999000	17.3585
22.241110000	22.6730
23.130754400	27.8302
22.423487102	31.1950
21.395947820	35.2830
19.990309668	39.7484
3.669783150	44.0252
2 660036756	48.4906
1.080917946	65.8491
1.948321236	90.7547
2.077319674	97.6730
2.095112562	100.3145

Test No. S12

Load kN	Deflection mm.
0.00000	0.000
1.11206	0.539
2.22411	0.958
3.33617	1.317
4.44822	2.635
6.67233	4.251
8.89644	6.168
11.12056	7.904
13.34467	10.299
15.56878	12.515
17.79289	15.569
20.01700	19.880
21.90749	29.042
20.13710	30.719
18.64695	33.353
15.07947	36.048
12.97991	39.162
7.02374	42.156
5.68928	45.389
4.79074	47.605
4.04343	50.180
2.60666	54.491
2.19297	96.347
2.09956	100.060
2.17073	101.557

A-2 The results of all concrete and mortar compression tests (three tests for each slab) are presented as follow:

Compression tests for concrete

Test No	First test 'lb'	Second test 'lb'	Third test 'lb'
S1	29150	30100	28550
S2	34150	31650	32250
S3	35700	30900	32800
S4	38400	32750	31050
S5	33100	36150	35750
S6	32550	28800	38850
S7	46700	44500	49200
S8	40150	33500	41850
S9	28700	32500	39350
S10	39500	36000	40250
S11	30500	38150	45350
S12	33200	48250	37250

Compression tests for mortar

Test No	First test 'lb'	Second test 'lb'	Third test 'lb'
S1	27100	23850	24850
S2	34550	26850	35800
S3	37000	36500	35500
S4	35000	28750	34250
S9	35350	27200	39300
S10	-	-	-
S11	23150	25000	29050
S12	23100	36200	42150

A-3 The load-deflection curve, for each slab test, is presented, in Figure A-1 through Figure A-12, as follows:

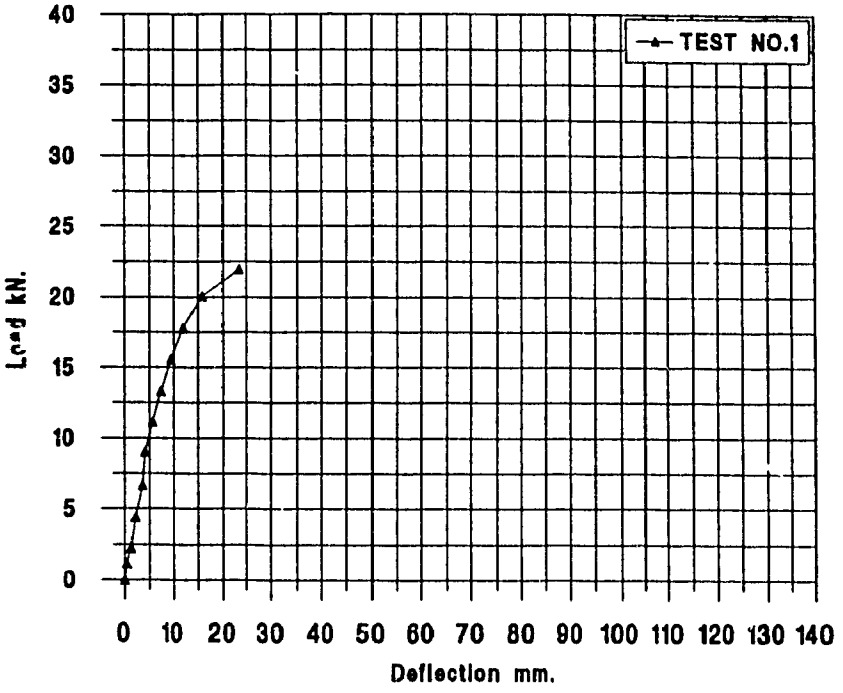

Figure A-1 Load-deflection curve for test S1 (restrained boundaries)

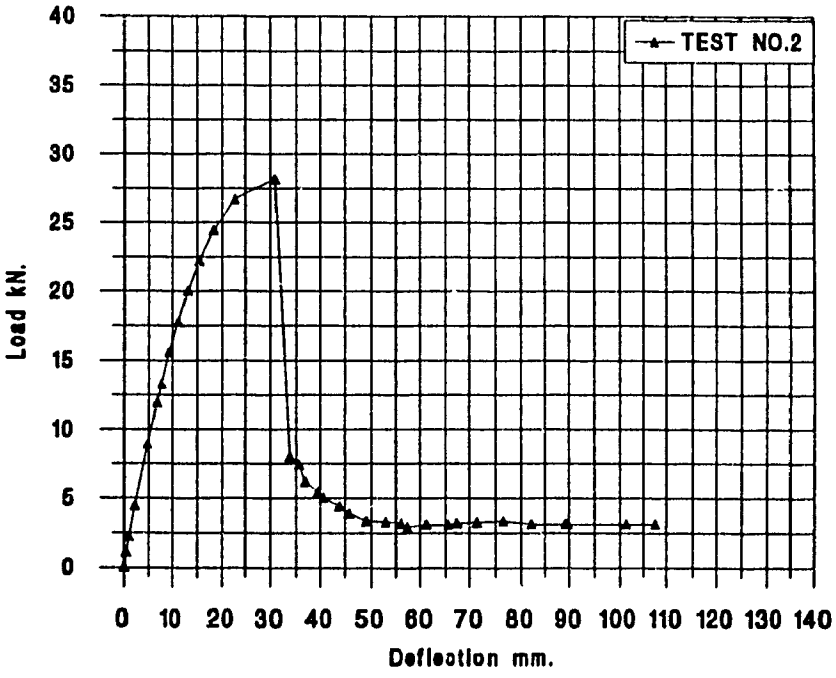

Figure A-2 Load-deflection curve for test S2 (restrained boundaries)

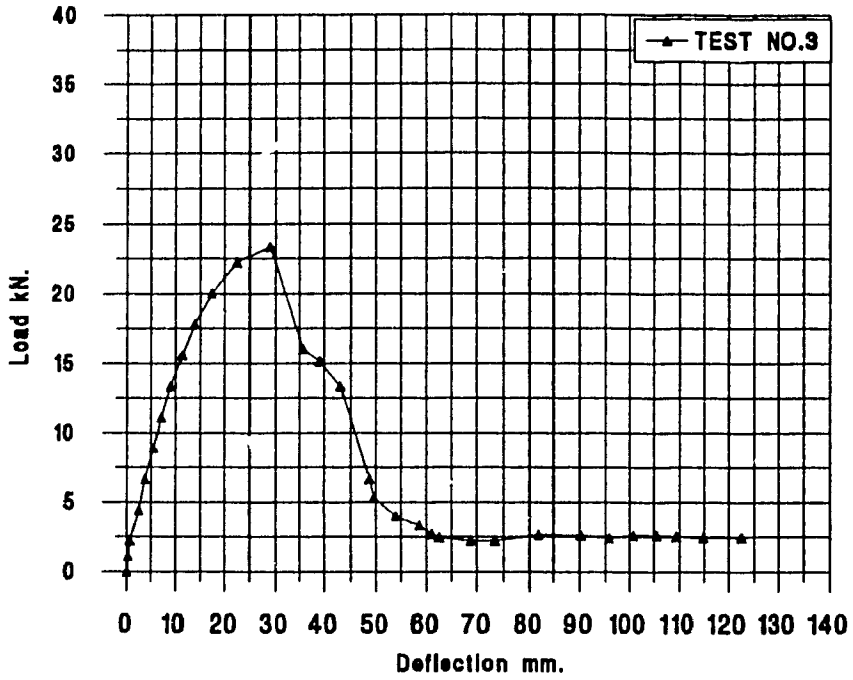

Figure A-3 Load-deflection curve for test S3 (restrained boundaries)

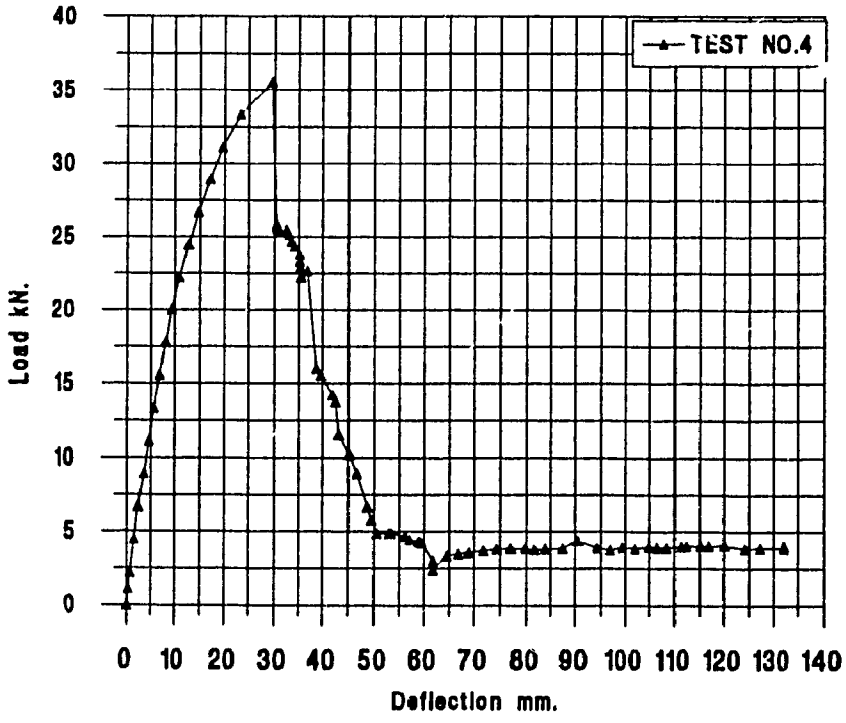

Figure A-4 Load-deflection curve for test S4 (restrained boundaries)

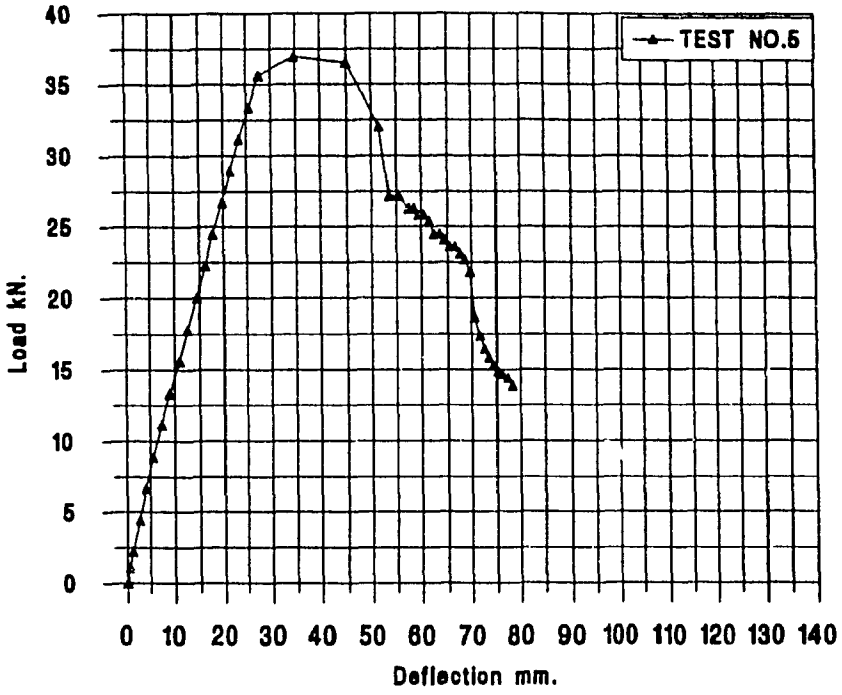

Figure A-5 Load-deflection curve for test S5 (simply supported boundaries)

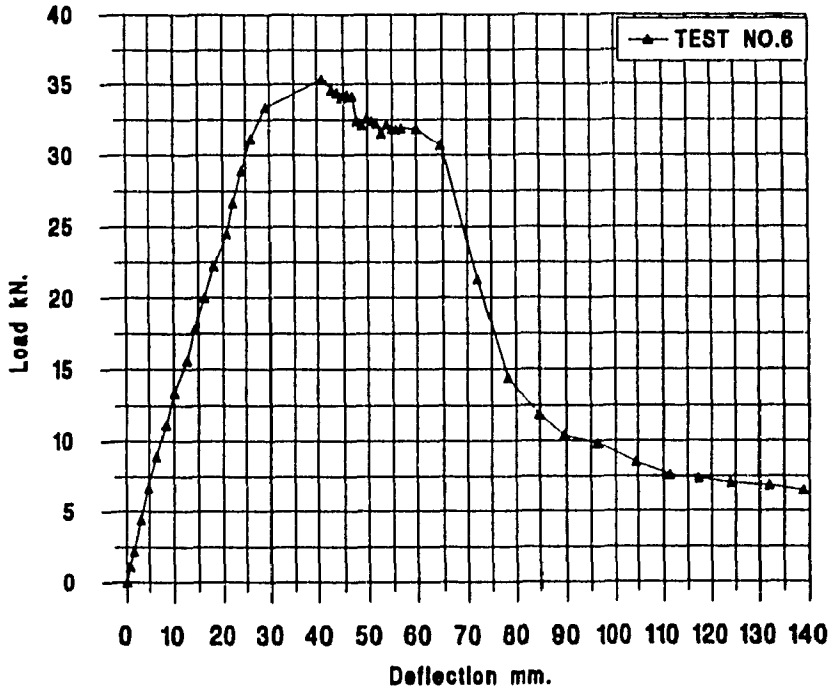

Figure A-6 Load-deflection curve for test S6 (simply supported boundaries)

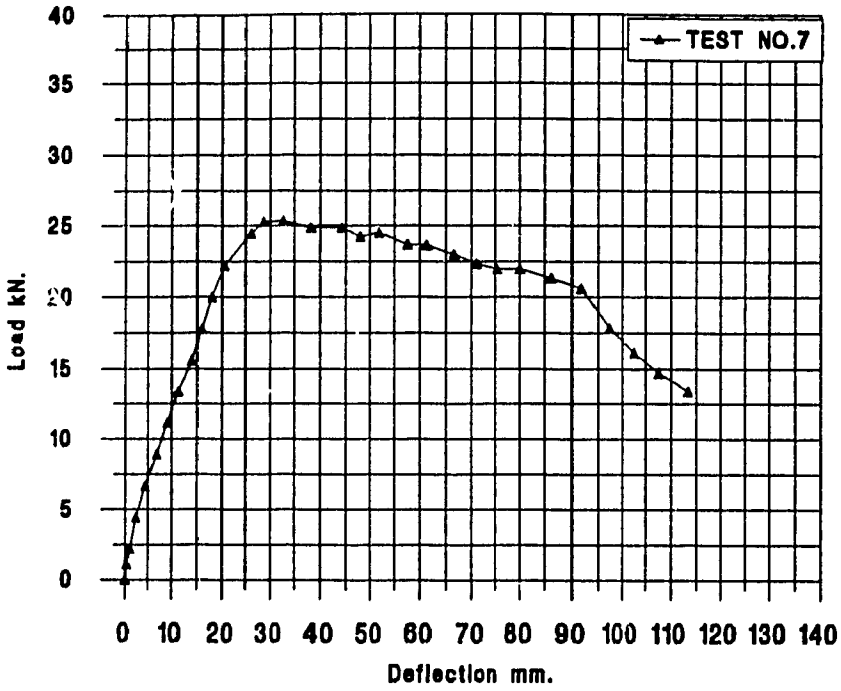

Figure A-7 Load-deflection curve for test S7 (simply supported boundaries)

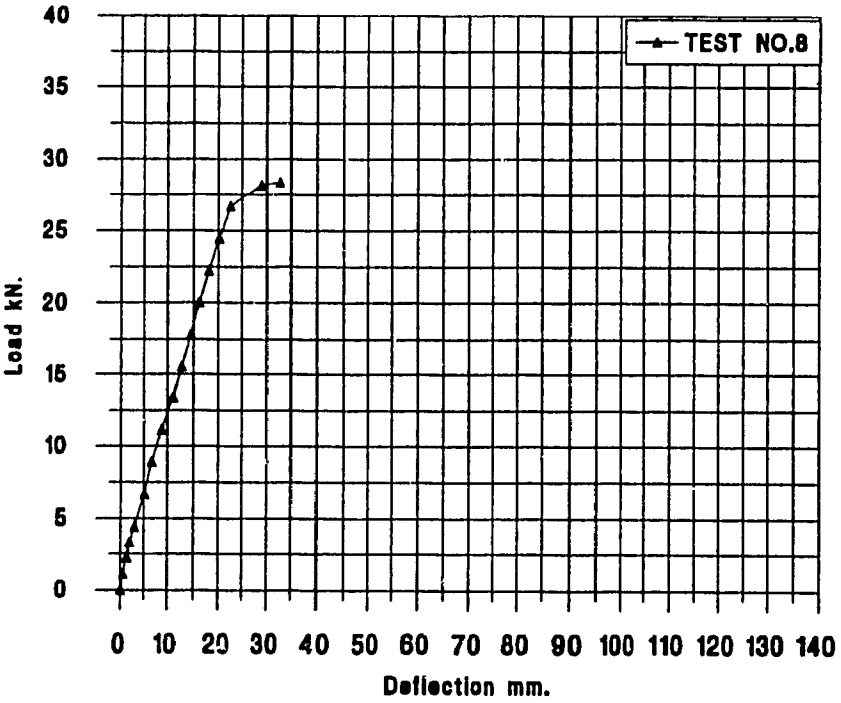

Figure A-8 Load-deflection curve for test S8 (simply supported boundaries)

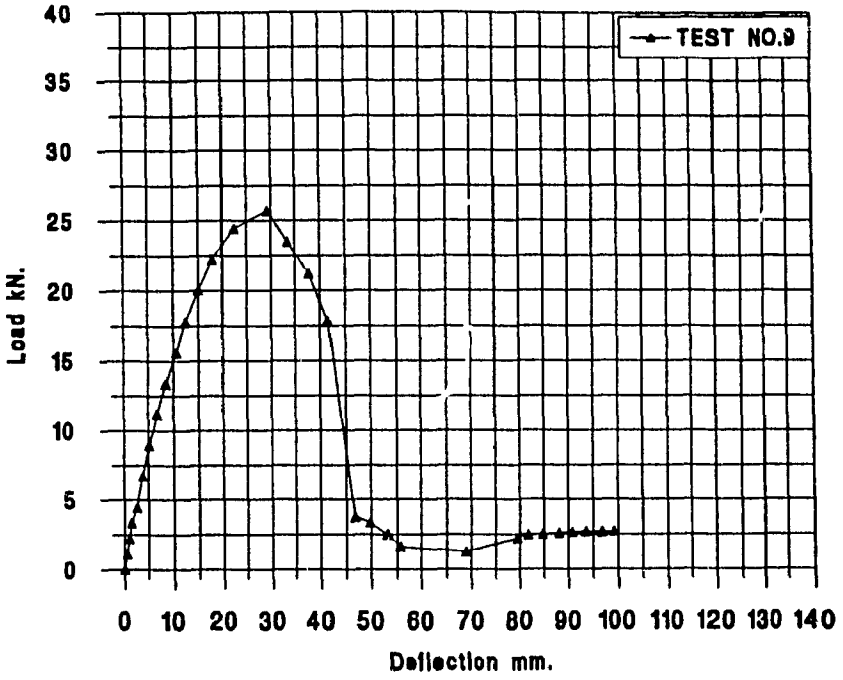

Figure A-9 Load-deflection curve for test S9 (restrained boundaries)

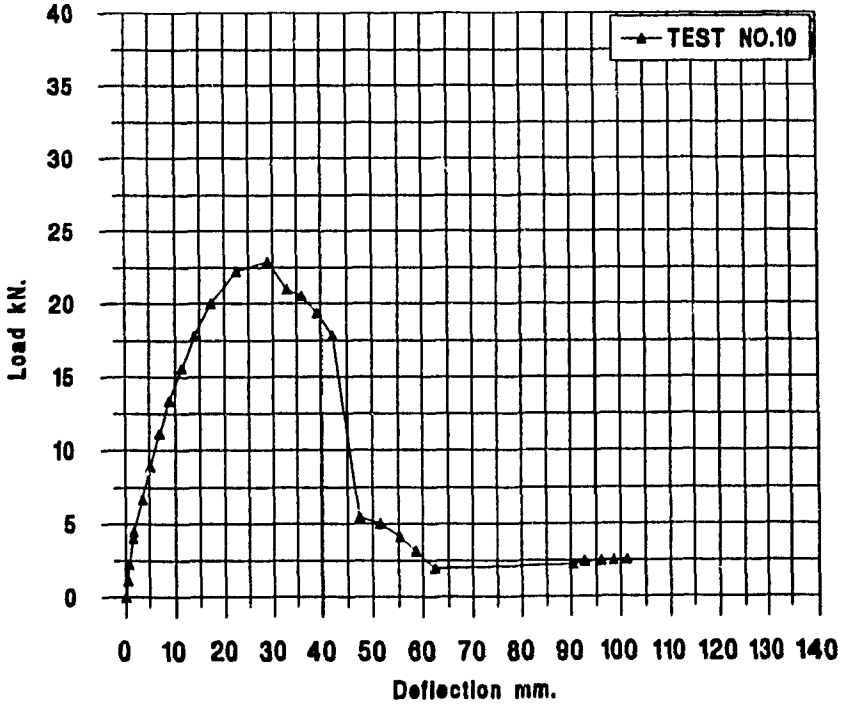

Figure A-10 Load-deflection curve for test S10 (restrained boundaries)

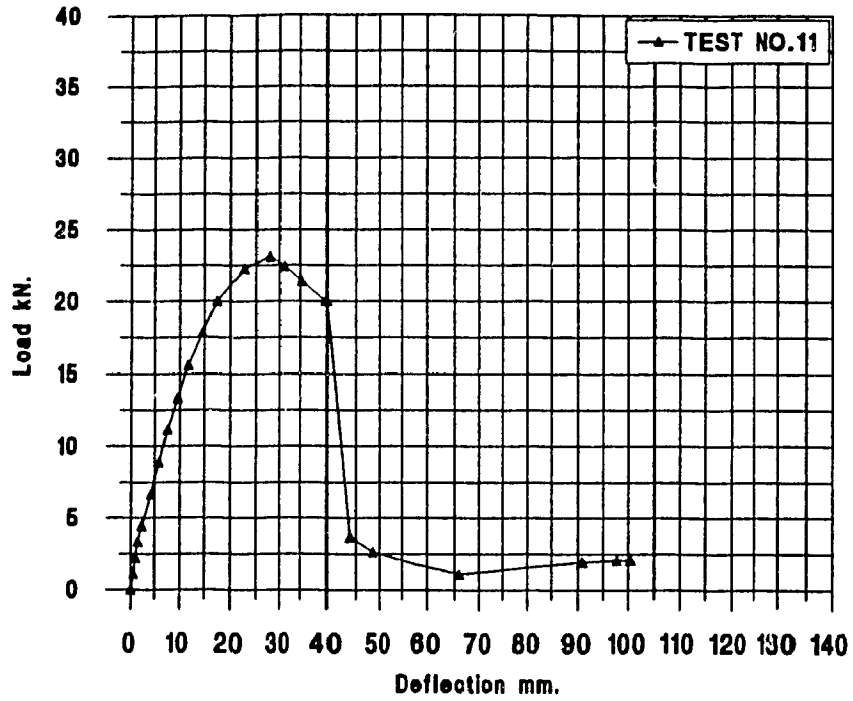

Figure A-11 Load-deflection curve for test S11 (restrained boundaries)

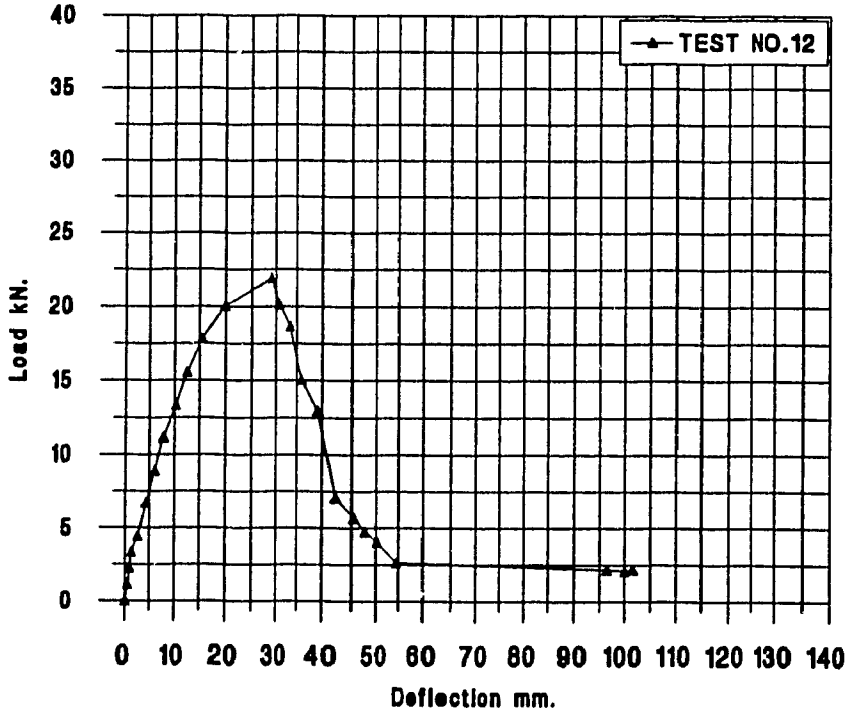

Figure A-12 Load-deflection curve for test S12 (restrained boundaries)

A-4 The graphs of the stress-strain curves that are obtained from the steel tests are shown as follows:

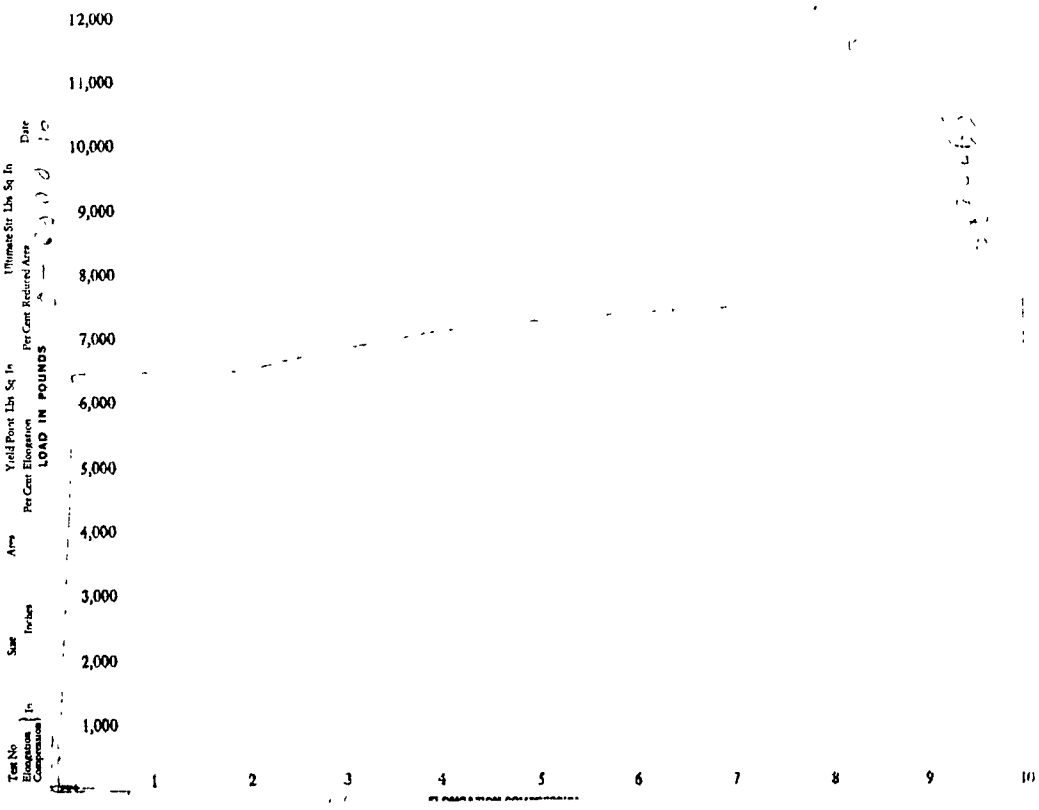

Figure A-13 Load-deformation test no.1 for bar 6M (first series)

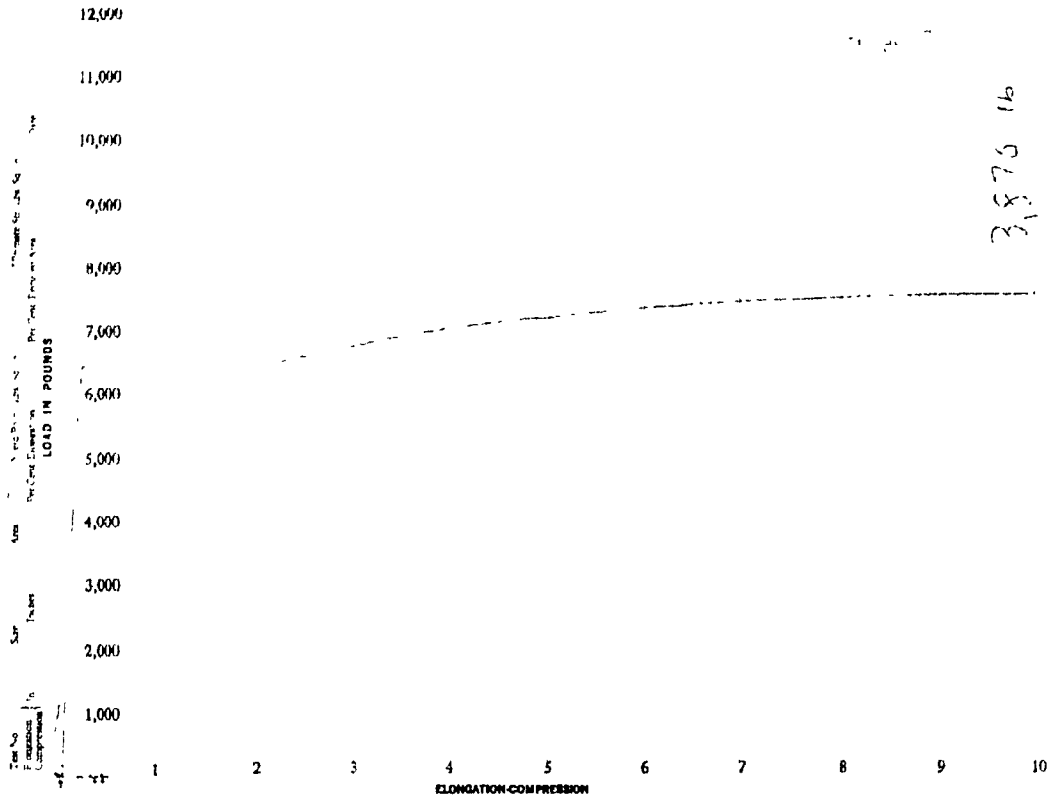

Figure A-14 Load-deformation test no.2 for bar 6M (first series)

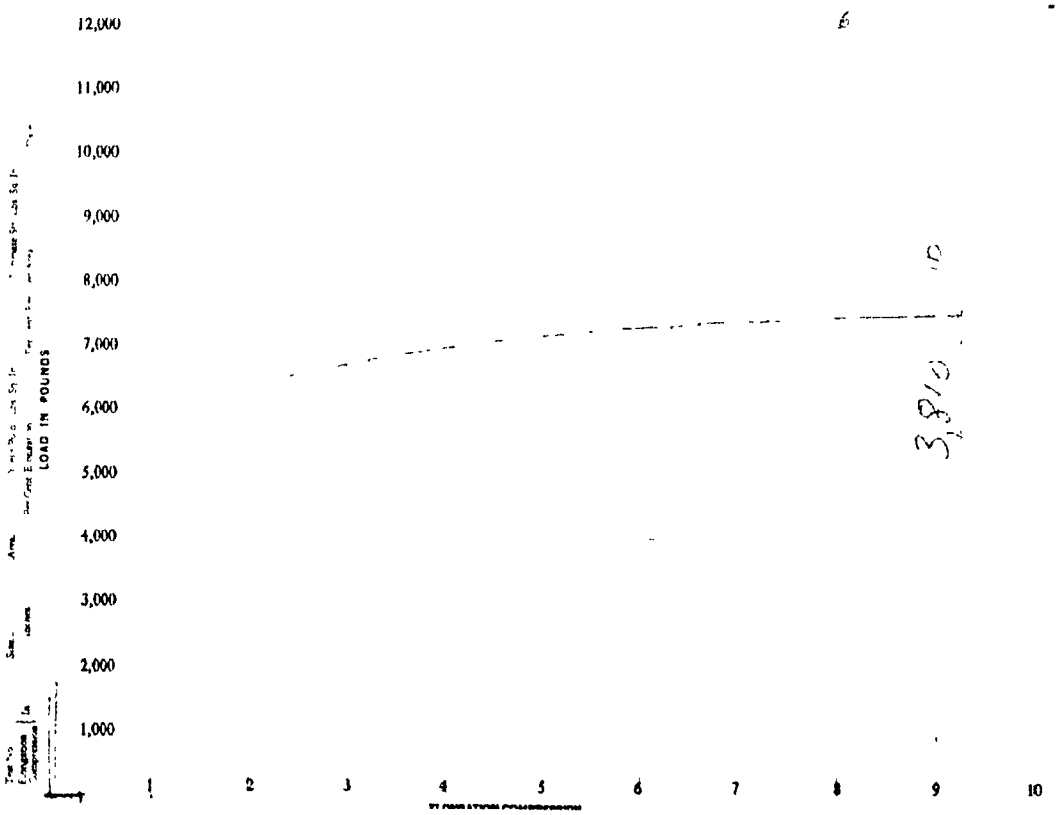

Figure A-15 Load-deformation test no.3 for bar 6M (first series)

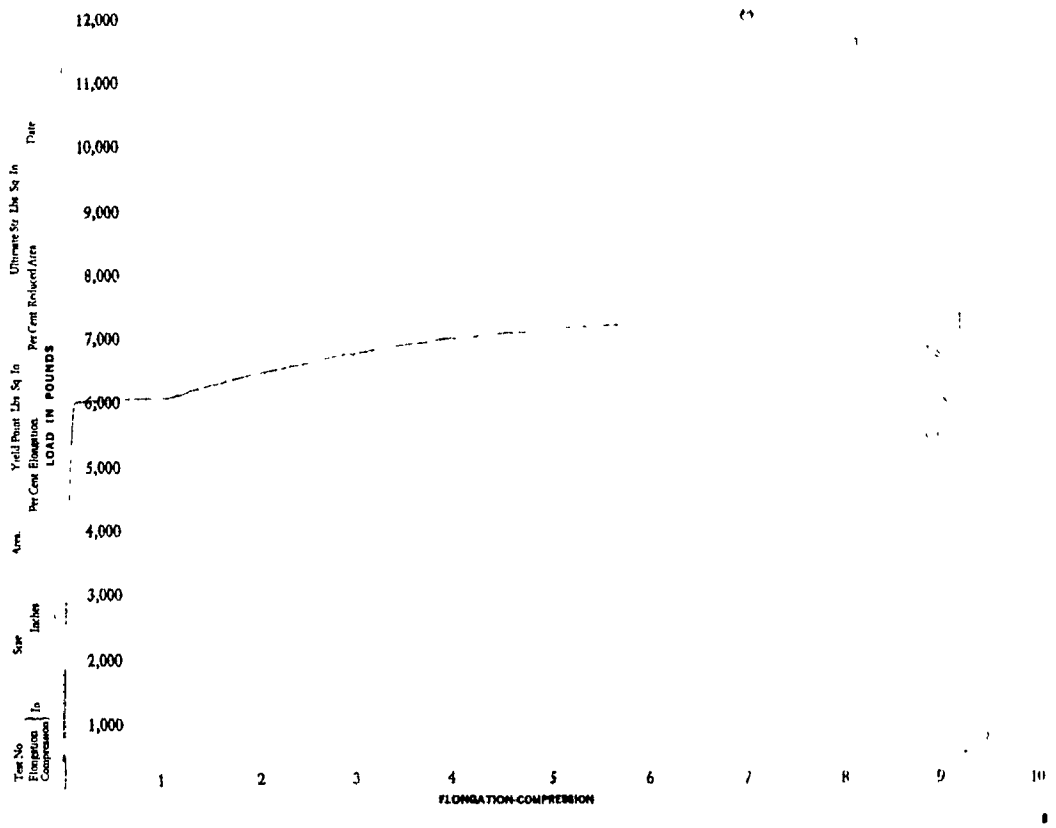

Figure A-16 Load-deformation test no.1 for bar 6M (second series)

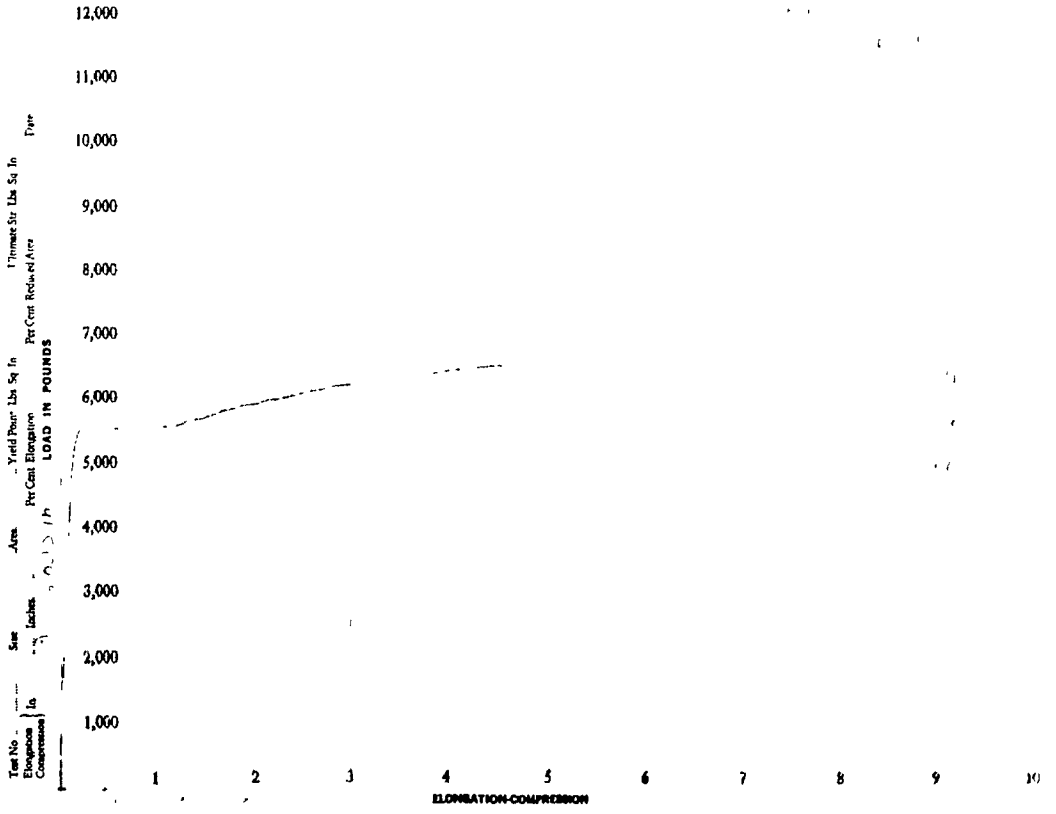

Figure A-17 Load-deformation test no.2 for bar 6M (second series)

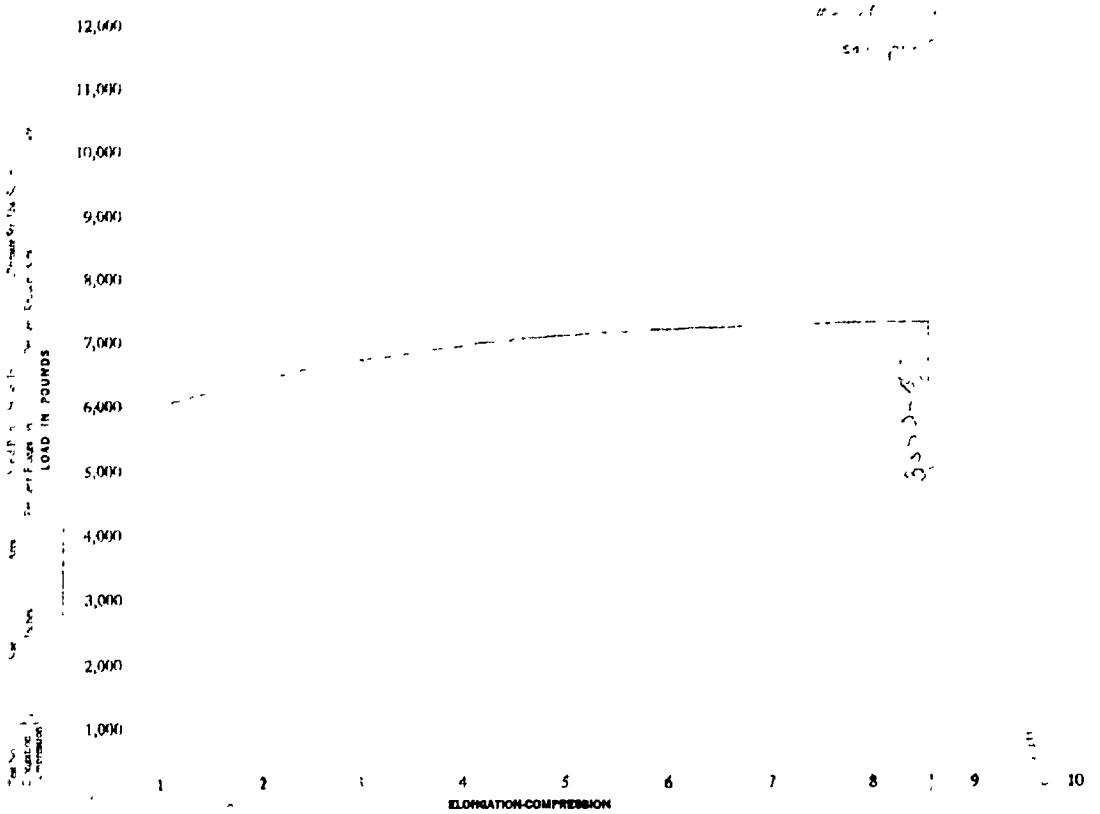

Figure A-18 Load-deformation test no.3 for bar 6M (second series)

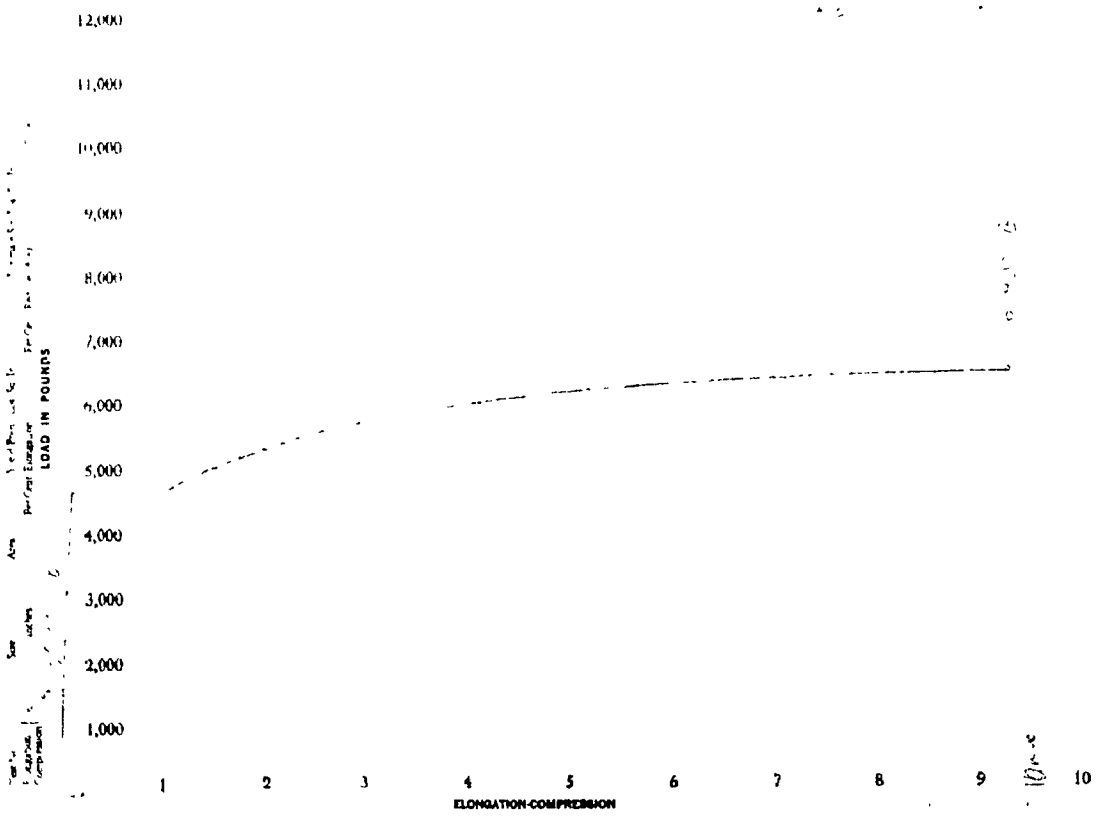

Figure A-19 Load-deformation test no.1 for bar 10M (first series)

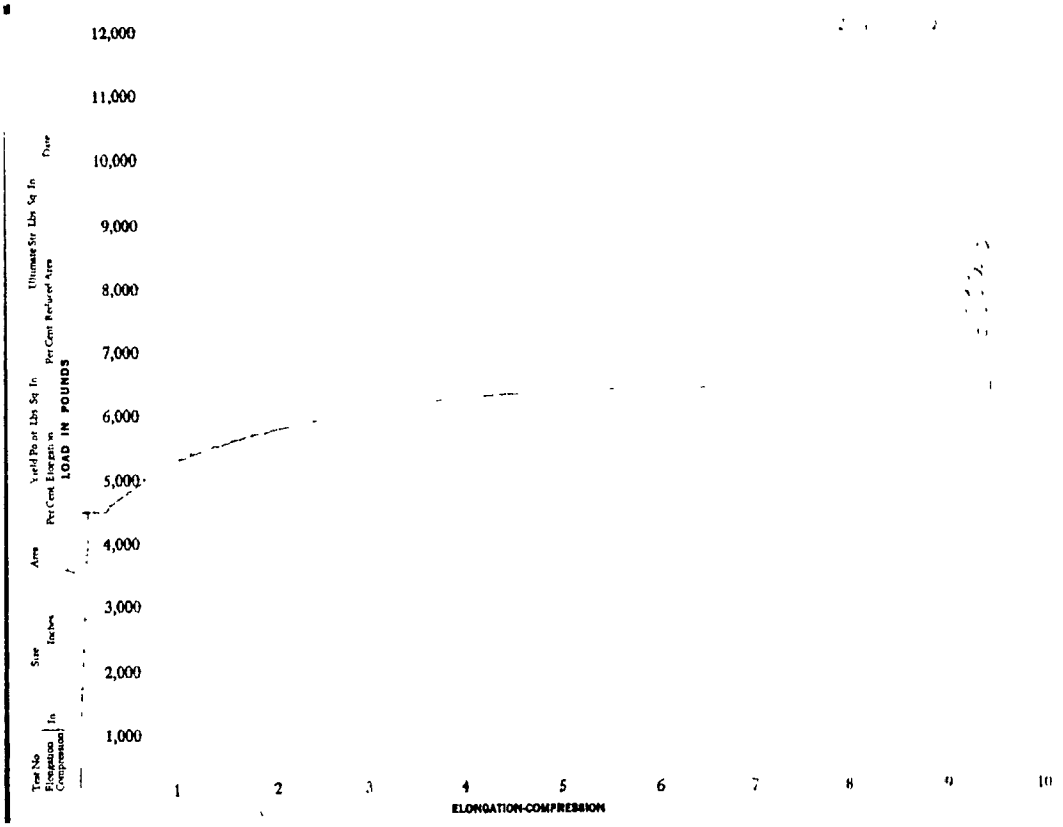

Figure A-20 Load-deformation test no.2 for bar 10M (first series)

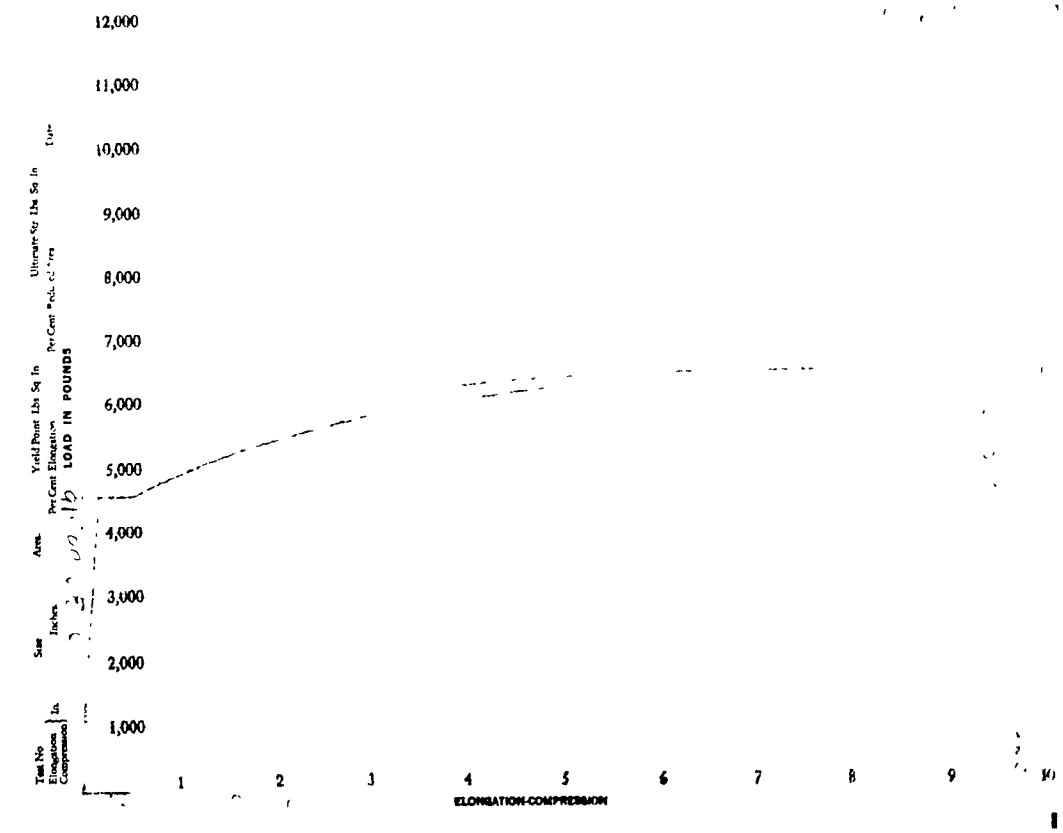

Figure A-21 Load-deformation test no.3 for bar 10M (first series)

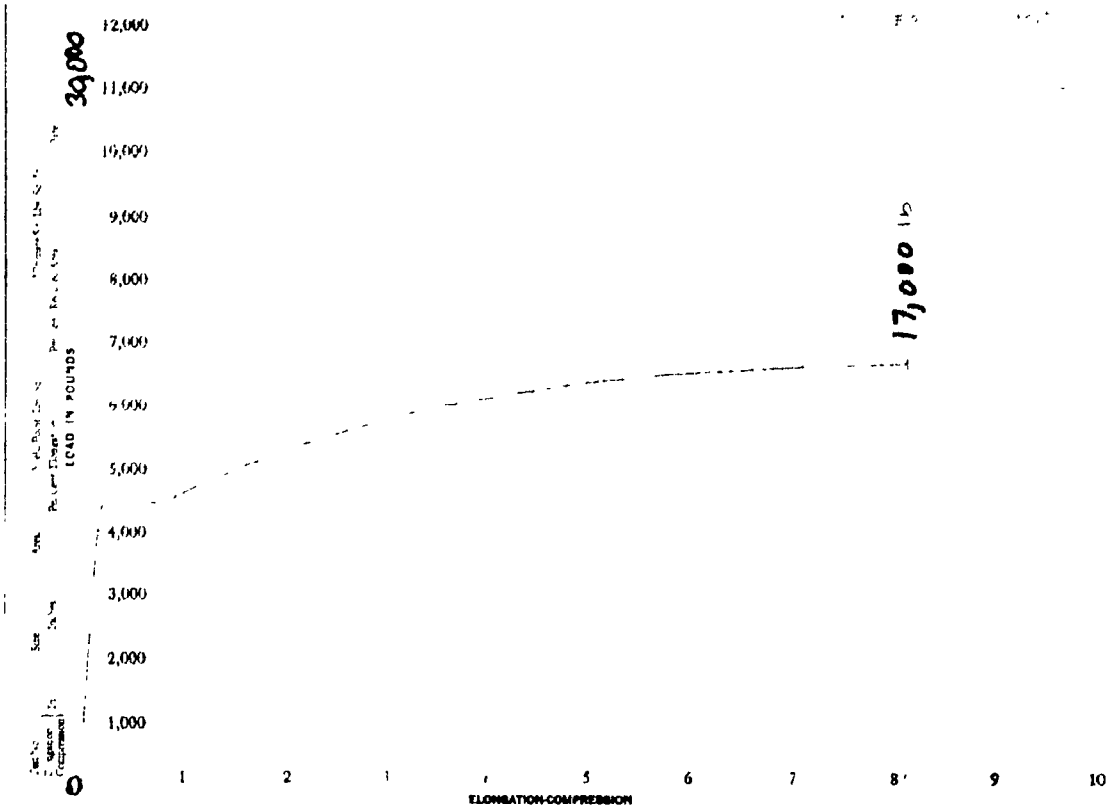

Figure A-22 Load-deformation test no.1 for bar 10M (second series)

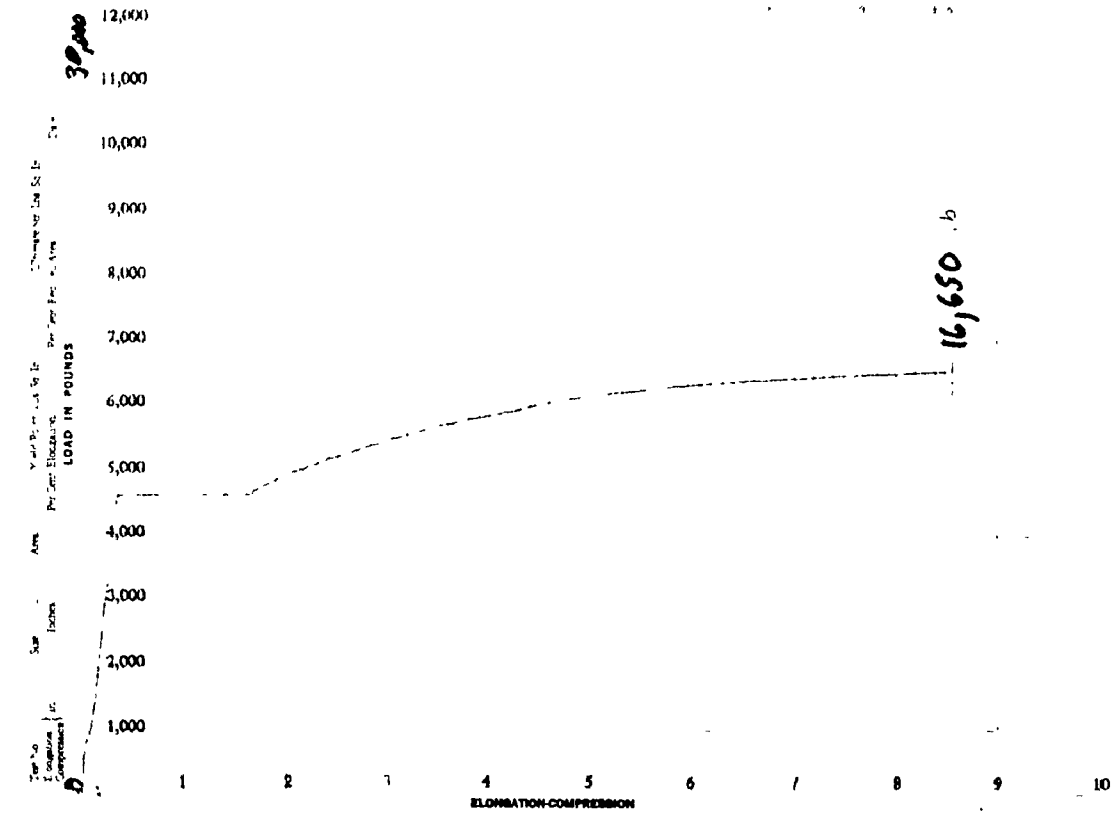

Figure A-23 Load-deformation test no.2 for bar 10M (second series)

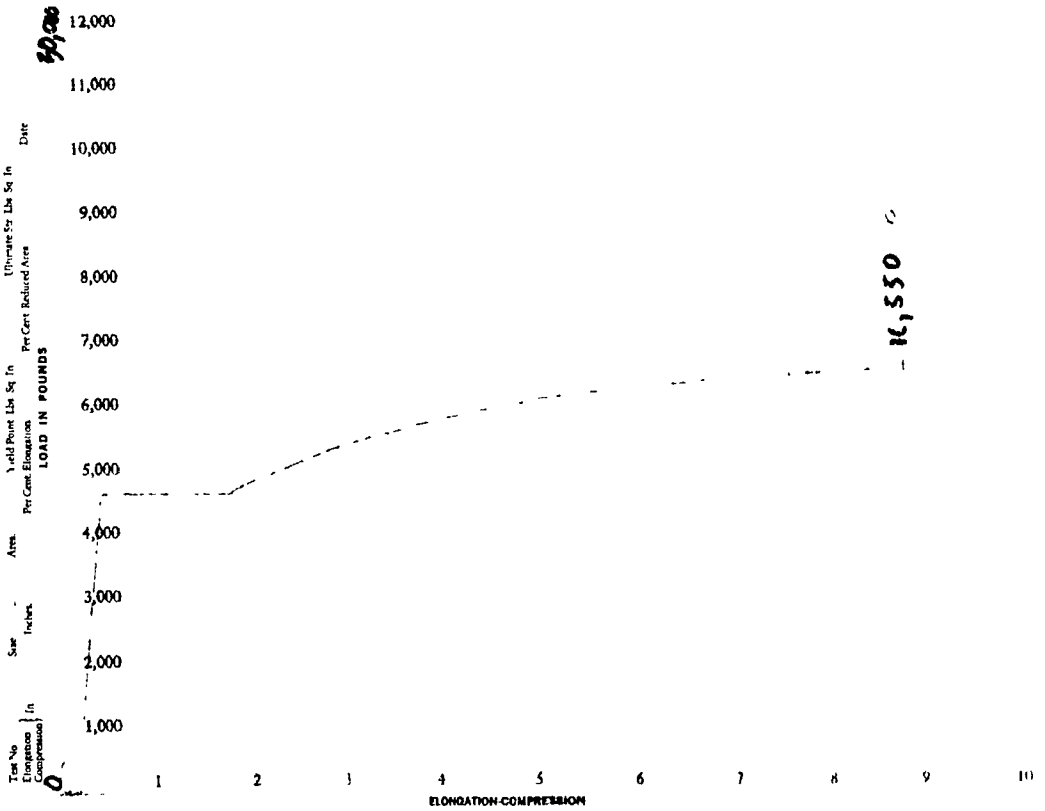

Figure A-24 Load-deformation test no.3 for bar 10M (second series)

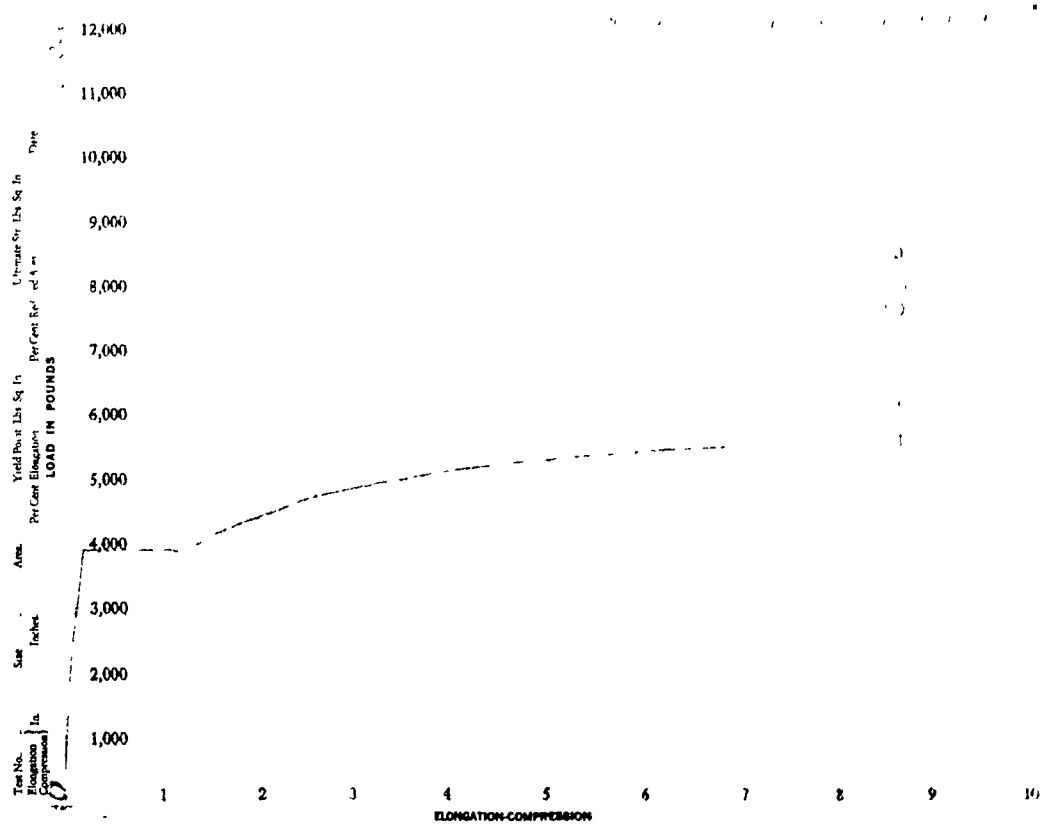

Figure A-25 Load-deformation test no.1 for bar 15M (first series)

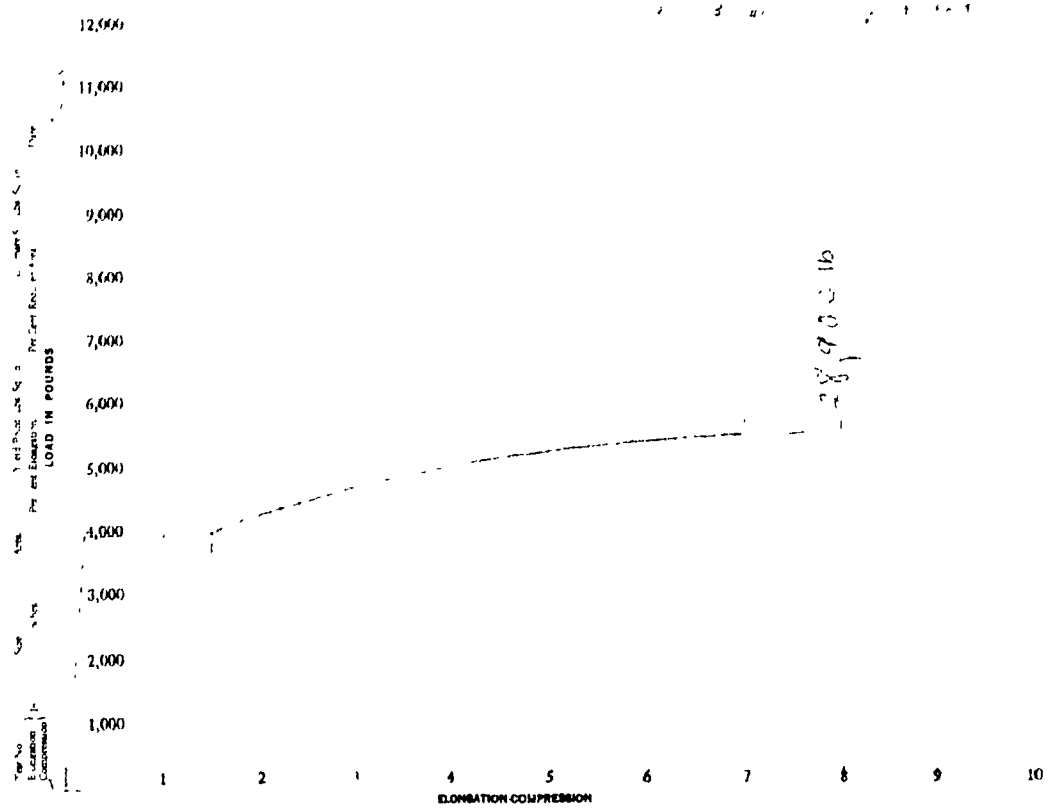

Figure A-26 Load-deformation test no.2 for bar 15M (first series)

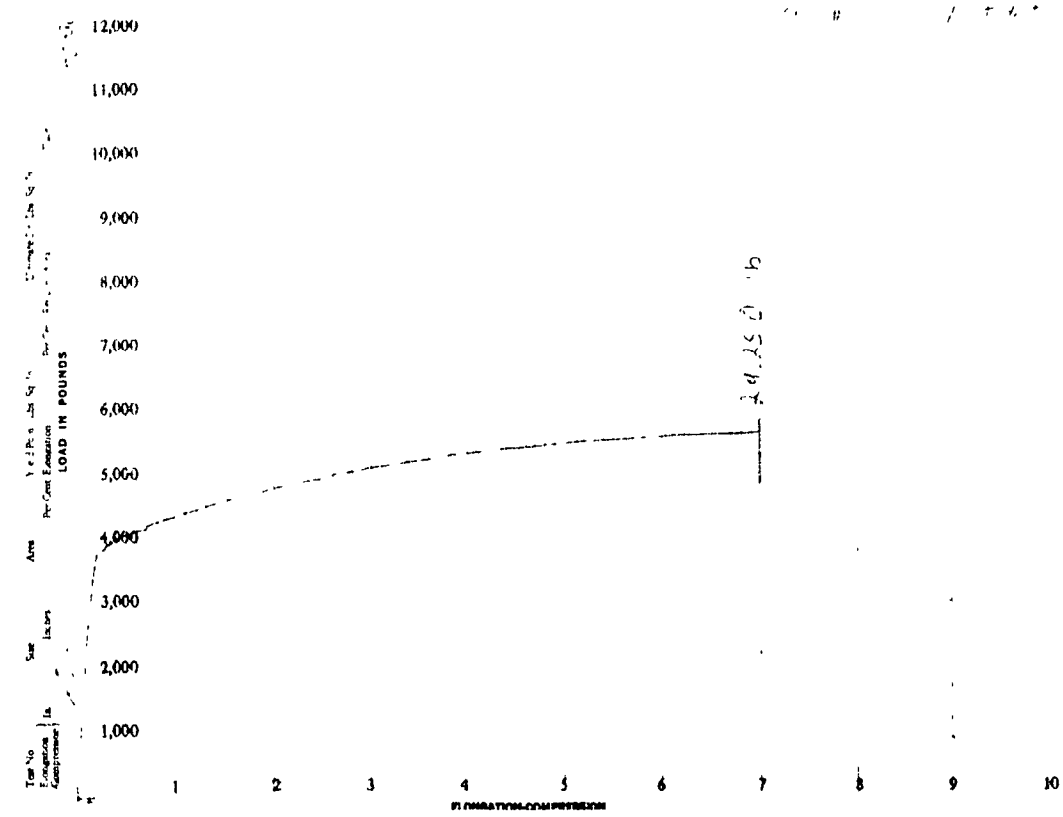

Figure A-27 Load-deformation test no 3 for bar 15M (first series)

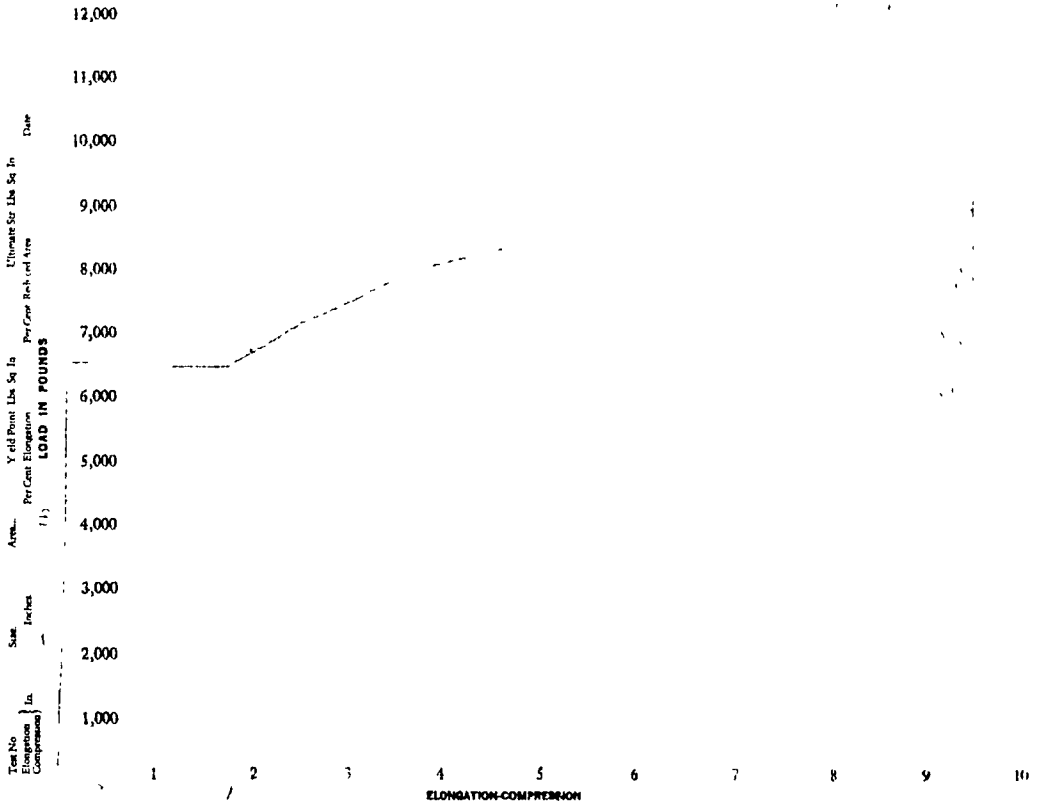

Figure A-28 Load-deformation test no.1 for bar 15M (second series)

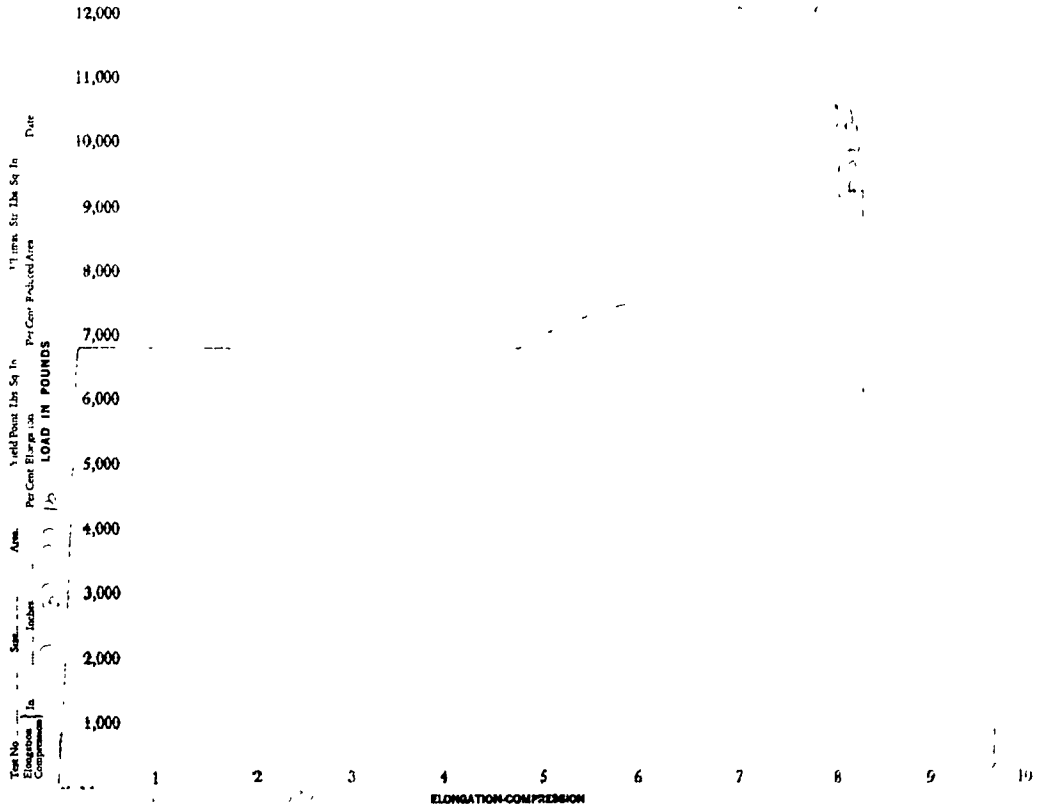

Figure A-29 Load-deformation test no.2 for bar 15M (second series)

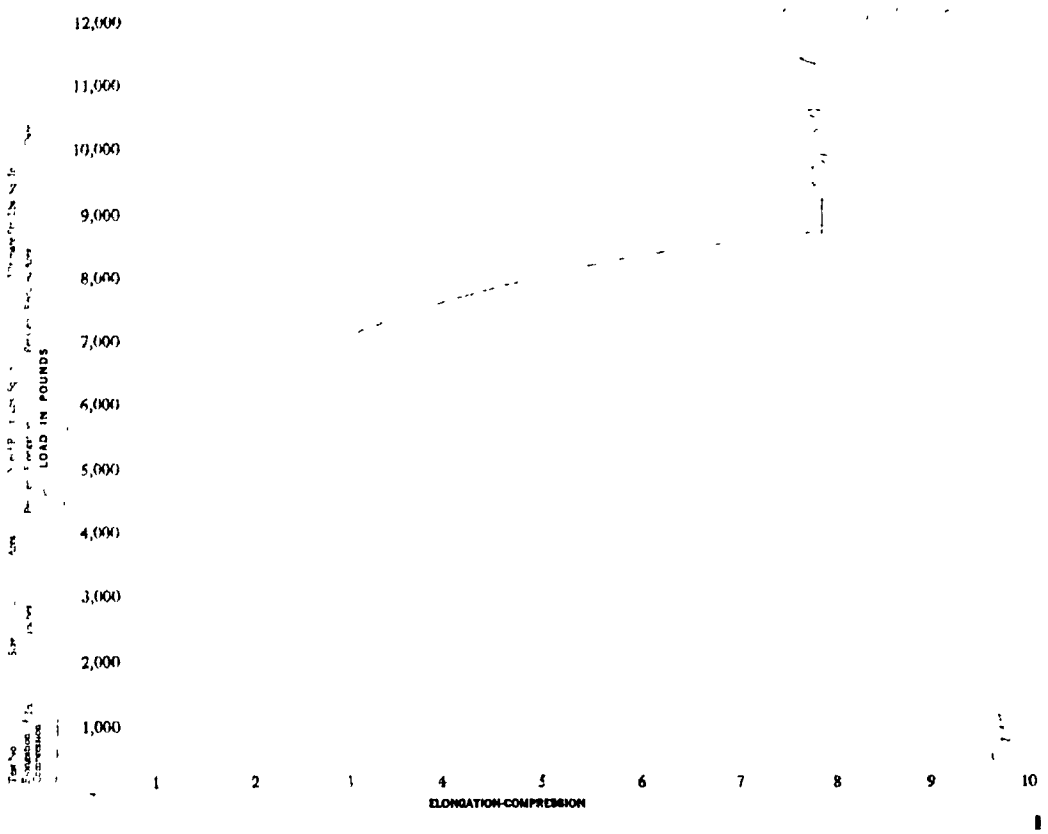

Figure A-30 Load-deformation test no.3 for bar 15M (second series)

Appendix B

B-1 Program 'ss2.in'

The following command program Adina is for modeling the strip slab of 2400 mm span. Eight-node elements are used.

```
*    ADINA-IN INPUT FILE
*
*    PROGRAM SS2 IS AN PLASTIC ANALSIS OF OF ONE WAY CONCRETE STRIP SLAB
*
     FILEUNITS  LIST=6 LOG=6 ECHO=6
     LIST FILEUNITS
*
     CONTROL  PLOTUNIT=CM,
     PLOTSAVE=YES
     LIST CONTROL
*
     DATABASE CREATE 7
*
     HEADING ' SS2 IS AN PLASTIC ANALSIS OF ONE WAY CONCRETE STRIP SLAB '
     LIST HEADING
*
     MASTER  IDOF=000111  NSTEP=2  REACTIONS=YES
     LIST MASTER
*
     ANALYSIS  TYPE=STATIC
     LIST ANALYSIS
*
     ITERATION  METHOD=FULL-NEWTON  LINE-SEARCH=YES
     LIST ITERATION
*
     TOLERANCES  PRINT=1  ITEMAX=35
     LIST TOLERANCES
*
     PRINTOUT  VOLUME=MAXIMUM CA=NO IPDA=4 PRINT=NO IPRIC=0,
     IPRIT=0 IVC=0 IAC=1 ST=NO
*
     TIMESTEP
      6   1
      8   1
      5   1
      8   1
      1   1
      6   1
```

```
*
    PORTHOLE  FORMATTED=YES  FILE=60
*
    TIMEFUNCTION  1
      0.  0.
      2   0.25
      8   0.625
      16  1.0
      21  1.1
      29  1.18
      30  1.184
      36  1.3
*
    COORDINATES
    ENTRIES     NODE      X       Y       Z
                  1       0       0       .100
                  2       .200    0       .100
                  3       .200    2.400   .100
                  4       0       2.400   .100
                  5       0       0       0
                  6       .200    0       0
                  7       .200    2.400   0
                  8       0       2.400   0
*
    EGROUP  1  THREEDSOLID  DISPL=SMALL  STRAINS=SMALL  MATERIAL=1
*
    GVOLUME  1  2  3  4  5  6  7 8  2 25 3 8
*
    MATERIAL  N=1  TYPE=CONCRETE,
    E0=28E+9  NU=0.20  SIGMAT=3E+6 SIGMAC=-30E+6 EPSC=-0.002,
    SIGMAU=-20E6  EPSU=-0.003  BETA=.75 DENSITY=2400
*   C1=0.0 C2=0.0 XSI=0.0 STIFAC=0.0 OPTION=INPUT
*   SP11=0 SP12=0.25 SP13=0.5 SP14=0.75 SP15=1.0  SP16=1.25
*   SP311=1.0  SP321=1.4  SP331=1.8,
*   SP341=2.2  SP351=2.5  SP361=2.8  SP312=1.25  SP322=1.7,
*   SP332=2.1  SP342=2.55  SP352=2.95  SP362=3.3  SP313=1.25,
*   SP323=1.6  SP333=2.0  SP343=2.4  SP353=2.8  SP363=3.15
*
    LOADS ELEMENT
    25  3  1E6   1E6   1E6   1E6   1
    26  3  1E6   1E6   1E6   1E6   1
*
    FIXBOUNDRIES  DIRECTIONS=123456  TYPE=SURFACES/ 1 2 6 5
    FIXBOUNDRIES  DIRECTIONS=123456  TYPE=SURFACES/ 4 3 7 8
*
    ADINA
    LIST ADINA
*
    END
```

B-2 Program 'ss2_r.in' to reduce the difficulty of convergence

Program 'ss2_r.in' is a recommended command program by the designer of Adina, to help reducing the difficulty of convergence. This command program is to be run to reduce the difficulty of convergence for program 'ss2.in'.

```
*    ADINA-IN INPUT FILE
*
     FILEUNITS  LIST=6 LOG=6  ECHO=6
     LIST FILEUNITS
*
     CONTROL  PLOTUNIT=CM,
     PLOTSAVE=YES
     LIST CONTROL
*
     DATABASE CREATE 7
*
     HEADING ' SS2 IS AN PLASTIC ANALSIS OF ONE WAY CONCRETE STRIP SLAB '
     LIST HEADING
*
     MASTER  IDOF=000111 MODE=2 TSTART=30  NSTEP=23 DT=0.25,
     REACTIONS=YES
     LIST MASTER
*
     ANALYSIS  TYPE=STATIC
     LIST ANALYSIS
*
     ITERATION  METHOD=BFGS
     EQUILIBRIUM 23 23 1
*
     ITERATION  METHOD=FULL-NEWTON   LINE-SEARCH=YES
     LIST ITERATION
     AUTOMATIC-ATS 10
*
     TOLERANCES  PRINT=2   ITEMAX=35
     LIST TOLERANCES
     PRINTNODES 1 8 1
     ESAVE 1 0 1
     NSAVE 1 0 1
*
     PRINTOUT  VOLUME=MINIMUM CA=NO IPDA=4 PRINT=NO IPRIC=0,
     IPRIT=0 IVC=0  IAC=1  ST=NO
*
*    TIMESTEP
*     6    1
```

```
*     8   1
*     5   1
*     8   1
*     1   1
*     15  1
*
      PORTHOLE  FORMATTED=NO  FILE=60
*
      TIMEFUNCTION  1
        0.   0.
        2    0.25
        8    0.625
        16   1.0
        21   1.1
        29   1.18
        30   1.184
        36   1.3
*
      COORDINATES
      ENTRIES    NODE      X       Y       Z
1       0        0        .100
                  2        .200    0       .100
                  3        .200    2.400   .100
                  4        0       2.400   .100
                  5        0       0       0
                  6        .200    0       0
                  7        .200    2.400   0
                  8        0       2.400   0
*
      EGROUP 1 THREEDSOLID  DISPL=SMALL  STRAINS=SMALL  MATERIAL=1
*
      GVOLUME  1  2  3  4  5  6  7 8  2 25 3 8
*
      MATERIAL  N=1  TYPE=CONCRETE,
      E0=28E+9  NU=0.20  SIGMAT=3E+6 SIGMAC=-30E+6 EPSC=-0.002,
      SIGMAU=-20E6  EPSU=-0.003  BETA=.75 DENSITY=2400,
      XSI=1. OPTION=SANDIA
*     C1=0.0 C2=0.0 XSI=0.0 STIFAC=0.0 OPTION=INPUT
*     SP11=0 SP12=0.25 SP13=0.5 SP14=0.75 SP15=1.0  SP16=1.25
*     SP311=1.0  SP321=1.4  SP331=1.8,
*     SP341=2.2  SP351=2.5  SP361=2.8  SP312=1.25  SP322=1.7,
*     SP332=2.1  SP342=2.55  SP352=2.95  SP362=3.3  SP313=1.25,
*     SP323=1.6  SP333=2.0  SP343=2.4  SP353=2.8  SP363=3.15
*
      LOADS ELEMENT
      25  3  1E6   1E6   1E6   1E6   1
      26  3  1E6   1E6   1E6   1E6   1
*
      FIXBOUNDRIES  DIRECTIONS=123456  TYPE=SURFACES/ 1 2 6 5
      FIXBOUNDRIES  DIRECTIONS=123456  TYPE=SURFACES/ 4 3 7 8
*
      ADINA
*
      END
```

B-3 Program 'ss4.in'

The following command program Adina is for modeling the strip slab of 2400 mm span. Twenty-node elements are used.

```
*   ADINA-IN INPUT FILE
*
*   SS4 IS AN PLASTIC ANALSIS OF CONCRETE STRIP SLAB
*
    FILEUNITS  LIST=7 LOG=7 ECHO=7
    LIST FILEUNITS
*
    CONTROL  PLOTUNIT=CM,
    PLOTSAVE=YES
    LIST CONTROL
*
    DATABASE CREATE
*
    HEADING ' SS4 IS AN PLASTIC ANALSIS OF CONCRETE STRIP SLAB '
    LIST HEADING
*
    MASTER  IDOF=000111  NSTEP=2  REACTIONS=YES
    LIST MASTER
*
    ANALYSIS  TYPE=STATIC
    LIST ANALYSIS
*
    ITERATION  METHOD=FULL-NEWTON  LINE-SEARCH=YES
    LIST ITERATION
*
    AUTOMATIC-ATS 10
*
    TOLERANCES  PRINT=1  ITEMAX=35
    LIST TOLERANCES
*
    PRINTOUT  VOLUME=MAXIMUM CA=NO IPDA=4 PRINT=NO IPRIC=0,
    IPRIT=0 IVC=0 IAC=1 ST=NO
*
    TIMESTEP
     6   1
     8   1
     5   1
     8   1
     1   1
     1   1
     6   1
*
```

```
    PORTHOLE  FORMATTED=YES  FILE=60
*
    TIMEFUNCTION  1
      0.   0.
      2    0.25
      8    0.625
      16   1.0
      21   1.1
      29   1.18
      30   1.184
      31   1.1852
      37   1.3
*
    COORDINATES
    ENTRIES     NODE      X       Y       Z
                  1       0       0      .100
                  2      .200     0      .100
                  3      .200    2.400   .100
                  4       0      2.400   .100
                  9       0       0       0
                 10      .200     0       0
                 11      .200    2.400    0
                 12       0      2.400    0
*
    EGROUP 1 THREEDSOLID DISPL=SMALL  STRAINS=SMALL  MATERIAL=1
*
    GVOLUME  1  2  3  4  9  10  11  12  1  25  2  20 NCOI=ALL
*
    MATERIAL  N=1  TYPE=CONCRETE,
    E0=28E+9  NU=0.20  SIGMAT=3E+6 SIGMAC=-30E+6 EPSC=-0.002,
    SIGMAU=-20E6  EPSU=-0.003  BETA=.75 DENSITY=2400
*   C1=0.0 C2=0.0 XSI=0.0 STIFAC=0.0 OPTION=INPUT
*   SP11=0 SP12=0.25 SP13=0.5 SP14=0.75 SP15=1.0  SP16=1.25
*   SP311=1.0  SP321=1.4  SP331=1.8,
*   SP341=2.2  SP351=2.5  SP361=2.8  SP312=1.25  SP322=1.7,
*   SP332=2.1  SP342=2.55  SP352=2.95  SP362=3.3  SP313=1.25,
*   SP323=1.6  SP333=2.0  SP343=2.4  SP353=2.8  SP363=3.15
*
    LOADS ELEMENT
    13  3  1E6   1E6  1E6   1E6  1
*
    FIXBOUNDRIES  DIRECTIONS=123456  TYPE=SURFACES/ 1  2  10 9
    FIXBOUNDRIES  DIRECTIONS=123456  TYPE=SURFACES/ 3  4  12 11
*
    ADINA
*
    END
```

B-4 Program 's5ms150.in'

The following command program Adina is for modeling a horizontally restrained strip slab with area steel equal to 150 mm^2 (as given in Section 6-2-1). Nine-node elements are used.

```
*    ADINA-IN INPUT FILE
*
*
     FILEUNITS  LIST=7 LOG=7 ECHO=7
     LIST FILEUNITS
*
     CONTROL  PLOTUNIT=CM,
     PLOTSAVE=YES
     LIST CONTROL
*
     DATABASE CREATE
*
     HEADING ' S5MS150 PLASTIC ANALYSIS OF CONCRETE STRIP SLAB '
     LIST HEADING
*
     MASTER  IDOF=100111  NSTEP=2  REACTIONS=YES
     LIST MASTER
*
     ANALYSIS  TYPE=STATIC
     LIST ANALYSIS
*
     KINEMATICS DISP=LARGE
*
     ITERATION  METHOD=FULL-NEWTON  LINE-SEARCH=YES
     LIST ITERATION
*
     AUTOMATIC-ATS 10
*
     TOLERANCES  PRINT=1  ITEMAX=35
     LIST TOLERANCES
*
     PRINTNODES 1 12 1
*
*    PRINTOUT  VOLUME=MAXIMUM CA=NO IPDA=4 PRINT=NO IPRIC=0,
*    IPRIT=0 IVC=0 IAC=1 ST=NO
*
     TIMESTEP
      6   1
      8   1
      5   1
      8   1
      1   1
```

```
    1   1
    6   1
*
    PORTHOLE FORMATTED=YES FILE=60
*
    TIMEFUNCTION 1
     0.  0.
     2   0.25
     8   0.625
     16  1.0
     21  1.1
     29  1.18
     30  1.184
     31  1.1852
     37  1.3
*
*
    COORDINATES
    ENTRIES    NODE      y       z
                  1      0       0.100
                  2      0       0.050
                  3      0       0.035
                  4      0       0.020
                  5      0       0.010
                  6      0       0.000
                  7      1.200   0.100
                  8      1.200   0.050
                  9      1.200   0.035
                  10     1.200   0.020
                  11     1.200   0.010
                  12     1.200   0.000
*
    EGROUP 1 TRUSS MATERIAL=1
    GLINE 4  10 EL=6 NODES=3 NCOIN=ALL
*
    EDATA
     ENTRIES EL  AREA    PRINT    SAVE
          1  150E-6  NO      YES
          STEP 1 TO
          6  150E-6  NO      YES
*
    MATERIAL 1 PLASTIC E=200000E6  YIELD=400E6 DENSITY=7850 ET=2000E6

    EGROUP 2 TWODSOLID  STRESS2 DISPL=LARG  MATERIAL=2
*
    GSURFACE 1  2  8  7  1  6  9 NCOI=ALL
    GSURFACE 2  4  10 8  1  6  9 NCOI=ALL
    GSURFACE 4  6  12 10 1  6  9 NCOI=ALL
*
    EDATA
     ENTRIES   EL PRINT SAVE  THICK
           1   NO  YES  0.200
           STEP  1 TO
          18   NO  YES  0.200
```

```
*
    MATERIAL  N=2   TYPE=CONCRETE,
    E0=28E+9   NU=0.20   SIGMAT=3E+6 SIGMAC=-30E+6 EPSC=-0.002,
    SIGMAU=-20E6   EPSU=-0.003  BETA=.75 DENSITY=2400
*   C1=0.0 C2=0.0 XSI=0.0 STIFAC=0.0 OPTION=INPUT
*   SP11=0 SP12=0.25 SP13=0.5 SP14=0.75 SP15=1.0  SP16=1.25
*   SP311=1.0  SP321=1.4  SP331=1.8,
*   SP341=2.2  SP351=2.5  SP361=2.8  SP312=1.25  SP322=1.7,
*   SP332=2.1  SP342=2.55  SP352=2.95  SP362=3.3  SP313=1.25,
*   SP323=1.6  SP333=2.0  SP343=2.4  SP353=2.8  SP363=3.15
*
*
    LOADS CONCENTRATED
    7  3  -9600
*
    FIXBOUNDRIES   DIRECTIONS=13456  TYPE=NODES/4
    FIXBOUNDRIES   DIRECTIONS=12456  TYPE=LINES/7  8
    FIXBOUNDRIES   DIRECTIONS=12456  TYPE=LINES/8  10
    FIXBOUNDRIES   DIRECTIONS=12456  TYPE=LINES/10 12
    FIXBOUNDRIES   DIRECTIONS=12456  TYPE=LINES/2  4
    FIXBOUNDRIES   DIRECTIONS=12456  TYPE=LINES/4  6
*
*
    ADINA
*
    END
```

B-5 Program 's5md2.in'

The following command program Adina is for modeling a horizontally restrained strip slab with a span equal to 1.6 m and a shear span to depth ratio equal to 8 (as given in Section 6-2-2). Nine-node elements are used.

```
*   ADINA-IN INPUT FILE
*
*
    FILEUNITS   LIST=7 LOG=7 ECHO=7
    LIST FILEUNITS
*
    CONTROL   PLOTUNIT=CM,
    PLOTSAVE=YES
    LIST CONTROL
*
    DATABASE CREATE
*
    HEADING 'S5MD2 PLASTIC ANALYSIS OF CONCRETE STRIP SLAB '
    LIST HEADING
*
    MASTER  IDOF=100111  NSTEP=2  REACTIONS=YES
    LIST MASTER
*
    ANALYSIS  TYPE=STATIC
    LIST ANALYSIS
*
    KINEMATICS DISP=LARGE
*
    ITERATION  METHOD=FULL-NEWTON  LINE-SEARCH=YES
    LIST ITERATION
*
    AUTOMATIC-ATS 10
*
    TOLERANCES  PRINT=1  ITEMAX=35
    LIST TOLERANCES
*
    PRINTNODES  1  12  1
*
*
    TIMESTEP
     6   1
     8   1
     5   1
     8   1
```

```
    1   1
    1   1
    6   1
    23  1
    60  1
    120 1
*
    PORTHOLE  FORMATTED=YES  FILE=60
*
    TIMEFUNCTION  1
     0.   0.
     2    0.25
     8    0.625
     16   1.0
     21   1.1
     29   1.18
     30   1.184
     31   1.1852
     37   1.3
     60   2.0
     120  4.0
     240  20

*
*
    COORDINATES
    ENTRIES     NODE      y        z
                1         0        0.100
                2         0        0.050
                3         0        0.035
                4         0        0.020
                5         0        0.010
                6         0        0.000
                7         0.800    0.100
                8         0.800    0.050
                9         0.800    0.035
                10        0.800    0.020
                11        0.800    0.010
                12        0.800    0.000
*
    EGROUP  1 TRUSS  MATERIAL=1
    GLINE 4  10 EL=4  NODES=3  NCOIN=ALL
*
*
    EDATA
     ENTRIES EL  AREA     PRINT    SAVE
          1   10E-6  NO      YES
          STEP 1 TO
          4   10E-6  NO      YES
*
    MATERIAL 1 PLASTIC E=200000E6  YIELD=400E6 DENSITY=7850 ET=2000E6

    EGROUP  2  TWODSOLID  STRESS2 DISPL=LARG  MATERIAL=2
*
```

```
    GSURFACE  1  2  8  7  1  4 9 NCOI=ALL
    GSURFACE  2  4  10 8  1  4 9 NCOI=ALL
    GSURFACE  4  6  12 10 1  4 9 NCOI=ALL
*
    EDATA
      ENTRIES   EL PRINT SAVE  THICK
              1  NO  YES  0.200
             STEP 1 TO
             12  NO  YES  0.200
*
    MATERIAL  N=2   TYPE=CONCRETE,
    E0=28E+9  NU=0.20  SIGMAT=3E+6 SIGMAC=-30E+6 EPSC=-0.002,
    SIGMAU=-20E6  EPSU=-0.003  BETA=.75 DENSITY=2400
*   C1=0.0 C2=0.0 XSI=0.0 STIFAC=0.0 OPTION=INPUT
*   SP11=0 SP12=0.25 SP13=0.5 SP14=0.75 SP15=1.0  SP16=1.25
*   SP311=1.0  SP321=1.4  SP331=1.8,
*   SP341=2.2  SP351=2.5  SP361=2.8  SP312=1.25  SP322=1.7,
*   SP332=2.1  SP342=2.55  SP352=2.95  SP362=3.3  SP313=1.25,
*   SP323=1.6  SP333=2.0  SP343=2.4  SP353=2.8  SP363=3.15
*
*
    LOADS CONCENTRATED
    7  3  -9600
*
*   FIXBOUNDRIES   DIRECTIONS=13456  TYPE=NODES/6
    FIXBOUNDRIES   DIRECTIONS=13456  TYPE=NODES/4
    FIXBOUNDRIES   DIRECTIONS=12456  TYPE=LINES/7  8
    FIXBOUNDRIES   DIRECTIONS=12456  TYPE=LINES/8  10
    FIXBOUNDRIES   DIRECTIONS=12456  TYPE=LINES/10 12
*   FIXBOUNDRIES   DIRECTIONS=12456  TYPE=LINES/1  2
    FIXBOUNDRIES   DIRECTIONS=12456  TYPE=LINES/2  4
    FIXBOUNDRIES   DIRECTIONS=12456  TYPE=LINES/4  6
*   FIXBOUNDRIES   DIRECTIONS=12456  TYPE=NODES/12
*
*
    ADINA
*   LIST ADINA
*
    END
```

B-6 Program 's5mr6.in'

The following command program Adina is for modeling a horizontally restrained strip slab with an elastic support stiffness of approximately 180 kN per mm (as given in Section 6-2-3). Nine-node elements are used.

```
*   ADINA-IN INPUT FILE
*
*
    FILEUNITS  LIST=7 LOG=7 ECHO=7
    LIST FILEUNITS
*
    CONTROL  PLOTUNIT=CM,
    PLOTSAVE=YES
    LIST CONTROL
*
    DATABASE CREATE
*
    HEADING ' S5MR6 PLASTIC ANALYSIS OF CONCRETE STRIP SLAB '
    LIST HEADING
*
    MASTER  IDOF=100111  NSTEP=2  REACTIONS=YES
    LIST MASTER
*
    ANALYSIS  TYPE=STATIC
    LIST ANALYSIS
*
    KINEMATICS DISP=LARGE
*
    ITERATION  METHOD=FULL-NEWTON  LINE-SEARCH=YES
    LIST ITERATION
*
    AUTOMATIC-ATS 10
*
    TOLERANCES  PRINT=1  ITEMAX=35
    LIST TOLERANCES
*
    PRINTNODES 1 12 1
*
    TIMESTEP
     6   1
     8   1
     5   1
     8   1
     1   1
```

```
    1   1
    6   1
*
    PORTHOLE  FORMATTED=YES  FILE=60
*
    TIMEFUNCTION  1
     0.   0.
     2    0.25
     8    0.625
     16   1.0
     21   1.1
     29   1.18
     30   1.184
     31   1.1852
     37   1.3
*
*
    COORDINATES
    ENTRIES     NODE      y        z
                   1      0        0.100
                   2      0        0.050
                   3      0        0.035
                   4      0        0.020
                   5      0        0.010
                   6      0        0.000
                   7      1.200    0.100
                   8      1.200    0.050
                   9      1.200    0.035
                   10     1.200    0.020
                   11     1.200    0.010
                   12     1.200    0.000
*
    EGROUP 1 TRUSS  MATERIAL=1
    GLINE 4  10 EL=6  NODES=3  NCOIN=ALL
*
*
    EDATA
     ENTRIES EL  AREA     PRINT    SAVE
          1   10E-6   NO      YES
          STEP 1 TO
          6   10E-6   NO      YES
*
    MATERIAL 1 PLASTIC E=200000E6  YIELD=400E6 DENSITY=7850 ET=2000E6
*
    EGROUP 2  TWODSOLID  STRESS2 DISPL=LARG  MATERIAL=2
*
    GSURFACE  1  2  8  7  1  6  9 NCOI=ALL
    GSURFACE  2  4  10 8  1  6  9 NCOI=ALL
    GSURFACE  4  6  12 10 1  6  9 NCOI=ALL
*
    EDATA
     ENTRIES   EL PRINT SAVE  THICK
           1   NO  YES   0.200
           STEP  1 TO
```

```
          18  NO  YES  0.200
*
    MATERIAL  N=2  TYPE=CONCRETE,
    E0=28E+9  NU=0.20  SIGMAT=3E+6 SIGMAC=-30E+6 EPSC=-0.002,
    SIGMAU=-20E6  EPSU=-0.003  BETA=.75 DENSITY=2400
*   C1=0.0 C2=0.0 XSI=0.0 STIFAC=0.0 OPTION=INPUT
*   SP11=0 SP12=0.25 SP13=0.5 SP14=0.75 SP15=1.0  SP16=1.25
*   SP311=1.0  SP321=1.4  SP331=1.8,
*   SP341=2.2  SP351=2.5  SP361=2.8  SP312=1.25  SP322=1.7,
*   SP332=2.1  SP342=2.55  SP352=2.95  SP362=3.3  SP313=1.25,
*   SP323=1.6  SP333=2.0  SP343=2.4  SP353=2.8  SP363=3.15
*
    EGROUP 3 SPRING
    PROPERTYSET N=1 K=40.97E6
    PROPERTYSET N=2 K=65.43E6
    PROPERTYSET N=3 K=72.17E6
*
    ENODES
*       1  1  2
*       2  2  2
*       3  3  2
        4  4  2
        5  5  2
        6  6  2
*
    EDATA
     ENTRIES    EL     PROPERTYSET  PRINT   SAVE
*           1       1      YES     YES
*           2       1      YES     YES
*           3       1      YES     YES
            4       1      YES     YES
            5       2      YES     YES
            6       3      YES     YES
*
    LOADS CONCENTRATED
    7  3  -9600
*
    FIXBOUNDRIES  DIRECTIONS=13456  TYPE=NODES/4
    FIXBOUNDRIES  DIRECTIONS=12456  TYPE=LINES/7  8
    FIXBOUNDRIES  DIRECTIONS=12456  TYPE=LINES/8  10
    FIXBOUNDRIES  DIRECTIONS=12456  TYPE=LINES/10 12
*
*
    ADINA
*
    END
```

B-7 Program 's5mm1.in'

The following command program Adina is for modeling a strip slab horizontally restrained by a layer of mortar 200 mm thick (as given in Section 6-4). Nine-node elements are used.

```
*   ADINA-IN INPUT FILE
*
*
    FILEUNITS   LIST=7 LOG=7 ECHO=7
    LIST FILEUNITS
*
    CONTROL   PLOTUNIT=CM,
    PLOTSAVE=YES
    LIST CONTROL
*
    DATABASE CREATE
*
    HEADING ' S5MM1 PLASTIC ANALYSIS OF CONCRETE STRIP SLAB '
    LIST HEADING
*
    MASTER  IDOF=100111  NSTEP=2  REACTIONS=YES
    LIST MASTER
*
    ANALYSIS  TYPE=STATIC
    LIST ANALYSIS
*
    KINEMATICS DISP=LARGE
*
    ITERATION  METHOD=FULL-NEWTON   LINE-SEARCH=YES
    LIST ITERATION
*
    AUTOMATIC-ATS  10
*
    TOLERANCES  PRINT=1   ITEMAX=35
    LIST TOLERANCES
*
    PRINTNODES  1  12  1
*
*
    TIMESTEP
     6   1
     8   1
     5   1
     8   1
     1   1
     1   1
     6   1
```

```
*
   PORTHOLE  FORMATTED=YES  FILE=60
*
   TIMEFUNCTION  1
     0.   0.
     2    0.25
     8    0.625
     16   1.0
     21   1.1
     29   1.18
     30   1.184
     31   1.1852
     37   1.3
*
*
   COORDINATES
   ENTRIES     NODE      y        z
                  1      0        0.100
                  2      0        0.050
                  3      0        0.035
                  4      0        0.020
                  5      0        0.010
                  6      0        0.000
                  7      1.200    0.100
                  8      1.200    0.050
                  9      1.200    0.035
                 10      1.200    0.020
                 11      1.200    0.010
                 12      1.200    0.000
                 13      -0.200   0.050
                 14      -0.200   0.020
                 15      -0.200   0.000
*                16      -0.200   0.050
                 17      -0.200   0.010
*                18      -0.200   0.000
*
   EGROUP 2 TWODSOLID  STRESS2 DISPL=LARG  MATERIAL=2
*
   GSURFACE  1  2  8  7  1  6  9 NCOI=ALL
   GSURFACE  2  4  10 8  1  6  9 NCOI=ALL
   GSURFACE  4  6  12 10 1  6  9 NCOI=ALL
*
   EDATA
     ENTRIES   EL PRINT SAVE  THICK
           1   NO  YES  0.200
          STEP 1 TO
          18   NO  YES  0.200
*
   MATERIAL  N=2   TYPE=CONCRETE,
   E0=28E+9   NU=0.20   SIGMAT=3E+6 SIGMAC=-30E+6 EPSC=-0.002,
   SIGMAU=-20E6   EPSU=-0.003  BETA=.75 DENSITY=2400
*  C1=0.0 C2=0.0 XSI=0.0 STIFAC=0.0 OPTION=INPUT
*  SP11=0 SP12=0.25 SP13=0.5 SP14=0.75 SP15=1.0  SP16=1.25
*  SP311=1.0  SP321=1.4  SP331=1.8,
```

```
*    SP341=2.2  SP351=2.5  SP361=2.8  SP312=1.25  SP322=1.7,
*    SP332=2.1  SP342=2.55  SP352=2.95  SP362=3.3  SP313=1.25,
*    SP323=1.6  SP333=2.0  SP343=2.4  SP353=2.8  SP363=3.15
*
     EGROUP 3 SPRING
     PROPERTYSET N=1 K=143.4E6
     PROPERTYSET N=2 K=229E6
     PROPERTYSET N=3 K=252.6E6
*
     ENODES
*       1  1  2
*       2  2  2
*       3  3  2
        14  14  2
        17  17  2
        15  15  2
*
     EDATA
       ENTRIES    EL     PROPERTYSET  PRINT   SAVE
*             1       1       NO      YES
*             2       1       NO      YES
*             3       1       NO      YES
             14       1       NO      YES
             17       2       NO      YES
             15       3       NO      YES
*
     EGROUP 4 TWODSOLID  STRESS2 DISPL=LARG  MATERIAL=4
*
     GSURFACE  13  2  4  14  1  1 9 NCOI=ALL
     GSURFACE  14  4  6  15  1  1 9 NCOI=ALL
*
     EDATA
       ENTRIES    EL PRINT SAVE  THICK
             1   NO  YES   0.200
            STEP 1 TO
             2   NO  YES   0.200
*
     MATERIAL  N=4  TYPE=CONCRETE,
     E0=32E+9   NU=0.20   SIGMAT=3E+6 SIGMAC=-28E+6 EPSC=-0.002,
     SIGMAU=-20E6   EPSU=-0.003   BETA=.75  DENSITY=2400
*
     LOADS CONCENTRATED
     7  3  -9600
*
*
     FIXBOUNDRIES   DIRECTIONS=13456   TYPE=NODES/4
     FIXBOUNDRIES   DIRECTIONS=12456   TYPE=LINES/7  8
     FIXBOUNDRIES   DIRECTIONS=12456   TYPE=LINES/8  10
     FIXBOUNDRIES   DIRECTIONS=12456   TYPE=LINES/10 12
*
*
     ADINA
*
     END
```

Appendix C

C-1 The structural scheme of the set-up

All the members of the test set-up that are shown in Figure C-1 are steel members unless indicated otherwise.

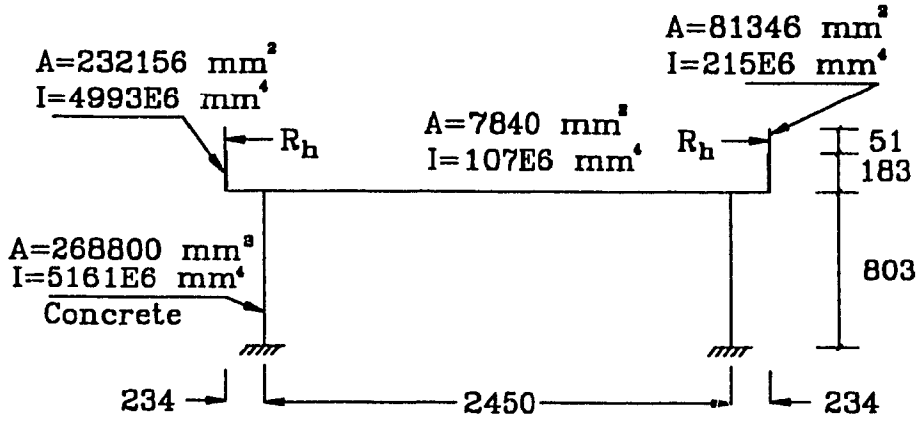

Figure C-1 The structure scheme of the set-up

C-2 The calculation of the load 'P_{cod}' and the deflection for the slab S1

The cross sectional dimensions of slab S1 are 104 mm in depth and 203 mm in width. The concrete compression strength is 28.55 MPa. The span of the slab is 2400 mm. The maximum load 'P_{cod}' that can be carried by the strip slab S1 is calculated according to the present codes of practice, assuming a non-reinforced concrete strip slab, as will be shown below. The rupture strength of the concrete 'f_r' is given as follows:

$$f_r = 0.6\sqrt{f_c'} = 0.6\sqrt{28.55} = 3.21\ MPa$$

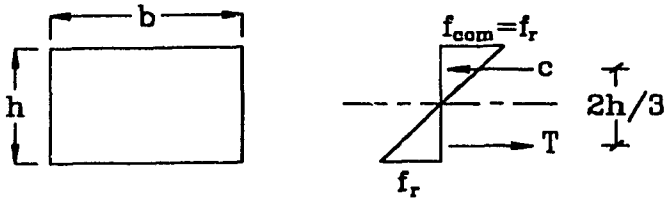

Figure C-2 The internal forces at the cross section of S1 at midspan

As shown in Figure C-2, the internal resultant forces in the concrete forming the internal resisting couple are C and T and the lever arm of this couple is $\frac{2h}{3}$, where

$$C = T = \frac{1}{2} \times 3.21 \times \frac{104}{2} \times 203 = 16,942.38\ N$$

The internal moment of resistance is calculated as follows:

$$M = C \times \frac{2h}{3} = 16,942.38 \times \frac{2 \times 104}{3} = 1,174,671.68\ N.mm$$

The external bending moment and the load 'P_{cod}' are given as follows:

$$M = \frac{P_{cod} \times L}{4}$$

Where L is the span length = 2400 mm

$$\text{i.e. } P_{cod} = \frac{4 \times M}{L} = \frac{4 \times 1,174,671.68}{2400} \times 10^{-3} = 1.96\ kN$$

The corresponding deflection 'w' is given as follows:

$$w = \frac{1}{48} \times \frac{P_{cod} \times L^3}{E \times I}$$

Where E is the modulus of elasticity of the concrete and given as

$$E = 5000\sqrt{f_c'} = 5000\sqrt{28.55} = 26{,}716.1\ MPa$$

and I is the moment of inertia of the cross section of the strip slab and is given as

$$I = \frac{b \times h^3}{12} = 19{,}028{,}949.3\ mm^4$$

$$\text{i.e. } w = \frac{1}{48} \times \frac{1{,}960.0 \times 2400^3}{26{,}716.1 \times 19{,}028{,}949.3} = 1.11\ mm$$

C-3 Calculations of 'P_{theo}' theoretical failure load for slab S5

The theoretical failure load 'P_{theo}' is calculated according to the Canadian Code CSA for the fully reinforced horizontally non-restrained strip slab S5. The reduction factors presented in the code are ignored. The cross sectional dimensions of the slab are 117 mm in depth and 203 mm in width. The compression strength of the concrete is 34.14 MPa. The span of the slab is 2400 mm. The yield strengths of the tension and compression reinforcement are 441.12 MPa and 504.40 MPa respectively. The reinforcement of this strip slab is shown in Figure 6-7 in Chapter 6. The calculation of 'P_{theo}' is as given below.

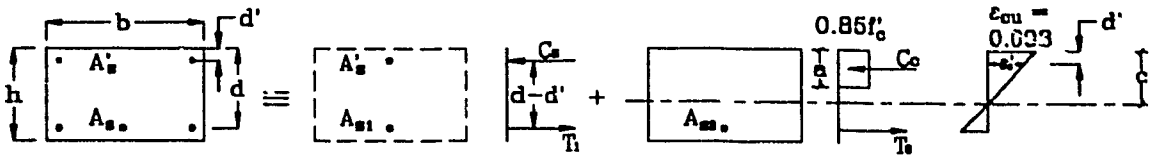

Figure C-3 The internal forces at the cross section of S5 at midspan

Referring to Figure C-3, the value of 'A_{s1}' is given as follows:

$$A_{s1} = \frac{A_s'}{f_y} \times (f_y' - 0.85 f_c') \qquad \text{..... (C-1)}$$

$$A_{s1} = \frac{56.55}{441.12} \times (504.40 - 0.85 \times 34.14) = 60 \ mm^2$$

Where:

A_{s1} is the area of tension reinforcement which has a tension force equivalent to the compression force in the compression reinforcement

A_s' is the compression area steel

f_y is the yield strength of the tension reinforcement

f_y' is the yield strength of the compression reinforcement

The area of the tension reinforcement 'A_{s2}' which has a tension force equivalent to the compressive force in the concrete can be calculated as follows:

$$A_{s2} = A_s - A_{s1} \qquad \text{..... (C-2)}$$

$$A_{s2} = 600 - 60.942 = 539.058 \ mm^2$$

Where 'A_s' is the total area of the tension steel

The depth of the compression zone 'a', as shown in Figure C-3, is given as follows:

$$a = \frac{A_{s2} \times f_y}{0.85 \times f_c' \times b} \quad \text{..... (C-3)}$$

$$a = \frac{539.058 \times 441.12}{0.85 \times 34.14 \times 203} = 40.366\, mm^2$$

Where 'b' is the width of the cross section = 203 mm

The value of 'c' which is the distance from the extremity of the compression fibers to the neutral axis, as shown in Figure C-3, is given as follows:

$$c = \frac{a}{\beta_1} = \frac{40.366}{0.817} = 49.407\, mm$$

Where 'β_1' is taken as 0.85 for concrete strength f_c' up to and including 30 MPa and beyond this it is reduced continuously at a rate of 0.08 for each additional 10 MPa of strength, but with a minimum value for 'β_1' of 0.65 which is calculated as follows:

$$\beta_1 = 0.85 - \frac{0.08}{10}(34.14 - 30) = 0.817$$

Since the depth of the neutral axis $c = a/\beta_1$, from the strain diagram in Figure C-3, the strain in the compression reinforcement can now be computed to confirm whether that steel has yielded.

$$\epsilon_s' = \frac{0.003}{c}(c - d') \qquad \text{..... (C-4)}$$

$$\epsilon_s' = \frac{0.003}{49.407}(49.407 - 36) = 0.000814$$

Where d' is the distance from the center of the compression reinforcement to the top of the cross section as shown in Figure C-3.

$$\epsilon_s' < \epsilon_y' = \frac{f_y'}{E_s} = \frac{504.4}{200,000.0} = 0.0025$$

Where ϵ_s' and ϵ_y' are the actual strain of the compression reinforcement and the strain of the reinforcement at the yielding point respectively. E_s is the modulus of elasticity of the steel.

The actual stress in the compression reinforcement is calculated as follows:

$$f_s' = \epsilon_s' \times E_s \qquad \text{..... (C-5)}$$

$$f_s' = 0.000814 \times 200,000.0 = 162.818 \ MPa$$

Equation (C-1) will become

$$A_{s1} = \frac{A_s'}{f_y} \times (f_s' - 0.85 f_c')$$

$$A_{s1} = \frac{56.55}{441.12} \times (162.818 - 0.85 \times 34.14) = 17.153 \ mm^2$$

Substituting in Equation (C-2), (C-3), (C-4) and (C-5)

$$A_{s2} = 600 - 17.153 = 528.847 \ mm^2$$

$$a = \frac{528.847 \times 441.12}{0.85 \times 34.14 \times 203} = 43.645 \ mm^2$$

$$c = \frac{a}{\beta_1} = \frac{43.645}{0.817} = 53.421\,mm$$

$$\epsilon_s' = \frac{0.003}{53.421}(53.421 - 36) = 0.000978$$

$$f_s' = 0.000978 \times 200{,}000.0 = 195.664\ MPa$$

The bending moment 'M_1' due to the compression reinforcement and its corresponding tension reinforcement is calculated as follows:

$$M_1 = A_{s1}'(f_s' - 0.85 f_c')(d - d')$$

$$M_1 = 17.153\ (195.664\ -\ 0.85 \times 34.14\ )(92 - 36) \times 10^{-6} = 0.16\ kN.m$$

Where d is shown in Figure C-3

The bending moment 'M_2' due to the Whitney compression zone of the concrete and its corresponding tension reinforcement is calculated as follows:

$$M_2 = A_{s2} \times f_y(d - \frac{a}{2})$$

$$M_2 = 582.847 \times 441.12\ (92 - \frac{43.645}{2}) 10^{-6} = 18.043\ kN.m$$

The total resisting moment at midspan is calculated as follows:

$$M = M_1 + M_2$$

$$M = 0.16 + 18.043 = 18.203\ kN.m$$

The value of the bending moment 'M' for a simply supported strip beam subjected to the load 'P_{theo}' at its midspan, can be calculated as follows:

$$M = \frac{P_{theo} \times L}{4}$$

$$\text{i.e. } P_{theo} = \frac{M \times 4}{L} = \frac{18.203 \times 4}{2.4} = 30.34 \ kN$$

C-4 Calculations for reinforcement ratios for slab S5

Referring to Figure C-3, the maximum value of 'c' is given as:

$$c_{max} = \frac{600}{600 + f_y} d$$

Substituting in the above equation,

$$c_{max} = \frac{600}{600 + 441.12} \times 92 = 53.0198 \ mm$$

The total internal compressive force 'C' due to the Whitney compression zone of the concrete and the compression reinforcement is calculated as follows:

$$C = A_s'(f_s' - 0.85 f_c') + (0.85 \times f_c' \times b \times \beta_1 \times c_{max})$$

$$C = 56.55(195.664 - 0.85 \times 34.14) + (0.85 \times 34.14 \times 203 \times 0.817 \times 53.0198) = 264,599.187 \ N$$

Where A_s', f_s', b, β_1 and f_c' are given in the above Section C-3.

The maximum area steel $A_{s(max)}$ is calculated as follows:

$$A_{s(max)} = \frac{C}{f_y} = \frac{264,599.187}{441.12} = 599.835 \ mm^2$$

The maximum reinforcement ratio 'ρ_{max}' is calculated as follows:

$$\rho_{max} = \frac{A_{s(max)}}{b \times d} = \frac{599.835}{203 \times 92} = 0.0032118$$

The actual reinforcement ratio 'ρ_{act}' is calculated as follows:

$$\rho_{max} = \frac{A_s}{b \times d} = \frac{600}{203 \times 92} = 0.0032127$$

The minimum reinforcement ratio 'ρ_{min}' is calculated as follows:

$$\rho_{min} = \frac{1.4}{f_y} = \frac{1.4}{441.12} = 0.003174$$

Appendix D

D-1 Program 'wall.in'

The following command program Adina is for modeling the segment of the slab shown in Figure 7-4. Eight-node elements are used.

```
*   wall.in
*
*   ADINA-IN INPUT FILE
*
*   SLB1 PLASTIC ANALYSIS OF TWO WAY WALL
*
*
    FILEUNITS  LIST=7 LOG=7 ECHO=7
    LIST FILEUNITS
*
    CONTROL  PLOTUNIT=CM,
    PLOTSAVE=YES
    LIST CONTROL,
*
    DATABASE CREATE
*
    HEADING ' SLB1 PLASTIC ANALYSIS OF TWO WAY WALL '
    LIST HEADING
*
    MASTER  IDOF=000111  NSTEP=2  REACTIONS=YES
    LIST MASTER
*
    ANALYSIS  TYPE=STATIC
    LIST ANALYSIS
*
    ITERATION  METHOD=FULL-NEWTON  LINE-SEARCH=YES
    LIST ITERATION
*
    AUTOMATIC-ATS  10
*
    TOLERANCES  PRINT=1  ITEMAX=35
    LIST TOLERANCES
*
    PRINTNODES  1  4  1
*
    ESAVE  1 0 1
*
    NSAVE  1 0 1
*
    PRINTOUT  VOLUME=MIN  CA=NO  IPDA=4  PRINT=NO  IPRIC=0,
```

```
   IPRIT=0 IVC=0 IAC=1 ST=NO
*
   TIMESTEP
    4   1
*
   PORTHOLE  FORMATTED=YES  FILE=60
*
   TIMEFUNCTION  1
    0.   0.
    2    0.25
    6    0.5
*
   COORDINATES
   ENTRIES     NODE      X      Y      Z
             1       1.12   0      1.12
             2       1.28   0      1.12
             3       1.28   0.1    1.12
             4       1.12   0.1    1.12
             5       0      0      0
             6       2.4    0      0
             7       2.4    0.1    0
             8       0      0.1    0
*
   EGROUP 1 THREEDSOLID  DISPL=SMALL  STRAINS=SMALL  MATERIAL=1
*
   GVOLUME  1  2  3  4  5  6  7 8  15 1 7 8
*
   MATERIAL  N=1   TYPE=CONCRETE,
   E0=28E+9   NU=0.20   SIGMAT=3E+6 SIGMAC=-30E+6 EPSC=-0.002,
   SIGMAU=-20E6   EPSU=-0.003  BETA=.75 DENSITY=2400
*
   LOADS ELEMENT
   1   3  25.5E6   25.5E6   25.5E6   25.5E6   1
   2   3  25.5E6   25.5E6   25.5E6   25.5E6   1
   3   3  25.5E6   25.5E6   25.5E6   25.5E6   1
   4   3  25.5E6   25.5E6   25.5E6   25.5E6   1
   5   3  25.5E6   25.5E6   25.5E6   25.5E6   1
   6   3  25.5E6   25.5E6   25.5E6   25.5E6   1
   7   3  25.5E6   25.5E6   25.5E6   25.5E6   1
   8   3  25.5E6   25.5E6   25.5E6   25.5E6   1
   9   3  25.5E6   25.5E6   25.5E6   25.5E6   1
   10  3  25.5E6   25.5E6   25.5E6   25.5E6   1
   11  3  25.5E6   25.5E6   25.5E6   25.5E6   1
   12  3  25.5E6   25.5E6   25.5E6   25.5E6   1
   13  3  25.5E6   25.5E6   25.5E6   25.5E6   1
   14  3  25.5E6   25.5E6   25.5E6   25.5E6   1
   15  3  25.5E6   25.5E6   25.5E6   25.5E6   1
*
   FIXBOUNDRIES   DIRECTIONS=123456  TYPE=SURFACES/ 5  6  7  8
*
    ADINA
*
   END
```

D-2 Program 'slb2.in'

The following command program Adina is for modeling the slab shown in Figure 7-9. Eight-node elements are used.

```
*    SLB2.IN
*
*    ADINA-IN INPUT FILE
*
*    SLB2 IS PLASTIC ANALYSIS PROGRAM FOR TWO WAY SLAB
*
*
     FILEUNITS   LIST=7  LOG=7  ECHO=7
     LIST FILEUNITS
*
     CONTROL   PLOTUNIT=CM,
     PLOTSAVE=YES
     LIST CONTROL
*
     DATABASE CREATE
*
     HEADING ' SLB2 IS PLASTIC ANALYSIS PROGRAM FOR TWO WAY SLAB'
     LIST HEADING
*
     MASTER  IDOF=000111  NSTEP=2  REACTIONS=YES
     LIST MASTER
*
     ANALYSIS  TYPE=STATIC
     LIST ANALYSIS
*
     ITERATION  METHOD=FULL-NEWTON   LINE-SEARCH=YES
     LIST ITERATION
*
     AUTOMATIC-ATS  10
*
     TOLERANCES  PRINT=1   ITEMAX=35
     LIST TOLERANCES
*
     PRINTNODES 640 670 1
*
     PRINTOUT   VOLUME=MIN CA=NO IPDA=4 PRINT=NO IPRIC=0,
     IPRIT=0 IVC=0 IAC=1 ST=NO
*
*
     TIMESTEP
      6   1
      1   1
      1   1
      1   1
      1   1
```

```
 13  1
*
 PORTHOLE  FORMATTED=YES  FILE=60
*
 TIMEFUNCTION  1
  0.   0.
  2    0.25
  8    0.625
  9    0.6485
  10   0.6719
  11   0.6777
  12   0.6799
  25   1.0
*
 COORDINATES
 ENTRIES    NODE      X       Y       Z
              1       0       0       .100
              2       2.400   0       .100
              3       2.400   2.400   .100
              4       0       2.400   .100
              9       0       0       0
              10      2.400   0       0
              11      2.400   2.400   0
              12      0       2.400   0
              5       0       0       .03333333333
              6       2.400   0       .03333333333
              7       2.400   2.400   .03333333333
              8       0       2.400   .03333333333
*
 EGROUP 1 THREEDSOLID DISPL=SMALL  STRAINS=SMALL  MATERIAL=1,
 RESULTS=FORCES
*
 EDATA
 ENTRIES EL  PRINT
      15  Y
      14  Y
      28  Y
      42  Y
      56  Y
      70  Y
      84  Y
      98  Y
*
      240 Y
      239 Y
      253 Y
      267 Y
      281 Y
      295 Y
      309 Y
      323 Y
*
      465 Y
      464 Y
```

```
        478 Y
        492 Y
        506 Y
        520 Y
        534 Y
        548 Y
*
    GVOLUME  1  2  3  4  5  6  7 8  15 15 2 8
    GVOLUME  5  6  7  8  9  10 11 12 15 15 1 8
*
    MATERIAL  N=1   TYPE=CONCRETE,
    E0=28E+9   NU=0.20   SIGMAT=3E+6 SIGMAC=-30E+6 EPSC=-0.002,
    SIGMAU=-20E6   EPSU=-0.003   BETA=.75 DENSITY=2400
*
*
    LOADS ELEMENT
    113  3   10E6   10E6   10E6   10E6   1
*
    FIXBOUNDRIES   DIRECTIONS=123456  TYPE=SURFACES/ 9 5 6 10
    FIXBOUNDRIES   DIRECTIONS=123456  TYPE=SURFACES/ 10 6 7 11
    FIXBOUNDRIES   DIRECTIONS=123456  TYPE=SURFACES/ 11 7 8 12
    FIXBOUNDRIES   DIRECTIONS=123456  TYPE=SURFACES/ 12 8 5 9
*
    ADINA

*
    END
```

D-3 Program 'slb1.in'

The following command program Adina is for modeling the slab shown in Figure D-1 and Figure 7-19. Eight-node elements are used. The summation of the vertical reaction forces at the locations of the nodes at the boundary of one side of the slab is obtained from the finite element output and the distribution of the reaction is presented as shown in Figure D-2. The vertical coordinate that is shown in Figure D-2 represents the downward reaction with negative numbers and the upward reaction is represented with positive numbers.

The values of the forces that are acting on the diagonal lines, at each layer, at the locations of the nodes in a direction perpendicular to the base of the segment (corresponding to Figure 7-12-A) are presented in Figure D-3.

Similar values for the forces that are acting on the diagonal lines in a direction parallel to the base of the segment are presented in Figure D-4. This direction corresponds to the direction that is shown in Figure 7-12-B.

The values of the forces presented in Figure D-4 are used in combination with the values presented in Figure D-3 to obtain the values of the forces presented in Figure D-5 and Figure D-6.

```
*    SLB1.IN
*
*    ADINA-IN INPUT FILE
*
*    SLB1 IS PLASTIC ANALSIS PROGRAM FOR TWO WAY SLAB
*
*
     FILEUNITS   LIST=7  LOG=7  ECHO=7
     LIST FILEUNITS
*
     CONTROL   PLOTUNIT=CM,
     PLOTSAVE=YES
     LIST CONTROL
*
     DATABASE CREATE
*
     HEADING ' SLB1 IS PLASTIC ANALYSIS PROGRAM FOR TWO WAY  SLAB'
     LIST HEADING
*
     MASTER  IDOF=000111  NSTEP=2  REACTIONS=YES
     LIST MASTER
*
     ANALYSIS  TYPE=STATIC
     LIST ANALYSIS
*
     ITERATION  METHOD=FULL-NEWTON   LINE-SEARCH=YES
```

```
   LIST ITERATION
*
   AUTOMATIC-ATS 10
*
   TOLERANCES PRINT=1  ITEMAX=35
   LIST TOLERANCES
*
   PRINTNODES 650 655 1
*
   PRINTOUT  VOLUME=MIN CA=NO IPDA=4 PRINT=NO IPRIC=0,
   IPRIT=0 IVC=0 IAC=1 ST=NO
*


*
   TIMESTEP
    6   1
    1   1
    1   1
    1   1
    14  1
*
   PORTHOLE  FORMATTED=YES  FILE=60
*
   TIMEFUNCTION  1
    0.   0.
    2    0.25
    8    0.625
    9    0.6719
    10   0.6777
    11   0.6799
    25   1.0
*
   COORDINATES
   ENTRIES     NODE      X       Y       Z
                 1       0       0       .100
                 2       2.400   0       .100
                 3       2.400   2.400   .100
                 4       0       2.400   .100
                 5       0       0       0
                 6       2.400   0       0
                 7       2.400   2.400   0
                 8       0       2.400   0
*
   EGROUP 1 THREEDSOLID  DISPL=SMALL  STRAINS=SMALL  MATERIAL=1,
   RESULTS=FORCES
*
   EDATA
   ENTRIES EL PRINT
        15  Y
        14  Y
        28  Y
        42  Y
        56  Y
        70  Y
```

```
        84  Y
        98  Y
*
        240 Y
        239 Y
        253 Y
        267 Y
        281 Y
        295 Y
        309 Y
        323 Y
*
        465 Y
        464 Y
        478 Y
        492 Y
        506 Y
        520 Y
        534 Y
        548 Y
*
    GVOLUME  1  2  3  4  5  6  7 8  15 15 3 8
*
    MATERIAL  N=1   TYPE=CONCRETE,
    E0=28E+9  NU=0.20  SIGMAT=3E+6 SIGMAC=-30E+6 EPSC=-0.002,
    SIGMAU=-20E6  EPSU=-0.003  BETA=.75 DENSITY=2400
*
    LOADS ELEMENT
    113  3  10E6   10E6   10E6   10E6   1
*
    FIXBOUNDRIES   DIRECTIONS=123456  TYPE=SURFACES/ 1  2  6  5
    FIXBOUNDRIES   DIRECTIONS=123456  TYPE=SURFACES/ 4  3  7  8
    FIXBOUNDRIES   DIRECTIONS=123456  TYPE=SURFACES/ 1  4  8  5
    FIXBOUNDRIES   DIRECTIONS=123456  TYPE=SURFACES/ 2  3  7  6
*
    ADINA
*
    END
```

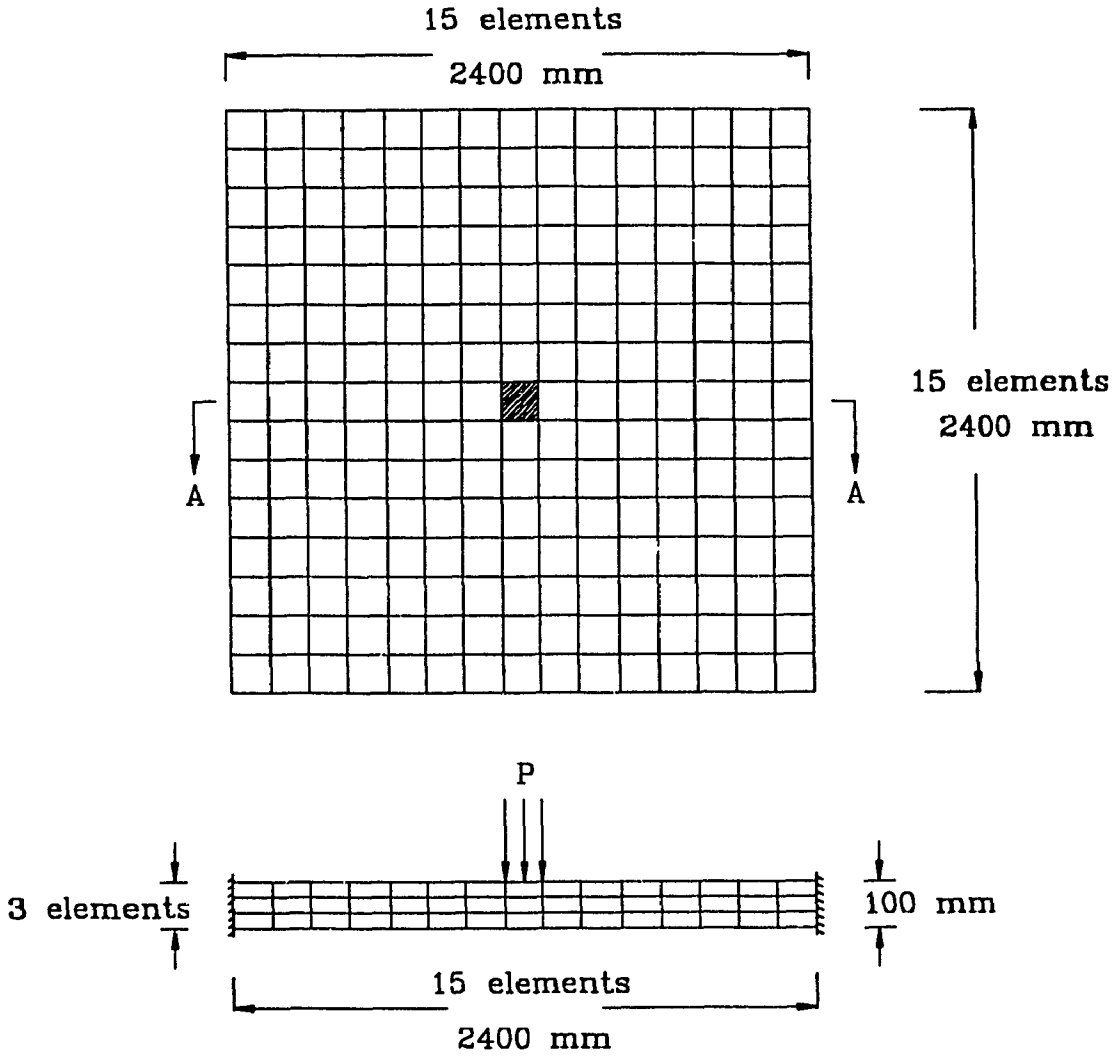

Figure D-1 A square slab with fixed boundaries analyzed by the finite element method

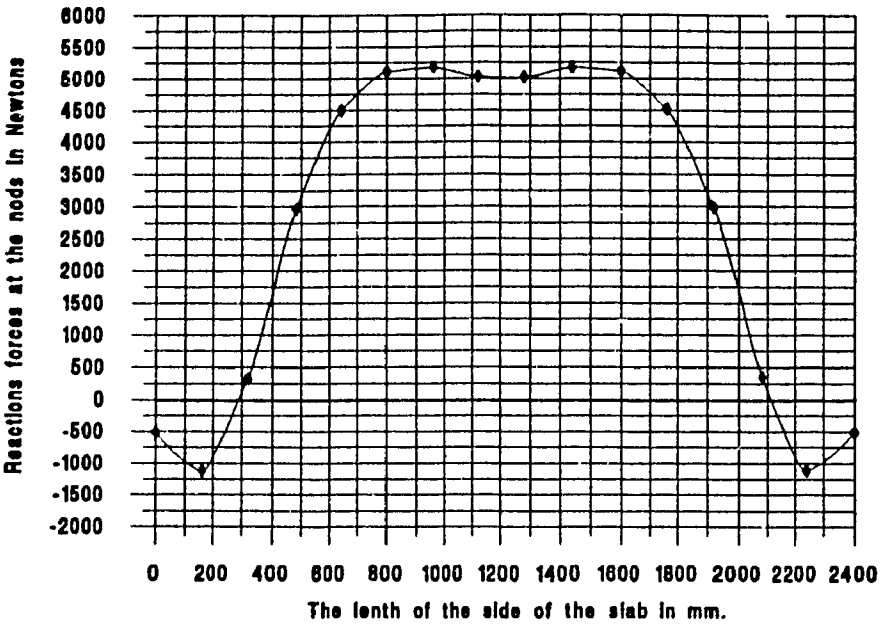

Figure D-2 The distribution of the vertical reaction at one side of the slab

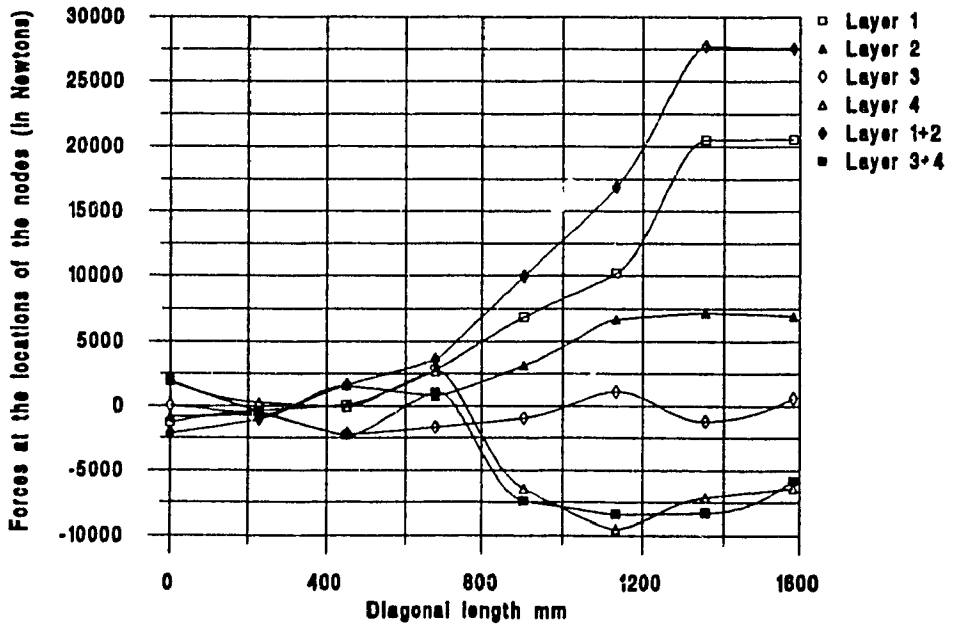

Figure D-3 Forces acting on the diagonal lines in a direction perpendicular to the base of the segment

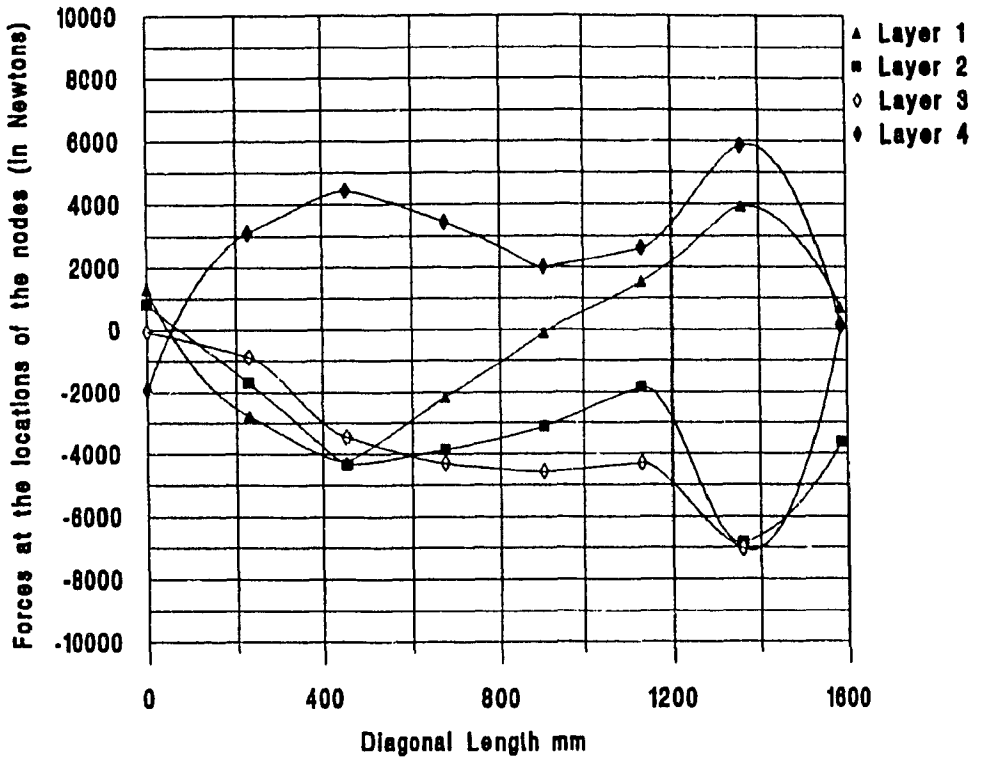

Figure D-4 Forces acting on the diagonal lines in a direction parallel to the base of the segment

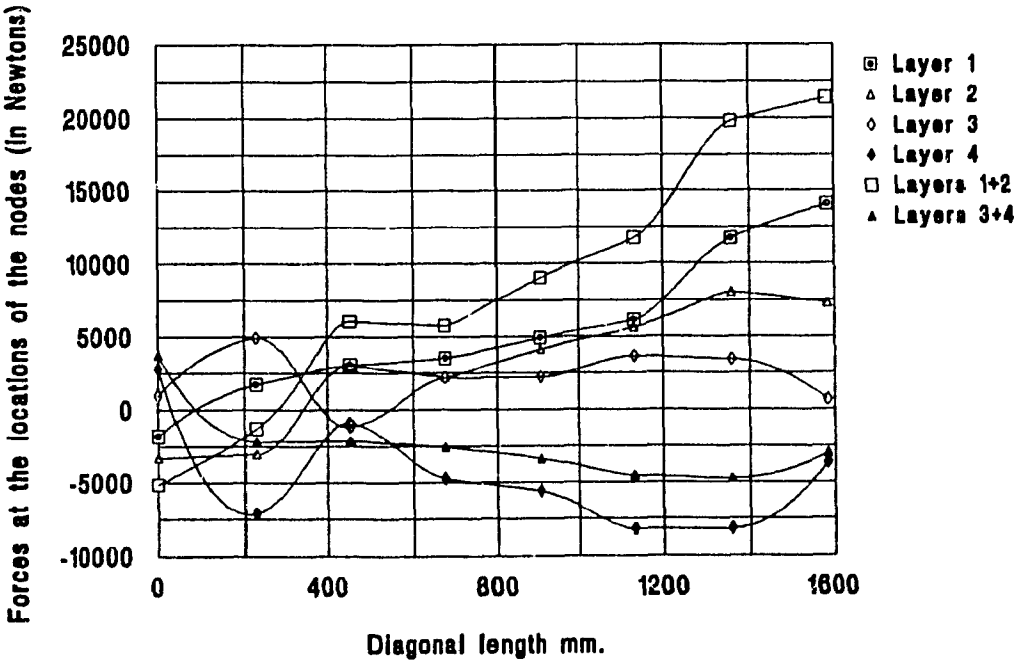

Figure D-5 Forces perpendicular to the diagonal lines

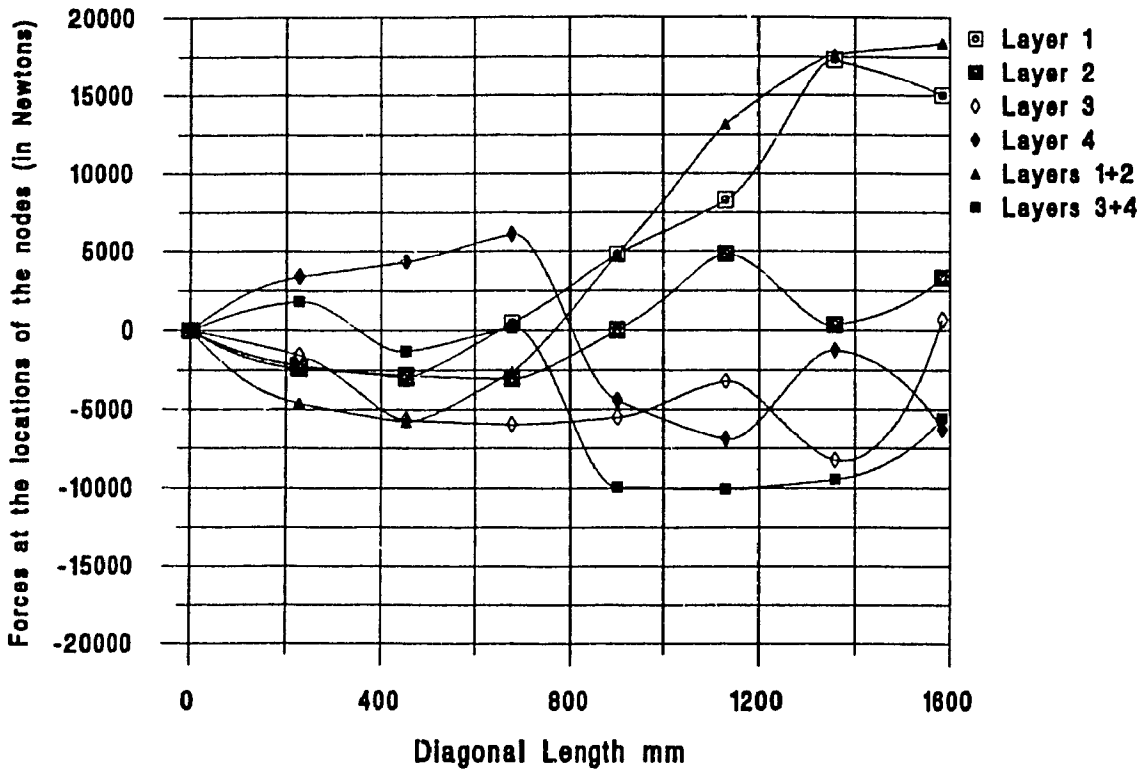

Figure D-6 Forces parallel to the diagonal lines

D-4 Program 'Slb7.in'

The following command program Adina is for modeling the slab shown in Figure 7-19. Twenty-node elements are used.

```
*  SLB7.IN
*
*  ADINA-IN INPUT FILE
*
*  SLB1 IS PLASTIC ANALYSIS PROGRAM FOR TWO WAY SLAB
*
*  CONTROL MODE=I PLOTUNIT=CM PLOTSAVE=YES
*  LIST CONTROL
```

```
*
   FILEUNITS  LIST=7 LOG=7 ECHO=7
   LIST FILEUNITS
*
   CONTROL  PLOTUNIT=CM,
   PLOTSAVE=YES
   LIST CONTROL
*
   DATABASE CREATE
*
   HEADING ' SLB1 IS PLASTIC ANALYSIS PROGRAM FOR TWO WAY SLAB'
   LIST HEADING
*
   MASTER  IDOF=000111  NSTEP=2  REACTIONS=YES MTOT=10000
   LIST MASTER
*
   ANALYSIS  TYPE=STATIC
   LIST ANALYSIS
*
   ITERATION  METHOD=FULL-NEWTON  LINE-SEARCH=YES
   LIST ITERATION
*
   AUTOMATIC-ATS 10
*
   TOLERANCES  PRINT=1  ITEMAX=35
   LIST TOLERANCES
*
   PRINTNODES 1  27  1
*
*   ESAVE  1 0 1
*
*   NSAVE  1 0 1
*
   PRINTOUT  VOLUME=MIN CA=NO IPDA=4  PRINT=NO  IPRIC=0,
   IPRIT=0 IVC=0 IAC=1 ST=NO
*
*   PRINTSTEPS FIRST1=LAST1
*
   TIMESTEP
    6   1
    1   1
    1   1
    1   1
    1   1
    13   1
*
   PORTHOLE  FORMATTED=YES  FILE=60
*
   TIMEFUNCTION  1
    0.   0.
    2    0.25
    8    0.625
    9    0.6485
    10   0.6719
```

```
  11  0.6777
  12  0.6799
  25  1.0
*
  COORDINATES
  ENTRIES    NODE      X       Y       Z
        1      0       0      .100
        2     .080     0      .100
        3     1.200    0      .100
        4     1.200    .080   .100
        5     1.200    1.200  .100
        6     .080     1.200  .100
        7     0        1.200  .100
        8     0        .080   .100
        9     .080     .080   .100
        10    0        0      .03333333333
        11    .080     0      .03333333333
        12    1.200    0      .03333333333
        13    1.200    .080   .03333333333
        14    1.200    1.200  .03333333333
        15    .080     1.200  .03333333333
        16    0        1.200  .03333333333
        17    0        .080   .03333333333
        18    .080     .080   .03333333333
        19    0        0      0
        20    .080     0      0
        21    1.200    0      0
        22    1.200    .080   0
        23    1.200    1.200  0
        24    .080     1.200  0
        25    0        1.200  0
        26    0        080    0
        27    .080     .080   0
*
  EGROUP 1 THREEDSOLID DISPL=SMALL STRAINS=SMALL MATERIAL=1,
  RESULTS=STRESS
*
  GVOLUME 1 2 9 8 19 20 27 26 1 1 3 20
  GVOLUME 8 9 6 7 17 18 15 16 1 7 2 20
  GVOLUME 17 18 15 16 26 27 24 25 1 7 1 20
  GVOLUME 2 3 4 9 11 12 13 18 7 1 2 20
  GVOLUME 11 12 13 18 20 21 22 27 7 1 1 20
  GVOLUME 9 4 5 6 18 13 14 15 7 7 2 20
  GVOLUME 18 13 14 15 27 22 23 24 7 7 1 20
*
  MATERIAL N=1 TYPE=CONCRETE,
  E0=28E+9 NU=0.20 SIGMAT=3E+6 SIGMAC=-30E+6 EPSC=-0.002,
  SIGMAU=-20E6 EPSU=-0.003 BETA=.75 DENSITY=2400
*
  LOADS ELEMENT
  1 3 10E6 10E6 10E6 10E6 1
*
  FIXBOUNDRIES DIRECTIONS=1456 TYPE=SURFACES/ 1 8 26 19
  FIXBOUNDRIES DIRECTIONS=1456 TYPE=SURFACES/ 8 7 16 17
```

```
    FIXBOUNDRIES   DIRECTIONS=1456    TYPE=SURFACES/ 17 16 25  26
    FIXBOUNDRIES   DIRECTIONS=2456    TYPE=SURFACES/ 1  2  20  19
    FIXBOUNDRIES   DIRECTIONS=2456    TYPE=SURFACES/ 2  3  12  11
    FIXBOUNDRIES   DIRECTIONS=2456    TYPE=SURFACES/ 11 12 21  20
    FIXBOUNDRIES   DIRECTIONS=123456  TYPE=SURFACES/ 16 15 24  25
    FIXBOUNDRIES   DIRECTIONS=123456  TYPE=SURFACES/ 15 14 23  24
    FIXBOUNDRIES   DIRECTIONS=123456  TYPE=SURFACES/ 12 13 22  21
    FIXBOUNDRIES   DIRECTIONS=123456  TYPE=SURFACES/ 13 14 23  22
*
    ADINA
*
    END
```